eCAM Evidence-Based Complementary and Alternative Medicine

Diabetes and Metabolism Disorders Medicinal Plants: A Glance at the Past and a Look to the Future 2018

Lead Guest Editor: Hilal Zaid
Guest Editors: Akhilesh K. Tamrakar, Mohammed S. Razzaque, and Thomas Efferth

Diabetes and Metabolism Disorders Medicinal Plants: A Glance at the Past and a Look to the Future 2018

Evidence-Based Complementary and Alternative Medicine

Diabetes and Metabolism Disorders Medicinal Plants: A Glance at the Past and a Look to the Future 2018

Lead Guest Editor: Hilal Zaid
Guest Editors: Akhilesh K. Tamrakar, Mohammed S. Razzaque, and Thomas Efferth

Editorial Board

Contents

Hindawi
Evidence-Based Complementary and Alternative Medicine
Volume 2018, Article ID 5843298, 3 pages
https://doi.org/10.1155/2018/5843298

Editorial

Diabetes and Metabolism Disorders Medicinal Plants: A Glance at the Past and a Look to the Future 2018

Hilal Zaid,[1,2] **Akhilesh K. Tamrakar**,[3] **Mohammed S. Razzaque**,[3,4] **and Thomas Efferth**[5]

[1]*Qasemi Research Center, Al-Qasemi Academy, P.O. Box 124, Baqa-El-Gharbia 30100, Israel*
[2]*Faculty of Sciences, Arab American University, P.O. Box 240, Jenin, State of Palestine*
[3]*CSIR-Central Drug Research Institute, Lucknow 226031, India*
[4]*The Forsyth Institute, Cambridge, USA*
[5]*Johannes Gutenberg University, Mainz, Germany*

Correspondence should be addressed to Hilal Zaid; hilal.zaid@gmail.com

Received 26 September 2018; Accepted 26 September 2018; Published 30 September 2018

Diabetes is one of the world's most widespread diseases, characterized by persistent hyperglycemia and related to metabolic disorder, affecting over 327 million people and causing about 300,000 deaths annually [1]. Despite great advances in prevention and therapy, existing treatments for this disorder have serious side effects. On the other hand, in the modern and contemporary world, the incidence of metabolic disorders and diabetes is rising continuously due to modernization in life style and unhealthy dietary habits, imposing an urgent need for new therapies for the management of this deadly disease. Plants used in traditional medicine represent a valuable source in the search for new medicinal compounds. In traditional system of medicine, at least 1200 species of medicinal plants are used for their antidiabetic attributes. However, only a small proportion of such plants have been scientifically validated [2].

Currently, we are witnessing a great progress in evidence-based modern medicine and pharmacology. The characterization of pharmacological and biological effects of herbal-based medicines is becoming more competitive and complex, with the involvement of experts in this research area belonging to different scientific fields, including botany, chemistry, biochemistry, immunology, molecular biology, and bioinformatics. However, despite this great progress in evidence-based modern medicine and pharmacology, traditional medicinal plants continue to be practiced without regulations in many countries [3]. It is crucial hence to keep on studying medicinal plants efficacy including their toxicity in order to prevent their abuse. This special issue provides a comprehensive overview on physiological as well as molecular and biochemical efficacy of medicinal plants and natural active compounds in treating metabolic disorders and diabetes. For this special issue, the editorial office received 23 papers, and after rigorous peer review process 12 papers were accepted for publication. All published articles focused on the theme of this special issue, dealing with biochemical efficacy, molecular mechanism, or clinical efficacy of plant-derived samples for the management of diabetes or associated metabolic disorders.

C. Rugerio-Escalona et al. evaluated the antihyperglycemic potential of the crude and fractional methanolic extracts of *Hamelia patens* Jacq in streptozotocin-induced hyperglycemic rats. They reported that repeated administrations of the crude or fractional methanolic extract for 20 days lowered blood glucose to a normal level. The extracts were also shown to have significant α-glucosidase inhibitory activity and protective effects of kidney and liver function parameters. They further subjected the plant extract for quantitative phytochemical and chromatographic analysis and identified five compounds. Out of those, epicatechin and chlorogenic acid had demonstrated antihyperglycemic effect. Considering its antihyperglycemic potential, the authors proposed the extracts of *Hamelia patens* as efficacious source for the treatment of diabetes.

Increased incidences of diabetes are closely associated with increase in obesity and related hyperlipidemia. Currently available synthetic drugs to lower weight or serum lipid in obese patients have been associated with adverse effect

progression of drug resistance. Therefore a well-designed clinical trial to establish the efficacy of an intended molecule is very important. In the clinical study by S. Kang et al., the authors evaluated the impact of *Citrus unshiu* peel pellet (CUPP) on obesity and lipid profile. They selected 118 patients, including 88 females with body mass index > 23 and gave them *Citrus unshiu* peel pellet for 4 weeks and observed a significant decrease in BMI in all subjects after CUPP treatment. They also observed a significant decrease in total cholesterol and triglycerides levels. The authors concluded that CUPP could aid in weight control and improve total cholesterol level, and they proposed a large-scale trial to establish the clinical benefits of CUPP.

In another pilot study performed by P. Algenstaedt et al., the authors test the effect of daily consumption of *Morinda citrifolia* (Noni) fruit juice on the physiological status of type 2 diabetic patients. They treated twenty patients with type 2 diabetes with *Morinda citrifolia* fruit juice for eight weeks with regular monitoring of blood glucose levels and other biochemical parameters. They observed that *Morinda citrifolia* fruit juice consumption decreased fasting blood glucose level in diabetic patients but it did not cause hypoglycemia in normoglycemic patients. They also reported decrease in mean HbA1c and CRP values and improvement in insulin excretion and blood cholesterol status in *Morinda citrifolia* fruit juice treated patients. The authors proposed *Morinda citrifolia* fruit juice as a suitable additive to the diet of diabetic patients.

Enhanced rate of morbidity and mortality of diabetics has become a global health problem and puts a huge economic burden on the world population, urging researchers to clarify the pathogenesis of diabetes using advanced techniques. Proteomic technologies are large-scale research tools that can provide abundant data regarding the pattern of protein expression and are widely used to explore the molecular mechanisms underlying the function of complex bioactive mixtures. X. Qiu and colleagues reported a comparative proteomic analysis of two differently extracted *Coptis Chinensis* (CC) in the treatment of type 2 diabetes. They established a rat model of type 2 diabetes, treated it with supercritical-extracted CC and gastric juice extracted CC, and compared various phenotypic and biochemical parameters between the groups. The report showed a significant decrease in triglyceride, total cholesterol, and low density lipoprotein in both CC-treated groups. Additionally, they reported 15 proteins to be differentially regulated in both CC-treated groups. These proteins were found to be associated with glucose metabolism, insulin action, immunity, inflammation, lipid metabolism, oxidation, and antioxidation. From the data authors established that the two differently extracted CC did not show significant differences in terms of their treatment efficacy.

Type 2 diabetes is characterized by insulin resistance in peripheral tissues, including skeletal muscle, liver, and adipose. Skeletal muscle is the major site for glucose utilization and insulin resistance in skeletal muscle is characterized by impaired translocation of insulin sensitive glucose transporter, GLUT4, to cell surface causing decreased rate of glucose uptake. Therefore, interventions with ability to increase GLUT4 translocation to cell surface can be beneficial for the management of insulin resistance. In the *in vitro* study by S. Kadan et al., the authors assessed the chemical composition, cytotoxicity, and antidiabetic activity of *Gundelia tournefortii* extracts. They revealed 39 compounds in the extracts and found both the methanol and hexane extract to be safe up to 250 μg/ml *in vitro*. Effect of extracts on glucose metabolism was assessed by measuring GLUT4 translocation in muscle cells, and it was found that methanol extract is more efficient in GLUT4 translocation enhancement. The authors proposed that *Gundelia tournefortii* exerts antidiabetic activity by enhancing GLUT4 translocation to the cell surface in skeletal muscle.

Inhibition of α-glucosidase and α-amylase, which digest dietary starch into glucose, has been an established method for controling blood sugar levels. However, currently available drugs under this category have been reported with unpleasant gastrointestinal side effects that frequently result in therapy abandonment. Therefore, it is necessary to continue the search for new alternatives to α–glucosidase and pancreatic lipase inhibitors, with milder side effects and which contribute to the treatment of obesity and type 2 diabetes mellitus, in conjunction with current therapies. With the aim of identifying new pancreatic lipase and α–glucosidase inhibitors for the management of diabetes, D. Morales et al. reported potential inhibitor for these enzymes from the hydroalcoholic extract of *Ludwigia octovalvis*. The authors reported identifying and characterizing one flavone (isoorientin) with considerable inhibitory effect of pancreatic lipase and two compounds with potential inhibitory effect against α–glucosidases (ethyl gallate and gallic acid). These findings might be useful in the development of a potential novel phytomedicine.

In a similar study, R. S. Shenoy et al. investigated the triterpene glycoside (TG) fraction, isolated from the ethanolic extract of *Gymnema sylvestre*, for inhibitory activity against different glucosidases. TG was characterized by being a mixture of triterpene glycosides, gymnemic acid I, IV, VII, and gymnemagenin and exhibited effective inhibition of yeast α- glucosidase, sucrase, maltase, and pancreatic α-amylase. TG did not exhibit any toxic effects on β-cell viability, showed protection against H2O2 induced ROS generation, and stimulated glucose-induced insulin secretion in β-cells. The authors proposed TG as a functional food ingredient and a safe nutraceutical candidate for management of diabetes.

Metabolomics is used to evaluate the characteristics and interactions of low molecular weight metabolites under a specific set of conditions. It is a powerful analytical strategy to identify the metabolites *in vivo* and clarify metabolic pathways. Especially for metabolic disease, such as T2DM, metabolomics offers an opportunity to test multiple metabolic markers in large settings. J. Liu et al. reported a metabolomics-based clinical efficacy of Tangzhiqing tablet (TZQ), a Chinese patent medicine, consisting of five herbs, *Paeonia lactiflora, Morus alba, Nelumbo nucifera, Salvia miltiorrhiza,* and *Crataegus pinnatifida,* for type 2 diabetes mellitus with hypertriglyceridemia. In clinical study with type 2 diabetic patients, they observed that TZQ could reduce glycosylated hemoglobin (HbA1c) and fasting insulin, correlated

with the baseline level of triglyceride. In metabolomics data they observed a significant difference between patients and healthy volunteers and identified 17 biomarkers. After 12-week treatment with TZQ they found significant decrease in 11 biomarkers and suggested that TZQ could improve the metabolomic abnormalities in the participants.

Obesity is the major risk factor for increasing incidences of diabetes. Therefore, search towards a molecule that can mitigate both hyperglycemia and obesity is of higher priority for the management of metabolic syndrome. R. O. Malematja et al. evaluated the acetone leaf extract of *Senna italic* for its cytotoxic, antiglycation, and lipolytic effect. They also evaluated its effect on glucose uptake and GLUT4 translocation to cell surface and adipogenesis in 3T3-L1 adipocytes. They found that extract had no adverse effect on cell viability. It showed significant antiglycation effect and decreased the expression of various adipokines. They also observed increased rate of glucose uptake associated with enhanced GLUT4 translocation and expression upon extract treatment in combination with insulin, mediated through the PI3K-dependent pathway. In independent study by J. Lee et al., authors investigated the synergistic effect of Bupleuri Radix and Scutellariae Radix, an herbal combination from Korean medicine on obesity model of 3T3-L1 adipocytes. They reported that combination significantly decreased lipid accumulation and expression of the important adipogenic factor PPARγ and C/EBPα and their downstream genes in 3T3-L1 adipocytes. Furthermore, the combination was reported to activate AMP-activated protein kinase alpha, thereby regulating energy metabolism.

In the study by C. Tian et al., the authors investigated the effect and mechanism of action of Wushenziye formula, a traditional Chinese medicine, on skeletal muscle insulin resistance in type 2 diabetes. They observed significant improvement in fasting blood glucose, glycosylated serum proteins, glycosylated hemoglobin, insulin, and insulin resistance index in type 2 diabetic Goto-Kakizaki rats. Under *in vitro* condition, they observed increased glucose consumption, upregulated expression of IRS-1, Akt, and GLUT4, and decreased expression of PTP1B in skeletal muscle cells treated with Wushenziye formula. The author demonstrated that Wushenziye formula regulated glucose metabolism through modulating PTP1B/ IRS-1/AKT/GLUT4 signaling and offered Wushenziye formula as a potential candidate for the management of type 2 diabetes.

The study by Q. Liang et al. aimed to understand the molecular mechanisms of Zuo Gui Wan (ZGW), classic formula in traditional Chinese medicine, on impaired glucose tolerance in mouse embryo. They used high glucose loaded two-cell stage mouse embryos as a model and utilized single-cell RNA sequencing technology for transcriptome analysis. They observed that ZGW reversed high glucose-mediated downregulation of genes in the ribosome pathway, leading to prevention of high glucose-mediated embryo cell death. They also observed that ZGW promoted sugar metabolism via tricarboxylic acid cycle through upregulating the genes in the respiratory chain and oxidative phosphorylation. The study revealed the global gene regulation changes of high glucose affecting two-cell stage embryos and also provided insight into the potential molecular mechanisms of ZGW on the IGT.

Overall, in light of this special issue, plant based therapeutics can be a better option for the management of diabetes and related metabolic complications. However, proper scientific validation of efficacy in established experimental models, clinical efficacy, and assessment for the adverse side effects is of utmost important, for their further development.

Conflicts of Interest

The editors declare that they have no conflicts of interest regarding the publication of this special issue.

Acknowledgments

We are thankful to all contributors of this special issue for their valuable research papers. We are grateful to the reviewers for their constructive criticism and timely response that made this special issue possible. Our sincere thanks and gratitude go to the editorial board of eCAM for inviting us to edit this special issue. The editorial board hopes that readers will enjoy this special issue.

Hilal Zaid
Akhilesh K. Tamrakar
Mohammed S. Razzaque
Thomas Efferth

References

[1] H. Zaid, B. Saad, A. A. Mahdi, A. K. Tamrakar, P. S. Haddad, and F. U. Afifi, "Medicinal Plants and Natural Active Compounds for Diabetes and/or Obesity Treatment," *Evidence-Based Complementary and Alternative Medicine*, vol. 2015, Article ID 469762, 2 pages, 2015.

[2] B. Saad, H. Zaid, S. Kadan, and S. Shanak, *Anti-diabetes and Anti-obesity Medicinal Plants and Phytochemicals: Safety, Efficacy, and Action Mechanisms*, Springer International Publishing AG, 2017.

[3] H. Zaid, A. A. Mahdi, A. K. Tamrakar, B. Saad, M. S. Razzaque, and A. Dasgupta, "Natural active ingredients for diabetes and metabolism disorders treatment," *Evidence-Based Complementary and Alternative Medicine*, vol. 2016, Article ID 2965214, 2 pages, 2016.

Hindawi
Evidence-Based Complementary and Alternative Medicine
Volume 2018, Article ID 4341961, 6 pages
https://doi.org/10.1155/2018/4341961

Research Article

Clinical Investigations of the Effect of *Citrus unshiu* Peel Pellet on Obesity and Lipid Profile

Seongil Kang,[1] Sangyeol Song,[1] Joosang Lee,[1] Hyekyung Chang,[2] and Sanghun Lee[3]

[1]*Jeju Institute of Korean Medicine, Republic of Korea*
[2]*Department of Surgery, College of Medicine, Kyunghee University, Republic of Korea*
[3]*Department of Medical Consilience, Graduate School, Dankook University, Republic of Korea*

Correspondence should be addressed to Sanghun Lee; integrative@korea.com

Received 26 March 2018; Revised 5 June 2018; Accepted 4 July 2018; Published 19 September 2018

Academic Editor: Mohammed S. Razzaque

Objectives. Several experimental studies have reported antiobesity and lipid-improving effects of *Citrus unshiu*. However, clinical studies on its effects are lacking. This study was designed to evaluate the impact of *Citrus unshiu* peel pellet (CUPP) on obesity and lipid profile. *Methods*. For 118 patients with body mass index (BMI) > 23 who took *Citrus unshiu* peel pellet (CUPP) for 4 weeks in a Public Health Center, laboratory and biometric readings before and after CUPP administration were analyzed. *Results*. Mean age of these subjects was 53.8±10.6 years (range: 18-75 years). There were 88 (74.6%) females in the study sample (n = 118). A significant ($p < 0.01$) decrease in BMI from 27.47±2.24 to 27.27±2.22 was observed in all subjects after CUPP treatment and 65.3% (N = 77) of them lost 1.03±0.83 kg of weight after 4 weeks of treatment. Total cholesterol level was significantly ($p < 0.01$) decreased from 204.0±37.4 mg/dL to 193.5±36.5 mg/dL. Significant ($p < 0.05$) decreases in levels of low-density lipoprotein, cholesterol, and triglyceride were also observed. *Conclusions*. These results suggest that CUPP in practice could help weight control and improve total cholesterol level. Findings of this study provide clinical foundation for future large-scale trials to establish clinical benefits of CUPP.

1. Introduction

Obesity and related hyperlipidemia have become major worldwide health problems. With sharply increasing incidence of metabolic disease and associated morbidity and mortality, both medical and economical costs are also expected to increase [1]. Nowadays, synthetic drugs to lower weight or serum lipid in obese patients with hyperlipidemia are available. However, they have limitations such as adverse effects and progression of drug resistance [2]. In this regard, application of medicinal plants is necessary.

Citrus flavonoids as polyphenolic compounds have emerged as promising therapeutic agents for the treatment of obesity, insulin resistance, and dyslipidemia [3, 4]. Flavonoids such as naringin, hesperidin, and nobiletin have been experimentally proven to be able to lower lipid levels with insulin-sensitizing and anti-inflammatory properties primarily through inhibition of hepatic fatty acid synthesis and induction of increased fatty acid oxidation [5–8]. *Citrus aurantium* has been used as one of common dietary supplements for weight loss in the US because it increases energy expenditure and lipolysis and acts as a mild appetite suppressant [9, 10]. Synephrine, its proposed active constituent, can mimic the action of epinephrine and norepinephrine as alpha-adrenergic agonists. However, human clinical studies have demonstrated that naringin or hesperidin supplement exerts no effect on lipid profile [11, 12]. Active compound isolated from herbs rarely demonstrates high pharmacological activity against metabolic dysregulation because there is no synergistic interaction or multifactorial effects between various compounds present in herbal extract [13]. Therefore, clinical study of citrus extract itself, not isolated flavonoid on the metabolic diseases, is required.

Dried peel of *Citrus unshiu* Markov has been traditionally used as a popular herbal ingredient for treatment of various digestive dysfunctions, including abdominal distension, nausea, vomiting, and dyspepsia in East Asia such as Korea and Japan [14]. Based on its excellent properties and safe use,

this herb has been commonly used for a long time in food or medicine preparation which was registered and managed as policy documents of Korea Food and Drug Administration [15, 16]. The dried peel of *Citrus unshiu*, like other citrus species, has been experimentally proven to be able to ameliorate hyperglycemia through inhibition of hepatic gluconeogenic enzyme and induction of insulin/glucagon secretion. It can also ameliorate hypertriglyceridemia via inhibition of lipid absorption and lipogenesis. In addition, it promotes lipolytic effects in the liver [17–20]. However, clinical studies on the effect of *Citrus unshiu* on obesity and lipid metabolism are insufficient [21]. Therefore, the objective of this study was to explore the efficacy and safety of *Citrus unshiu* in overweight or obese subjects. Results of this study will provide a clinical foundation for future large-scale clinical trials.

2. Patients and Methods

2.1. Subjects and Ethics. The Public Health Center in Jejusi, Republic of Korea, has provided a variety of weight management programs including exercise, diet, and behavior modification to local residents. Herbal medicines were also provided to those who did not lose weight after such effort with voluntary consent. According to the Asia-Pacific obesity classification, all subjects were classified into five different groups: underweight (< 18.5 kg/m^2), normal weight (18.5 to 22.99 kg/m^2), overweight (23 to 24.99 kg/m^2), class I obese (25 to 29.99 kg/m^2), and class II obese (≥ 30 kg/m^2) [22]. Therefore, all 157 adult patients with BMI greater than 23 kg/m^2 were treated with *Citrus unshiu* peel pellet (CUPP) for 4 weeks between September and October 2017. After excluding cases with missing data on anthropometric and biochemical parameters before and after CUPP administration, 118 patients were finally analyzed. This project was approved by the Institutional Review Board of Dankook University (DKU 2017-11-001). It was conducted in accordance with the Declaration of Helsinki.

2.2. Citrus unshiu Peel Pellet (CUPP) and Treatment Course. CUPP was prepared from dried peels of *Citrus unshiu* cultivated organically in Jeju Island, Republic of Korea. After juice extraction process, *Citrus unshiu* peels were collected and dried in an air-oven at 50°C. Subsequently, they were crushed and sieved to particle size of 0.25 mm. They then underwent agglomeration to form larger pellet size of 5 mm.

For analysis of CUPP components, 10 grams of the final CUPP was extracted with 10 ml of 80% methanol under ultrasonication for 30 min and centrifuged at 3000 rpm for 5 min. The supernatant was filtered through a Whatman No. 1 filter paper. The filtrate was concentrated using a vacuum rotary evaporator (Büchi R-100, Germany) and lyophilized using a freeze dryer (Ilshin Biobase, Korea). The extract was dissolved in high-performance liquid chromatography (HPLC) grade methanol to a final concentration of 10 mg/mL. The solution was filtered through a 0.45-μm membrane and 20 μL of the filtrate was subjected to HPLC analysis. HPLC

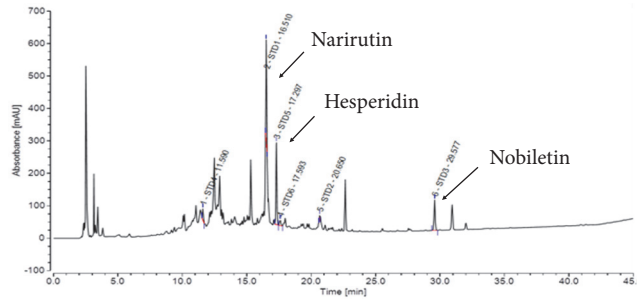

Figure 1: Major constituents of *Citrus unshiu* peel pellet (CUPP) revealed by HPLC.

profile of CUPP is shown in Figure 1, showing the presence of narirutin, hesperidin, and nobiletin. The quality of CUPP was tested and controlled according to quality standards of the Korea Food and Drug Administration (hesperidin content > 4.0%). The proximate composition of CUPP following AOAC method was carbohydrate (82.4%), sugar (18.9%), crude protein (5.8%), crude fat (0.0%), and caloric value (353.2 kcal/100 g). Daily oral administration of 18 mg (6 mg three times a day) of CUPP was prescribed.

2.3. Protocols and Procedures. Demographic and clinical variables including gender, age, waist circumference, weight, height, and medical comorbidities were collected from patients. Waist circumference was measured at the midway between the last rib and the iliac crest. BMI was calculated as kg/m^2. Body composition, particularly the amount of body fat, was measured by multifrequency tetrapolar bioelectrical impedance method (InBody230®, Biospace, Seoul, South Korea) after at least 8 hours of fasting. Fasting blood samples were also obtained for laboratory analysis of aspartate aminotransferase (AST), alanine aminotransferase (ALT), γ-glutamyltranspeptidase (γ-GTP), total cholesterol (TC), triglyceride (TG), high-density lipoprotein (HDL) cholesterol, and low-density lipoprotein (LDL) cholesterol levels. These clinical data including anthropometric and biochemical parameters were repeatedly measured after 4 weeks of CUPP treatment under similar fasting conditions. Medications for commodities were not changed during the 4 weeks of CUPP treatment. Recorded adverse effects during CUPP administration were also checked.

2.4. Statistical Analyses. Baseline demographic and clinical characteristics of patients are reported as mean ± standard deviation for continuous variables and as frequencies and percentages for categorical variables. Differences in anthropometric and biochemical parameters between groups were examined by Student's t-test. Paired samples t-test was used to evaluate the significance and difference in data obtained from quantitative laboratory and biometric tests before and after treatment with CUPP. Pearson correlation analysis was performed for weight loss and changes in TC level. Statistical significance was considered when p value was equal to or

Table 1: Changes in clinical variables after 4 weeks of CUPP treatment (N = 118).

	Baseline	4th Week	p
Waist circumference (cm)	91.53±7.55	90.36±7.27	0.0002
Weight (kg)	71.09±9.52	70.59 ±9.40	< 0.0001
BMI (kg/m^2)	27.47±2.24	27.27±2.22	< 0.0001
Body fat mass (kg)	24.98±4.78	24.87±4.61	0.481
Fat free mass (kg)	46.11±8.57	45.68±8.84	0.023
Systolic blood pressure (mmHg)	128.9±16.6	126.9 ±14.8	0.554
Diastolic blood pressure (mmHg)	81.4±10.8	81.9±10.7	0.558
Total cholesterol (mg/dL)	201.5±37.4	192.8±36.5	< 0.0001
LDL cholesterol (mg/dL)	117.3±34.5	111.8±34.6	0.011
HDL cholesterol (mg/dL)	56.3±14.6	55.8±13.2	0.482
Triglyceride (mg/dL)	139.7±78.0	126.1±74.5	0.026
AST (U/L)	24.1±8.1	22.4±8.1	0.0093
ALT (U/L)	23.3±12.3	21.2±11.6	0.0167
γ-GTP (U/L)	29.9 ±38.5	32.0 ±35.9	0.153

BMI: body mass index; AST: aspartate aminotransferase; ALT: alanine aminotransferase; and γ-GTP: γ-glutamyltranspeptidase.

less than 0.05. All statistical analyses were carried out using R, a free package from the R Foundation for Statistical Computing.

3. Results

The study population was composed of 30 males and 88 females with a mean age of 53.8±10.6 years (range: 18-75 years) and a median BMI of 27.1 kg/m^2 (range: 23.4-36.1 kg/m^2). Around a third of these subjects (N = 38, 32.2%) were taking antihypertension medication along with dyslipidemia medication including statin (N = 29, 24.6%) or oral hypoglycemic drugs for type 2 diabetes (N = 7, 5.9%). With respect to smoking history, there were five (4.2%) current smokers, 13 (11.0%) former smokers, and 100 (84.7%) never-smokers. Regarding alcohol consumption, there were 66 (55.9%) current drinkers, 5 (4.2%) former drinkers, and 47 (39.8%) never-drinkers.

Main characteristics of anthropometric and biochemical measurements between baseline and 4th week after CUPP administration are summarized in Table 1. BMI, weight, and waist circumference were significantly decreased after CUPP treatment. However, the reduction volume of BMI was only about 0.2 kg/m^2 with weight reduction of 500 grams during 4 weeks. There was no change in fat mass based on bioelectrical impedance method. However, 77 (65.3%) responders experienced weight loss after CUPP treatment, amounting to 1.03±0.83 kg in 4 weeks.

Based on laboratory tests, TC exhibited significantly more decrease compared to other lipid levels. This could be explained by LDL cholesterol reduction, but not HDL cholesterol reduction. Subanalysis after separating normal and abnormal TC or LDL cholesterol range also demonstrated that TC and LDL cholesterol levels in the abnormal group were decreased more by CUPP treatment compared to those in the normal group (Figures 2 and 3). Moreover,

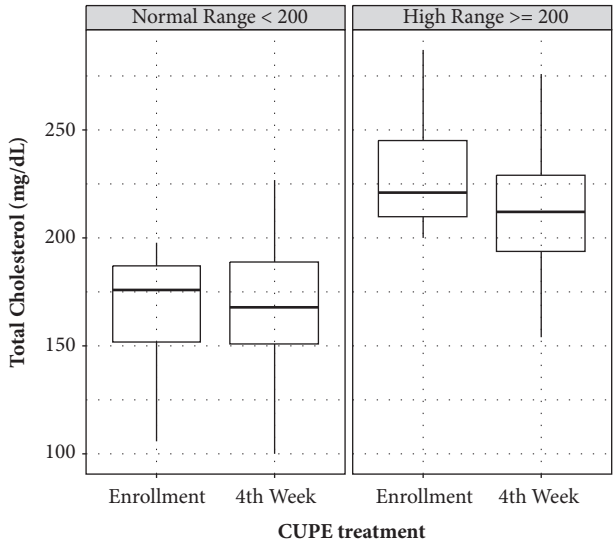

Figure 2: Total cholesterol changes in subjects with normal range (< 200 mg/dL) and abnormal range (≥ 200 mg/dL) of cholesterol before CUPP treatment, showing definite improvement in the abnormal group after treatment.

TC reduction subsequent to CUPP treatment was independent of statin medications (p = 0.797) or weight loss (r = 0.0597, 95% CI: −0.122 to 0.238, p = 0.521, Figure 4), suggesting that CUPP treatment could complement statin with different mechanism of action. AST and ALT levels were also significantly decreased below their normal ranges. This suggests that CUPP treatment is safe for the liver.

Adverse events related to CUPP treatment were not serious. Gastrointestinal discomfort (N = 19, 16.1%), mild diarrhea (N = 8, 6.8%), headache (N = 1, 0.8%), and dizziness (N = 1, 0.8%) were reported which resolved later without any intervention.

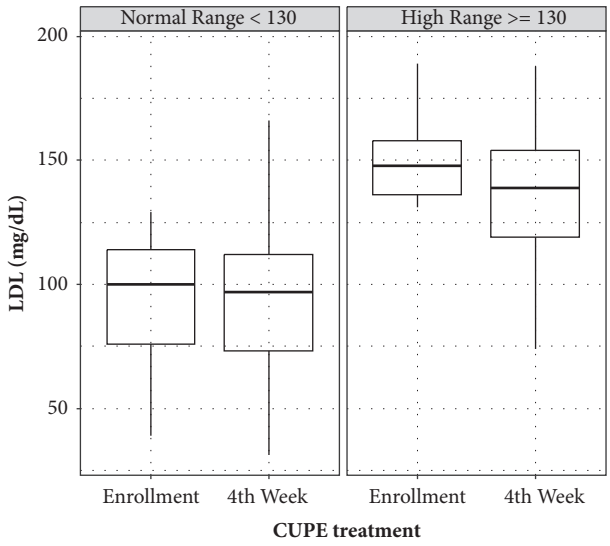

Figure 3: Changes in low-density lipoprotein (LDL) in subjects with normal range (< 130 mg/dL) and abnormal range (≥ 130 mg/dL) of LDL before CUPP treatment, showing definite improvement in the abnormal group after treatment.

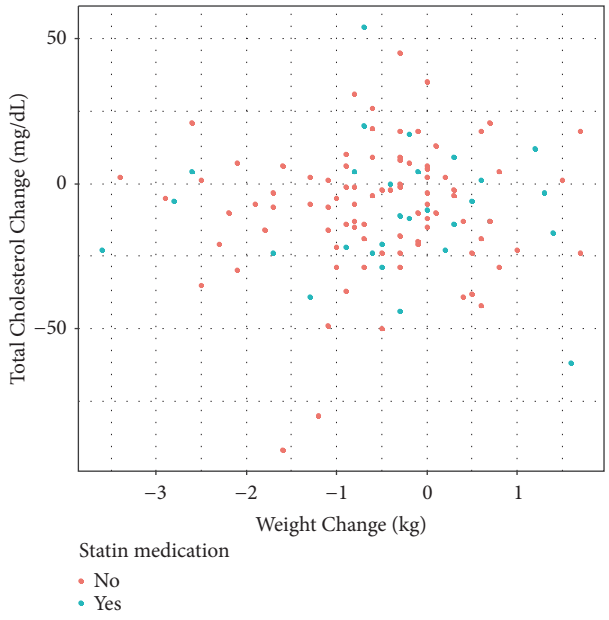

Figure 4: Total cholesterol versus weight change during CUPP treatment based on taking or not taking statin medication (correlation coefficient r = 0.0597, $p = 0.521$).

4. Discussion

Compounds present in CUPP are naririutin, its isomer naringin, hesperidin, and nobiletin. They have been proven to exert antiobesity effects both *in vitro* and *in vivo* [5–8]. Furthermore, these compounds have been found to display strong anti-inflammatory and antioxidant activities [23]. A number of molecular mechanisms particularly underlying lipid metabolism in obesity have been explained [3, 4]. It has been reported that hesperidin possesses inhibitory activity against lipase, resulting in inhibition of fat absorption [6]. Nobiletin can improve obesity and insulin resistance in rats fed a high-fat diet by increasing PPARγ expression or regulating NF-κB and Nrf2 pathways [7, 24]. However, therapeutic uses of these flavonoids are significantly limited due to the lack of adequate clinical evidence.

Peel extracts of *Citrus unshiu* have shown antiobesity effects through inhibition of lipogenesis and adipogenesis in both normal and high-fat diet fed animal models compared to peel extracts of other citrus such as *Citrus aurantium* L. which does not demonstrate any improvement in obesity in normal diet fed mice [17, 20, 25, 26]. The preventive effect of *Citrus unshiu* on atrophy of skeletal muscle and weight loss by suppressing systemic inflammation and production of procachectic factors in tumor-bearing mice has been reported [27]. Our results showed that CUPP has antiobesity effect after 4 weeks of treatment, with 500 grams of reduction in weight of obese subjects. Previous studies on *Citrus unshiu* have shown its antiobesity effect after 9 weeks of administration in high-fat diet fed Sprague-Dawley male rats as well as after 5 or 6 weeks of administration in normal diet fed mouse [17, 20]. Therefore, it has been proposed that the observation period should be longer than 4 weeks to notice sufficient effect of CUPP on weight loss.

Effects of *Citrus unshiu* on lowering cholesterol and TG have been repeatedly confirmed in many preclinical studies [17, 19, 28]. A mixture of naringin and hesperidin can also significantly lower levels of plasma and hepatic cholesterol and TG levels as well as 3-hydroxy-3-methylglutaryl-CoA (HMG-CoA) reductase activity in rats [29]. However, in human studies, citrus flavonoids such as naringin (500 mg/day) or hesperidin (800 mg/day) did not exhibit any lipid-lowering activity on TC, LDL cholesterol, or TG levels after 4 weeks of administration in moderately hypercholesterolemic individuals [11]. Another clinical study has demonstrated that peel extract of *Citrus unshiu* could significantly suppress elevated TG level, but not TC level [21]. Our study showed that CUPP administration for only 4 weeks significantly decreased TC, LDL cholesterol, and TG concentrations in plasma. The lipid-lowering mechanism of *Citrus unshiu* is suggested as follows. Reduced hepatic steatosis along with increased hepatic insulin sensitivity and fatty acid oxidation can promote apolipoprotein B degradation, thereby contributing to lowering the secretion of LDL and LDL particle and circulating cholesterol level [3]. The beneficial effect of *Citrus unshiu* is associated with 5′-adenosine monophosphate-activated protein kinase activation in adipose tissue [30]. Additionally, *Citrus unshiu* could change microbiota in the colon. The white part of the peel from *Citrus unshiu* can decrease serum TG due to increased levels of bifidobacteria in rat cecum [31].

Our study population was chiefly middle-aged women experiencing estrogen hormone changes at menopause, a condition well known to be associated with obesity and hyperlipidemia [32]. The peel of *Citrus unshiu* can significantly lower TC and TG concentrations in the liver of ovariectomized rats showing obvious lipid metabolic disturbance [28]. Therefore, it was hypothesized that CUPP could be

more beneficial for individuals with dyslipidemia and those who were suffering from a reduction in estrogen levels. In our study, lipid-lowering effect of CUPP treatment was independent of weight loss or statin medications. Therefore, CUPP could help the condition of dyslipidemia in individuals with lean body mass or in patients whose lipid levels remain uncontrolled even by statin medication. CUPP treatment is tolerable with only minor nonhematologic adverse effects including gastrointestinal discomfort (16.1%) and mild diarrhea (6.8%). In some cases, improvement in constipation was observed. It could be explained by increased gastrointestinal motility by CUPP based on a preclinical study [14]. None of our patients discontinued CUPP treatment due to CUPP-related adverse events.

This study has several limitations that should be considered. Firstly, this study was planned as part of a health promotion program at a Public Health Center, not for clinical trial. Thus, the absence of a control group to make a comparison led to careful interpretation of results. However, most of enrolled subjects had failed in weight loss in spite of a variety of weight management programs including exercise, diet, and behavior modification previously provided by the Public Health Center for more than 6 months. Therefore, the improvement of weight circumference, weight, or total cholesterol without lifestyle changes could be interpreted by the effect of CUPP treatment. Secondly, the observation period was only for 4 weeks, which is relatively short compared to most intervention trials on obesity. If CUPP treatment would be administered for a longer observation period, the effect of weight loss could be even greater. Finally, there was no inquiry of daily intake showing the changes of calorie intake. Therefore, it is difficult to distinguish whether the effect of CUPP treatment is due to a decrease in the amount of diet through loss of appetite or an increase of the basal metabolic rate which were suggested by the mechanism of action in Citrus flavonoids.

In conclusion, this study shows that CUPP treatment is well tolerated in overweight or obese patients for weight control. It can improve lipid levels in those with moderate dyslipidemia either alone or in combination with statin. Therefore, our results encourage further studies on the lipid-lowering effect of CUPP or its flavonoids due to low toxicity and different mechanism of action compared to conventional statin medication. Additional randomized and well-controlled multicenter clinical trials involving large populations are necessary to evaluate the efficacy and safety of CUPP in the treatment of obesity and dyslipidemia.

Data Availability

The data used to support the findings of this study are available at http://jikom.or.kr/.

Conflicts of Interest

The authors declare that they have no conflicts of interest related to this study.

Acknowledgments

This study was supported by the Bio-Synergy Research Project (NRF-2017M3A9C4065964) of the Ministry of Science, ICT and Future Planning through the National Research Foundation and by Jeju Institute of Korean Medicine (JIKM), Republic of Korea.

References

[1] E. A. Finkelstein, J. G. Trogdon, J. W. Cohen, and W. Dietz, "Annual medical spending attributable to obesity: payer- and service-specific estimates," *Health Affairs*, vol. 28, no. 5, pp. w822–w831, 2009.

[2] C. N. Bang and P. M. Okin, "Statin Treatment, New-Onset Diabetes, and Other Adverse Effects: A Systematic Review," *Current Cardiology Reports*, vol. 16, no. 3, 2014.

[3] J. M. Assini, E. E. Mulvihill, and M. W. Huff, "Citrus flavonoids and lipid metabolism," *Current Opinion in Lipidology*, vol. 24, no. 1, pp. 34–40, 2013.

[4] V. M. Nakajima, G. A. Macedo, and J. A. Macedo, "Citrus bioactive phenolics: Role in the obesity treatment," *LWT- Food Science and Technology*, vol. 59, no. 2, pp. 1205–1212, 2014.

[5] M. A. Alam, N. Subhan, M. M. Rahman, S. J. Uddin, H. M. Reza, and S. D. Sarker, "Effect of citrus flavonoids, naringin and naringenin, on metabolic syndrome and their mechanisms of action," *Advances in Nutrition*, vol. 5, no. 4, pp. 404–417, 2014.

[6] K. Kawaguchi, T. Mizuno, K. Aida, and K. Uchino, "Hesperidin as an inhibitor of lipases from porcine pancreas and pseudomonas," *Bioscience, Biotechnology, and Biochemistry*, vol. 61, no. 1, pp. 102–104, 1997.

[7] E. Yoshigai, T. Machida, T. Okuyama et al., "Citrus nobiletin suppresses inducible nitric oxide synthase gene expression in interleukin-1β-treated hepatocytes," *Biochemical and Biophysical Research Communications*, vol. 439, no. 1, pp. 54–59, 2013.

[8] J. Jia, W. Yao, M. Guan et al., "Glucocorticoid dose determines osteocyte cell fate," *The FASEB Journal*, vol. 25, no. 10, pp. 3366–3376, 2011.

[9] S. Haaz, K. R. Fontaine, G. Cutter, N. Limdi, S. Perumean-Chaney, and D. B. Allison, "Citrus aurantium and synephrine alkaloids in the treatment of overweight and obesity: an update," *Obesity Reviews*, vol. 7, no. 1, pp. 79–88, 2006.

[10] S. J. Stohs, H. G. Preuss, and M. Shara, "A review of the human clinical studies involving citrus aurantium (bitter orange) extract and its primary protoalkaloid p-synephrine," *International Journal of Medical Sciences*, vol. 9, no. 7, pp. 527–538, 2012.

[11] I. Demonty, Y. Lin, Y. E. M. P. Zebregs et al., "The citrus flavonoids hesperidin and naringin do not affect serum cholesterol in moderately hypercholesterolemic men and women," *Journal of Nutrition*, vol. 140, no. 9, pp. 1615–1620, 2010.

[12] U. J. Jung, H. J. Kim, J. S. Lee et al., "Naringin supplementation lowers plasma lipids and enhances erythrocyte antioxidant enzyme activities in hypercholesterolemic subjects," *Clinical Nutrition*, vol. 22, no. 6, pp. 561–568, 2003.

[13] H. Wagner and G. Ulrich-Merzenich, "Synergy research: approaching a new generation of phytopharmaceuticals," *Phytomedicine*, vol. 16, no. 2-3, pp. 97–110, 2009.

[14] J. H. Lyu and H.-T. Lee, "Effects of dried Citrus unshiu peels on gastrointestinal motility in rodents," *Archives of Pharmacal Research*, vol. 36, no. 5, pp. 641–648, 2013.

[15] J. Seo, H. Lim, Y.-H. Chang et al., "Effects of jeju citrus unshiu peel extracts before and after bioconversion with cytolase on anti-inflammatory activity in RAW264.7 cells," *Journal of the Korean Society of Food Science and Nutrition*, vol. 44, no. 3, pp. 331–337, 2015.

[16] S. Lee, S. Suh, K. Lee, J. Yang, S. Choi, and S. Park, "Anti-Inflammatory Effect of Peel Extracts from Citrus Fruits," *Journal of Food Hygiene and Safety*, vol. 28, no. 4, pp. 342–348, 2013.

[17] S. Jung, *Anti-obesity effect of Citrus unshiu peel in rats fed a high-fat diet*, Graduate School, Kyung Hee University, Seoul, South Korea, 2013.

[18] G. N. Kim, M. R. Shin, S. H. Shin et al., "Study of Antiobesity Effect through Inhibition of Pancreatic Lipase Activity of Diospyros kaki Fruit and Citrus unshiu Peel," *BioMed Research International*, vol. 2016, Article ID 1723042, 7 pages, 2016.

[19] H. Lim, E. Yeo, E. Song et al., "Bioconversion of Citrus unshiu peel extracts with cytolase suppresses adipogenic activity in 3T3-L1 cells," *Nutrition Research and Practice*, vol. 9, no. 6, pp. 599–605, 2015.

[20] H.-J. Park, U. J. Jung, S.-J. Cho, H.-K. Jung, S. Shim, and M.-S. Choi, "Citrus unshiu peel extract ameliorates hyperglycemia and hepatic steatosis by altering inflammation and hepatic glucose- and lipid-regulating enzymes in db/db mice," *The Journal of Nutritional Biochemistry*, vol. 24, no. 2, pp. 419–427, 2013.

[21] H. Fritzsch, "Composite weak bosons, leptons and quarks," *Modern Physics Letters A*, vol. 26, no. 31, pp. 2305–2312, 2011.

[22] R. C. Weisell, "Body mass index as an indicator of obesity," *Asia Pacific Journal of Clinical Nutrition*, vol. 11, no. s8, pp. S681–S684, 2002.

[23] X.-M. Chen, A. R. Tait, and D. D. Kitts, "Flavonoid composition of orange peel and its association with antioxidant and anti-inflammatory activities," *Food Chemistry*, vol. 218, pp. 15–21, 2017.

[24] Y.-S. Lee, B.-Y. Cha, S.-S. Choi et al., "Nobiletin improves obesity and insulin resistance in high-fat diet-induced obese mice," *The Journal of Nutritional Biochemistry*, vol. 24, no. 1, pp. 156–162, 2013.

[25] M. D. Arbo, G. C. Schmitt, M. F. Limberger et al., "Subchronic toxicity of Citrus aurantium L. (Rutaceae) extract and p-synephrine in mice," *Regulatory Toxicology and Pharmacology*, vol. 54, no. 2, pp. 114–117, 2009.

[26] G. Yang, J. Lee, E.-D. Jung, I. Ham, and H.-Y. Choi, "Lipid lowering activity of Citri unshii pericarpium in hyperlipemic rats," *Immunopharmacology and Immunotoxicology*, vol. 30, no. 4, pp. 783–791, 2008.

[27] A. Kim, M. Im, M. J. Gu, and J. Y. Ma, "Citrus unshiu peel extract alleviates cancer-induced weight loss in mice bearing CT-26 adenocarcinoma," *Scientific Reports*, vol. 6, Article ID 24214, 2016.

[28] D. W. Lim, Y. Lee, and Y. T. Kim, "Preventive effects of citrus unshiu peel extracts on bone and lipid metabolism in OVX rats," *Molecules*, vol. 19, no. 1, pp. 783–794, 2014.

[29] S.-H. Bok, S.-H. Lee, Y.-B. Park et al., "Plasma and hepatic cholesterol and hepatic activities of 3-hydroxy-3- methyl-glutaryl-CoA reductase and acyl CoA: cholesterol transferase are lower in rats fed citrus peel extract or a mixture of citrus bioflavonoids," *Journal of Nutrition*, vol. 129, no. 6, pp. 1182–1185, 1999.

[30] M. Z. Karagozlu, M. Kim, and M. Lee, "Citrus Peel Ethanol Extract Inhibits the Adipogenesis Caused from High Fat-Induced DIO Model," *Journal of Food and Nutrition Sciences*, vol. 07, no. 01, pp. 8–19, 2016.

[31] E. Iwata, H. Hotta, and M. Goto, "Hypolipidemic and bifidogenic potentials in the dietary fiber prepared from Mikan (Japanese mandarin orange: Citrus unshiu) albedo," *Journal of Nutritional Science and Vitaminology*, vol. 58, no. 3, pp. 175–180, 2012.

[32] H. N. Polotsky and A. J. Polotsky, "Metabolic implications of menopause," *Seminars in Reproductive Medicine*, vol. 28, no. 5, pp. 426–434, 2010.

Hindawi
Evidence-Based Complementary and Alternative Medicine
Volume 2018, Article ID 3248521, 22 pages
https://doi.org/10.1155/2018/3248521

Research Article

Comparative Proteomic Analysis of Two Differently Extracted Coptis chinensis in the Treatment of Type 2 Diabetic Rats

Xin Qiu,[1] Xinyu Wei,[2] Hongwei Guan,[1] Hao Su,[1] Jing Gong,[1] Ke Fang,[3] Xin Zou,[1] Hui Dong,[1] Lijun Xu,[1] and Fuer Lu[1]

[1]*Institute of Integrated Traditional Chinese and Western Medicine, Tongji Hospital, Tongji Medical College, Huazhong University of Science and Technology, Wuhan 430030, China*
[2]*Accounting Department, Lowa State University, Lowa State 50011, USA*
[3]*Department of Integrated Traditional Chinese and Western Medicine, Tongji Hospital, Tongji Medical College, Huazhong University of Science and Technology, Wuhan 430030, China*

Correspondence should be addressed to Fuer Lu; felu@tjh.tjmu.edu.cn

Received 21 March 2018; Revised 8 August 2018; Accepted 16 August 2018; Published 13 September 2018

Academic Editor: Akhilesh K. Tamrakar

Coptis chinensis (CC) is widely used to treat diabetes in traditional Chinese medicine due to its significant hypoglycemic and hypolipidemic effects. It was reported that CC powders are more effective than CC decoctions. In this study, a rat model of type 2 diabetes was established and treated with supercritical-extracted CC and gastric juice extracted CC, respectively. Body weight, fasting plasma insulin, insulin resistance index, and lipid profiles were measured along with oral glucose tolerance tests (OGTTs). In addition, the levels of plasma proteins were compared between type 2 diabetic rats and CC-treated rats using an iTRAQ-based quantitative proteomic analysis. The results showed that the plasma levels of triglyceride (TC), total cholesterol (TG), and low-density lipoprotein (LDL) in rats of both CC-treated groups were significantly decreased. In addition, the proteomic analysis identified 929 proteins, while 15 proteins were selected from these 929 proteins based on their expression levels and bioinformatic results. Among these 15 proteins, 9 proteins (IGF-1, Igfbp4, Igfbp-6, Igfals, C2, C4, Cfi, Prdx-2, and Prdx-3) were upregulated in the two CC-treated groups, while 6 proteins (Pla2g7, Pcyox1, ApoC-1, ApoC-3, ApoB-100, and ApoE) were downregulated. The functions of these proteins are associated with glucose metabolism, insulin action, immunity, inflammation, lipid metabolism, oxidation, and antioxidation. The two differently extracted CC did not show significant differences in terms of their treatment efficacy. This research expanded our understanding on the therapeutic effects and mechanisms of CC in the treatment of type 2 diabetes.

1. Introduction

The number of diabetic patients in the past 35 years has increased by four times. It was estimated that the global incidence of diabetes was about 9% in 2014 [1]. In China, the incidence of adult diabetes reached 11.6% and the rate of prediabetes was 50.1%. However, only 25.8% of diabetics received hypoglycemic treatment, and only 39.7% of treated diabetics achieved successful glucose control [2]. It has been reported that poor control of blood glucose led to the deaths of 370 million diabetics in 2012 [3]. High mortality of diabetes has become a global health problem and puts a huge economic burden on the world population, urging researchers to clarify the pathogenesis of diabetes using advanced techniques.

Proteomic technologies are large-scale research tools that can provide abundant data regarding the pattern of protein expression and are widely used to explore the molecular mechanisms underlying the function of complex bioactive mixtures, including traditional Chinese medicine (TCM). Recently, a new method, isobaric tags for relative and absolute quantity (iTRAQ), has been used to simultaneously measure protein content in multiple test samples. As an automatic, multidimensional, and more sensitive tool, iTRAQ labeling

coupled with liquid-phase secondary mass spectrometry (LC-MS/MS) is more suitable for the study of pathogenic mechanisms and pathophysiology of diseases [4, 5].

Coptis chinensis (CC, Huanglian in Chinese) has been used to treat diabetes for thousands of years in China. The main components of CC are berberine, epiberberine, coptisine, palmatine, ferulic acid, and berberrubine (Figure 1) [6]. Berberine has been proved to reduce insulin resistance and promote insulin secretion [7]; epiberberine, coptisine, and palmatine exert a strong effect on aldose reductase inhibition [8]; jatrorrhizine and ferulic acid [9, 10] also play a certain hypoglycemic and lipid-regulating role. All above components might contribute to the effect of CC in the treatment of type 2 diabetes mellitus (T2DM). In addition, evidence has shown that CC powders have better pharmacokinetic properties than CC decoctions. For example, our previous work showed that, as compared with a CC decoction, CC powders demonstrated higher bioavailability, slower in vivo elimination, and better absorption and distribution profiles [11]. CC powders also exert excellent hypoglycemic and lipid-lowering effects [12]. However, the mechanisms underlying the functions of CC and its molecular targets in the treatment of T2DM remain unclear.

In this study, the iTRAQ technology was used to compare the effect of CC obtained by two different extracted methods in the treatment of diabetic rats. In addition, differentially expressed proteins in the plasma of diabetic rats and CC-treated rats were identified using a proteomic technology. At the same time, the potential pathways of these proteins implicated in the pathogenesis of T2DM were elucidated using pathway and network analyses.

2. Materials and Method

2.1. Substances. Dried rhizoma of CC was purchased from Hubei Herbal Medicine Company (Wuhan, China) and was identified by Prof. Zhang Xiu-Qiao from Hubei University of Chinese Medicine as Coptis chinensis Franch, which was called "Wei Lian" in Chinese. The purchased CC was ground into powders and kept in a desiccator at ambient temperature. In order to obtain homogenous powders, the dried powders were filtered through a sieve of 450 ± 20 μm meshes.

Supercritical extraction of CC was carried out as follows: 200 g of CC powder was placed into an extraction kettle (HA221-40-11-C supercritical fluid extractor, Nantong, China). The extraction conditions were as follows: extraction time, 5 min of static extraction followed by up to 2 h of dynamic extraction; temperature, 50°C; pressure, 200 Mpa; entrainer, 300 ml of 90% methanol; flow rate of carbon dioxide (gaseous state), 30 L/h; temperature or extraction and separation: 45°C. With the 200 g input, about 11.59 g of dried powder was extracted and stored in a refrigerator at 4°C before use.

Gastric juice extracted CC was prepared as follows: 20 g of CC powder was mixed with an artificial gastric juice (pH 1.2, obtained by dissolving 2.0 g of sodium chloride in 7.0 mL of hydrochloric acid and further diluted with water to a final volume of 1,000 mL [13]) for 30 min at 37°C. Subsequently, the mixture was filtered twice and the filtrate was combined. After being evaporated in a rotary evaporator and freeze-dried, about 4.00 g of extract were obtained and stored at 4°C for subsequent use.

2.2. Animals, Groups, and Intervention. Male Wistar rats with a weight of between 190 and 210 g were purchased from WeiTongLiHua Co., Ltd, and housed in SPF Grade facilities in the experimental animal center of Huazhong University of Science and Technology (SCXK (Jing)2012-0001). After 10 days of acclimatization, the rats were randomly divided into a normal group (N group) and a high glucose fatty diet group (HGFD group). The rats in the N group was fed with a standard diet (containing 35% flour, 20% corn meal, 20% soy meal, 15.5% bran, 5% fish meal, 1% dusty yeast, 0.5% bean oil, 2.5% bone meal, and 0.5% salt), while the diet in the HGFD group contained 67.5% of the standard diet, 12% lard, 2% cholesterol, 0.5% bile salts, and 20% sugar. The dietary regimens of the rats in different groups were maintained the same throughout the entire experiment. Forty days later, each rat in the HGFD group received an intravenous injection of 24 mg/kg streptozotocin (STZ) [14]. Subsequently, the normal 95% confidence intervals (CIs) at various time points of the oral glucose tolerance test (OGTT) were calculated based on the blood glucose level of the rats in the N group. If the blood glucose was greater than 20% of the upper limit of CI at any time point, the rats were considered as successfully modeled diabetic rats. These diabetic rats were then randomly divided into a model group (M group) and different treatment groups, with 15 rats in each group. All experiments were approved by the animal ethics committee of Huazhong University of Science and Technology (No. 2016S615).

The treatment groups included a group treated by CC obtained using supercritical extraction (A group), a group treated by CC obtained using artificial gastric juice extraction (B group), and a group treated by metformin (D group). All test compounds were dissolved in a 1: 1 oil-water mixture. CC obtained using supercritical extraction was administered in the A group at a dose of 85mg/kg/day. CC obtained using artificial gastric juice extraction was administered in the B group at a dose of 333 mg/kg/day [15]. In the D group, the daily dose of metformin was 184 mg/kg. Daily lavage volume of each rat was 1 ml/100 g body weight, and the solution concentration was calculated according to the lavage volume. In addition, a 1:1 mixture of oil and water was given to the rats in N and M groups via intragastric administration. The doses of gastric irrigation were given for 9 weeks and adjusted weekly based on the weight of the rats.

2.3. OGTT, Plasma Lipid, and Insulin Measurement. After the interventions were carried out, all rats were subjected to OGTT. During OGTT, the rats were fasted for 12 h before 2 g/kg of glucose was administrated. Tail vein blood samples were collected from each rat at 0, 60, and 120 min after the intragastric administration to detect the blood glucose levels using a glucose monitor (Roche, German).

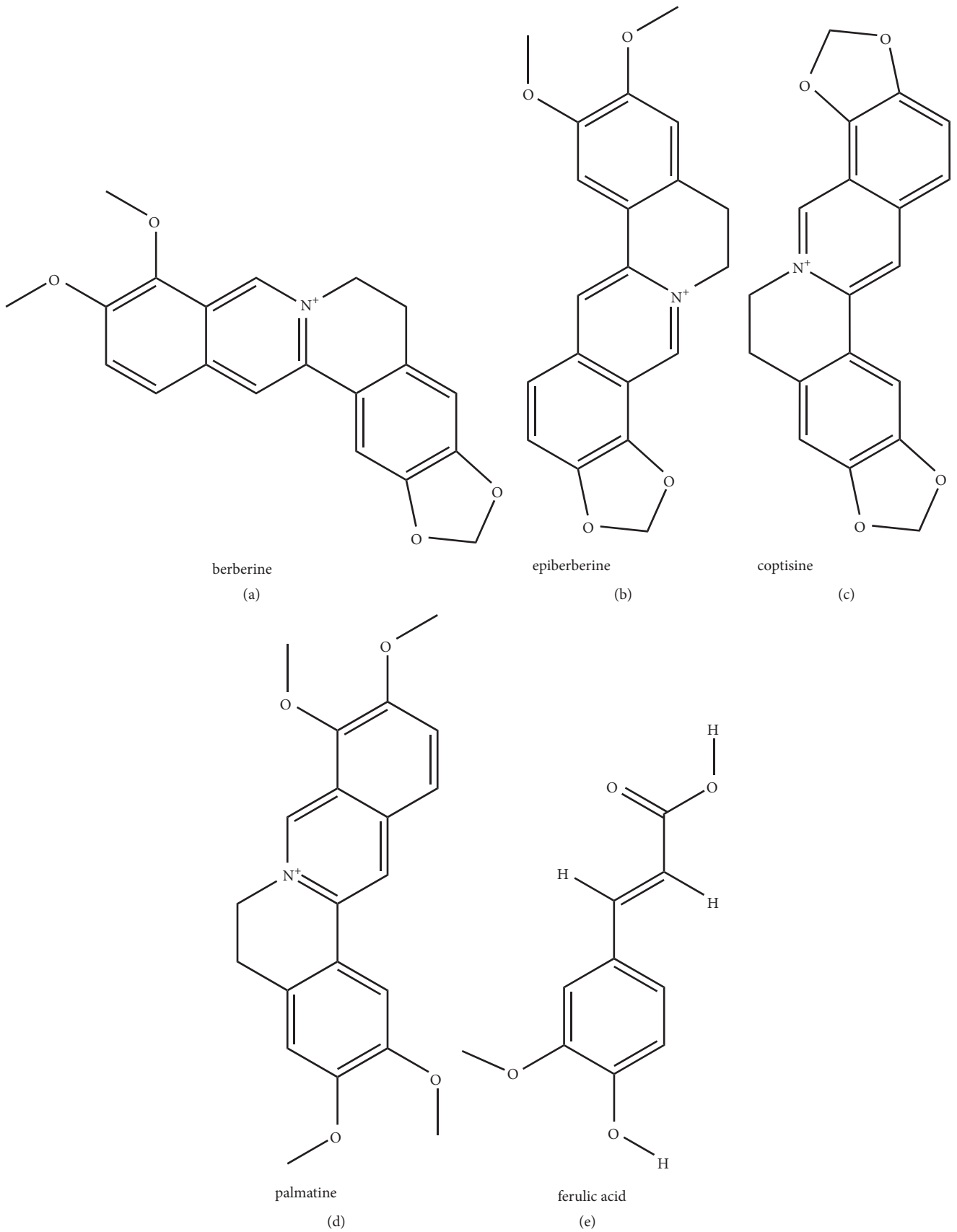

Figure 1: **The main component of Coptis chinensis: (a)** berberine; **(b)** epiberberine; **(c)** coptisine; **(d)** palmatine; **(e)** ferulic acid.

After the experiment was completed, all animals were anesthetized by intraperitoneal injection of 50 mg/kg pentobarbital sodium. Abdominal aorta blood samples were then collected using heparin sodium anticoagulant tubes. Subsequently, the blood samples were centrifuged at 3000 rpm for 10 min to separate plasma. A part of the separated plasma was used to measure the levels of lipids, while the remaining part of the separated plasma was rapidly frozen under liquid nitrogen and stored at −80°C for proteomic analysis.

The concentration of plasma insulin was measured using a Rat/Mouse Insulin ELISA kit (Millipore, German). For the detection of triglyceride (TG) content and total cholesterol (T-CHO), a colorimetric assay (Jiancheng, Nanjing, China) was used. A double reagent direct method (Jiancheng, Nanjing, China) was used to detect the level of low-density lipoprotein (LDL).

2.4. Protein Extraction, Digestion, and iTRAQ Labeling. The plasma samples were transferred into 5-mL centrifuge tubes, which were then centrifuged at 12,000 g and 4°C for 10 min to collect the supernatant. Subsequently, the samples were processed by a ProteoMiner™ Protein Enrichment Small-Capacity Kit (Bio-Rad, US) to enrich low abundance proteins. Finally, the protein concentration was determined with a BCA kit (Biyuntian, China) according to the manufacturer's instructions.

For digestion, the protein solution was reduced with 5 mM dithiothreitol for 30 min at 56°C and alkylated with 11 mM iodoacetamide for 15 min at room temperature away from light. Each protein sample was then diluted by 100 mM TEAB until the urea concentration was less than 2M. Finally, trypsin was added to the samples at a 1:50 trypsin-to-protein mass ratio and incubated overnight to carry out the first digestion, followed by another 4 h digestion using a 1:100 trypsin-to-protein mass ratio.

After trypsin digestion, peptides were desalted by a Strata X C18 SPE column (Phenomenex), vacuum-dried, reconstituted in 0.5 M TEAB, and processed with an iTRAQ kit according to the manufacturer's protocol. In brief, one unit of iTRAQ reagent was thawed and reconstituted in acetonitrile. The peptide mixtures were then incubated with the iTRAQ reagent for 2 h at room temperature, pooled, desalted, and dried by vacuum centrifugation.

2.5. HPLC Fractionation. The tryptic peptides were fractionated into fractions by high pH reverse-phase HPLC using an Agilent 300Extend C18 column (5 μm particles, 4.6 mm ID, 250 mm length). In brief, peptides were initially separated into 60 fractions over 60 min with 8% to 32% gradient acetonitrile (pH 9.0). Subsequently, the peptides were combined into 18 fractions and dried by vacuum centrifugation.

2.6. LC-MS/MS Analysis. The tryptic peptides were dissolved in 0.1% formic acid (solvent A) and then directly loaded onto a homemade reversed-phase analytical column (15-cm length, 75 μm ID). The gradient elution included an increase from 6% to 23% of solvent B (0.1% formic acid in 98% acetonitrile) over 26 min, followed by an increase from 23% to 35% of solvent B in 8 min, an increase to 80% of solvent B in 3 min, and holding at 80% of solvent B for 3 min. All elution was carried out at a constant flow rate of 400 nL/min on an EASY-nLC 1000 UPLC system.

The peptides were ionized by an NSI source and analyzed online by Q ExactiveTM Plus (Thermo) tandem mass spectrometry (MS/MS) coupled to UPLC. The electrospray voltage was 2.0 kV. The m/z scan range was 350 to 1800 for full scan, and intact peptides were detected in the Orbitrap at a resolution of 70,000. Peptides were subsequently selected for MS/MS using an NCE setting of 28, and the fragments were detected in the Orbitrap at a resolution of 17,500. A data-dependent procedure was used and contained cycles of one MS scan followed by 20 MS/MS scans with 15.0 s dynamic exclusion. Automatic gain control (AGC) was set at 5E4. Fixed first mass was set as 100 m/z.

2.7. Database Search. The resulting MS/MS data were processed using a Maxquant search engine (v.1.5.2.8). Tandem mass spectra were searched against the UniprotKB Rattus norvegicus database, which covered 35842 of protein sequences concatenated with reverse decoy database. Trypsin/P was specified as the cleavage enzyme and up to 2 missing cleavages were allowed. The range of the initial search was set to 5 ppm for precursor ions, while the range of the primary search was set to 5 ppm and 0.02 Da for fragment ions. Carbamidomethyl on Cys was specified as fixed modification, while the oxidation on Met was specified as variable modifications. FDR was adjusted to $< 1\%$ and minimum score for peptides was set to > 40. To evaluate the significant changes in protein expression, cut-off values of $>$ 1.5- or < 0.667-fold changes in protein expression were used.

2.8. Bioinformatics Methods

2.8.1. Annotation Methods

GO Annotation. Gene Ontology (GO) annotation proteome was derived from the UniProt-GOA database (www.http://www.ebi.ac.uk/GOA/). Firstly, each identified protein ID was converted to a UniProt ID and subsequently mapped to a GO ID based on the protein ID. If some identified proteins were not annotated by the UniProt-GOA database, InterProScan software would be used to annotate the GO functions of the proteins using a protein sequence alignment method. Subsequently, the proteins were classified by Gene Ontology annotations based on three categories: biological process, cellular component, and molecular function.

Domain Annotation. Using the InterPro domain database (http://www.ebi.ac.uk/interpro/), a freely accessible database that integrates diverse information about protein families, domains, and functional sites, the domain functional descriptions of identified proteins were annotated by InterProScan (a sequence analysis tool) based on a protein sequence alignment method. The key elements of the InterPro domain

database are diagnostic models, known as signatures, against which protein sequences can be mapped to determine their potential functions. InterPro has been used in the large-scale analysis of whole genomes and metagenomes, as well as in characterizing individual protein sequences.

KEGG Pathway Annotation. Kyoto Encyclopedia of Genes and Genomes (KEGG) database was used to annotate protein pathways. Firstly, using KAAS, a KEGG online service tool, the KEGG database description of the proteins was annotated. Subsequently, the annotation results were mapped to the KEGG pathway database using KEGG mapper, a KEGG online service tool.

2.8.2. Functional Enrichment

Enrichment of Gene Ontology. Proteins were classified by GO annotation into three categories: biological process, cellular compartment, and molecular function. For each category, a two-tailed Fisher's exact test was employed to test the enrichment of the differentially expressed protein against all identified proteins. The GO with a corrected p value of < 0.05 was considered significant.

Enrichment of Pathways. Encyclopedia of Genes and Genomes (KEGG) database was used to identify enriched pathways by a two-tailed Fisher's exact test, so that the enrichment of differentially expressed proteins could be tested against all identified proteins. The pathways with a corrected p value of < 0.05 were considered significant. These pathways were then classified into hierarchical categories according to the instruction on the KEGG website.

Enrichment of Protein Domains. For the proteins in each category, the InterPro (a tool used for the functional analysis of protein sequences by classifying them into families and by predicting the presence of domains and important sites) database was searched and a two-tailed Fisher's exact test was employed to test the enrichment of differentially expressed proteins against all identified proteins. Protein domains with a p value of < 0.05 were considered significant.

2.8.3. Enrichment-Based Clustering. For further hierarchical clustering based on different functional classifications of proteins (such as GO, Domain, Pathway, and Complex), all categories obtained after enrichment were first collated along with their P values and subsequently filtered to select categories which were at least enriched in one of the clusters with a P value of <0.05. This filtered matrix of P values was then transformed using the formula $x = -\log 10$ (P value). Finally, these x values were z-transformed for each functional category and the z scores were subsequently clustered by one-way hierarchical clustering (Euclidean distance, average linkage clustering) in Genesis. Cluster memberships were visualized by a heat map using the "heatmap.2" function in the "gplots" R-package.

2.9. Statistical Analysis. Statistical analyses were performed with GraphPad Prism version 5.01 (GraphPad Software, Inc., San Diego, CA, USA). The variables in each group were tested to determine if they were normally distributed. Analysis of variance was used for the comparisons of sample means among multiple groups. The SNK method was used for pairwise comparison. $P < 0.05$ was considered to be significant.

3. Results

3.1. CC Decreases Plasma Glucose and Lipid in Diabetic Rats. Consistent with a previous study, diabetic rats showed weight loss, abnormal OGTT results, an elevated plasma lipid level, and a reduced concentration of fasting plasma insulin [16]. CC intervention did not significantly increase body weight and fasting concentration of plasma insulin. However, CC reversed elevated levels of fasting and postprandial blood glucose, plasma TG, and T-CHO in diabetic rats. Furthermore, CC decreased insulin resistance index (IRI) as well as LDL in diabetic rats. Among the above indicators, there were no significant differences between the two extracted CC. These data indicated that CC exerted beneficial effects on metabolic parameters (Figure 2).

3.2. Comparative Analysis of Plasma Proteomic Changes in Each Group. This study measured a total of 929 proteins, of which 789 proteins produced quantitative information. In this study, more than 1.5 times increase in protein expression was considered as a significant increase, while a reduction in protein expression to a level less than 0.67 of the normal level was considered as a significant reduction. Subsequently, in the N and M groups, the expression of 115 proteins was upregulated and the expression of 116 proteins was downregulated. In the A and M groups, the expression of 101 proteins was upregulated and the expression of 59 proteins was downregulated. In both N and M groups, the expression of 70 proteins was upregulated and the expression of 58 proteins was downregulated. In both B and M groups, the expression of 109 proteins was upregulated and the expression of 71 proteins was downregulated (Table 1).

3.3. Functional Classification and Functional Enrichment of GO Annotation. Based on the above data, a bioinformatics analysis of proteins containing quantitative information, including protein annotation, functional classification, and functional enrichment, was carried out systematically.

3.3.1. N versus M Group. Differentially expressed proteins in the N and M groups were categorized based on the results of GO enrichment analysis. In terms of biological processes, 14% of the proteins with elevated expression were related to each of the "biological regulation", "single-organism process", "response to stimulus", and "cellular process" (Figure 3(a)), while each of "cellular process" and "metabolic process" involved 15% of the proteins with decreased expression. Around 13% of the proteins with decreased expression were related to "single-organism process" (Figure 3(b)). In terms of cellular components, 32% and 21% of the proteins with elevated expression were related to the extracellular region

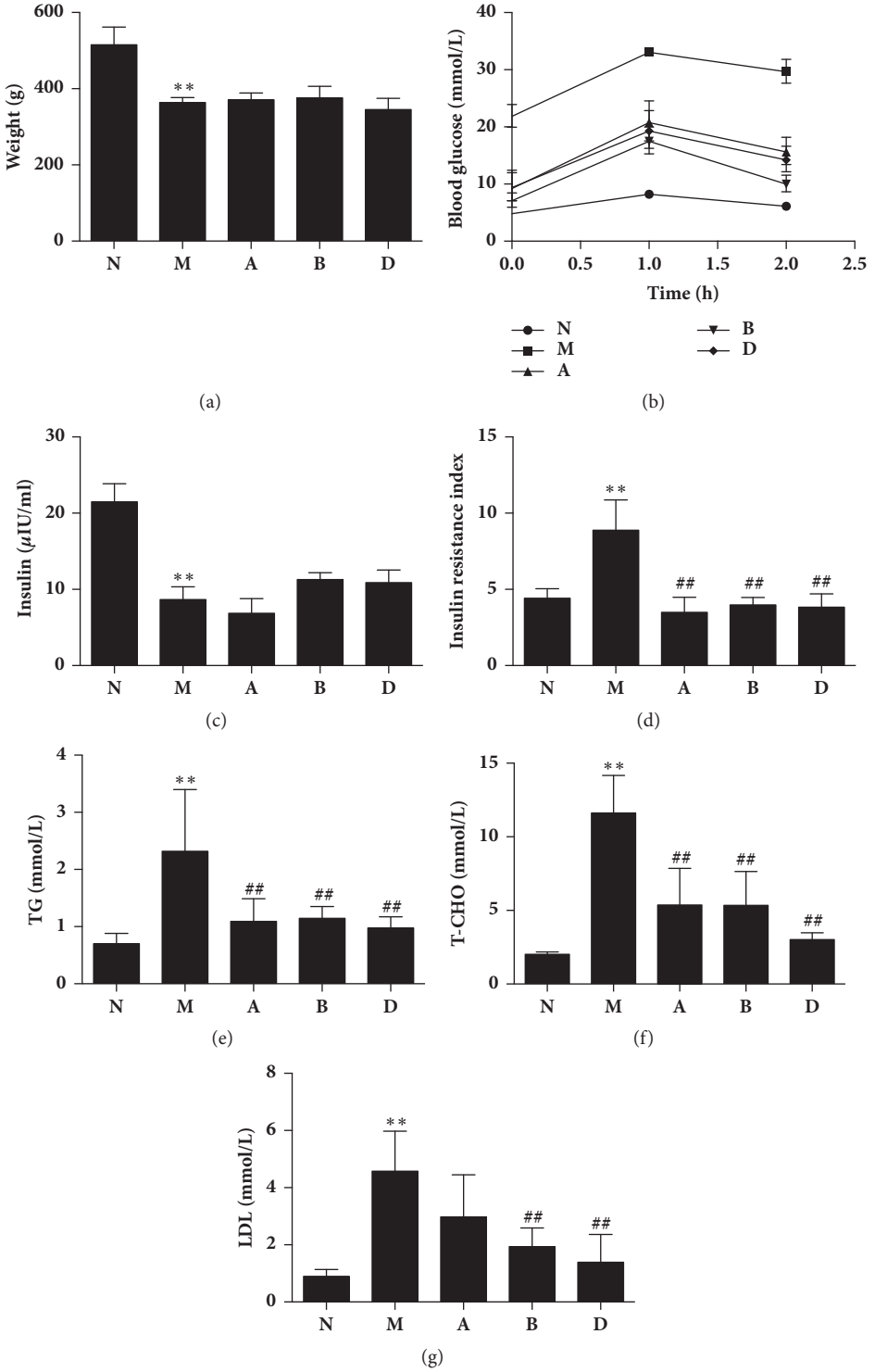

FIGURE 2: **Coptis chinensis (CC) is effective in decreasing plasma glucose and lipid. (a)** Body weight of rats in each group; **(b)** OGTT of rats after oral gavage with 2.0 g / kg glucose. Data is expressed as mean ± SE. P <0.01 for each of the N versus M, A versus M, B versus M, and D versus M group at each time point; **(c)** plasma insulin concentration in the rat; **(d)** IRI after treatment; **(e)** plasma TG concentration; **(f)** plasma T-CHO concentration; **(g)** plasma LDL concentration. N: normal control group; M: diabetic model group; A: supercritical extraction of Coptis chinensis group; B: simulated gastric juice extraction of Coptis chinensis group; D: metformin treatment group; mean ± SD of data except OGTT. n=6 rats in each group. **P <0.01 relative to group N, $^{\#\#}$P <0.01 relative to group M.

Table 1: Differentially expressed protein summary (P value < 0.05).

Compared sample name	1.5-fold change	
	Upregulated	Downregulated
A/M	101	59
B/M	109	71
D/M	93	128
N/M	115	116
A/B	27	16

and cells, respectively, followed by the proteins involving organelle (20%; Figure 3(c)). Approximately 24% and 22% of the proteins with decreased expression were linked to cell and extracellular region, respectively, followed by the proteins involving organelle (19%; Figure 3(d)). For molecular functions, 54% of the upregulated proteins were associated with binding, followed by the proteins involving catalytic activity (18%; Figure 3(e)). Approximately 50% of the downregulated proteins were associated with binding, while 38% of these proteins were related to catalytic activity (Figure 3(f)). Subsequently, an enrichment analysis of the GO function annotation was performed, and "membrane attack complex", "endopeptidase inhibitor activity", and "negative regulation of peptidase activity" were the most common functions of "cellular component", "molecular function", and "biological process" of upregulated proteins (Figure 4(a)). For the downregulated proteins, "proteasome core complex", "threonine-type endopeptidase activity", and "protein catabolic process" were the most common functions (Figure 4(b)).

3.3.2. A versus M Groups. Differentially expressed proteins in the A and M groups were categorized based on the results of GO enrichment analysis. In terms of biological processes, 14% of upregulated proteins were related to "biological regulation", while 13% were related to each of the "single-organism process", "metabolic process", and "cellular process" (Figure 5(a)). Around 15% of the downregulated proteins were related to each of "cellular process", "single-organism process", and "metabolic process" (Figure 5(b)). In terms of cellular components, 31% and 23% of upregulated proteins were related to the extracellular region and the organelle, respectively, followed by proteins involving cells (22%; Figure 5(c)). Approximately 26% and 21% of the downregulated proteins were linked to extracellular region and organelle, respectively, followed by proteins involving cells (19%; Figure 5(d)). For molecular functions, 47% of the upregulated proteins were associated with binding, followed by proteins involving catalytic activity (25%; Figure 5(e)). Approximately 51% of downregulated proteins were associated with binding, followed by 29% of downregulated proteins related to catalytic activity (Figure 5(f)). Subsequently, the enrichment analysis of GO function annotation was performed, and "membrane attack complex", "endopeptidase inhibitor activity", and "negative regulation of peptidase activity" were the most common functions of "cellular component", "molecular function", and "biological process" of upregulated proteins (Figure 6(a)). For downregulated proteins, "proteasome core complex", "threonine-type endopeptidase activity", and "protein catabolic process" were the most common functions (Figure 6(b)).

3.3.3. B versus M Groups. Differentially expressed proteins in the B and M groups were categorized based on the results of GO enrichment analysis. In terms of biological processes, 14% of upregulated proteins were related to each of "biological regulation", "single-organism process", "metabolic process", and "response to stimulus" (Figure 7(a)). Around 15% of the downregulated proteins were related to each of "cellular process", "metabolic process", and "single-organism process" (Figure 7(b)). In terms of cellular components, 34% and 23% of upregulated proteins were related to the extracellular region and the organelle, respectively, followed by proteins involving cells (20%; Figure 7(c)). Approximately 24% and 22% of downregulated proteins were linked to extracellular region and cells, respectively, followed by proteins involving organelle (19%; Figure 7(d)). For molecular functions, 50% of upregulated proteins were associated with binding, followed by proteins involving catalytic activity (22%; Figure 7(e)). Approximately 51% of downregulated proteins were associated with binding, followed by 36% of downregulated proteins related to catalytic activity (Figure 7(f)). Subsequently, an enrichment analysis of GO function annotation was performed, and "extracellular space", "endopeptidase inhibitor activity", and "negative regulation of peptidase activity" were the most common functions of "cellular component", "molecular function", and "biological process" of upregulated proteins (Figure 8(a)). For downregulated proteins, "proteasome core complex", "threonine-type endopeptidase activity", and "proteolysis involved in cellular protein catabolic process" were the most common functions (Figure 8(b)).

3.3.4. A versus B Groups. Differentially expressed proteins in the A and M groups were categorized based on the results of GO enrichment analysis. In terms of biological processes, 15% of upregulated proteins were related to each of "metabolic process" and "response to stimulus". 13% of upregulated proteins were related to each of "immune system process", "single-organism process", and "cellular process" (Figure 9(a)). Around 15% of the downregulated proteins were related to each of "metabolic process" and "single-organism process". Around 13% of the downregulated proteins were related to each of "cellular process" and "biological regulation" (Figure 9(b)). In terms of cellular components, 31% and 19% of upregulated proteins were

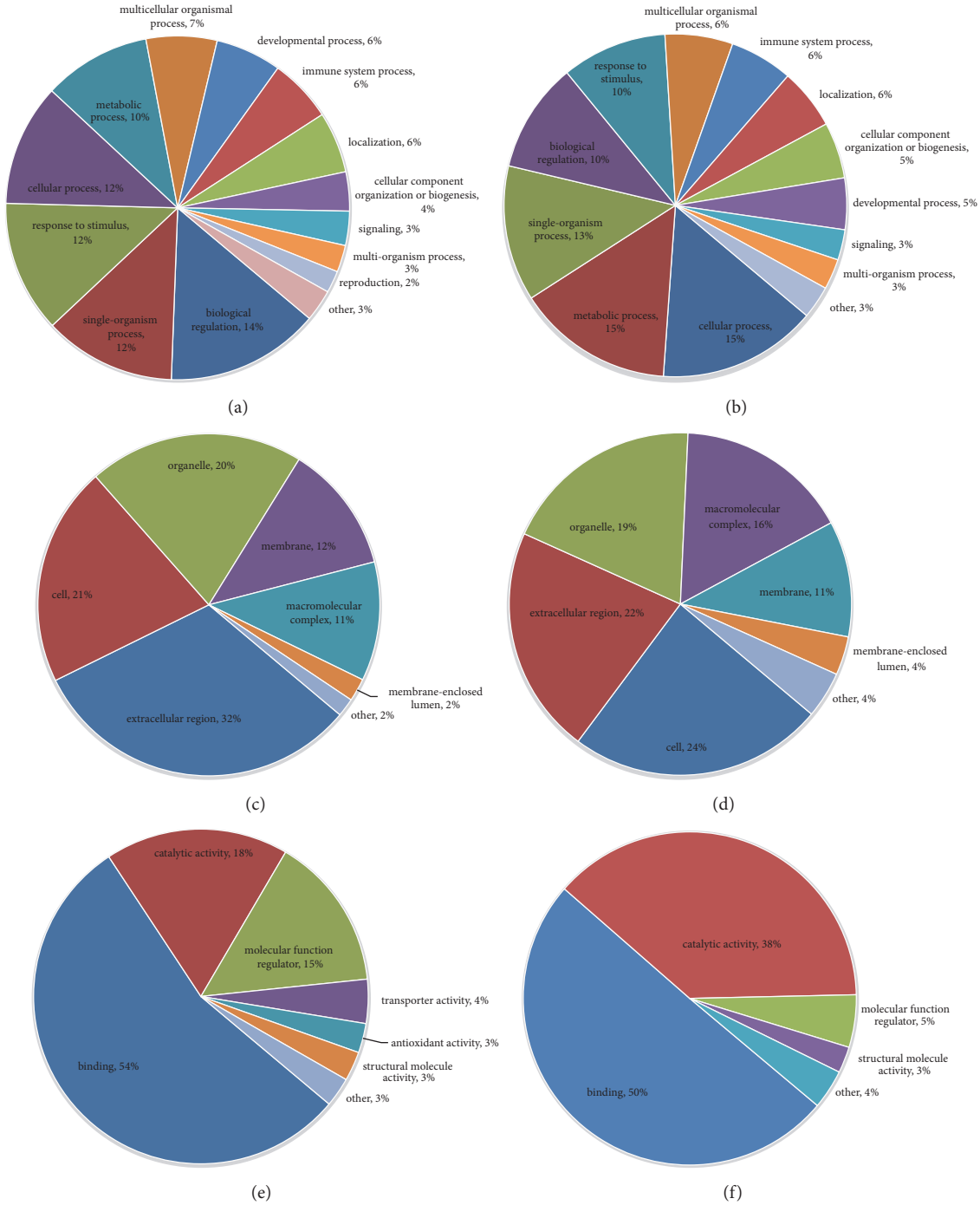

Figure 3: **Normal group versus model group (N versus M) Go analysis information. (a)** Biological process: upregulated proteins: the response to biological regulation (14%) was the major component. **(b)** Biological process: downregulated proteins: the responses to cellular processes (15%) and metabolic processes (15%) were the dominant features. **(c)** Cellular components: upregulated proteins: extracellular region (32%) formed the main component of the cellular component category. **(d)** Cellular components: downregulated proteins: cell (24%) was the major component. **(e)** Molecular function: upregulated proteins: binding (54%) was the dominant molecular function in the GO assignments. **(f)** Molecular function: downregulated proteins: binding represented 50% of the molecular function.

related to the extracellular region and the organelle, respectively, followed by proteins involving cells (19%; Figure 9(c)). Approximately 28% and 24% of downregulated proteins were linked to extracellular region and cells, respectively, followed by proteins involving organelle (17%; Figure 9(d)). For molecular functions, 59% of upregulated proteins were associated with binding, followed by proteins involving catalytic activity (32%; Figure 9(e)). Approximately 58% of

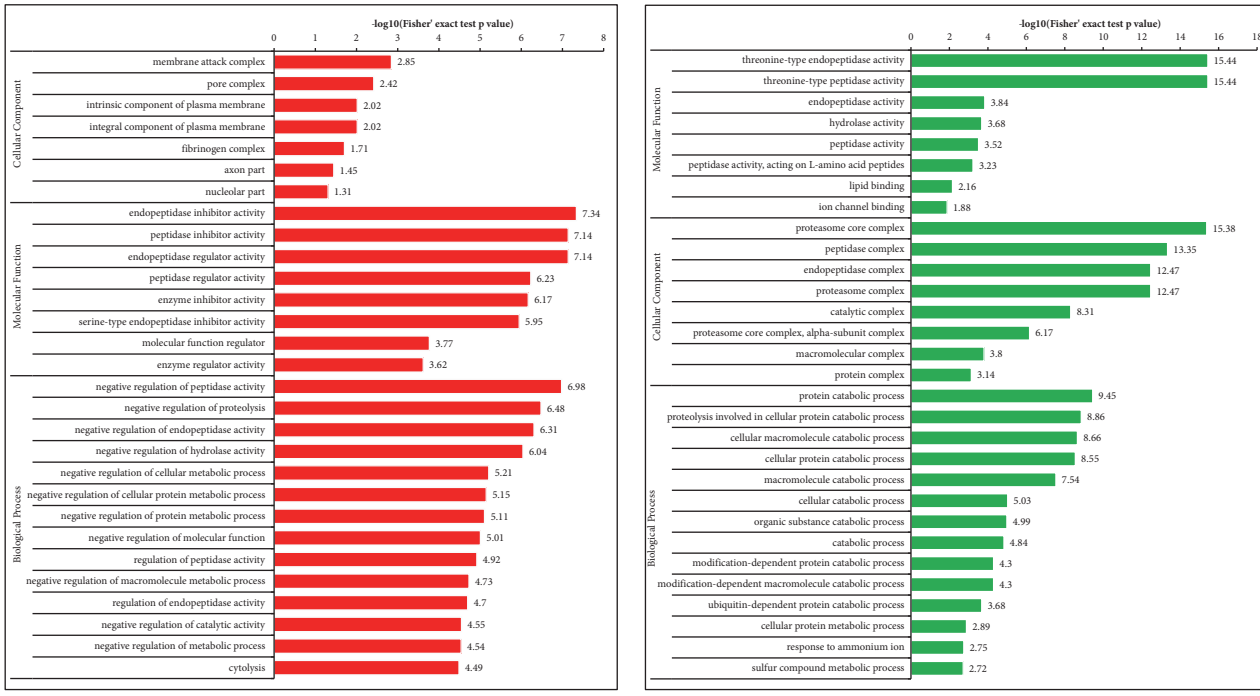

(a) (b)

FIGURE 4: **Enrichment analysis of the GO function annotation of normal versus model group (N versus M). (a)** Upregulated proteins: membrane attack complex, endopeptidase inhibitor activity, and negative regulation of peptidase activity of, respectively, cellular component, molecular function, and biological process were the most representative functions. **(b)** Downregulated proteins: proteasome core complex, threonine-type endopeptidase activity, and protein catabolic process were the most representative functions.

downregulated proteins were associated with binding, followed by 37% of downregulated proteins related to catalytic activity (Figure 9(f)). Subsequently, an enrichment analysis of GO function annotation was performed, and "oxidoreductase activity acting on the CH-CH group of donors", "organelle inner membrane", and "production of molecular mediator of immune response" were the most common functions of "cellular component", "molecular function", and "biological process" of upregulated proteins (Figure 10(a)). For downregulated proteins, "transferase activity" was the most common function of "molecular function", while other downregulated proteins did not produce a valid P value (Figure 10(b)).

3.4. KEGG Pathway Enrichment. In Figure 11, the different protein-enriched KEGG pathways were identified in each group. Differentially expressed proteins in the N and M groups were mapped to multiple pathways in the KEGG database to investigate their biological functions. "Complement and coagulation cascade" was the most common pathway enriched by upregulated proteins, followed by "systemic lupus erythematosus" and "Staphylococcus aureus infection". The downregulated proteins were significantly enriched in the pathways of "proteasome," "protein processing in endoplasmic reticulum", "biosynthesis of amino acids", and "alanine, aspartate and glutamate metabolism". Compared with those in A and M groups, the KEGG pathways enriched by upregulated proteins were similar in N and M groups, while the downregulated proteins in N and M groups were significantly enriched in the pathways of "proteasome," "gap junction," "Alzheimer's disease," and "ether lipid metabolism." Furthermore, in the B and M groups, "complement and coagulation cascade" was the most common pathway enriched by upregulated proteins, followed by "systemic lupus erythematosus" and "Prion diseases", while the pathways in B and M groups enriched by downregulated proteins were similar with those in A and M groups.

3.5. Protein Domain Enrichment. The protein domains refer to some components that repeat in different protein molecules and have similar sequences, structures, and functions. These protein domains are the units of protein evolution. Upregulated proteins in the N group were associated with "Serpin domain," "Serine proteases, trypsin domain," and "Peptidase S1, PA clan", whereas downregulated proteins in the N group were associated with Nucleophile aminohydrolases, N-terminal, Proteasome alpha-subunit, and N-terminal domain. Compared with those in A and M groups, the enriched domains of upregulated proteins in N and M groups were similar, while the downregulated proteins were significantly enriched in domains of "Nucleophile aminohydrolases, N-terminal," "Tubulin/FtsZ, C-terminal," "Tubulin/FtsZ, GTPase domain," "Tubulin/FtsZ, 2-layer sandwich domain," and "Tubulin, C-terminal." Upregulated proteins in the B group were associated with "Serpin domain," "Alpha-2-macroglobulin, N-terminal 2,"

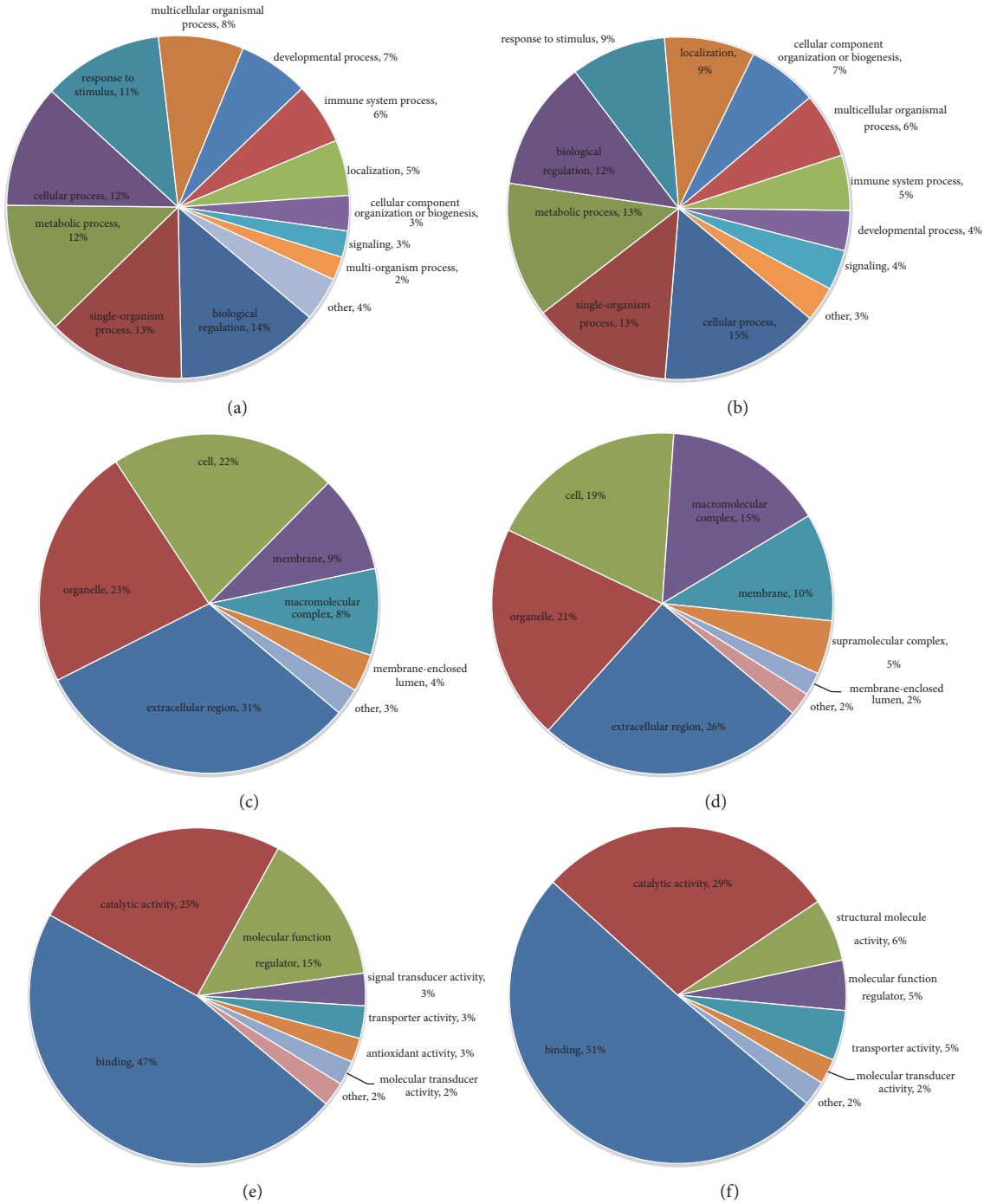

FIGURE 5: **Supercritical extraction of Coptis chinensis treatment group versus model group (A versus M) Go analysis information.** **(a)** Biological process: upregulated proteins: the response to biological regulation (14%) was the major component. **(b)** Biological process: downregulated proteins: the response to cellular processes (15%) was the dominant feature. **(c)** Cellular components: upregulated proteins: extracellular region (31%) formed the main component of the cellular component category. **(d)** Cellular components: downregulated proteins: extracellular region (26%) was the major component. **(e)** Molecular function: upregulated proteins: binding (47%) was the dominant molecular function in the GO assignments. **(f)** Molecular function: downregulated proteins: binding represented 51% of the molecular function.

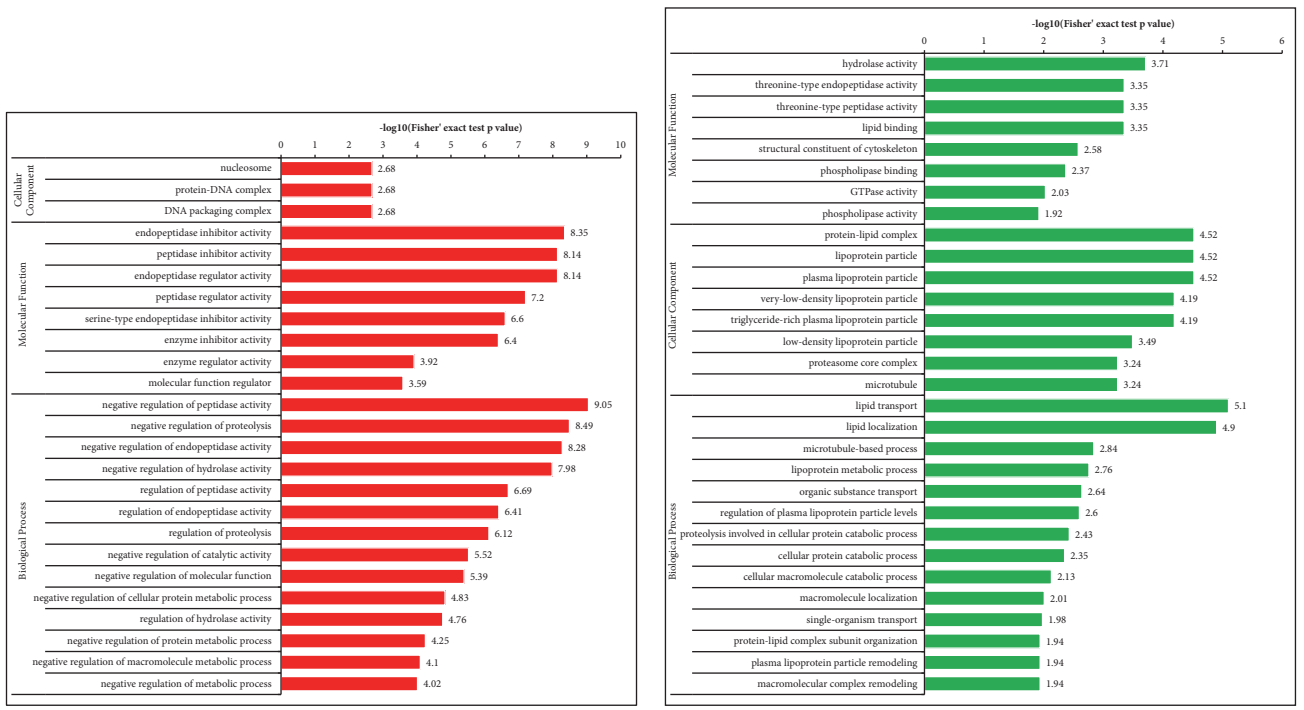

Figure 6: **Enrichment analysis of the GO function annotation of supercritical extraction of Coptis chinensis treatment group versus model group (A versus M). (a)** Upregulated proteins: membrane attack complex, endopeptidase inhibitor activity, and negative regulation of peptidase activity of, respectively, cellular component, molecular function, and biological process were the most representative functions. **(b)** Downregulated proteins: proteasome core complex, threonine-type endopeptidase activity, and protein catabolic process were the most representative functions.

"Alpha-macroglobulin, receptor-binding," and "Alpha-2-macroglobulin", while the enriched domains of downregulated proteins in the B group were similar to those in A and M groups (Figure 12(d)).

3.6. Cluster Analysis Based on Functional Enrichment. The differentially expressed proteins in different groups were classified based on GO annotation, KEGG pathway enrichment, and cluster analysis to determine the correlation in the functions of differentially expressed proteins among different groups (Figure 12).

4. Discussion

CC can effectively regulate blood lipid metabolism, improve glucose tolerance, reduce insulin resistance, improve insulin sensitivity, reduce serum inflammatory cytokines, and alleviate lipid peroxidation [7, 17]. In Table 2, the therapeutic targets for CC in the plasma of diabetic individuals, including insulin-like growth factor 1 (IGF-1), insulin-like growth factor binding protein 4 (IGFBP-4), insulin-like growth factor binding protein 6 (IGFBP-6), insulin-like growth factor binding protein, acid labile subunit (IGFALS), complement component 2 (C2), complement component (C4), complement factor I (Cfi), Apolipoprotein C-III (ApoC-III), Apolipoprotein C-I (ApoC-I), Apolipoprotein E (ApoE), Apolipoprotein B-100 (ApoB-100), Peroxiredoxin-2 (PRDX-2), Peroxiredoxin-3 (PRDX-3), prenylcysteine oxidase, and Group VII Phospholipase A2, were identified and validated by proteomic techniques. However, in different CC preparations, there was not much difference in terms of therapeutic targets and efficacy, and the advantages and disadvantages of different CC preparations were not demonstrated in this experiment. To identify therapeutically relevant drug targets of CC in individuals with diabetes, differentially expressed plasma proteins were divided into four regions according to their functions: glucose tolerance and insulin sensitivity, immunity and inflammation, lipoprotein metabolism and transport, and oxidation and antioxidation.

4.1. Effects of CC on Glucose Tolerance and Insulin Sensitivity. IGF-1 is an endocrine, paracrine, and autocrine hormone of a 70-amino acid polypeptide that shares structural homology (> 60%) with IGF-2 and proinsulin [18]. IGF-1 plays a number of physiological roles in tissue growth and development, proliferation, lipid metabolism, survival promotion, antiaging, anti-inflammation, anabolic and antioxidant properties, and neurological and hepatic protection [19–24]. IGF-1 exerts a protective effect on mitochondria by protecting it against oxidative damage, increasing ATP synthesis and reducing the production of free radicals in the mitochondria [19–21].

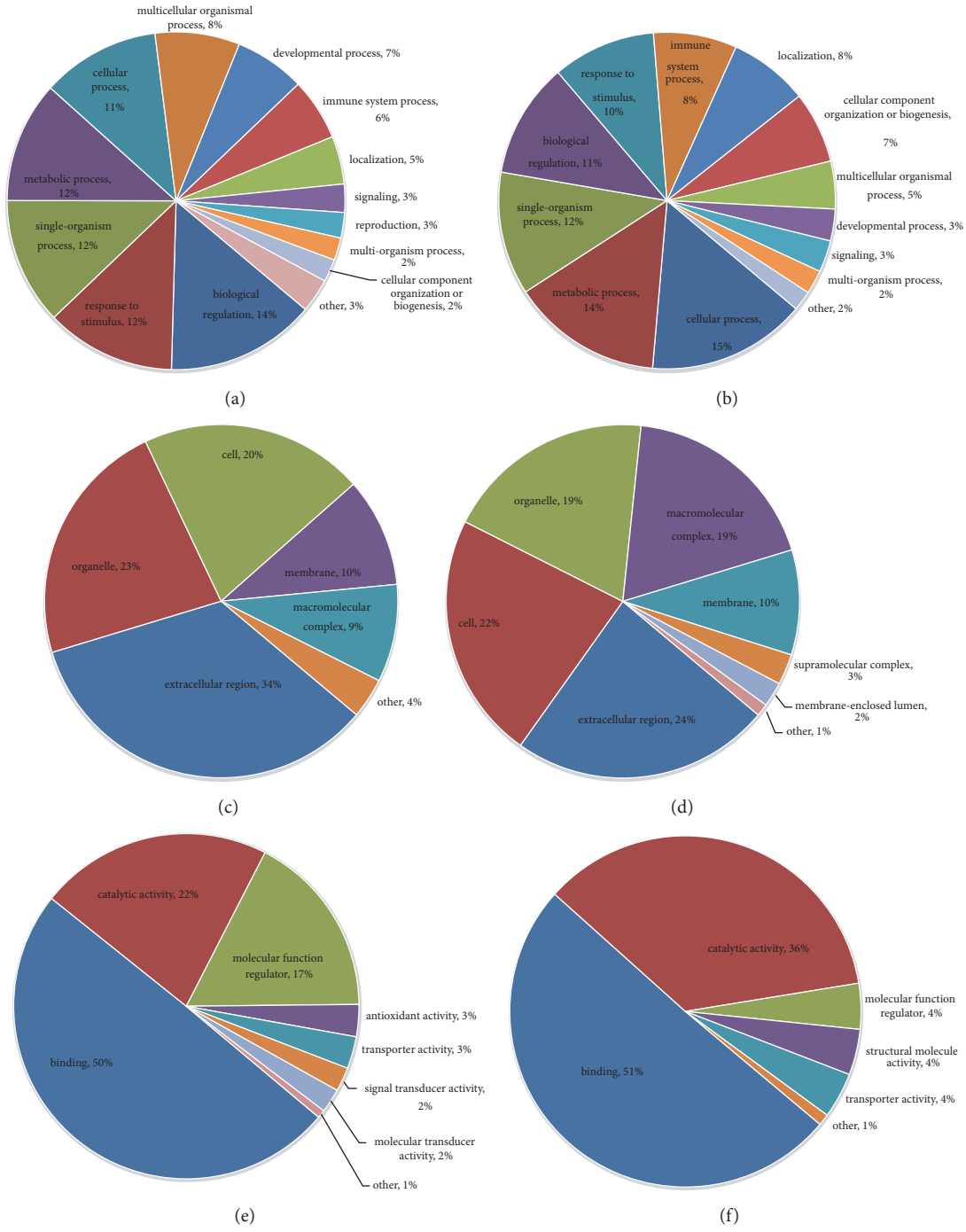

FIGURE 7: **Artificial gastric juice extraction of Coptis chinensis treatment group versus model group (B versus M) Go analysis information. (a)** Biological process: upregulated proteins: the response to biological regulation (14%) was the major component. **(b)** Biological process: downregulated proteins: the response to cellular processes (15%) was the dominant feature. **(c)** Cellular components: upregulated proteins: extracellular region (34%) formed the main component of the cellular component category. **(d)** Cellular components: downregulated proteins: extracellular region (24%) was the major component. **(e)** Molecular function: upregulated proteins: binding (50%) was the dominant molecular function in the GO assignments. **(f)** Molecular function: downregulated proteins: binding represented 51% of the molecular function.

Table 2: Significant differential expressions of proteins in Coptis chinensis-treated rats and the model rats.

Protein accession[a]	Protein description[b]	Gene name	MW [kDa]	A/M Ratio[c]	B/M Ratio[c]	D/M Ratio[c]	N/M Ratio[c]
Glucose Tolerance and Insulin Sensitivity							
P35572	Insulin-like growth factor-binding protein 6	Igfbp6	24.193	1.763	2.557	2.181	2.121
A0A0G2JX40	Insulin-like growth factor I	Igf1	16.075	1.422	1.877	1.880	2.001
P21744	Insulin-like growth factor-binding protein 4	Igfbp4	27.745	1.730	2.609	2.527	2.239
F1LRE2	Insulin-like growth factor binding protein, acid labile subunit, isoform CRA_b	Igfals	66.898	1.968	1.973	1.843	2.391
Immunity and Inflammation							
P08649	Complement C4	C4	192.16	1.787	1.770	1.868	1.532
Q6MG73	Complement component 2	C2	83.698	1.895	1.748	1.729	1.616
A0A0G2K135	Complement factor I	Cfi	69.774	1.537	1.674	1.808	1.753
Oxidation and Anti-oxidation							
A0A0G2JSH9	Peroxiredoxin-2	Prdx2	21.797	1.538	1.723	1.468	2.169
G3V7I0	Peroxiredoxin 3	Prdx3	28.299	2.219	1.992	1.333	2.800
Q5M7T7	Phospholipase A2, group VII (Platelet-activating factor acetylhydrolase, plasma)	Pla2g7	49.49	0.349	0.286	0.234	0.299
Q99ML5	Prenylcysteine oxidase	Pcyox1	56.287	0.530	0.449	0.363	0.371
Lipid Metabolism and Transport							
P19939	Apolipoprotein C-I	Apoc1	9.8606	0.498	0.410	0.541	0.581
A0A0G2K8Q1	Apolipoprotein C-III	Apoc3	11.029	0.318	0.284	0.308	0.623
A0A0G2K151	Apolipoprotein E	Apoe	41.199	0.251	0.198	0.203	0.259
F1M6Z1	Apolipoprotein B-100	Apob	509.69	0.426	0.299	0.285	0.286

[a]Database accession numbers; [b]name and categories of the proteins identified; [c]ratios of treatments/models.

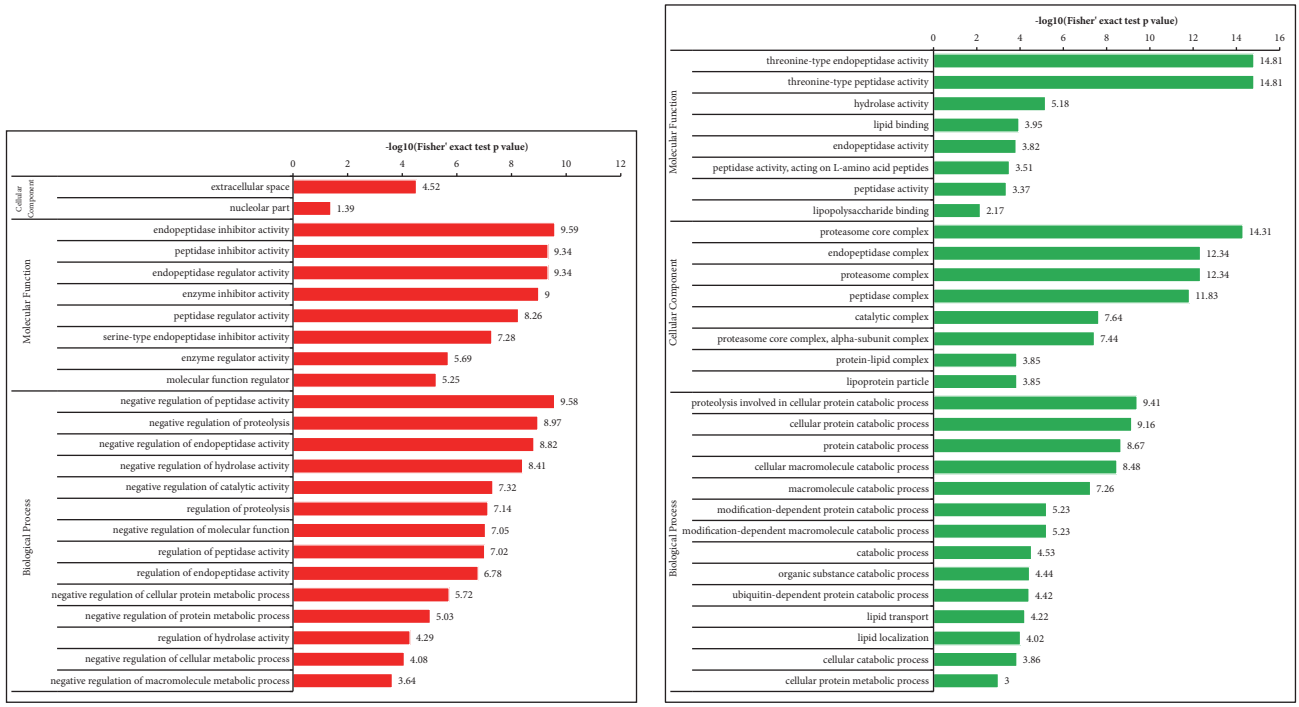

(a) (b)

FIGURE 8: **Enrichment analysis of the GO function annotation of artificial gastric juice extraction of Coptis chinensis treatment group versus model group (B versus M). (a)** Upregulated proteins: extracellular space, endopeptidase inhibitor activity, and negative regulation of peptidase activity of, respectively, cellular component, molecular function, and biological process were the most representative functions. **(b)** Downregulated proteins: proteasome core complex, threonine-type endopeptidase activity, and proteolysis involved in cellular protein catabolic process were the most representative functions.

IGF-1 can also promote glucose uptake in some peripheral tissues [25–30]. In addition, exogenous IGF-1 has been shown to lower serum glucose levels [31–33] not only in healthy individuals[34], but also in those with insulin resistance [35–37]. Low circulating levels of IGF-1 have also been associated with reduced insulin sensitivity [38], impaired glucose tolerance, and T2DM[38–40]. The experimental results of this study suggested that the level of IGF-1 in the A and B groups was higher than that in the M group.

In addition, IGF signaling is regulated by six binding proteins, IGFBP1-6. IGF-binding proteins can locally enhance or inhibit the effects of IGF [41]. IGFBP-4 is highly expressed in osteoblasts, while past in vivo studies indicated that IGFBP-4 can potentiate the effects of IGF-1 and IGF-2 [42]. The main function of IGFBP-6 is to inhibit the effects of IGF-II, although IGFBP-6 has no effect on IGF-I [43]. At present, the function of IGFBP-6 is not yet clear, but it may be involved in the pathogenesis of metabolic diseases.

IGFALS encodes a protein acid labile subunit (ALS), which forms a ternary complex with IGF-1, IGFBP-3, and IGFBP-5. The primary role of ALS is to extend the half-life of IGF1 by protecting the ternary complex against degradation [44, 45]. In addition, it was reported that mutations in the IGFALS gene lead to a syndrome of primary IGF-I deficiency [46]. Biallelic mutations in IGFALS may also be associated with insulin resistance [45, 47]. In this study, the expression of IGFBP-4, 6, and IGFALS was significantly increased in the A and B groups. Based on these findings, it is likely that CC can improve glucose tolerance and increase insulin sensitivity by upregulating the expression of IGF-1 and related insulin-like growth factor binding proteins in vivo.

4.2. Effects of CC on Immunity and Inflammation. The complement system is a crucial element of the immune defense system. A complex enzyme cascade containing more than 50 circulating and membrane-bound proteins plays an important role in the activation of natural and adaptive immune responses [48, 49]. The complement system is also involved in the process of tissue development, degeneration, and regeneration and plays an important metabolic and inflammatory role in adipose tissues [50]. The clinical status of T2DM is associated with chronic and mild inflammation, such as an increase in serum levels of inflammatory cytokines [51]. In previous proteomics studies, complement-related proteins were upregulated in T2DM [52]. In addition, in some cohort studies, it was found that the levels of complement-related proteins correlate with insulin resistance and elevated blood glucose and hence are considered as risk factors for the development of T2DM [53, 54].

However, in this study, conflicting results were found. In the diabetic model, the complement proteins C2, C4,

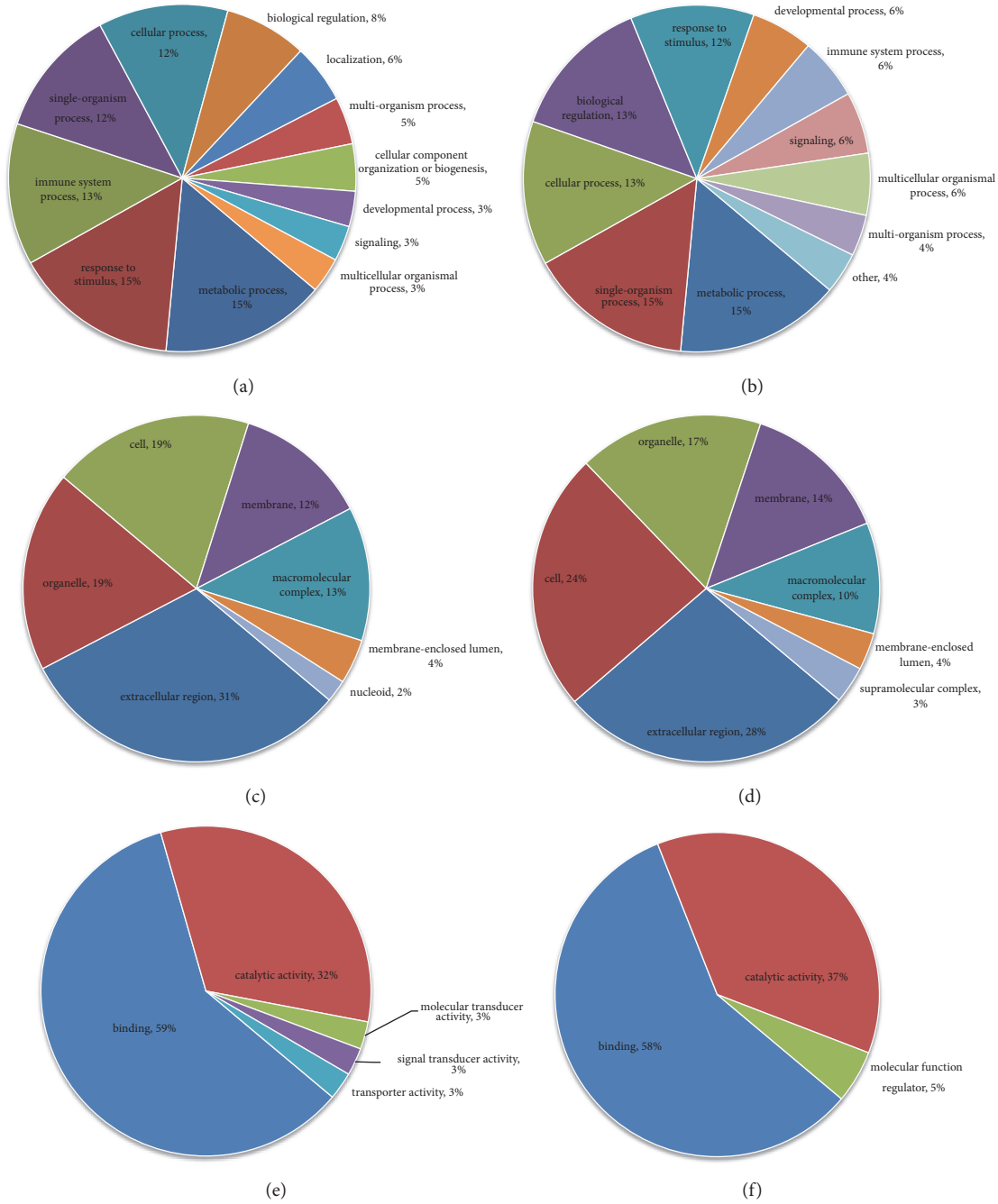

Figure 9: **Supercritical extraction of Coptis chinensis treatment group versus artificial gastric juice extraction of Coptis chinensis treatment group (A versus B) Go analysis information. (a)** Biological process: upregulated proteins: the response to metabolic process (15%) and response to stimulus (15%) were the major component. **(b)** Biological process: downregulated proteins: the responses to metabolic process (15%) and single-organism process (15%) were the dominant features. **(c)** Cellular components: upregulated proteins: extracellular region (31%) formed the main component of the cellular component category. **(d)** Cellular components: downregulated proteins: extracellular region (28%) was the major component. **(e)** Molecular function: upregulated proteins: binding (59%) was the dominant molecular function in the GO assignments. **(f)** Molecular function: downregulated proteins: binding represented 58% of the molecular function.

and Cfi were downregulated. However, after drug intervention (including metformin), these complement proteins were upregulated. In diabetes, the abnormal production or regulation of hundreds of immune mediators leads to changes in metabolic status. Given such complexity, different or even conflicting results are commonly observed [55]. It is believed that the upregulation of complement-associated proteins is most likely reactive. For example, CC may upregulate these proteins to enhance phagocytosis and hypersensitivity without causing direct cell-injury, suggesting that the tissues

(a)

(b)

Figure 10: **Enrichment analysis of the GO function annotation of supercritical extraction of Coptis chinensis treatment group versus artificial gastric juice extraction of Coptis chinensis treatment group (A versus B). (a)** Upregulated proteins: oxidoreductase activity, acting on the CH-CH group of donors, organelle inner membrane, and production of molecular mediator of immune response of, respectively, cellular component, molecular function, and biological process were the most representative functions in the upregulated proteins. **(b)** Downregulated proteins: transferase activity was the most representative function in molecular function, and others could not get a valid P value.

of the complement system can block the possible role of apoptotic debris and inflammation in tissues [56].

4.3. Effects of CC on Lipid Metabolism and Transport. The proteins in plasma lipoproteins are called apolipoproteins and their basic function is to carry lipids and stabilize the structure of lipoproteins. It was found in the present study that the level of apolipoproteins correlates with the level of insulin resistance. Haplotypes in the ApoC-III gene have been shown to lead to elevated ApoC-III levels and an increased susceptibility to type 1 diabetes [57]. ApoC-III gene mutations and ApoC-III levels are also associated with the development of nonalcoholic fatty liver, hepatic insulin resistance, and T2DM [58, 59]. In addition, it has also been reported that ApoC-III, which is produced locally under insulin resistance, is an important agent causing islet β-cell dysfunction in diabetes. Reduced ApoC-III in vivo by antisense treatment can improve glucose tolerance [60], and ApoC-I exerts a similar effect as ApoC-III. Prospective studies have shown that ApoC-I levels are higher in polycystic ovarian syndrome (PCOS) patients with insulin resistance [61]. It was also found that severe systemic and hepatic insulin resistance can occur in mice overexpressing ApoC-I [62].

Overproduction of VLDL particles containing hepatic Apo-B-100 has been well documented in animal models and in those with insulin resistance (such as Metabolic Syndrome and T2DM), which can result in the typical dyslipidemia in these disorders [63]. As for ApoE, previous findings suggest that mice carrying the ApoE-3-genotype are more prone to develop impaired glucose tolerance leading to obesity and metabolic complications [64]. In an aging brain, the increasing level of ApoE-4 can further aggravate the inhibitory effect of ApoE-4 on insulin signaling and act as an important pathogenic mechanism underlying insulin resistance [65]. This study showed that the treatment of CC downregulated the expression of above proteins. From these results, it is confirmed that C can reduce the level of lipoproteins, thus improving insulin resistance and glucose tolerance.

4.4. Effects of CC on Oxidation and Antioxidation. Oxidative stress is an important pathophysiological mechanism underlying the development and complications of T2DM [66]. A peroxidase system is present in somatic cells and plays a key role in counteracting oxidative stress. PRDX-2 is an antioxidant protein found to be downregulated in patients with T2DM and PCOS. The expression of PRDX-2 indicates the levels of oxidative stress and toxicity in T2DM [67]. Previous data also indicated that PRDX-2 is required for normal insulin secretion [68]. Like PRDX-2, PRDX-3 is also an antioxidant protein. A systemic knockdown of PRDX-3 in mice leads to oxidative stress, increased accumulation of white adipose tissues, dysregulated adiposity, and systemic insulin resistance [69]. In contrast, overexpression of PRDX-3 can reduce the levels of oxidative stress and alleviate insulin resistance, highlighting that oxidative stress plays a key role in maintaining insulin sensitivity [70–74]. In addition, PRDX-3 transcription is downregulated in adipose tissues in obese and insulin-resistant humans, while some studies have shown that diabetics are associated with increased levels of oxidative stress markers such as lipid peroxidation. In addition, PRDX3 can resist oxidative stress [71–77]. The experiment of this study confirmed that CC treatment could increase the expression of PRDX-2 and PRDX-3. It also indicates that CC is likely to improve the oxidation response in diabetes by upregulating the expression of proteins in the peroxidase family.

Prenylcysteine oxidase is detectable both in embryonic tissues and in various adult organs, particularly in the liver. The gene sequence Pcyox1 has also been described as a marker of toxicity in the liver [78]. In addition, Group VII Phospholipase A2 has been described as a novel risk factor for cardiovascular disease [79, 80]. Some reports also showed significant increases in Pla2g7 mRNA expression in the liver of metabolic syndrome rats [81, 82]. In this study, it was found that prenylcysteine oxidase and Group VII Phospholipase A2 were significantly downregulated after CC treatment. It was

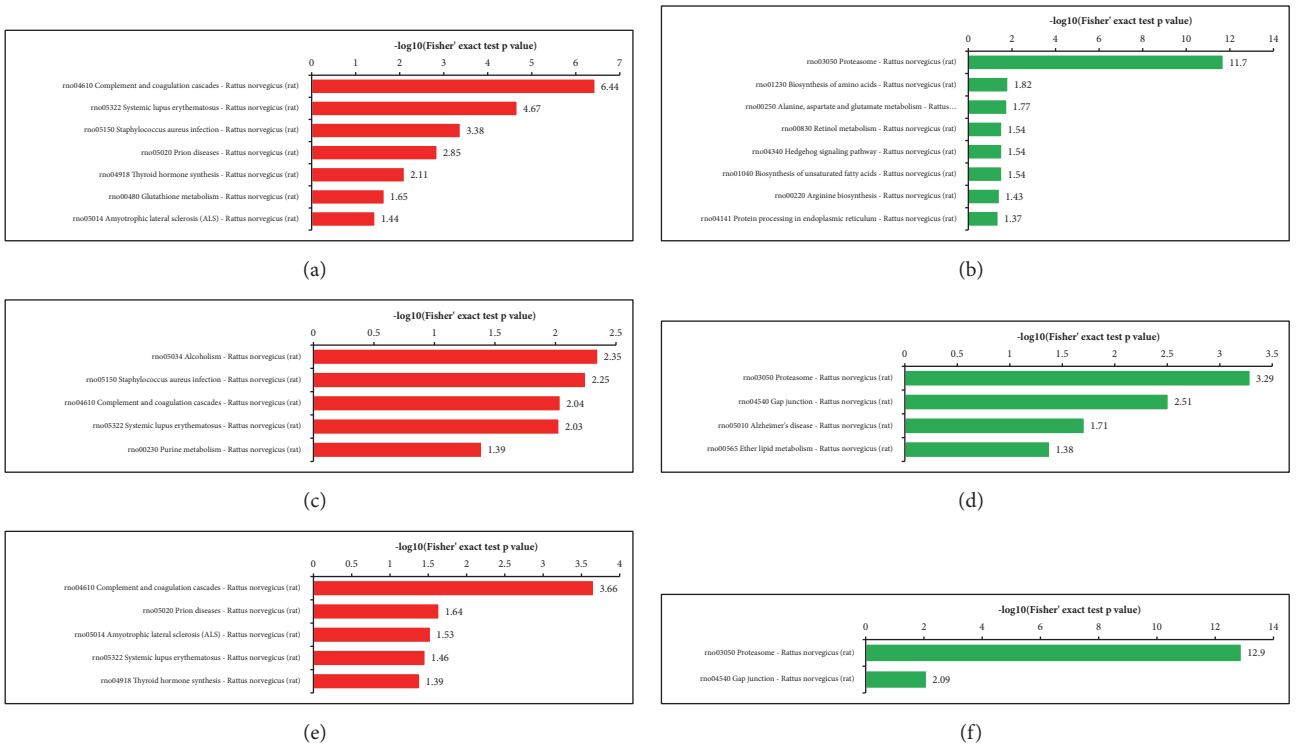

Figure 11: **KEGG Pathway enrichment. (a)** N versus M: KEGG pathway enrichment of upregulated proteins; **(b)** N versus M: KEGG pathway enrichment of downregulated proteins; **(c)** A versus M: KEGG pathway enrichment of increased proteins; **(d)** A versus M: KEGG pathway enrichment of decreased proteins; **(e)** B versus M: KEGG pathway enrichment of upregulated proteins; **(f)** B versus M: KEGG pathway enrichment of downregulated proteins.

Table 3: Significant differential expressions of proteins in two different extracted CC treatments.

Protein accession[a]	Protein description[b]	Gene name	MW [kDa]	A/M Ratio[c]	B/M Ratio[c]	D/M Ratio[c]	N/M Ratio[c]	A/B Ratio[c]
P21744	Insulin-like growth factor-binding protein 4	Igfbp4	27.745	1.730	2.609	2.527	2.239	0.663
A0A0G2JSP8	Creatine kinase M-type	Ckm	43.018	2.655	4.055	2.938	9.693	0.655
P02600	Myosin light chain 1/3, skeletal muscle isoform	Myl1	20.679	1.663	2.610	4.669	2.347	0.637
F1M171	Protein RGD1311933	RGD1311933	38.482	0.451	0.282	0.268	0.254	1.597

[a]Database accession numbers; [b]name and categories of the proteins identified; [c]ratios of treatments/models.

suggested that CC can improve insulin resistance and treat diabetes by reducing the expression of oxidative factors and increasing the level of antioxidants in the body.

4.5. Differences between A and B Groups. No significant difference was found in the two CC treatments in terms of the status of glycemic and lipid disorders. In proteomic analysis, although it was found that 27 proteins were upregulated and 16 proteins were downregulated in group A compared with those in group B, they showed no significant impact on the treatment of T2DM. Therefore, 43 proteins that did not differ between N and M groups were excluded. In addition, the proteins with less than 1.5-fold difference between A versus M and B versus M groups and the proteins with nonmeaningful P values were also eliminated. As a result, only four differentially expressed proteins were found between A and B groups, as shown in Table 3.

Based on the above discussion, IGFBP-4 can enhance the role of IGF-1 and IGF-2 [42], while both types of extracted CC can upregulate IGFBP-4. However, it is worth noting that IGF-1 did not show significant differences in the two CC treatments. Similarly, IGFBP-6 and IGFALS also showed no significant differences in the two CC treatments. Therefore, although the drug in group B can increase the level of IGFBP4, it does not show much difference in the improvement of glucose tolerance and insulin resistance as compared with the drug in group A.

Creatine kinase M-type is a creatine kinase isoenzyme found in muscles. Little information is available regarding the relation of this enzyme to diabetes, but a study using

Figure 12: Continued.

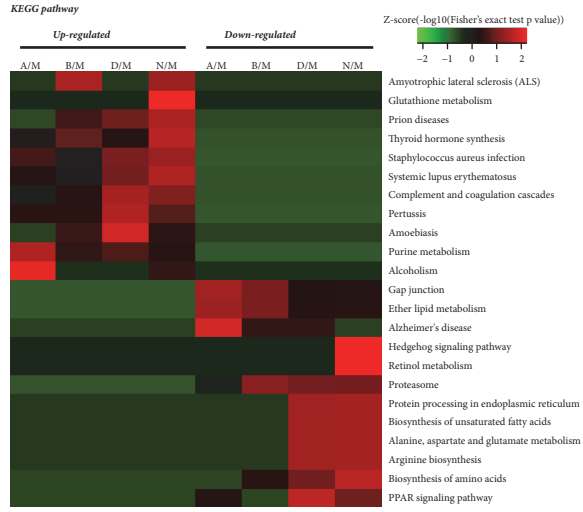

(e)

FIGURE 12: **Heat map obtained from GO and cluster based on feature enrichment. (a)** Biological process analysis; **(b)** cell component analysis; **(c)** molecular function analysis; **(d)** protein domain analysis; **(e)** KEGG pathway analysis. All corrected P values <0.05 passed two-tailed Fisher exact test.

nontargeted proteomics revealed that the expression of creatine kinase M-type in skeletal muscles of women with hyperandrogenism was downregulated, suggesting that the downregulation of this protein may cause insulin resistance [83]. Myosin light chain 1/3 (MLC 1/3) is a member of myosin light chains. A study has shown that muscle fiber components are related to insulin resistance, while exercises can increase the amount of myosin fibers, thereby reducing the risk of diabetes [84]. One study showed that, as compared with the control group, MLC in heart homogenates of diabetic rats was significantly reduced (40% to 45%), and MLC phosphorylation was also significantly reduced (30% to 45%). These results indicate that the decrease of protein content in MLC and the phosphorylation of MLC may lead to diabetic cardiomyopathy [85]. In this study, it was found that both CC A and B can effectively upregulate the expression of creatine kinase M-type and MLC 1/3, which can reduce the risk of diabetes.

As for Protein RGD1311933, it was found in this study that Protein RGD1311933 was upregulated in the M group compared with that in the N group, and the levels of Protein RGD1311933 were reversed after treatment with both types of CC. In addition, B drug decreased the level of Protein RGD1311933 to a greater extent. Although Protein RGD1311933 has yet to have functional annotations in the database, its relationship with diabetes shall be further studied.

In summary, although B drug showed a better efficacy in regulating the levels of above four proteins, the evidence is relatively weak. Therefore, it is very difficult to infer that B drug is more effective than A drug.

5. Conclusions

In this experiment, 15 differentially expressed proteins were identified as being related to the efficacy of CC. The functions of these proteins were related to improved glucose, insulin sensitivity, immunity, lipid metabolism, lipid transport, and antioxidant activity. Two differentially extracted CC treatments did not show significant differences in their treatment efficacy. In summary, this study deepens our understanding about the role of CC in the treatment of diabetes.

Data Availability

We guarantee the authenticity of the data. If the article is received, we can provide all the original data.

Conflicts of Interest

The authors declare that there are no conflicts of interest regarding the publication of this paper.

Authors' Contributions

Xin Qiu and Xinyu Wei contributed equally to this work.

Acknowledgments

This article is supported by the National Natural Science Foundation of China (No. 81473448).

References

[1] NCD Risk Factor Collaboration (NCD-RisC), "Worldwide trends in diabetes since 1980: a pooled analysis of 751 population-based studies with 4·4 million participants," *The Lancet*, vol. 387, no. 10027, pp. 1513–1530, 2016.

[2] Y. Xu, L. Wang, J. He et al., "Prevalence and control of diabetes in Chinese adults," *Journal of the American Medical Association*, vol. 310, no. 9, pp. 948–958, 2013.

[3] The Lancet, "Beat diabetes: an urgent call for global action," *The Lancet*, vol. 387, no. 10027, p. 1483, 2016.

[4] S. M. Herbrich, R. N. Cole, K. P. West Jr. et al., "Statistical inference from multiple iTRAQ experiments without using common reference standards," *Journal of Proteome Research*, vol. 12, no. 2, pp. 594–604, 2013.

[5] P. L. Ross, Y. N. Huang, J. N. Marchese et al., "Multiplexed protein quantitation in *Saccharomyces cerevisiae* using amine-reactive isobaric tagging reagents," *Molecular & Cellular Proteomics*, vol. 3, no. 12, pp. 1154–1169, 2004.

[6] S.-Y. Dai, B. Xu, Y. Zhang et al., "Establishment and reliability evaluation of the design space for HPLC analysis of six alkaloids in Coptis chinensis (Huanglian) using Bayesian approach," *Chinese Journal of Natural Medicines*, vol. 14, no. 9, pp. 697–708, 2016.

[7] S. H. Leng, F. E. Lu, and L. J. Xu, "Therapeutic effects of berberine in impaired glucose tolerance rats and its influence on insulin secretion," *Acta Pharmacologica Sinica*, vol. 25, no. 4, pp. 496-502.

[8] H. A. Jung, N. Y. Yoon, H. J. Bae, B. Min, and J. S. Choi, "Inhibitory activities of the alkaloids from Coptidis Rhizoma against aldose reductase," *Archives of Pharmacal Research*, vol. 31, no. 11, pp. 1405–1412, 2008.

[9] M. Ohnishi, T. Matuo, T. Tsuno et al., "Antioxidant activity and hypoglycemic effect of ferulic acid in STZ-induced diabetic mice and KK-Ay mice," *BioFactors*, vol. 21, no. 1-4, pp. 315–319, 2004.

[10] M. S. Balasubashini, R. Rukkumani, P. Viswanathan, and V. P. Menon, "Ferulic acid alleviates lipid peroxidation in diabetic rats," *Phytotherapy Research*, vol. 18, no. 4, pp. 310–314, 2004.

[11] S. C. Wei, L. J. Xu, and X. Zou, "Pharmacokinetics of berberine and jateorhizine from Rhizoma coptidis powder and decoction in diabetic rats," *Chinese Hospital Pharmacy*, no. 08, pp. 698-702.

[12] S.-C. Wei, L.-J. Xu, X. Zou et al., "Pharmacokinetic and pharmacodynamic characteristics of berberine and jateorhizine in Coptidis Rhizoma powder and their monomeric compounds in type 2 diabetic rats," *Zhongguo Zhongyao Zazhi*, vol. 40, no. 21, pp. 4262–4267, 2015.

[13] C. JPE, *The Japanese Pharmacopoeia*, Hirokawa Publishing Co, Tokyo, Japan, 2011.

[14] F. A. Duca, C. D. Côté, B. A. Rasmussen et al., "Metformin activates a duodenal Ampk-dependent pathway to lower hepatic glucose production in rats," *Nature Medicine*, vol. 21, no. 5, pp. 506–511, 2015.

[15] S. Wei, L. Xu, and X. Zou, "Preliminary study on secreting efects of Rhizoma Coptidis active ingredients and their combinations on insulin and glucagon-like peptide1 (GLP-1)in glucose feding mice," *Chinese Hospital Pharmaceutical Journal*, no. 14, pp. 1343-1347.

[16] J. Wang, L. Teng, Y. Liu et al., "Studies on the antidiabetic and antinephritic activities of paecilomyces hepiali water extract in diet-streptozotocin-induced diabetic sprague dawley rats," *Journal of Diabetes Research*, vol. 2016, 2016.

[17] J. Gong, M. Hu, Z. Huang et al., "Berberine Attenuates Intestinal Mucosal Barrier Dysfunction in Type 2 Diabetic Rats," *Frontiers in Pharmacology*, vol. 8, 2017.

[18] E. Rinderknecht and R. E. Humbel, "The amino acid sequence of human insulin-like growth factor I and its structural homology with proinsulin," *The Journal of Biological Chemistry*, vol. 253, no. 8, pp. 2769–2776, 1978.

[19] R. Pérez, M. García-Fernández, M. Díaz-Sánchez et al., "Mitochondrial protection by low doses of insulin-like growth factor-Iin experimental cirrhosis," *World Journal of Gastroenterology*, vol. 14, no. 17, p. 2731, 2008.

[20] J. E. Puche, M. García-Fernández, J. Muntané, J. Rioja, S. González-Barón, and I. C. Cortazar, "Low doses of insulin-like growth factor-I induce mitochondrial protection in aging rats," *Endocrinology*, vol. 149, no. 5, pp. 2620–2627, 2008.

[21] M. García-Fernández, G. Delgado, J. E. Puche, S. González-Barón, and I. C. Cortázar, "Low doses of insulin-like growth factor I improve insulin resistance, lipid metabolism, and oxidative damage in aging rats," *Endocrinology*, vol. 149, no. 5, pp. 2433–2442, 2008.

[22] M. Conchillo, R. J. de Knegt, M. Payeras et al., "Insulin-like growth factor I (IGF-I) replacement therapy increases albumin concentration in liver cirrhosis: results of a pilot randomized controlled clinical trial," *Journal of Hepatology*, vol. 43, no. 4, pp. 630–636, 2005.

[23] M. García-Fernández, I. Castilla-Cortázar, M. Díaz-Sanchez et al., "Antioxidant effects of insulin-like growth factor-I (IGF-I) in rats with advanced liver cirrhosis," *BMC Gastroenterology*, vol. 5, no. 1, 2005.

[24] I. Castilla-Cortázar, M. Pascual, E. Urdaneta et al., "Jejunal microvilli atrophy and reduced nutrient transport in rats with advanced liver cirrhosis: improvement by Insulin-like Growth Factor I," *BMC Gastroenterology*, vol. 4, no. 1, 2004.

[25] H. Laager, R. Ninnis, and U. Keller, "Comparison of the effects of recombinant human insulin-like growth factor-1 and insulin on glucose and leucine kinetics in humans," *The Journal of Clinical Investigation*, vol. 92, no. 4, pp. 1903–1909, 1993.

[26] D. Elahi, M. McAloon-Dyke, N. K. Fukagawa et al., "Effects of recombinant human IGF-I on glucose and leucine kinetics in men," *American Journal of Physiology-Endocrinology and Metabolism*, vol. 265, no. 6, pp. E831–E838, 1993.

[27] D. L. Russell-Jones, A. T. Bates, A. M. Umpleby et al., "A comparison of the effects of IGF-I and insulin on glucose metabolism, fat metabolism and the cardiovascular system in normal human volunteers," *European Journal of Clinical Investigation*, vol. 25, no. 6, pp. 403–411, 1995.

[28] S. D. Boulware, W. V. Tamborlane, N. J. Rennert, N. Gesundheit, and R. S. Sherwin, "Comparison of the metabolic effects of recombinant human insulin-like growth factor-I and insulin. Dose-response relationships in healthy young and middle-aged adults," *The Journal of Clinical Investigation*, vol. 93, no. 3, pp. 1131–1139, 1994.

[29] K. Sakai, H. B. Lowman, and D. R. Clemmons, "Increases in free, unbound insulin-like growth factor I enhance insulin responsiveness in human hepatoma G2 cells in culture," *The Journal of Biological Chemistry*, vol. 277, no. 16, pp. 13620–13627, 2002.

[30] J. Frystyk, T. Grøfte, C. Skjærbæk, and H. Ørskov, " The Effect of Oral Glucose on Serum Free Insulin-Like Growth Factor-I and -II in Healthy Adults ," *The Journal of Clinical Endocrinology & Metabolism*, vol. 82, no. 9, pp. 3124–3127, 1997.

[31] P. D. Zenobi, H.-P. Guler, J. Zapf, and E. R. Froesch, "Insulin-like growth factors in the Gottinger miniature-pig," *Acta Endocrinologica*, vol. 117, no. 3, pp. 343–352, 1988.

[32] J. Zapf, C. Hauri, M. Waldvogel, and E. R. Froesch, "Acute metabolic effects and half-lives of intravenously administered insulinlike growth factors I and II in normal and hypophysectomized rats," *The Journal of Clinical Investigation*, vol. 77, no. 6, pp. 1768–1775, 1986.

[33] R. G. Rosenfeld, V. Hwa, E. Wilson, S. R. Plymate, and Y. Oh, "The insulin-like growth factor-binding protein superfamily," *Growth Hormone & IGF Research*, vol. 10, pp. S16–S17, 2000.

[34] C. Schmid, T. Bianda, C. Zwimpfer, J. Zapf, and P. Wiesli, "Changes in insulin sensitivity induced by short-term growth hormone (GH) and insulin-like growth factor I (IGF-I) treatment in GH-deficient adults are not associated with changes in adiponectin levels," *Growth Hormone & IGF Research*, vol. 15, no. 4, pp. 300–303, 2005.

[35] P. D. Zenobi, Y. Glatz, A. Keller et al., "Beneficial metabolic effects of insulin-like growth factor I in patients with severe insulin resistant diabetes type A," *European Journal of Endocrinology*, vol. 131, no. 3, pp. 251–257, 1994.

[36] T. Saukkonen, R. Amin, R. M. Williams et al., "Dose-dependent effects of recombinant human insulin-like growth factor (IGF)-I/IGF binding protein-3 complex on overnight growth hormone secretion and insulin sensitivity in type 1 diabetes," *The Journal of Clinical Endocrinology & Metabolism*, vol. 89, no. 9, pp. 4634–4641, 2004.

[37] T. Pratipanawatr, W. Pratipanawatr, C. Rosen et al., "Effect of IGF-I on FFA and glucose metabolism in control and type 2 diabetic subjects," *American Journal of Physiology-Endocrinology and Metabolism*, vol. 282, no. 6, pp. E1360–E1368, 2002.

[38] E. Succurro, F. Andreozzi, M. A. Marini et al., "Low plasma insulin-like growth factor-1 levels are associated with reduced insulin sensitivity and increased insulin secretion in nondiabetic subjects," *Nutrition, Metabolism & Cardiovascular Diseases*, vol. 19, no. 10, pp. 713–719, 2009.

[39] M. S. Sandhu, A. H. Heald, J. M. Gibson, J. K. Cruickshank, D. B. Dunger, and N. J. Wareham, "Circulating concentrations of insulin-like growth factor-I and development of glucose intolerance: a prospective observational study," *The Lancet*, vol. 359, no. 9319, pp. 1740–1745, 2002.

[40] G. C. Mannino, A. Greco, C. De Lorenzo et al., "A fasting insulin-raising allele at IGF1 locus is associated with circulating levels of IGF-1 and insulin sensitivity," *PLoS ONE*, vol. 8, no. 12, 2013.

[41] C. G. Tahimic, Y. Wang, and D. D. Bikle, "Anabolic effects of IGF-1 signaling on the skeleton," *Frontiers in Endocrinology*, vol. 4, 2013.

[42] D. E. Maridas, V. E. DeMambro, P. T. Le et al., "IGFBP-4 regulates adult skeletal growth in a sex-specific manner," *Journal of Endocrinology*, vol. 233, no. 1, pp. 131–144, 2017.

[43] L. A. Bach, "IGFBP-6 five years on; not so "forgotten"?" *Growth Hormone & IGF Research*, vol. 15, no. 3, pp. 185–192, 2005.

[44] L. Guilin, N. Lili, L. Haifeng, and G. Jiazhong, "Structure and function of insulin-like growth factor acid-labile subunits in mammalian homologues," *Yi chuan*, vol. 37, no. 12, pp. 1185–1193, 2015.

[45] H. M. Domené, V. Hwa, H. G. Jasper, and R. G. Rosenfeld, "Acid-labile subunit (ALS) deficiency," *Best Practice & Research Clinical Endocrinology & Metabolism*, vol. 25, no. 1, pp. 101–113, 2011.

[46] T. Poukoulidou, J. Kowalczyk, L. Metherell, J. De Schepper, and M. Maes, "A novel homozygous mutation of the IGFALS gene in a female adolescent: Indirect evidence for a contributing role of the circulating IGF-I pool in the pubertal growth spurt," *Hormone Research in Paediatrics*, vol. 81, no. 6, pp. 422–427, 2014.

[47] O. Hess, M. Khayat, V. Hwa et al., "A novel mutation in IGFALS, c.380T>C (p.L127P), associated with short stature, delayed puberty, osteopenia and hyperinsulinaemia in two siblings: Insights into the roles of insulin growth factor-1 (IGF1)," *Clinical Endocrinology*, vol. 79, no. 6, pp. 838–844, 2013.

[48] S. I. Vlaicu, A. Tatomir, D. Boodhoo, S. Vesa, P. A. Mircea, and H. Rus, "The role of complement system in adipose tissue-related inflammation," *Immunologic Research*, vol. 64, no. 3, pp. 653–664, 2016.

[49] R. Lubbers, M. F. van Essen, C. van Kooten, and L. A. Trouw, "Production of complement components by cells of the immune system," *Clinical & Experimental Immunology*, vol. 188, no. 2, pp. 183–194, 2017.

[50] J. Phieler, R. Garcia-Martin, J. D. Lambris, and T. Chavakis, "The role of the complement system in metabolic organs and metabolic diseases," *Seminars in Immunology*, vol. 25, no. 1, pp. 47–53, 2013.

[51] B. C. King and A. M. Blom, "Non-traditional roles of complement in type 2 diabetes: Metabolism, insulin secretion and homeostasis," *Molecular Immunology*, vol. 84, pp. 34–42, 2017.

[52] R. Li, H. Chen, K. Tu et al., "Localized-Statistical Quantification of Human Serum Proteome Associated with Type 2 Diabetes," *PLoS ONE*, vol. 3, no. 9, p. e3224, 2008.

[53] N. Wlazlo, M. M. J. Van Greevenbroek, I. Ferreira et al., "Complement factor 3 is associated with insulin resistance and with incident type 2 diabetes over a 7-year follow-up period: The CODAM study," *Diabetes Care*, vol. 37, no. 7, pp. 1900–1909, 2014.

[54] G. Engström, B. Hedblad, K.-F. Eriksson, L. Janzon, and F. Lindgärde, "Complement C3 is a risk factor for the development of diabetes: A population-based cohort study," *Diabetes*, vol. 54, no. 2, pp. 570–575, 2005.

[55] G. S. Hotamisligil, "Foundations of Immunometabolism and Implications for Metabolic Health and Disease," *Immunity*, vol. 47, no. 3, pp. 406–420, 2017.

[56] S. Kaye, A. I. Lokki, A. Hanttu et al., "Upregulation of Early and Downregulation of Terminal Pathway Complement Genes in Subcutaneous Adipose Tissue and Adipocytes in Acquired Obesity," *Frontiers in Immunology*, vol. 8, 2017.

[57] J. E. Hokanson, G. L. Kinney, S. Cheng, H. A. Erlich, A. Kretowski, and M. Rewers, "Susceptibility to type 1 diabetes is associated with apoCIII gene haplotypes," *Diabetes*, vol. 55, no. 3, pp. 834–838, 2006.

[58] K. F. Petersen, S. Dufour, A. Hariri et al., "Apolipoprotein C3 gene variants in nonalcoholic fatty liver disease," *The New England Journal of Medicine*, vol. 362, no. 12, pp. 1082–1089, 2010.

[59] R. J. Perry, V. T. Samuel, K. F. Petersen, and G. I. Shulman, "The role of hepatic lipids in hepatic insulin resistance and type 2 diabetes," *Nature*, vol. 510, no. 7503, pp. 84–91, 2014.

[60] L. Juntti-Berggren and P.-O. Berggren, "Apolipoprotein CIII is a new player in diabetes," *Current Opinion in Lipidology*, vol. 28, no. 1, pp. 27–31, 2017.

[61] S. Huang, J. Qiao, R. Li, L. Wang, and M. Li, "Can serum apolipoprotein C-I demonstrate metabolic abnormality early in women with polycystic ovary syndrome?" *Fertility and Sterility*, vol. 94, no. 1, pp. 205–210, 2010.

[62] M. Muurling, A. M. Van Den Hoek, R. P. Mensink et al., "Overexpression of APOC1 in obob mice leads to hepatic steatosis and severe hepatic insulin resistance," *Journal of Lipid Research*, vol. 45, no. 1, pp. 9–16, 2004.

[63] C. Xiao, S. Dash, C. Morgantini, and G. F. Lewis, "New and emerging regulators of intestinal lipoprotein secretion," *Atherosclerosis*, vol. 233, no. 2, pp. 608–615, 2014.

[64] K. E. Slim, D. Vauzour, N. Tejera, P. J. Voshol, A. Cassidy, and A. M. Minihane, "The effect of dietary fish oil on weight gain & insulin sensitivity is dependent on APOE genotype in humanized targeted replacement mice," *The FASEB Journal*, vol. 31, no. 3, pp. 989–997, 2017.

[65] N. Zhao, C.-C. Liu, A. J. Van Ingelgom et al., "Apolipoprotein E4 Impairs Neuronal Insulin Signaling by Trapping Insulin Receptor in the Endosomes," *Neuron*, vol. 96, no. 1, pp. 115–129.e5, 2017.

[66] J. L. Evans, I. D. Goldfine, B. A. Maddux, and G. M. Grodsky, "Oxidative stress and stress-activated signaling pathways: a unifying hypothesis of type 2 diabetes," *Endocrine Reviews*, vol. 23, no. 5, pp. 599–622, 2002.

[67] M. Cortón, J. I. Botella-Carretero, J. A. López et al., "Proteomic analysis of human omental adipose tissue in the polycystic ovary syndrome using two-dimensional difference gel electrophoresis and mass spectrometry," *Human Reproduction*, vol. 23, no. 3, pp. 651–661, 2008.

[68] M. Oláhová and E. A. Veal, "A peroxiredoxin, PRDX-2, is required for insulin secretion and insulin/IIS-dependent regulation of stress resistance and longevity," *Aging Cell*, vol. 14, no. 4, pp. 558–568, 2015.

[69] J. Y. Huh, Y. Kim, J. Jeong et al., "Peroxiredoxin 3 is a key molecule regulating adipocyte oxidative stress, mitochondrial biogenesis, and adipokine expression," *Antioxidants & Redox Signaling*, vol. 16, no. 3, pp. 229–243, 2012.

[70] L. Chen, R. Na, M. Gu et al., "Reduction of mitochondrial H2O2 by overexpressing peroxiredoxin 3 improves glucose tolerance in mice," *Aging Cell*, vol. 7, no. 6, pp. 866–878, 2008.

[71] K. H. Fisher-Wellman and P. D. Neufer, "Linking mitochondrial bioenergetics to insulin resistance via redox biology," *Trends in Endocrinology & Metabolism*, vol. 23, no. 3, pp. 142–153, 2012.

[72] P. A. Grimsrud, M. J. Picklo Sr., T. J. Griffin, and D. A. Bernlohr, "Carbonylation of adipose proteins in obesity and insulin resistance: Identification of adipocyte fatty acid-binding protein as a cellular target of 4-hydroxynonenal," *Molecular & Cellular Proteomics*, vol. 6, no. 4, pp. 624–637, 2007.

[73] R. Monteiro and I. Azevedo, "Chronic inflammation in obesity and the metabolic syndrome," *Mediators of Inflammation*, vol. 2010, Article ID 289645, 10 pages, 2010.

[74] H. Xu, G. T. Barnes, Q. Yang et al., "Chronic inflammation in fat plays a crucial role in the development of obesity-related insulin resistance," *The Journal of Clinical Investigation*, vol. 112, no. 12, pp. 1821–1830, 2003.

[75] S. K. Jain, "Hyperglycemia can cause membrane lipid peroxidation and osmotic fragility in human red blood cells," *The Journal of Biological Chemistry*, vol. 264, no. 35, pp. 21340–21345, 1989.

[76] P. Peraldi and B. Spiegelman, "TNF-alpha and insulin resistance: summary and future prospects," *Molecular and Cellular Biochemistry*, vol. 182, no. 1-2, pp. 169-175.

[77] W. S. Hahn, J. Kuzmicic, J. S. Burrill et al., "Proinflammatory cytokines differentially regulate adipocyte mitochondrial metabolism, oxidative stress, and dynamics," *American Journal of Physiology-Endocrinology and Metabolism*, vol. 306, no. 9, pp. E1033–E1045, 2014.

[78] M. M. Wouters, J.-M. Neefs, A. D. Kerchove d'Exaerde, J.-M. Vanderwinden, and K. A. Smans, "Downregulation of two novel genes in Sl/Sld and WLacZ/Wv mouse jejunum," *Biochemical and Biophysical Research Communications*, vol. 346, no. 2, pp. 491–500, 2006.

[79] M. A. Corson, P. H. Jones, and M. H. Davidson, "Review of the Evidence for the Clinical Utility of Lipoprotein-Associated Phospholipase A2 as a Cardiovascular Risk Marker," *American Journal of Cardiology*, vol. 101, no. 12, pp. S41–S50, 2008.

[80] M. Ali and M. Madjid, "Lipoprotein-associated phospholipase A2: a cardiovascular risk predictor and a potential therapeutic target," *Future Cardiology*, vol. 5, no. 2, pp. 159–173, 2009.

[81] C. Fèvre, S. Bellenger, A.-S. Pierre et al., "The metabolic cascade leading to eicosanoid precursors - Desaturases, elongases, and phospholipases A2 - Is altered in Zucker fatty rats," *Biochimica et Biophysica Acta (BBA) - Molecular and Cell Biology of Lipids*, vol. 1811, no. 6, pp. 409–417, 2011.

[82] C. Mai, B. Wang, J. Wen, X. Lin, and J. Niu, "Lipoprotein-associated phospholipase A2 and AGEs are associated with cardiovascular risk factors in women with history of gestational diabetes mellitus," *Gynecological Endocrinology*, vol. 30, no. 3, pp. 241–244, 2014.

[83] M. Insenser, R. Montes-Nieto, M. Angeles Martinez-Garcia, and H. F. Escobar-Morreale, "A nontargeted study of muscle proteome in severely obese women with androgen excess compared with severely obese men and nonhyperandrogenic women," *European Journal of Endocrinology*, vol. 174, no. 3, pp. 389–398, 2016.

[84] C. A. Stuart, W. L. Stone, M. E. Howell et al., "Myosin content of individual human muscle fibers isolated by laser capture microdissection," *American Journal of Physiology-Cell Physiology*, vol. 310, no. 5, pp. C381–C389, 2016.

[85] X. Liu, N. Takeda, and N. S. Dhalla, "Myosin light-chain phosphorylation in diabetic cardiomyopathy in rats," *Metabolism - Clinical and Experimental*, vol. 46, no. 1, pp. 71–75, 1997.

Hindawi
Evidence-Based Complementary and Alternative Medicine
Volume 2018, Article ID 7926452, 9 pages
https://doi.org/10.1155/2018/7926452

Research Article

"Diabetes and Metabolism Disorders Medicinal Plants: A Glance at the Past and a Look to the Future 2018": Antihyperglycemic Activity of *Hamelia patens* Jacq. Extracts

Catalina Rugerio-Escalona,[1] Cynthia Ordaz-Pichardo,[2] Elvia Becerra-Martinez,[3] María del Carmen Cruz-López,[1] Victor E. López-y-López,[1] Aarón Mendieta-Moctezuma,[1] Ignacio E. Maldonado-Mendoza,[4] and Fabiola E. Jiménez-Montejo[1]

[1]*Centro de Investigación en Biotecnología Aplicada del Instituto Politécnico Nacional, Tlaxcala, Mexico*
[2]*Escuela Nacional de Medicina y Homeopatía del Instituto Politécnico Nacional, Ciudad de México, Mexico*
[3]*Centro de Nanociencias y Micro y Nanotecnología del Instituto Politécnico Nacional, Ciudad de México, Mexico*
[4]*Centro Interdisciplinario de Investigación para el Desarrollo Integral Regional, Unidad Sinaloa del Instituto Politécnico Nacional, Sinaloa, Mexico*

Correspondence should be addressed to Fabiola E. Jiménez-Montejo; fejimenezm@ipn.mx

Received 9 April 2018; Revised 21 June 2018; Accepted 31 July 2018; Published 27 August 2018

Academic Editor: Akhilesh K. Tamrakar

Diabetes is one the world's most widespread diseases, affecting over 327 million people and causing about 300,000 deaths annually. Despite great advances in prevention and therapy, existing treatments for this disorder have serious side effects. Plants used in traditional medicine represent a valuable source in the search for new medicinal compounds. *Hamelia patens* Jacq. has been used for treating diabetes and, so far, no reports have been made on the *in vivo* antihyperglycemic activity of this plant. The present study on *H. patens* aimed to test the antihyperglycemic effect of repeated administrations of the crude and fractional methanolic extracts (CME and FME, respectively) on rats with hyperglycemia induced by streptozotocin. After 10 administrations (20 days), each extract had lowered blood glucose to a normal level. The extracts produced effects similar to metformin. Of the five compounds identified by chromatographic analysis of the extracts, epicatechin and chlorogenic acid demonstrated antihyperglycemic effect. The antioxidant activity of the extracts was evidenced by their IC_{50} values (51.7 and 50.7 μg/mL, respectively). The LD_{50} ≥2000 mg/Kg suggests low toxicity for both CME and FME. Thus, considering that the antihyperglycemic and antioxidant effects of metformin and extracts from *H. patens* were comparable, the latter may be efficacious for treating diabetes.

1. Introduction

Diabetes mellitus (DM), characterized by hyperglycemia and related to metabolic disorder [1–3], is a worldwide health problem and still on the increase. According to the International Diabetes Federation (IDF), 327 million people currently suffer from DM, a figure estimated to reach 438 million by 2045. Diabetes type 2 (DM2) is the most common form of this disorder, representing 90% of the total affected population [4, 5].

Today therapeutic alternatives include various drugs administered orally, such as sulfonylureas (metformin), biguanides (glybenclamide), troglitazones (pioglitazone), and inhibitors of DPP-4 (gliptins), SGLT2 (gliflozin), and α-glucosidase (acarbose) [6]. However, the secondary effects of these treatments (e.g., gastrointestinal disorders and hepatotoxicity) [7], have led diabetic patients to seek natural alternatives [8]. At least 1,200 species of medicinal plants are used in traditional medicine for their antidiabetic attributes. A small proportion (450 plants) of such plants have been studied to

explore their effect and of these; only 109 have had their action mechanism analyzed [9–11]. It has been reported that in Mexico more than 383 plant species are employed for DM2 treatment [12].

Hamelia patens Jacq. (Rubiaceae, commonly known as "bayetilla, coralillo, firebush, or scarlet bush") is a subtropical and tropical shrub, native to the Americas (widespread from Florida to Argentina). Endemic to Mexico, it is used in traditional medicine for headaches, diarrhea, stomach ache, wound healing and diabetes, among other applications. Biological studies have demonstrated radical scavenging [13, 14] as well as anti-inflammatory [15], antibacterial [16], and cytotoxic [17] activity by *H. patens*. In an oral glucose tolerance test, this plant demonstrated inhibition of α-glucosidase [18] and a hypoglycemic effect [19]. Phytochemical analysis of the plant has established the presence of isopteropodin, rumberin, palmirin, maruquin, 24-methylenecicloartan-3ß-ol, 24-methylcicloart-24-en-3ß-ol, 2*E*-3,7,11,15,19-pentamethyl-2-eicosaen-1-ol, stigmasterol, ß-sitosterol, ursolic acid, aricin, (+)-catechin, (-)-epicatechin, and (-)-hammelin [20–22]. However, some of these compounds have not been shown to have biological effects.

The aim of the present study was to evaluate the antihyperglycemic effect of methanolic extracts of *H. patens* Jacq., by assessing repeated administrations to a hyperglycemia murine model, induced by streptozotocin (STZ). The extracts were subjected to quantitative phytochemical and chromatographic analysis, as well as examination of their antioxidant activity.

2. Materials and Methods

2.1. Reagents. All reagents were purchased and used without further purification. The Folin-Ciocalteu phenol reagent (F9252), (±)-catechin hydrate (C1788), (-)-epicatechin (E1753), 2,2-diphenyl-1-picrylhydrazyl (D9132), α-glucosidase (from *Saccharomyces cerevisiae*) type I (G5003), 4-nitrophenyl α-D-glucopyranoside (N1377), quercetin (Q4951), and tannic acid (403040) were acquired from Sigma-Aldrich. Aluminum chloride was obtained from Honeywell Fluka and gallic acid from Fermont.

2.2. Plant Material. H. patens leaves were collected in the municipality of Xicotepec de Juarez, in the State of Puebla, Mexico. The aerial parts were dried in the shade at room temperature and ground to a fine powder for extraction.

2.3. Extract Preparation. One kg of plant material (leaves) was subjected to a fractional extraction, using solvents of increasing polarity (hexane, dichloromethane, and methanol). Extraction from another kg of plant material was made separately, using methanol. In each case, the solvent was evaporated under reduced pressure to dryness, and subsequently extracts were lyophilized and stored at 4°C until use. We worked with methanolic extracts; specifically, the fractional methanol extract (FME) and the crude methanol extract (CME).

2.4. Total Phenolic Content. Total content of phenols was measured using the Folin-Ciocalteu method [23], with certain modifications. The reaction mixture was prepared with 0.2 mL of extract (5 mg/mL), 2 mL of solution A (2% Na_2CO_3, 1% $CuSO_4$ and 2.7% potassium sodium tartrate), and 0.4 mL of NaOH (5 N). Subsequently, 0.2 mL of the Folin-Ciocalteu solution (1:1, v/v) was added and the mixture was allowed to stand for 30 minutes at room temperature. Absorbance was measured at 750 nm. The standard curve was constructed based on various concentrations of gallic acid. The content of total phenols was expressed as milligram equivalents of gallic acid per gram of dried extract (mg EGA/g dried extract).

2.5. Total Flavonoid Content. Total flavonoid content was evaluated using an aluminum chloride method with slight modifications [23]. In brief, the reaction mixture consisted of 0.1 mL of extract, 0.30 mL of absolute ethanol, 0.02 mL $AlCl_3$ (10%), 0.02 mL CH_3COOK, and 0.56 mL of distilled water. This was left to stand for 30 min at room temperature and the reading was taken at 415 nm. Flavonoid content was determined from a calibration curve of quercetin and expressed as mg equivalents of quercetin per gram of dried extract (mg EQ/g dried extract).

2.6. Condensed Tannins Content. Tannins content was determined using the vanillin/HCl method [24]. 2 mL of extract was placed in a tube and heated in a water bath at 30°C for 20 min, 0.4 mL were removed from this sample, and then 2 mL of vanillin solution (1% in methanol) were added. The tube was placed in a water bath once again at 30°C for 20 min. Finally, the reading was made at 550 nm and tannins content was expressed as mg of catechin per gram of dried extract (mg ECat/g dried extract) from a standard curve for catechin.

2.7. Antioxidant Activity (DPPH Assay). Antioxidant activity was measured by employing the DPPH method described by Cevallos [25], with a number of modifications. Concentrations of 4, 0.4 and 0.04 mg/mL from each of the extracts were prepared, to which a solution of 2,2-diphenyl-1-picrylhydrazyl radical (DPPH) (133.33 μM) was added, at a ratio of 1:3 (v:v). The mixture was incubated at 37°C for 30 minutes and read at 517 nm. Antioxidant activity was expressed as mean effective concentration (EC_{50}).

2.8. In Vitro α-Glucosidase Inhibitory Activity. The evaluation of α-glucosidase inhibition was determined using Salehi's method [26], with slight modifications. The mixture containing 480 μL of phosphate buffer (0.1 M, pH 6.9), 40 μL of extract (4 mg/mL), and 80 μL of α-glucosidase (0.5 U/mL) was incubated at 37°C for 15 min in 96-well plates. The reaction was initiated by placing 80 μL *p*-nitrophenyl α-D-glucopyranoside solution (*p*-NPG, 5 mM) in phosphate buffer (0.1 M, pH 6.9). After 15 min of incubation at 37°C, the reaction was terminated by adding 320 μL of Na_2CO_3 (0.2 M). α-Glucosidase inhibition was determined by measuring the yellow-colored *p*-nitrophenolate ion released from *p*-NPG at 405 nm with a spectrophotometer. The inhibition of α-glucosidase by the extracts was expressed as the IC_{50} and

compared to the value found for chlorogenic acid, quercetin, and epicatechin.

2.9. Qualitative High-Performance Liquid Chromatography (HPLC) Analysis. Analytical HPLC was carried out using an Agilent 1100 series apparatus equipped with a diode array detector (DAD) (Agilent Technologies), using a XBD-C18 analytical column 4.6 × 150 mm, 3.5 μm particle size (Agilent Technologies), and a column temperature of 60°C. Elution was performed at a flow rate of 1 mL/min with 0.2% formic acid (solvent A) and acetonitrile (solvent B) for the mobile phase. The samples were eluted by applying the following gradient: 100% A as the initial condition for 3 min, 90% A and 10% B for 3 min, 85% A and 15% B for 3 min, 80% A and 20% B for 3 min, 70% A and 30% B for 3 min, 60% A and 40% B for 3 min, and finally 50% A and 50% B for 15 min. At 253, 290, and 349 nm, compounds were detected and identified by comparing them to known standards (caffeic acid, chlorogenic acid, trans-cinnamic acid, trans-ferulic acid, syringic acid, caffeine, (±)-catechin, (-)-epicatechin, kaempferol, naringenin, quercetin, and rutin), based on retention times and UV spectra.

2.10. Experimental Animals. Male (27±2 g) and female (20±2 g) ICR mice and male Wistar rats (180±30 g) were obtained from the Facultad de Estudios Superiores Acatlan, Universidad Nacional Autónoma de Mexico. The mice were housed under standard conditions and given a standard pellet feed and water *ad libitum*. All experiments with animals were authorized by the Ethics Committee of the Escuela Nacional de Medicina y Homeopatía of the Instituto Politécnico Nacional and complied with national and international principles for the care and use of lab animals.

2.11. Acute Oral Toxicity Testing. Toxicity assessment adhered to OECD (Organization of Economic Co-operation and Development) guidelines for testing chemicals (Acute Oral Toxicity–Acute Toxic Class Method, section 423). Three female and three male ICR mice (20-30 g) were given a single oral administration of 300 mg/kg of the plant extracts, after overnight fasting [27]. The control group received only water. Mice were observed for symptoms and weight variation at postadministration intervals of 1, 3, and 4 h and then twice per day for the subsequent 14 days. Animals were kept at 23±2°C and 50% humidity under a 12:12 h light/darkness cycle. They were provided with standard feed and water *ad libitum,* throughout the study. Results made it possible to classify the substance according to the Globally Harmonized System (GHS).

2.12. Streptozotocin-Induced Diabetic Rats. This parameter was explored among 110 male Wistar rats. They were kept at a temperature of 23±3°C and on a 12:12 h light/darkness cycle, with free access to food and water. For the induction of hyperglycemia, all groups of rats (except the healthy control) were administered a single dose of 50 mg/kg of streptozotocin (STZ) intraperitoneally. After three days of administration, the glucose level was measured on reactive strips and animals showing a blood glucose level of ≥ 200 mg/dL were selected for the test groups.

2.13. Antihyperglycemic Activity of H. patens Extracts. Extract concentrations necessary to induce the desired pharmacological responses were taken from previous studies. Rats were divided into eleven groups each consisting of ten animals. Group I: healthy control (water sterile), group II: diabetic control (STZ), group III: vehicle (300 μL propylene glycol, PPG), group IV: metformin (100 mg/kg), group V: acarbose (10 mg/kg), groups VI-VIII: FME extracts at doses of 35, 75, and 150 mg/kg, groups IX-XI: CME extracts at doses of 35, 75, and 150 mg/kg were all administered intragastrically every third day, monitoring the peripheral glucose 48 h postadministration. After the 15th administration, animals were euthanized and a blood sample was obtained for biochemical analysis [28].

2.14. Biochemical Determinations. Serum samples were collected in order to measure glucose concentration (SG), insulin (SIN), total cholesterol (TC), low-density lipoproteins (LDL), high-density lipoproteins (HDL), triglycerides (Tg), creatinine (SCr), urea (SUr), blood urea nitrogen (BUN), alanine aminotransferase (AlT), and aspartate aminotransferase (AsT). Detection was carried out, following the manufacturer's protocol for each diagnostic kit.

2.15. Statistical Analysis. Data are expressed as the mean ± standard error. Statistical differences were evaluated using the Tukey test with the SAS version 9 program. For the evaluation of antihyperglycemic activity and biochemical parameters, the comparison of multiple variance was analyzed by applying the Holm-Bonferroni method, utilizing GraphPad Prism software (version 5.0). In all cases, statistical significance was considered at $p<0.05$.

3. Results and Discussion

CME yield was 8.9% and 5.4% for FME. Chemical compositions of CME and FME are presented in Table 1. As apparent, CME and FME of *H. patens* are an excellent source of tannins, flavonoids, and phenols. Significant differences between CME and FME were apparent in the total content of phenols and flavonoids. The latter extract displayed the highest content of these metabolites. We relate this to the way extracts were obtained. These results concur with those reported by Flores-Sanchez in 2017 [29].

Pathogenesis of DM has been shown to relate to the generation of free radicals especially reactive oxygen species (ROS), glucose oxidation, increased lipid peroxidation, and greater insulin resistance. Recent studies have shown that phenolic compounds are well known for their great capacity for radical scavenging, especially flavonoids which may be effective in the management and prevention of diabetes mellitus, due to interference in the absorption, digestion, and metabolism of carbohydrates [30, 31]. When evaluating the antioxidant activity of both extracts (Table 2), no significant differences were observed between CME and FME in terms

Table 1: Metabolic content of the methanolic extracts of *H. patens*.

Metabolite	FME	CME
Condensed tannins (mg ECat/g of dried extract)	291.30 ± 0.00^{a}	313.20 ± 0.00^{a}
Total phenols (mg EGA/g of dried extract)	335.26 ± 0.20^{b}	322.40 ± 0.20^{c}
Flavonoids (mg EQ/g of dried extract)	399.94 ± 0.02^{d}	308.32 ± 0.02^{e}

Data are expressed as the mean ± SD. ECat: equivalents of catechin; EGA: equivalents of gallic acid; EQ: equivalents of quercetin. The mean values labeled with uppercase letters differ significantly compared to the control.

Table 2: DPPH radical scavenging activity and α-glucosidase inhibition by methanolic extracts of *H. patens*.

Extract	DPPH EC_{50} (μg/mL)	α-glucosidase inhibition (IC_{50} μg/mL)
FME	51.7 ± 1.1	67.8 ± 3.09
CME	50.7 ± 1.3	78.3 ± 1.88
BHT	201.0 ± 0.7	-
Acarbose	-	4996.7 ± 1.22
Epicatechin	-	282.6 ± 2.28
Ursolic acid	-	116.8 ± 1.15
Quercetin	-	2.7 ± 1.05
Chlorogenic acid	-	6167.1 ± 1.16

Data are expressed as the mean ± SD.

of their EC_{50} values (50.7 and 51.7 μg/mL, respectively). However, both extracts presented a better EC_{50} value than BHT, which is a synthetic phenolic antioxidant currently used in food, despite the evidence that it causes enzymatic or lipid alterations, as well as carcinogenic effects and mutagenic activity [32, 33].

α-Glucosidase inhibitors are targeted to delay carbohydrate absorption and reduce postprandial glucose. Several phenolic compounds containing a flavonoid nucleus in their structure are reportedly useful for the control of diabetes by improving glucose and lipid levels [30]. Moreover, studies have demonstrated that quercetin, epicatechin, kaempferol, and naringenin effectively inhibit the α-glucosidase enzyme [31, 34]. Consequently, the α-glucosidase inhibition assay was the first stage in the identification of antidiabetic agents. High α-glucosidase inhibitory activity was found in both extracts (FME IC_{50} = 67.8 and CME IC_{50} = 78.3 μg/mL; Table 2). Thus, the extracts are more active than acarbose (IC_{50}= 4996.6 μg/mL). Contrastingly, our low polarity extracts showed inhibitory activity of less than 10% at a concentration of 4000 μg/mL. However, in 2016 Jiménez [18] established that hexanic and methanol-ethyl acetate extracts of *H. patens* manifest better α-glucosidase inhibitory effect with IC_{50} = 26.07 μg/ml and 30.18 μg/ml, respectively, than dichloromethane-ethyl acetate and methanol-water extracts which did not exhibit activity. Their results coincide with those reported by other authors, who have demonstrated that high polarity extracts are more active than acarbose [35–37].

The compounds in the extracts which produce antagonistic activity are polar in nature and a chromatographic HPLC analysis was performed to determine their composition and identify the possible active principles. By using different standards (Figure 1), the resulting retention times (Table 3) reveal that chlorogenic acid is the main component in both extracts, constituting 13.5% of CME and 19.5% of FME. Catechin and epicatechin were also detected in the extracts, concurring with Wong's description of *H. patens* in 2017 [38]. Looking for a possible explanation for this behaviour, we decided to evaluate the inhibitory activity for the compounds epicatechin, chlorogenic acid, and quercetin, previously identified in the extracts. The first two showed IC_{50} values that were higher than those obtained from FME and CME, with IC_{50} = 282.6 μg/mL for epicatechin and $IC_{50} \geq$ 3000 μg/mL for chlorogenic acid. Notably, our results for chlorogenic acid differ from those previously reported (IC_{50} = 24, 461, 1000 and >2000 μg/mL) [39–42]. Although chlorogenic acid is the main component, the antagonistic activity against the enzyme is low, which does not correlate with the activity that both extracts manifested. Quercetin, previously isolated from *H. patens*, presented a similar inhibitory activity (IC_{50} = 2.7 μg/mL) to the one described by Indrianingsih in 2015 (IC_{50} = 4.2 μg/mL) [2]. A peak at 14.025 minutes was displayed in the spectrum for CME (10.7%) and at 14.075 minutes for FME (4.5%). Likewise, the peak with a retention time of 19.21 indicated a higher concentration for CME (5.9%) than for FME (0.9%). As these two components of low polarity may partly explain the perceived difference in activity, further research is necessary to isolate them for further structural characterization and biological evaluation. Using column chromatography, a light brown amorphous solid with a melting point of 236-238°C was isolated from CME. Nuclear magnetic resonance (NMR) analysis made it possible to identify a 3-flavonol skeleton, and the ^{1}H and ^{13}C NMR spectra and two-dimensional spectra established the structure as (-)-epicatechin, concurring with a recent report for *H. patens* [43]. The chemical shifts for this compound in the ^{1}H and ^{13}C NMR are presented in Table 4.

The second stage of the current study intended to explore the antihyperglycemic effect of the extracts in an *in vivo* murine model. The extracts were administered 15 times to rats

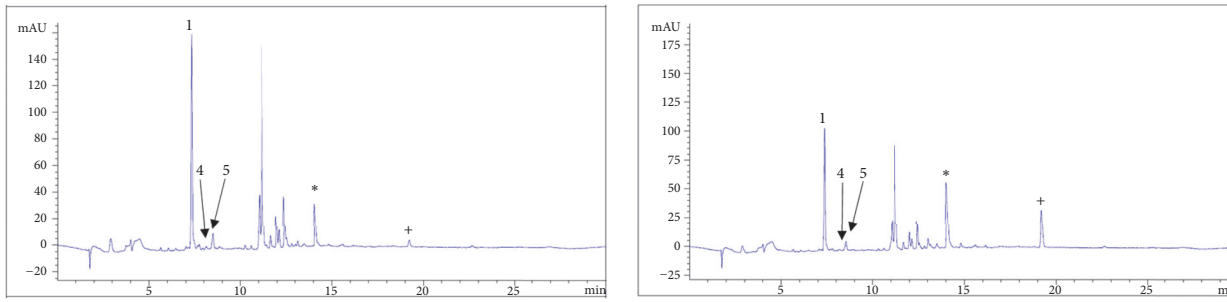

(a) FME (b) CME

Figure 1: HPLC chromatogram of fractional (FME) and crude (CME) methanolic extracts of *H. patens*. (1) chlorogenic acid, (4) catechin, and (5) (-) epicatechin. *Different component. +Different concentration.

Table 3: The retention time of phenolic compounds at 290 nm.

Number	Standard	Retention time (R_t) min
1	Chlorogenic acid	7.406
2	Caffeine	7.846
3	Caffeic acid	7.950
4	Epicatechin	8.417
5	Catechin	8.518
6	Syringic acid	8.639
7	Rutin	11.196
8	*trans*-Ferulic acid	11.326
9	Hesperidin	13.164
10	Quercetin	15.262
11	*trans*-Cinnamic acid	16.126
12	Naringenin	16.583
13	Kaempferol	16.920

Table 4: ^{1}H (400 MHz) and ^{13}C (100 MHz) NMR spectroscopic data for compound 1 in CD_3OD.

Position	δ_C	Type	δ_H, multiplicity (J in Hz)
C-2	80.0	CH	4.816, sl (8, 1.6)
C-3	67.6	CH	4.17, sept (16.8, 3.2, 1.6)
C-4	29.4	CH_2	2.86, dd (16.8, 4.4, α) 2.73, dd (16.8, 2.8, b)
C-4a	100.2	C	
C-5	158.1	C	
C-6	96.55	CH	5.94, d (2.4)
C-7	157.8	C	
C-8	96.05	CH	5.92, d (2.4)
C-8a	157.5	C	
C-1'	132.4	C	
C-2'	116.0	CH	6.97, d (2)
C-3'	145.9	C	
C-4'	146.1	C	
C-5'	115.5	CH	6.75, d (8)
C-6'	119.6	CH	6.79, dd (8, 2)

with hyperglycemia induced by STZ (glucose levels higher 300 mg/dL). FME and CME extracts produced a reduction in glucose concentration (Table 5), which reached a normal level after 10 administrations. At a concentration of 150 mg/kg, extracts showed a greater decrease in glucose level. Likewise, the extracts and metformin exhibited a decrease in serum insulin compared to the diabetic control. However in the diabetic control as well as in acarbose, this behaviour was not observed. Some studies explain that this increase in insulin levels is due to resistance to insulin, which leads to peripheral hyperglycemia and major insulin secretion, a process known as compensatory hyperinsulinemia [44, 45]. Levels of serum creatinine (SCr), serum urea (SUr), and blood urea nitrogen (BUN) were measured in order to assess the effects on the kidney, as this damage is one of the main collateral effects of hyperglycemia. The malfunction of this organ leads to an increase in metabolic waste products in the blood [46]. The 150 mg/kg concentration of CME and FME results in the best protective effect in relation to SCr, and no

Table 5: Glucose levels and serum insulin in experimental rats.

Sample	SG (mg/dL)	SIN (mUI/mL)
HC	112.70 ± 22.11	2.10 ± 1.27
DC	437.50 ± 0.71$^{###}$	2.50 ± 1.31
DCV	429.00 ± 2.83	1.95 ± 0.07
Metformin	123.90 ± 33.99***	1.74 ± 0.06
Acarbose	142.30 ± 31.99***	2.15 ± 0.39
CME 150	93.25 ± 20.22***	1.63 ± 0.71
CME 75	156.00 ± 15.13***	1.33 ± 0.15
CME 35	153.00 ± 30.36***	2.32 ± 1.32
FME 150	117.50 ± 41.35***	1.47 ± 0.55
FME 75	168.80 ± 11.67***	2.00 ± 0.87
FME 35	162.00 ± 28.77***	2.75 ± 0.35

(SG) concentration of glucose; (SIN) insulin; HC: healthy control; DC: diabetic control; DCV: diabetic control vehicle; CME 150: crude methanolic extract at a concentration of 150 mg/kg; CME 75: crude methanolic extract at a concentration of 75 mg/kg; CME 35: crude methanolic extract at a concentration of 35 mg/kg; FME 150: fractional methanolic extract at a concentration of 150 mg/kg; FME 75: fractional methanolic extract at a concentration of 75 mg/kg; FME 35: fractional methanolic extract at a concentration of 35 mg/kg. For the corresponding mean ± SD, $^{###}P < 0.001$ compared to the healthy control and $^{***}P < 0.01$ compared to the diabetic control.

Table 6: Kidney and liver profile of experimental rats.

Sample	SCr (mg/dL)	SUr (mg/dL)	BUN (mg/dL)	AlT (mg/dL)	AsT (μU/mL)
HC	1.20 ± 0.03	47.83 ± 15.20	23.94 ± 6.50	65.33 ± 21.72	156.20 ± 60.50
DC	1.05 ± 0.02	82.50 ± 24.69$^{\pm}$	38.53 ± 11.49	99.33 ± 26.27	208.50 ± 93.26
DCV	0.75 ± 0.01	76.00 ± 27.13	32.08 ± 16.24	61.33 ± 13.20	188.80 ± 81.49
Metformin	0.74 ± 0.02	34.50 ± 10.63$^{\blacksquare}$	20.53 ± 5.04$^{\blacksquare}$	65.50 ± 12.22	145.40 ± 26.60
Acarbose	0.83 ± 0.31	48.33 ± 1.53	22.67 ± 1.16	59.50 ± 14.57	136.00 ± 36.17
CME 150	0.63 ± 0.02	31.25 ± 1.71$^{\blacksquare\blacksquare\blacksquare}$	14.55 ± 0.81$^{\blacksquare}$	73.25 ± 24.68	138.00 ± 22.07
CME 75	0.90 ± 0.10	43.00 ± 3.61$^{\blacksquare}$	20.07 ± 1.65	69.67 ± 11.15	139.30 ± 31.18
CME 35	1.37 ± 0.38	54.33 ± 7.52	26.50 ± 3.66	73.25 ± 14.06	157.80 ± 28.49
FME 150	0.67 ± 0.05	31.50 ± 4.07$^{\blacksquare\blacksquare\blacksquare}$	14.68 ± 2.39$^{\blacksquare\blacksquare}$	45.50 ± 5.07$^{\blacksquare}$	141.00 ± 36.40
FME 75	1.20 ± 0.32	56.00 ± 5.77	24.68 ± 4.02	76.25 ± 19.28	136.30 ± 22.29
FME 35	1.10 ± 0.14	47.00 ± 10.86$^{\blacksquare}$	21.93 ± 5.07	76.75 ± 26.04	134.00 ± 31.23

(SCr) serum creatinine; (SUr) serum urea; (BUN) blood urea nitrogen; (AlT) alanine aminotransferase; (AsT) aspartate aminotransferase; HC: healthy control; DC: diabetic control; DCV: diabetic control vehicle; CME 150: crude methanolic extract at a concentration of 150 mg/kg; CME 75: crude methanolic extract at a concentration of 75 mg/kg; CME 35: crude methanolic extract at a concentration of 35 mg/kg; FME 150: fractional methanolic extract at a concentration of 150 mg/kg; FME 75: fractional methanolic extract at a concentration of 75 mg/kg; FME 35: fractional methanolic extract at a concentration of 35 mg/kg. For the corresponding mean ± SD, $^{\pm}P < 0.05$ compared to health control, $^{\blacksquare}P < 0.05$ compared to the diabetic control, $^{\blacksquare\blacksquare}P < 0.05$ compared to the diabetic control, and $^{\blacksquare\blacksquare\blacksquare}P < 0.05$ compared to the diabetic control.

Table 7: Lipid profile (mg/dL) among experimental rats.

Sample	TC	Tg	LDL	HDL
HC	68.60 ± 12.93	104.80 ± 25.42	17.00 ± 4.97	35.75 ± 7.27
DC	53.00 ± 10.00	160.30 ± 71.30	12.60 ± 3.58	24.40 ± 8.73
DCV	64.50 ± 5.32	147.30 ± 73.58	12.67 ± 6.43	34.25 ± 5.06
Metformin	58.38 ± 10.70	83.29 ± 20.86	21.83 ± 4.92	32.33 ± 10.93
Acarbose	48.25 ± 7.50	47.75 ± 13.10$^{\blacksquare\blacksquare}$	22.25 ± 10.81	18.75 ± 1.5
CME 150	61.50 ± 5.80	94.75 ± 13.38	13.33 ± 1.16	36.25 ± 3.59$^{\blacktriangle}$
CME 75	54.67 ± 7.37	47.67 ± 6.03$^{\blacksquare}$	32.00 ± 2.00$^{\blacksquare\blacksquare}$	13.33 ± 4.16$^{\Diamond\pm}$
CME 35	44.00 ± 7.07	50.25 ± 16.76$^{\blacksquare}$	17.00 ± 4.08	20.33 ± 8.39
FME 150	77.00 ± 8.20	99.25 ± 5.85	27.67 ± 6.81$^{\blacksquare}$	41.25 ± 4.19$^{\blacksquare\blacksquare\blacktriangle}$
FME 75	59.75 ± 12.42	76.50 ± 28.69	26.67 ± 3.06	23.00 ± 1.00
FME 35	60.75 ± 9.00	75.75 ± 48.42	29.67 ± 5.51$^{\blacksquare}$	22.33 ± 3.51

(TC) total cholesterol; (Tg) triglycerides; (LDL) low-density lipoproteins; (HDL) high-density lipoproteins; HC, healthy control; DC, diabetic control; DCV, diabetic control vehicle; CME 150, crude methanolic extract at a concentration of 150 mg/kg; CME 75, crude methanolic extract at a concentration of 75 mg/kg; CME 35, crude methanolic extract at a concentration of 35 mg/kg; FME 150, fractional methanolic extract at a concentration of 150 mg/kg; FME 75, fractional methanolic extract at a concentration of 75 mg/kg; FME 35, fractional methanolic extract at a concentration of 35 mg/kg. For the corresponding mean ± SD: $^{\blacksquare}P < 0.05$ compared to the diabetic control, $^{\blacksquare\blacksquare}P < 0.05$ compared to the diabetic control, $^{\pm}P < 0.05$ compared to health control, $^{\blacktriangle}P < 0.05$ compared to acarbose, $^{\Diamond}P < 0.05$ compared to metformin.

difference was observed between the two extracts (Table 6). Enzymes AlT and AsT are an indicator of liver injury, as enzymes leaking from cytosol liver cells into bloodstream correlate with insulin resistance, diabetes, and inflammatory processes of the liver [47, 48]. FME induced a marked decrease in AlT, making further histopathological studies necessary to confirm whether there is protection or damage to the liver as a result of the treatments. The effect of the extracts on the lipid profile was also examined (Table 7). Patients with DM type 2 have been characterized by high triglycerides levels, low high-density lipoprotein cholesterol (HDL) levels, normal low-density lipoprotein (LDL) levels, and normal or slightly increased total cholesterol levels [49–51]. This characteristic was observed in the group treated with extracts and diabetic control, where no significant differences were evident between treatments in terms of total cholesterol; nevertheless a sharp decline in triglyceride value was perceived in the acarbose and CME treatments (75 and 35 mg/kg). The capacity of acarbose for lowering triglycerides has been described previously, finding that 200 mg constitutes an effective dose for reducing the risk of cardiovascular events in humans, implying a minimal risk of hypoglycemia [52, 53]. Various studies have provided evidence that phenolic compounds such as flavonoids may be involved in decreased glucose levels in the *in vivo* model. It has been suggested that the flavonoids naringenin and hesperetin may produce antiatherogenic effects, partly by means of the activation of the peroxisome proliferator activated receptor gamma PPAR-γ and the upregulation of adiponectin expression in adipocytes. Numerous reports document the antidiabetic effects of flavan-3-ols, especially epigallocatechin gallate (EGCG), in animals and cell-cultures. EGCG can elicit

various changes that are associated with beneficial effects for diabetes, including improvements in insulin secretion, glucose uptake, insulin resistance, glucose tolerance, oxidative stress, inflammation, and mitochondrial function [54, 55]. CME and FME comprise a mixture of compounds and appear to inhibit the α-glucosidase enzyme; however the inhibitory activity of the identified compounds suggests that this is not the only way to reduce hyperglycemia. As this is a mixture of multitarget molecules, it is impossible to assess the antihyperglycemic mechanism, as this would imply identifying the two additional compounds and performing complementary studies. For the acute toxicity study which involved dosing ≥2000 mg/kg, there was no apparent mortality, suggesting low toxicity, within category 5 according to the OECD Globally Harmonized Classification System (GHS) (2014) [27]. This is advantageous should you wish to concoct an herbal preparation.

4. Conclusions

These results reveal that extracts of *Hamelia patens* with a high content of phenolic compounds elicit α-glucosidase inhibition and an antihyperglycemic effect. At a concentration of 150 mg/kg, they produce an equivalent effect to metformin. Epicatechin and chlorogenic acid contribute to the antihyperglycemic activity of *H. patens*; however it is necessary to carry out the structural identification of any other components present. Further research is necessary to elucidate the activity mechanisms.

Data Availability

The data used to support the findings of this study are available from the corresponding author upon request.

Conflicts of Interest

The authors declare that there are no conflicts of interest regarding the publication of this paper.

Acknowledgments

The authors are grateful for technical support provided by the personnel at the Laboratory of Natural Products and Molecular Biology of the ENMyH at IPN. Catalina Rugerio-Escalona thanks CONACYT for the graduate scholarships awarded (264517) and SIP-IPN (BEIFI) for a complementary scholarship. Cynthia Ordaz-Pichardo, Fabiola E. Jiménez-Montejo, Ignacio E. Maldonado-Mendoza, María del Carmen Cruz-López, and Victor E. López-y-López are Fellows of the Estímulos al Desempeño de los Investigadores (EDI)-IPN. Cynthia Ordaz-Pichardo, Ignacio E. Maldonado-Mendoza, María del Carmen Cruz-López, and Victor E. López-y-López thank the Comisión de Operación y Fomento de Actividades Académicas (COFAA), an IPN program that provides support to researchers. This work was financially supported by a project (20161781) from the Secretaría de Investigación y Posgrado, Instituto Politécnico Nacional.

References

[1] F. A. Matough, S. B. Budin, Z. A. Hamid, N. Alwahaibi, and J. Mohamed, "The role of oxidative stress and antioxidants in diabetic complications," *SQU Medical Journal*, vol. 12, no. 1, pp. 5–18, 2012.

[2] A. W. Indrianingsih, S. Tachibana, R. T. Dewi, and K. Itoh, "Antioxidant and α-glucosidase inhibitor activities of natural compounds isolated from *Quercus gilva* Blume leaves," *Asian Pacific Journal of Tropical Biomedicine*, vol. 5, no. 9, pp. 748–755, 2015.

[3] M. Gondi and U. J. S. Prasada Rao, "Ethanol extract of mango (*Mangifera indica* L.) peel inhibits α-amylase and α-glucosidase activities, and ameliorates diabetes related biochemical parameters in streptozotocin (STZ)-induced diabetic rats," *Journal of Food Science and Technology*, vol. 52, no. 12, pp. 7883–7893, 2015.

[4] A. Rayar and R. Manivannan, "In-vitro alpha-amylase and alpha-glucosidase inhibition activity of umbelliferone and beta-ionone isolated from *Coriandrum sativum* Linn," *World Journal of Pharmacy and Pharmaceutical Sciences*, vol. 5, no. 1, pp. 1280–1289, 2016.

[5] *Atlas de la Diabetes de la FID-Octava edición*, International Diabetes Federation, 2017.

[6] American Diabetes Association, "Pharmacologic Approaches to Glycemic Treatment," *Journal of Clinical and Applied Resarch and Education*, vol. 40, no. 1, pp. S64–S76, 2017.

[7] J. J. Marín-Peñalver, I. Martín-Timón, C. Sevillano-Collantes, and F. J. del Cañizo-Gómez, "Update on the treatment of type 2 diabetes mellitus," *World Journal of Diabetes*, vol. 7, no. 17, pp. 354–395, 2016.

[8] H.-Y. Chang, M. Wallis, and E. Tiralongo, "Use of complementary and alternative medicine among people living with diabetes: literature review," *Journal of Advanced Nursing*, vol. 58, no. 4, pp. 307–319, 2007.

[9] A. B. Medagama and R. Bandara, "The use of Complementary and Alternative Medicines (CAMs) in the treatment of diabetes mellitus: Is continued use safe and effective?" *Nutrition Journal*, vol. 13, no. 1, 2014.

[10] B. Baharvand-Ahmadi, M. Bahmani, P. Tajeddini, N. Naghdi, and M. Rafieian-Kopaei, "An ethno-medicinal study of medicinal plants used for the treatment of diabetes," *Journal of Nephropathology*, vol. 5, no. 1, pp. 44–50, 2016.

[11] S. Verma, M. Gupta, H. Popli, and G. Aggarwal, "Diabetes mellitus treatment using herbal drugs," *International Journal of Phytomedicine*, vol. 10, no. 1, pp. 1–10, 2018.

[12] B. Ovalle-Magallanes, O. N. Medina-Campos, J. Pedraza-Chaverri, and R. Mata, "Hypoglycemic and antihyperglycemic effects of phytopreparations and limonoids from *Swietenia humilis*," *Phytochemistry*, vol. 110, pp. 111–119, 2015.

[13] S. Singh and M. Vyas, "Comparative *in-vitro* biological study of aerial parts of plant *Hamelia patens*," *International Journal of Pharmaceutical Sciences and Research*, vol. 7, no. 4, pp. 1793–1808, 2016.

[14] F. Ruiz-Terán, A. Medrano-Martínez, and A. Navarro-Ocaña, "Antioxidant and free radical scavenging activities of plant extracts used in traditional medicine in Mexico," *African Journal of Biotechnology*, vol. 7, no. 12, pp. 1886–1893, 2008.

[15] S. Sosa, M. J. Balick, R. Arvigo et al., "Screening of the topical anti-inflammatory activity of some Central American plants," *Journal of Ethnopharmacology*, vol. 81, no. 2, pp. 211–215, 2002.

[16] A. Camporese, M. J. Balick, R. Arvigo et al., "Screening of anti-bacterial activity of medicinal plants from Belize (Central

America)," *Journal of Ethnopharmacology*, vol. 87, no. 1, pp. 103–107, 2003.

[17] G. Mena-Rejon, E. Caamal-Fuentes, Z. Cantillo-Ciau, R. Cedillo-Rivera, J. Flores-Guido, and R. Moo-Puc, "*In vitro* cytotoxic activity of nine plants used in Mayan traditional medicine," *Journal of Ethnopharmacology*, vol. 121, no. 3, pp. 462–465, 2009.

[18] V. Jiménez-Suárez, A. Nieto-Camacho, M. Jiménez-Estrada, and B. Alvarado Sánchez, "Anti-inflammatory, free radical scavenging and alpha-glucosidase inhibitory activities of *Hamelia patens* and its chemical constituents," *Pharmaceutical Biology*, vol. 54, no. 9, pp. 1822–1830, 2016.

[19] A. Andrade-Cetto, S. Escandón-Rivera, and V. Garcia-Luna, "Hypoglycemic effect of *Hamelia patens* Jacq., aerial part in STZ-NA-induced diabetic rats," *Pharmacologyonline*, vol. 3, pp. 65–69b, 2015.

[20] A. Ahmad, A. Pandurangan, N. Singh, and P. Ananad, "A mini review on chemistry and biology of *Hamelia Patens* (Rubiaceae)," *Pharmacognosy Journal*, vol. 4, no. 29, pp. 1–4, 2012.

[21] J. Bano, S. Santra, and E. Menghani, "*Hamelia patens* a potential plant from Rubiaceae family: A review," *International Journal of Scientific & Engineering Research*, vol. 6, no. 12, pp. 960–973, 2015.

[22] E. C. Cruz and A. Andrade-Cetto, "Ethnopharmacological field study of the plants used to treat type 2 diabetes among the Cakchiquels in Guatemala," *Journal of Ethnopharmacology*, vol. 159, pp. 238–244, 2015.

[23] D. A. Sampietro, M. A. Sgariglia, J. R. Soberón, E. N. Quiroga, and M. A. Vattuone, "Colorimetric reactions," in *Isolation, Identification and Characterization of Allelochemicals/Natural Products*, chapter 4, pp. 78–82, 2009.

[24] H. P. S. Makkar and K. Becker, "Vanillin-HCl method for condensed tannins: effect of organic solvents used for extraction of tannins," *Journal of Chemical Ecology*, vol. 19, no. 4, pp. 613–621, 1993.

[25] B. A. Cevallos-Casals and L. Cisneros-Zevallos, "Stoichiometric and kinetic studies of phenolic antioxidants from Andean purple corn and red-fleshed sweetpotato," *Journal of Agricultural and Food Chemistry*, vol. 51, no. 11, pp. 3313–3319, 2003.

[26] P. Salehi, B. Asghari, M. A. Esmaeili, H. Dehghan, and I. Ghazi, "α-Glucosidase and α-amylase inhibitory effect and antioxidant of ten plant extracts traditionally used in Iran for diabetes," *Journal of Medicinal Plants Research*, vol. 7, no. 6, pp. 257–266, 2013.

[27] OECD/OCDE 423, *OECD Guideline for testing of chemicals, Acute Oral Toxicity – Acute Toxic Class Method*, Environment Directorate Organisation for Economic Co-Operation and Development, Paris, France, 2001.

[28] B. L. Furman, "Streptozotocin-induced diabetic models in mice and rats," *Current Protocols in Pharmacology*, vol. 70, pp. 5.47.1–5.47.20, 2015.

[29] I. J. Flores-Sanchez and A. C. Ramos-Valdivia, "A review from patents inspired by two plant genera: *Uncaria* and *Hamelia*," *Phytochemistry Reviews*, vol. 16, no. 4, pp. 693–723, 2017.

[30] R. Vinayagam and B. Xu, "Antidiabetic properties of dietary flavonoids: A cellular mechanism review," *Journal of Nutrition and Metabolism*, vol. 12, no. 60, pp. 1–20, 2015.

[31] S. Marella, "Flavonoids-The most potent poly-phenols as antidiabetic agents: an overview," *Modern Approaches in Drug Designing*, vol. 1, no. 3, pp. 2–5, 2017.

[32] A. Ullah, A. Khan, and I. Khan, "Diabetes mellitus and oxidative stress-A concise review," *Saudi Pharmaceutical Journal*, vol. 24, pp. 547–553, 2016.

[33] D. Shasha, C. Magogo, and P. Dzomba, "Reversed phase HPLC-UV Quantitation of BHA, BHT and TBHQ in food items sold in bindura supermarkets, Zimbabwe," *International Research Journal of Pure & Applied Chemistry*, vol. 4, no. 5, pp. 578–584, 2014.

[34] M. Vessal, M. Hemmati, and M. Vasei, "Antidiabetic effects of quercetin in streptozocin-induced diabetic rats," *Comparative Biochemistry and Physiology Part C: Toxicology & Pharmacology*, vol. 135, no. 3, pp. 357–364, 2003.

[35] P.-C. Hsieh, G.-J. Huang, Y.-L. Ho et al., "Activities of antioxidants, α-glucosidase inhibitors and aldose reductase inhibitors of the aqueous extracts of four *Flemingia* species in Taiwan," *Botanical Studies*, vol. 51, no. 3, pp. 293–302, 2010.

[36] W. Kang, Y. Song, and X. Gu, "α-glucosidase inhibitory *in vitro* and antidiabetic activity *in vivo* of *Osmanthus fragrans*," *Journal of Medicinal Plants Research*, vol. 6, no. 14, pp. 2850–2856, 2012.

[37] N. Zahratunnisa, B. Elya, and A. Noviani, "Inhibition of Alpha-glucosidase and antioxidant test of stem bark extracts of *Garcinia fruticosa* Lauterb," *Pharmacognosy Journal*, vol. 9, no. 2, pp. 273–275, 2017.

[38] J. E. Wong, C. Rubio, A. Reyes, C. N. Aguilar, and M. L. Carrillo, "Phenolic content and antibacterial activity of extracts of *Hamelia patens* obtained by different extraction methods," *Brazilian Journal of Microbiology*, vol. 49, no. 3, pp. 656–661, 2017.

[39] G. Oboh, O. M. Agunloye, S. A. Adefegha, A. J. Akinyemi, and A. O. Ademiluyi, "Caffeic and chlorogenic acids inhibit key enzymes linked to type 2 diabetes (in vitro): a comparative study," *Journal of Basic and Clinical Physiology and Pharmacology*, vol. 26, no. 2, pp. 165–170, 2015.

[40] S.-Y. Chiou, J.-M. Sung, P.-W. Huang, and S.-D. Lin, "Antioxidant, Antidiabetic, and Antihypertensive Properties of *Echinacea purpurea* Flower Extract and Caffeic Acid Derivatives Using *in Vitro* Models," *Journal of Medicinal Food*, vol. 20, no. 2, pp. 171–179, 2017.

[41] C.-M. Ma, M. Hattori, M. Daneshtalab, and L. Wang, "Chlorogenic acid derivatives with alkyl chains of different lengths and orientations: Potent α-glucosidase inhibitors," *Journal of Medicinal Chemistry*, vol. 51, no. 19, pp. 6188–6194, 2008.

[42] C. Tan, Q. Wang, C. Luo, S. Chen, Q. Li, and P. Li, "Yeast α-glucosidase inhibitory phenolic compounds isolated from *Gynura medica* leaf," *International Journal of Molecular Sciences*, vol. 14, no. 2, pp. 2551–2558, 2013.

[43] A. I. Suárez, B. Diaz, S. Tillett, E. Valdivieso, and R. S. Compagnone, "Leishmanicidal activity of alkaloids from *Hamelia patens*," *Ciencia*, vol. 16, no. 2, pp. 148–155, 2008.

[44] C. Gutiérrez-Rodelo, A. Roura-Guiberna, and J. A. Olivares-Reyes, "Mecanismos moleculares de la resistencia a la insulina: una actualización," *Gaceta Médica de México*, vol. 153, pp. 215–228, 2017.

[45] J. Rojas, V. Berm, E. Leal, V. Bermúdez et al., "Insulinoresistencia e hiperinsulinemia como factores de riesgo para enfermedad cardivascular," *Revista Latinoamericana de Hipertensión*, vol. 2, no. 6, pp. 179–190, 2007.

[46] S. A. Bamanikar, A. A. Bamanikar, and A. Arora, "Study of serum urea and creatinine in diabetic and non-diabetic patients in a tertiary teaching hospital," *The Journal of Medical Research*, vol. 2, no. 1, pp. 12–15, 2016.

[47] M. Music, A. Dervisevic, E. Pepic et al., "Metabolic Syndrome and Serum Liver Enzymes Level at Patients with Type 2 Diabetes Mellitus," *Medical Archives*, vol. 69, no. 4, pp. 251–255, 2015.

[48] S. Kazemi, S. Asgary, J. Moshtaghian et al., "Liver-protective effects of hydroalcoholic extract of *Allium hirtifolium* Boiss in rats with alloxan-induced diabetes mellitus," *ARYA Atherosclerosis Journal*, vol. 6, no. 1, pp. 11–15, 2010.

[49] G. A. Bonneau, M. S. Castillo Rascón, R. A. Sánchez, W. R. Pedrozo, and C. Castro Olivera, "Colesterol-IDL y parámetros lipídicos en diabéticos tipo 2," *Revista Argentina de Endocrinología y Metabolismo*, vol. 44, no. 4, pp. 215–222, 2007.

[50] A. Husni, D. Purwanti, and Ustadi, "Blood glucose level and lipid profile of streptozotocin-induced diabetes rats treated with sodium alginate from *Sargassum crassifolium*," *Journal of Biological Sciences*, vol. 16, no. 3, pp. 58–64, 2016.

[51] S. Palazhy and V. Viswanathan, "Lipid abnormalities in type 2 diabetes mellitus patients with overt nephropathy," *Diabetes & Metabolism Journal*, vol. 41, no. 2, pp. 128–134, 2017.

[52] J. J. DiNicolantonio, J. Bhutani, and J. H. O'Keefe, "Acarbose: safe and effective for lowering postprandial hyperglycaemia and improving cardiovascular outcomes," *Open Heart*, vol. 2, no. 1, 2015.

[53] S. Ogawa, K. Takaeuchi, and S. Ito, "Acarbose lowers serum triglyceride and postprandial chylomicron levels in type 2 diabetes," *Diabetes, Obesity and Metabolism*, vol. 6, no. 5, pp. 384–390, 2004.

[54] L. Liu, S. Shan, K. Zhang, Z.-Q. Ning, X.-P. Lu, and Y.-Y. Cheng, "Naringenin and hesperetin, two flavonoids derived from *Citrus aurantium* up-regulate transcription of adiponectin," *Phytotherapy Research*, vol. 22, no. 10, pp. 1400–1403, 2008.

[55] E. P. Cai and J.-K. Lin, "Epigallocatechin gallate (EGCG) and rutin suppress the glucotoxicity through activating IRS2 and AMPK signaling in rat pancreatic β cells," *Journal of Agricultural and Food Chemistry*, vol. 57, no. 20, pp. 9817–9827, 2009.

Hindawi
Evidence-Based Complementary and Alternative Medicine
Volume 2018, Article ID 5269731, 10 pages
https://doi.org/10.1155/2018/5269731

Research Article

Synergistic Effect of Bupleuri Radix and Scutellariae Radix on Adipogenesis and AMP-Activated Protein Kinase: A Network Pharmacological Approach

Jueun Lee,[1] Jinbong Park,[1,2] Hyewon Park,[3] Dong-Hyun Youn,[1,2] Jaehoon Lee,[4] Seokbeom Hong,[4] and Jae-Young Um[1,2]

[1]*Department of Pharmacology, College of Korean Medicine, Kyung Hee University, Seoul, Republic of Korea*
[2]*Basic Research Laboratory for Comorbidity Regulation, Comorbidity Research Institute, Kyung Hee University, Seoul, Republic of Korea*
[3]*Department of Biological Sciences in Korean Medicine, Graduate School, Kyung Hee University, Seoul, Republic of Korea*
[4]*Department of Korean Medicine, Graduate School, Kyung Hee University, Seoul, Republic of Korea*

Correspondence should be addressed to Jae-Young Um; jyum@khu.ac.kr

Received 20 April 2018; Revised 11 July 2018; Accepted 26 July 2018; Published 23 August 2018

Academic Editor: Hilal Zaid

Obesity has become a major health threat in developed countries. However, current medications for obesity are limited because of their adverse effects. Interest in natural products for the treatment of obesity is thus rapidly growing. Korean medicine is characterized by the wide use of herbal formulas. However, the combination rule of herbal formulas in Korean medicine lacks experimental evidence. According to *Shennong's Classic of Materia Medica*, the earliest book of herbal medicine, Bupleuri Radix (BR) and Scutellariae Radix (SR) possess the Sangsoo relationship, which means they have synergistic features when used together. Therefore these two are frequently used together in prescriptions such as Sosiho-Tang. In this study, we used the network pharmacological method to predict the interaction between these two herbs and then investigated the effects of BR, SR, and their combination on obesity in 3T3-L1 adipocytes. BR, SR, and BR-SR mixture significantly decreased lipid accumulation and the expressions of two major adipogenic factors, peroxisome proliferator-activated receptor-gamma (PPARγ) and CCAAT/enhancer-binding protein-alpha (C/EBPα), and their downstream genes, *Adipoq*, *aP2,* and *Lipin1* in 3T3-L1 cells. In addition, the BR-SR mixture had synergistic effects compared with BR or SR on inhibition of adipogenic-gene expressions. BR and SR also inhibited the protein expressions of PPARγ and C/EBPα. Furthermore, the two extracts successfully activated AMP-activated protein kinase alpha (AMPK α), the key regulator of energy metabolism. When compared to those of BR or SR, the BR-SR mixture showed higher inhibition rates of PPARγ and C/EBPα, along with higher activation rate of AMPK. These results indicate a new potential antiobese pharmacotherapy and also provide scientific evidence supporting the usage of herbal combinations instead of mixtures in Korean medicine.

1. Introduction

The epidemiology of obesity is constantly increasing, becoming a health threat all over the world. The World Health Organization has reported that over 1.4 billion adults worldwide are overweight (BMI $\geq$ 25 kg/m^2) or obese (BMI $\geq$ 30 kg/m^2) [1]. However, there are only 5 treatments (orlistat, lorcaserin, liraglutide, phentermine/topiramate, and bupropion/naltrexone) approved by the United States Food and Drug Administration. Despite their efficacies, adverse effects of these drugs lead to search for other options [2].

Obesity is caused by a simple process: when energy intake exceeds expenditure, the excess energy is saved in as a form of lipid. On the other hand, in the perspective of selecting treatments, there are more than pathways to resolve this metabolic syndrome. Pharmacological approach for obesity treatment can be subcategorized into two methods: inhibiting lipid accumulation or consuming accumulated lipids. Former

method inhibits lipid accumulation in adipose tissues by decreasing appetite, lowering fat absorption, and inhibiting adipogenesis, and the latter is by increasing energy expenditure via fatty acid oxidation or brown adipose tissue- (BAT-) related thermogenesis [3]

Network pharmacology is a system biology-based methodology for pharmacological research [4, 5]. Network pharmacological research replaces the dominant paradigm of drug design based on "one gene, one drug, one disease," into multitarget drugs that act on biological networks. These unique characteristics of network pharmacology expand the potential use of traditional herbal medicine including Korean medicine, Japanese Kampo medicine, and Traditional Chinese Medicine [6]. In this premise, as obesity is a multipathway-involved disease, and the multicomponent-multitarget herbal drugs may provide an answer to its treatment.

Bupleuri Radix (BR) and Scutellariae Radix (SR) are both components of Sosiho-Tang, a traditional Korean herbal formula which is originally used to treat chronic herbal diseases. The antiobese effect of Sosiho-Tang is reported in a study using 3T3-L1 adipocytes and high fat diet- (HFD-) induced obese C57BL/6J mice [7]. In the current study, Yoo et al. show Sosiho-Tang can inhibit adipogenesis by suppressing CCAAT/enhancer-binding protein-alpha (C/EBPα) and peroxisome proliferator-activated receptor-gamma (PPARγ), two key regulators of adipogenesis *in vivo* and *in vitro*. Furthermore, other studies demonstrate that BR can attenuate obesity in rats by regulating adipogenic factors [8], while its active compound saikosaponin A inhibits inflammatory markers in adipocytes [9]. Several reports also demonstrate the antiobese and antiadipogenic effect of SR [10] and its active compounds such as baicalin [11–14], baicalein [15, 16], and wogonin [17–19].

Based on these studies, we expected that BR and SR are the major components of Sosiho-Tang responsible for antiobese effects. They are used for specific types of obesity patients after diagnosis by a Korean medicine practitioner, and, in addition, several experimental studies also report the possibility. According to *Shennong's Classic of Materia Medica*, a classic of oriental medicine introducing 365 kinds of herbs and their features [20], BR and SR are Sangsoo (synergistic) pairs. As a pair of Sangsoo (synergism), our hypothesis herein is that BR and SR may show synergistic effects in obesity-related mechanisms. Therefore, in this study, we evaluate the synergistic potential between BR and SR by the network pharmacological approach and assess their effects on obesity by investigating related mechanisms.

2. Materials and Methods

2.1. Reagents. 3-Isobutylmethylxanthine (IBMX), dexamethasone (Dex), and Insulin were purchased from Sigma Chemicals (St Louis, MO, USA). Dulbecco's modified Eagle's medium (DMEM), penicillin-streptomycin, bovine serum (BS), and fetal bovine serum (FBS) were purchased from Gibco BRL (Grand Island, NY, USA).

Table 1: Nineteen active main components of Scutellariae Radix and Bupleuri Radix.

Scutellariae Radix	Bupleuri Radix
(S)-camphor	(-)-alpha-Pinene
apigenin	(Z,Z)-farnesol
baicalein	Baicalin
Baicalin	beta-Eudesmol
beta-sitosterol	coumarin
scutellarein	kaempferol
palmitic acid	quercetin
wogonin	capsaicin
Linolenic acid methyl ester	saikosaponin a
	oleanolic acid

2.2. Preparation of Water Extracts of BR and SR. BR (the root of Bupleurum falcatum Linne) and SR (the root of Scutellaria baicalensis Georgi), both originated from China, were purchased from Omniherb Co. (Daegu, Republic of Korea) identified by a specialist of herbs. 100 g of BR was extracted in 1000 ml of distilled water at 100°C for 4 h. 100 g of SR was extracted by the same method. Then, the water extracted BR and SR were freeze dried. The yields were 15.9% and 17.6% for BR and SR, respectively. The same amounts of BR and SR were mixed to prepare the BR-SR mixture.

2.3. Network Pharmacological Analysis. The herbal compound-target gene information was analyzed using the Traditional Chinese Medicine Systems Pharmacology Database (TCMSP). The major chemical components of SR and BR were collected and extracted from TCMSP. We collected each 99 and 147 compounds that encompassed the main components of SR and BR, taking into account the relevant reports. Then we selected the 9 and 10 chemical compounds that satisfied an oral bioavailability (OB) $\geq$ 10% and drug-likeness (DL) $\geq$ 0.04 and provide further extraction and optimization of the medicinal ingredients. Nineteen pharmacological ingredients that satisfied the above conditions are showed in Table 1. In a biological network, nodes are visual representations proteins, genes, or metabolites. An edge is a visual representation of a relation. It is a line that connects two nodes and represents biological relationships, such as physical interactions or gene expression regulation [21]. In this study, nodes mean compounds and targets, and edges are relationships between compounds and target. Degree is the number of connected nodes.

To construct a compound-target network, we used Cytoscape 3.6.0 software. By compound-target network, we studied Sangsoo relationships between SR and BR. Multiple targets that participate in 3T3-L1 adipocytes were shared by each compound of SR and BR.

2.4. Cell Culture and Adipocyte Differentiation. 3T3-L1 preadipocytes (American Type Culture Collection, Rockville, MD, USA) was cultured and differentiated as previously described [22]. Briefly, 3T3-L1 preadipocytes were cultured in DMEM containing 1% penicillin-streptomycin and 10%

BS in 6-well plates until confluence at 37°C. Two days after 100% confluence (day 0), cells were differentiated for 48 h in differentiation medium composed of DMEM containing 10% FBS and differentiation inducers (MDI: 0.5 mM IBMX, 1 μM Dex, and 1 μg/ml insulin). From day 2 to day 4, the cells were incubated in culture medium (DMEM plus 10% FBS and 1 μg/ml insulin) supplemented with BR, SR, or BR-SR mixture. Then, at day 4, the medium was changed into fresh culture medium and the cells were cultured for 48 h.

2.5. Cell Viability Assay. Cytotoxicity of BR, SR, and BR-SR mixture was evaluated using the MTS assay, as previously described [23]. The absorbance was measured at 490 nm using a VERSAmax microplate reader (Molecular Devices, Sunnyvale, CA, USA).

2.6. Oil Red O Staining. Intracellular lipid accumulation was measured by Oil Red O staining as previously described [24]. The absorbance, which is proportional to intracellular lipid, was measured at 500 nm with a VERSAmax microplate reader (Molecular Devices, Sunnyvale, CA, USA).

2.7. RNA Isolation and Real-Time Reverse-Transcription Polymerase Chain Reaction (RT-PCR). Total RNA was extracted from BR, SR, or BR-SR mixture-treated cells using QIAzol lysis reagent (Qiagen Sciences Inc., Germantown, MD, USA) and GeneAll RiboEx Total RNA extraction kit (GeneAll Biotechnology, Seoul, Republic of Korea) as previously described [25]. mRNA evaluation was performed using a StepOnePlus Real-time RT-PCR System (Applied Biosystems, Foster City, CA, USA). Primer sequences used in this study are described in Table 2.

2.8. Protein Extraction and Western Blot Analysis. BR, SR, or BR-SR mixture-treated cells were harvested and lysed in Cell Lysis Buffer (Cell Signaling Technology Inc., Danvers, MA, USA). Determination of total protein concentration and western blot analysis were performed as described previously [25, 26].

2.9. Statistical Analysis. Results are expressed as mean ± standard error mean (SEM). Student *t*-test was used to determine statistical relevance. All statistical analyses were performed using GraphPad Prism 5 (GraphPad Software, La Jolla, CA, USA).

Table 2: Primer sequences (5′ to 3′) for real-time RT-PCR.

Genes	5′ to 3′ Oligonucleotide Sequences
Mouse *Pparg*	
Sense (Forward)	TTT TCA AGG GTG CCA GTT TC
Antisense (Reverse)	TTA TTC ATC AGG GAG GCC AG
Mouse *Cebpa*	
Sense (Forward)	GCC GAG ATA AAG CCA AAC AA
Antisense (Reverse)	CCT TGA CCA AGG AGC TCT CA
Mouse *aP2*	
Sense (Forward)	CGTAAATGGGGATTTGGTCA
Antisense (Reverse)	TCGACTTTCCATCCCACTTC
Mouse *Adipoq*	
Sense (Forward)	AGACCTGGCCACTTTCTCCTCATT
Antisense (Reverse)	AGAGGAACAGGAGAGCTTGCAACA
Mouse *Lipin1*	
Sense (Forward)	TTCCTTGTCCCTGAACTGCT
Antisense (Reverse)	TGAAGACTCGCTGTGAATGG
Mouse *Gapdh*	
Sense (Forward)	AAC TTT GGC ATT GTG GAA GG
Antisense (Reverse)	GGA TGC AGG GAT GAT GTT CT

3. Results

3.1. Compound-Compound Target Network Analysis of BR and SR. For prediction analysis of Sangsoo relationship between BR and SR, we constructed the compound-target network (Figure 1(a)) based on data mining. This network consists of 19 compounds and 504 candidate targets in which pink circles and blue ones correspond to active components and targets, respectively. In the relationships between compounds and targets, we found 265 nodes and 504 edges. The means of degree value (the number of associated targets) of the compounds were 18, indicating that most of the compounds regulated multiple targets to exert various therapeutic effects. The mean compounds of each target were 6, showing that most of the targets can interact with multiple compounds simultaneously.

Among the active compounds, quercetin of BR exhibits the highest number of target candidate target interactions (degrees =154), followed by apigenin from SR (degrees = 80), kaempferol from BR (degrees = 59), and wogonin from SR (degrees = 52).

In the 504 targets of active compounds, prostaglandin G/H syntheses 2 showed the highest degree (degrees = 12), which was followed by apoptosis regulator Bcl-2 and caspase-3 (degrees = 10), prostaglandin G/H synthase 1 and phosphatidylinositol-4,5-bisphosphate 3-kinase catalytic subunit, and gamma isoform (degrees = 9). The network pharmacological analysis result demonstrates the potential synergistic effect of SR and BR on adipogenesis and energy expenditure through modulating these relevant proteins.

3.2. BR and SR Inhibit Lipid Accumulation in 3T3-L1 Adipocytes. First, we evaluated the cytotoxicity of BR and SR on 3T3-L1 adipocytes. As shown in Figure 2(a), BR and SR did not affect cell viability up to concentration of 10 μg/ml and 1 μg/ml, respectively, when analyzed by an MTS assay. Further experiments were conducted using concentrations which did not decrease cell viability. Next, to evaluate the effect of BR and SR on lipid accumulation, Oil Red O staining assay was performed. Adipocytes treated with BR and SR both showed concentration-dependent decrease of intracellular lipids (Figure 2(b)).

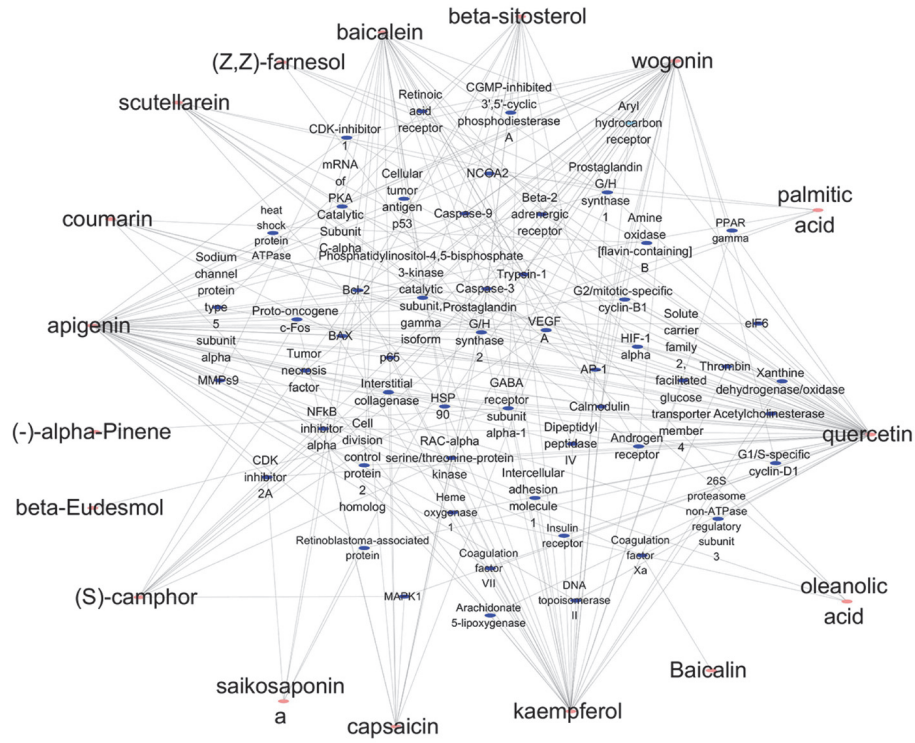

(a)

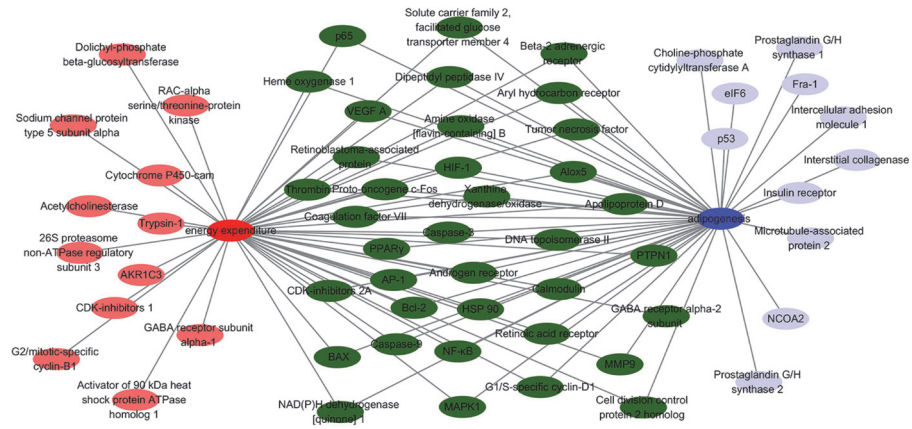

(b)

Figure 1: Compound-compound target network of BR and SR. (a) Compound-compound target network of BR and SR. (b) Synergistic target network of BR and SR. Blue ovals represent targets related in adipogenesis, red ovals represent targets related in energy expenditure, and green ovals represent targets related in both.

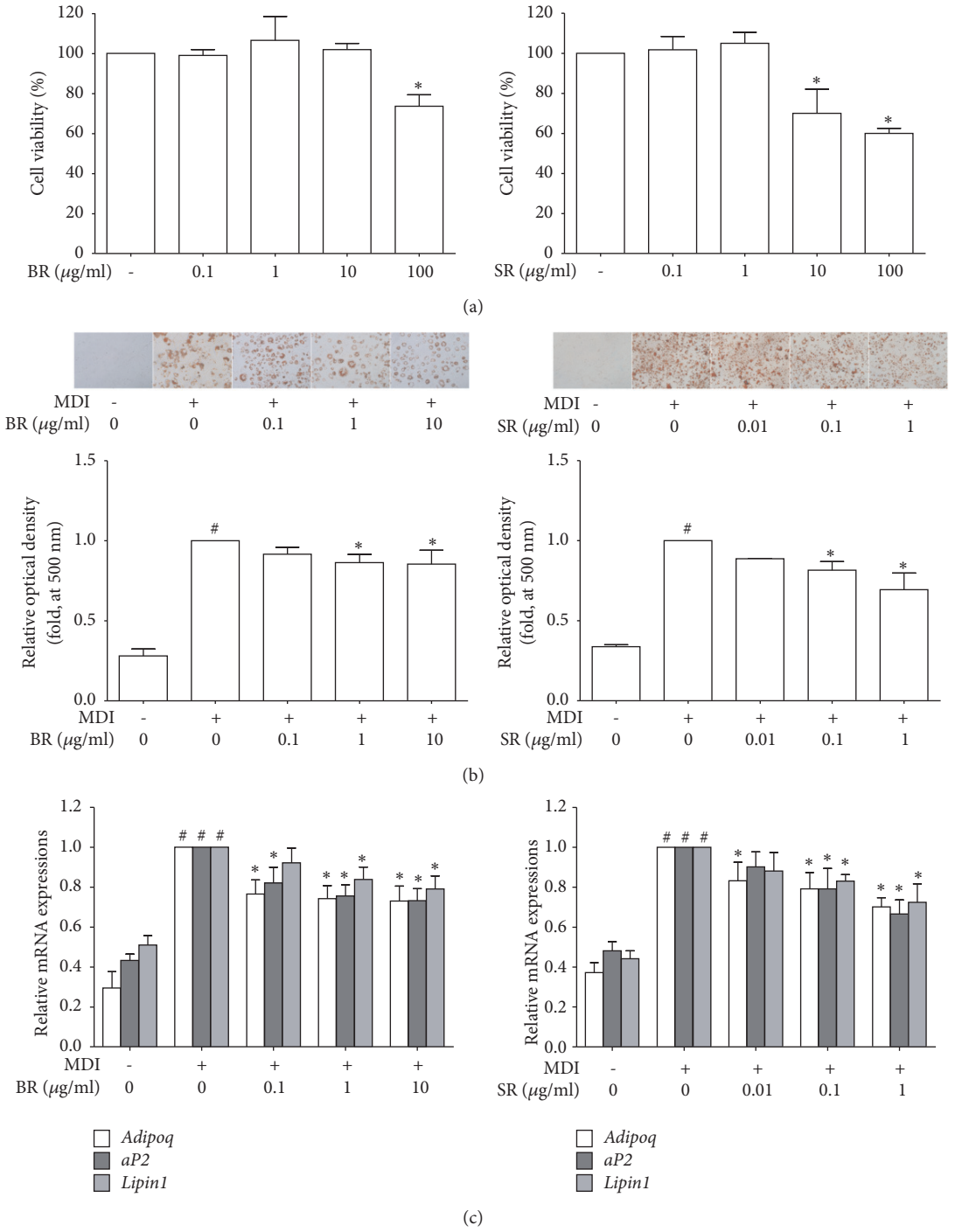

Figure 2: BR and SR inhibit lipid accumulation in 3T3-L1 adipocytes. (a) An MTS assay was performed in order to measure the effects of Bupleuri Radix and Scutellariae Radix on cell viability in 3T3-L1 cells. (b) An Oil Red O assay was performed in order to measure the effect of Bupleuri Radix and Scutellariae Radix on lipid accumulation in 3T3-L1 cells. (c) A Real-Time RT-PCR assay was performed in order to measure the effect of Bupleuri Radix and Scutellariae Radix on mRNA expressions of *AdipoQ*, *aP2,* and *Lipin1*. *Gapdh* mRNA was analyzed as an internal control. Experiments were repeated at least three times. Data represented are the relative expression. All values are mean ± SEM. $^{*}p < 0.05$, significantly different from untreated adipocytes. BR, Bupleuri Radix; SR, Scutellariae Radix.

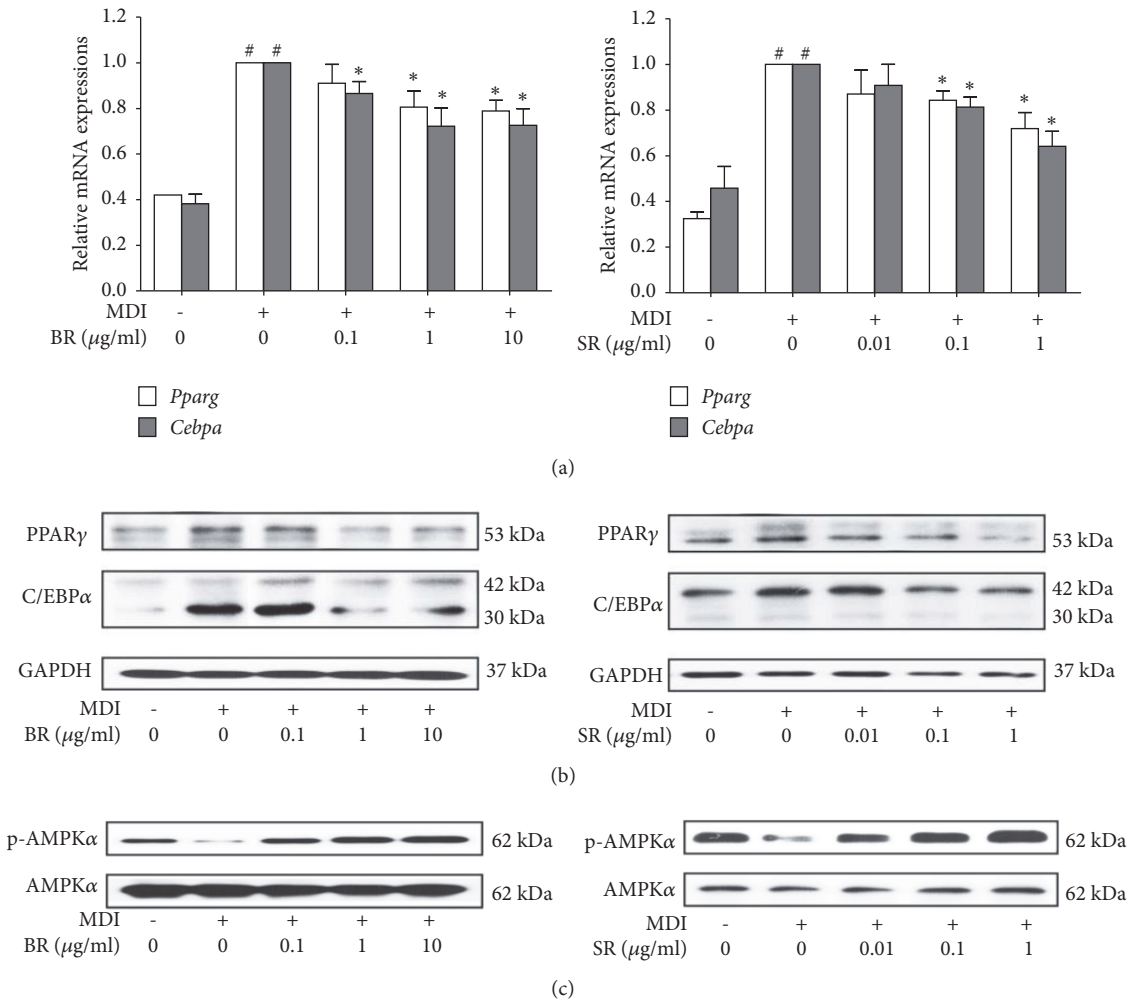

Figure 3: BR and SR suppress adipogenesis and increase energy expenditure in 3T3-L1 adipocytes. (a) A real-time RT-PCR assay was performed in order to measure the effect of Bupleuri Radix and Scutellariae Radix on mRNA expressions of *Cebpa* and *Pparg*. (b) A western blot assay was performed in order to measure the effect of Bupleuri Radix Scutellariae Radix on protein expressions of C/EBPα, PPARγ, and (c) p-AMPKα. *Gapdh* mRNA was analyzed as an internal control for Real-Time RT-PCR assays. Experiments were repeated at least three times. Data represented are the relative expression. All values are mean ± SEM. $^{*}p < 0.05$, significantly different from untreated adipocytes. BR, Bupleuri Radix; SR, Scutellariae Radix.

3.3. BR and SR Decrease Adipokines in 3T3-L1 Adipocytes. Real-time RT-PCR assays revealed adipokine genes including *Adipoq*, *aP2*, and *Lipin1* were decreased as well (Figure 2(c)). Adiponectin, an adipokine transcripted by the *Adipoq* gene, promotes adipocyte differentiation by increasing C/EBPα and PPARγ in 3T3-L1 adipocytes [27], and also secreted adiponectins are considered as a marker to evaluate adipogenic differentiation [28]. Adipocyte protein 2 (aP2) is a mediator of intracellular transport of fatty acids which is primarily expressed in adipocytes and macrophages [29]. Inhibition of this protein leads to a potential amelioration of obesity [30]. The role of Lipin-1, a protein with the most prominent expression in adipose tissue, skeletal muscle, and testis [31], in adipogenesis is complex. Several studies indicate its importance since the lack of Lipin-1 results in disturbed adipogenesis both *in vivo* and *in vitro* [32–34].

3.4. BR and SR Suppress Adipogenesis and Increase Energy Expenditure in 3T3-L1 Adipocytes. To investigate the action mechanism in lipid inhibition by BR and SR, we assessed the change in adipogenic factors. Two major controllers in adipogenesis, C/EBPα and PPARγ, were significantly decreased by BR and SR treatment at mRNA level and protein level both (Figures 3(a) and 3(b)), suggesting suppressed adipogenesis was responsible for the antilipogenic effect of BR. Then, we evaluated the effect of BR and SR on AMP-activated protein kinase alpha (AMPKα). As a result, we observed concentration-dependent increase in phosphorylation of AMPKα in BR- and SR-treated adipocytes (Figure 3(c)). Through these results, we could conclude that BR and SR suppress lipid accumulation in 3T3-L1 adipocytes by two action mechanisms: inhibition of adipogenesis and increase of energy expenditure.

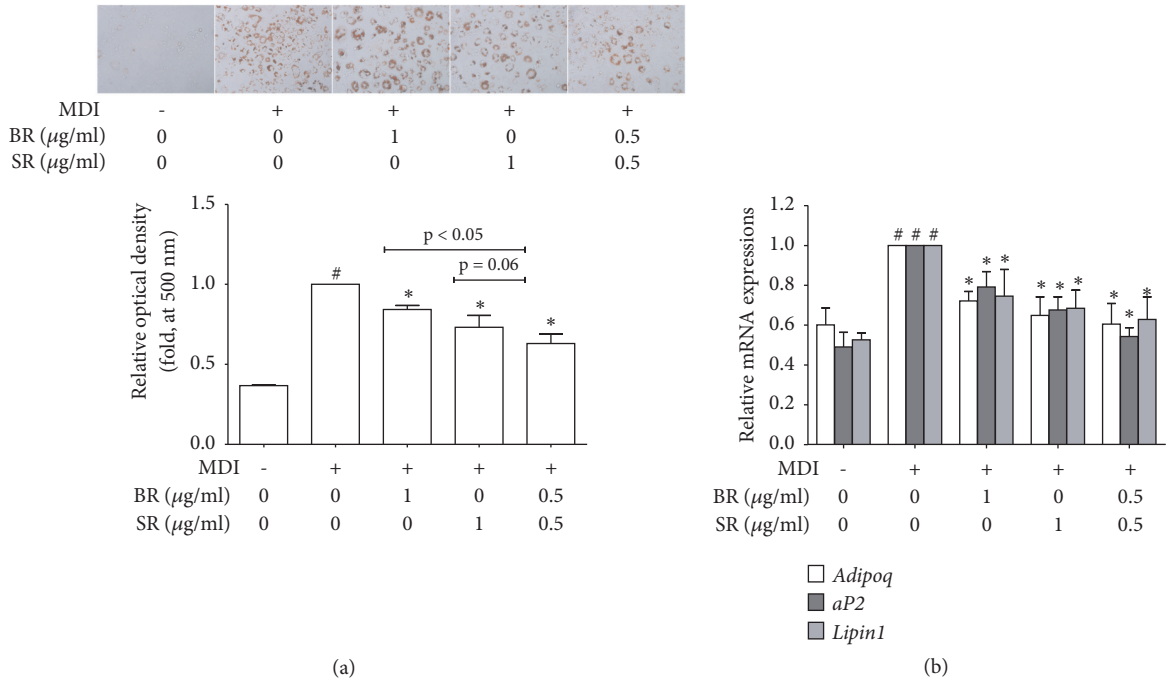

Figure 4: BR-SR mixture synergistically suppresses lipid accumulation in 3T3-L1 adipocytes. (a) An Oil Red O assay was performed in order to measure the effect of Bupleuri Radix, Scutellariae Radix, and their 1:1 mixture on lipid accumulation in 3T3-L1 cells. (b) A Real-Time RT-PCR assay was performed in order to measure the effect of Bupleuri Radix, Scutellariae Radix, and their 1:1 mixture on mRNA expressions of *AdipoQ*, *aP2,* and *Lipin1. Gapdh* mRNA was analyzed as an internal control. Experiments were repeated at least three times. Data represented are the relative expression. All values are mean ± SEM. $^{*}p < 0.05$, significantly different from untreated adipocytes. BR, Bupleuri Radix; SR, Scutellariae Radix.

3.5. BR-SR Mixture Synergistically Suppress Lipid Accumulation in 3T3-L1 Adipocytes. To confirm whether our hypothesis is correct or not, we then performed experiments to evaluate the synergism between BR and SR. BR and SR are contained in Sosiho-Tang at a 3:2 ratio (12 g and 8 g, respectively), and our results on separate extracts showed 1 μg/ml was the most efficient concentration of SR while 1 μg/ml and 10 μg/ml of BR did not differ significantly. Therefore, we used BR-SR mixture at 1 μg/ml of which extracts were mixed at 1:1 ratio. As shown in Figure 4(a), BR-SR 1:1 mixture suppressed lipid accumulation in 3T3-L1 adipocytes, whose inhibition rate was higher than BR 1 μg/ml or SR 1 μg/ml ($p < 0.05$ and $p = 0.06$, respectively). Further qPCR results indicated synergistic inhibition of adipokine genes such as *Adipoq*, *aP2,* and *Lipin1* (Figure 4(b)).

3.6. BR-SR Mixture Synergistically Inhibits Adipogenesis and Increases Energy Expenditure. To investigate the effect of BR-SR mixture on adipogenesis, we analyzed expression levels of *Cebpa* and *Pparg* using Real-Time RT-PCR. As in Figure 5(a), BR-SR 1:1 mixture showed higher inhibition rate in the two factors when compared to separate extracts at the same concentration. Consistently, BR-SR mixture showed synergistic inhibitory effect on protein levels of C/EBPα and PPARγ as well (Figure 5(b)). Mixture of BR and SR also enhanced the activation of AMPKα (Figure 5(c)), implying that these two herbal extracts synergistically interact in two different pathways of obesity treatment: inhibiting adipogenesis and increasing energy expenditure.

4. Discussion

The emerging crisis of obesity impacts the world. A more serious problem is that obesity can lead to other metabolism-related diseases, such as diabetes, cardiovascular diseases, and even cancer [35]. Current available medications for obesity are however limited; therefore the necessity of new options are growing. Nature-derived materials, in this case, have gained interest in the field of obesity treatment due to their positive effects with pharmacological safety [36]. Sosiho-Tang is a Korean medical formula composed of seven herbs: BR (12 g), SR (8 g), Pinelliae Tuber (4 g), Ginseng Radix (4 g), Zizyphi Fructus (4 g), Zingiberis Rhizoma (4 g), and Glycyrrhizae Radix (2 g). This herbal formula is a candidate for optional treatments as Yoo et al. reported its show antiobese effects *in vivo* and *in vitro* [7].

Several studies report the synergistic interaction in nature-derived materials. Our previous study has reported synergistic effect of two herbal pairs, *Vertrum nigrum* and *Panax ginseng* [37]. Zhao et al. used HFD-induced rats to show synergism between quercetin and resveratrol [38]. Another group has also reported the synergistic effect of this pair "browning" of white adipose tissue [39]. In this

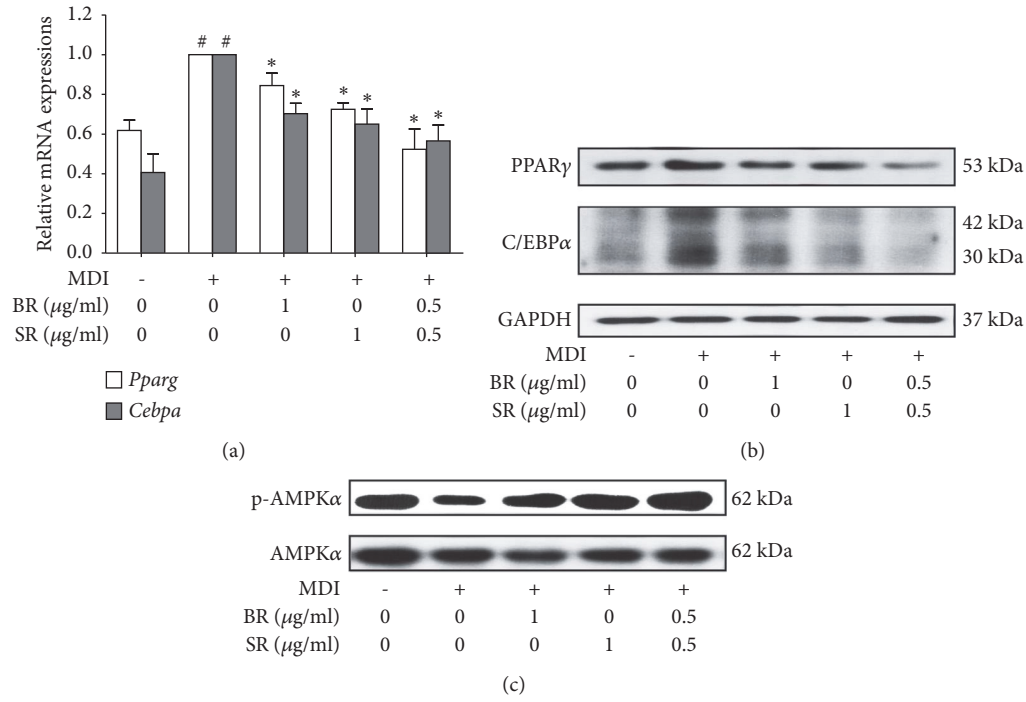

Figure 5: BR-SR mixture synergistically inhibits adipogenesis and increases energy expenditure. (a) A real-time RT-PCR assay was performed in order to measure the effect of Bupleuri Radix, Scutellariae Radix, and their 1:1 mixture on mRNA expressions of *Cebpa* and *Pparg*. (b) A western blot assay was performed in order to measure the effect of Bupleuri Radix, Scutellariae Radix, and their 1:1 mixture on protein expressions of C/EBPα, PPARγ, and (c) p-AMPKα. *Gapdh* mRNA was analyzed as an internal control for Real-Time RT-PCR assays. Experiments were repeated at least three times. Data represented are the relative expression. All values are mean ± SEM. $^{*}p < 0.05$, significantly different from untreated adipocytes. BR, Bupleuri Radix; SR, Scutellariae Radix.

study, we first analyzed the possible synergy of BR-SR pair by a network pharmacological approach. In the compound-target analysis, we observed several active compounds of BR and SR regulate targets related to adipogenesis and energy expenditure.

Obesity results from accumulation of excess energy in the form of lipid in adipocytes. Adipogenesis is a process of differentiation of preadipocyte into adipocytes. Numerous transcriptional factors form a complex cascade of adipogenesis, of which process changes in shape, genes, proteins, and hormones are accompanied [40, 41]. Among them, C/EBPα and PPARγ are considered to be the master regulators in adipogenesis [42]. In the current study, BR-SR mixture showed significant synergism on the inhibition of these two key adipogenic factors.

In addition to inhibiting adipogenesis, pharmacological activation of AMPKα is another potential pathway for obesity treatment. The energy storing WAT expresses AMPK, a serine/threonine protein kinase complex composed of three subunits (AMPKα, β and γ) which is activated in low energy-conditions [43]. Activated AMPK induces catalytic ATP generation while inhibiting anabolic process of energy consumption in order to maintain cellular energy homeostasis [44]. Thus, AMPK is one of the key regulators in energy homeostasis that mediate glucose and lipid metabolism to modulate energy levels [45]. Although previous studies allow the anticipation of AMPK elevation by BR [46] and SR [47, 48], the significance of our study was that, by network pharmacological analysis, a possible synergy mechanism on AMPK induction could be expected. Our results show that BR and SR extracts can activate AMPKα, suggesting their ability to increase energy expenditure. Furthermore, the 1:1 mixture of these two herbs interacted synergistically, phosphorylating AMPKα at a higher level.

Besides energy expenditure, AMPKα is also a regulator of adipogenesis by suppressing C/EBPα and PPARγ [49]. These reports again provide substantial evidence of synergy between BR and SR on adipogenesis. However, further study is required to fully understand the synergy mechanism of this Sangsoo pair of BR and SR.

5. Conclusion

Taken together, we analyzed the network pharmacological action of the Sangsoo herbal pair BR and SR, the two major components of Sosiho-Tang to predict their synergistic possibility. The compound-target relevance showed that these two herbs share two major antiobese targets: adipogenesis and energy expenditure. Then we used 3T3-L1 adipocytes to investigate whether the herbal pair do synergistically interact. As expected, BR-SR mixture showed synergism on suppressing intracellular lipid accumulation

and adipokine genes, which resulted from inhibition of adipogenic factors, C/EBPα and PPARγ, and activation of the key regulator of energy metabolism, AMPKα. Despite the fact that further mechanism study is required and that our results lack in vivo effects of BR-SR herbal pair, our results provide experimental evidence for the Korean medical theory of Sangsoo and also suggest this herbal pair BR and SR may benefit as a potential antiobese therapeutic agent.

Data Availability

The authors will retain all data and can provide it when requested.

Conflicts of Interest

The authors declare that they have no conflicts of interest.

Authors' Contributions

The first three authors (Jueun Lee, Jinbong Park, and Hyewon Park) contributed equally to this paper and share first authorship. Jae-Young Um developed the experimental design and conducted all of the manuscript. Jueun Lee performed the network pharmacology analysis. Hyewon Park and Dong-Hyun Youn performed the in vitro experiments. Jaehoon Lee and Seokbeom Hong provided technical and material support. Jinbong Park wrote the manuscript. All authors read and approved the final manuscript for submission.

Acknowledgments

This study was supported by the National Research Foundation of Korea (NRF-2015R1A41042399 and 2018R1D1A1B07049882) and Kyung Hee University in 2018 (KHU-1051).

References

[1] World Health Organization Media Centre, *WHO Media Centre Fact Sheets: Obesity and Overweight*, World Health Organization Media Centre, 2015.

[2] M. Solas, F. I. Milagro, D. Martínez-Urbistondo, M. J. Ramirez, and J. A. Martínez, "Precision obesity treatments including pharmacogenetic and nutrigenetic approaches," *Trends in Pharmacological Sciences*, vol. 37, no. 7, pp. 575–593, 2016.

[3] H. R. Wyatt, "Update on treatment strategies for obesity," *The Journal of Clinical Endocrinology & Metabolism*, vol. 98, no. 4, pp. 1299–1306, 2013.

[4] A. L. Hopkins, "Network pharmacology," *Nature Biotechnology*, vol. 25, no. 10, pp. 1110-1111, 2007.

[5] A. L. Hopkins, "Network pharmacology: the next paradigm in drug discovery," *Nature Chemical Biology*, vol. 4, no. 11, pp. 682–690, 2008.

[6] G.-b. Zhang, Q.-y. Li, Q.-l. Chen, and S.-b. Su, "Network pharmacology: a new approach for chinese herbal medicine research," *Evidence-Based Complementary and Alternative Medicine*, vol. 2013, Article ID 621423, 9 pages, 2013.

[7] S.-R. Yoo, M.-Y. Lee, B.-K. Kang, H.-K. Shin, and S.-J. Jeong, "Soshiho-tang aqueous extract exerts antiobesity effects in high fat diet-fed mice and inhibits adipogenesis in 3T3-L1 adipocytes," *Evidence-Based Complementary and Alternative Medicine*, vol. 2016, Article ID 2628901, 2016.

[8] T. F. Tzeng, H. J. Lu, S. S. Liou, C. J. Chang, and I. M. Liu, "Vinegar-baked radix bupleuri regulates lipid disorders via a pathway dependent on peroxisome-proliferator-activated receptor-alpha in high-fat-diet-induced obese rats," *Evidence-Based Complementary and Alternative Medicine*, vol. 2012, Article ID 827278, 12 pages, 2012.

[9] S. O. Kim, J. Y. Park, S. Y. Jeon, C. H. Yang, and M. R. Kim, "Saikosaponin a, an active compound of Radix Bupleuri, attenuates inflammation in hypertrophied 3T3-L1 adipocytes via ERK/NF-κB signaling pathways," *International Journal of Molecular Medicine*, vol. 35, no. 4, pp. 1126–1132, 2015.

[10] S.-J. Hong, J. C. Fong, and J.-H. Hwang, "Effects of crude drugs on glucose uptake in 3T3-L1 adipocytes," *Kaohsiung Journal of Medical Sciences*, vol. 16, no. 9, pp. 445–451, 2000.

[11] H. Lee, R. Kang, Y. Hahn et al., "Antiobesity effect of baicalin involves the modulations of proadipogenic and antiadipogenic regulators of the adipogenesis pathway," *Phytotherapy Research*, vol. 23, no. 11, pp. 1615–1623, 2009.

[12] D. H. Kwak, J.-H. Lee, K. H. Song, and J. Y. Ma, "Inhibitory effects of baicalin in the early stage of 3T3-L1 preadipocytes differentiation by down-regulation of PDK1/Akt phosphorylation," *Molecular and Cellular Biochemistry*, vol. 385, no. 1-2, pp. 257–264, 2014.

[13] L.-L. Yang, N. Xiao, J. Liu et al., "Differential regulation of baicalin and scutellarin on AMPK and Akt in promoting adipose cell glucose disposal," *Biochimica et Biophysica Acta*, vol. 1863, no. 2, pp. 598–606, 2017.

[14] P. Fang, M. Yu, W. Min et al., "Beneficial effect of baicalin on insulin sensitivity in adipocytes of diet-induced obese mice," *Diabetes Research and Clinical Practice*, vol. 139, pp. 262–271, 2018.

[15] M.-H. Cha, I.-C. Kim, B.-H. Lee, and Y. Yoon, "Baicalein inhibits adipocyte differentiation by enhancing COX-2 expression," *Journal of Medicinal Food*, vol. 9, no. 2, pp. 145–153, 2006.

[16] Y. Nakao, H. Yoshihara, K. Fujimori, and H. Xu, "Suppression of very early stage of adipogenesis by baicalein, a plant-derived flavonoid through reduced Akt-C/EBPα-GLUT4 signaling-mediated glucose uptake in 3T3-L1 adipocytes," *PLoS ONE*, vol. 11, no. 9, Article ID e0163640, 2016.

[17] E.-J. Bak, J. Kim, Y. H. Choi et al., "Wogonin ameliorates hyperglycemia and dyslipidemia via PPARα activation in db/db mice," *Clinical Nutrition*, vol. 33, no. 1, pp. 156–163, 2014.

[18] T. Yang, H. Liu, B. Zhao et al., "Wogonin enhances intracellular adiponectin levels and suppresses adiponectin secretion in 3T3-L1 adipocytes," *Endocrine Journal*, vol. 64, no. 1, pp. 15–26, 2017.

[19] J. Chen, J. Liu, and Y. Wang, "Wogonin mitigates nonalcoholic fatty liver disease via enhancing PPARα/AdipoR2, in vivo and in vitro," *Biomedicine & Pharmacotherapy*, vol. 91, pp. 621–631, 2017.

[20] R. Jin, B. Zhang, C.-M. Xue, S.-M. Liu, Q. Zhao, and K. Li, "Classification of 365 Chinese medicines in Shennong's Materia Medica Classic based on a semi-supervised incremental clustering method," *Journal of Chinese Integrative Medicine*, vol. 9, no. 6, pp. 665–674, 2011.

[21] D. Merico, D. Gfeller, and G. D. Bader, "How to visually interpret biological data using networks," *Nature Biotechnology*, vol. 27, no. 10, pp. 921–924, 2009.

[22] J. Park, Y.-D. Jeon, H.-L. Kim et al., "Veratri Nigri Rhizoma et Radix (Veratrum nigrum L.) and its constituent jervine prevent adipogenesis via activation of the LKB1-AMPKalpha-ACC axis in vivo and in vitro," *Evidence-Based Complementary and Alternative Medicine*, vol. 2016, Article ID 8674397, 12 pages, 2016.

[23] Y. Jung, J. Park, H. Kim et al., " Vanillic acid attenuates obesity ," *The FASEB Journal*, vol. 32, no. 3, pp. 1388–1402, 2018.

[24] M.-Y. Jeong, H.-L. Kim, J. Park et al., "Rubi Fructus (*Rubus coreanus*) activates the expression of thermogenic genes in vivo and in vitro," *International Journal of Obesity*, vol. 39, no. 3, pp. 464-456, 2015.

[25] M.-Y. Jeong, J. Park, D.-H. Youn et al., "Albiflorin ameliorates obesity by inducing thermogenic genes via AMPK and PI3K/AKT in vivo and in vitro," *Metabolism - Clinical and Experimental*, vol. 73, pp. 85–99, 2017.

[26] H. Kim, Y. Jung, J. Park et al., "Farnesol has an anti-obesity effect in high-fat diet-induced obese mice and induces the development of beige adipocytes in human adipose tissue derived-mesenchymal stem cells," *Frontiers in Pharmacology*, vol. 8, article 654, 2017.

[27] Y. Fu, N. Luo, R. L. Klein, and W. Timothy Garvey, "Adiponectin promotes adipocyte differentiation, insulin sensitivity, and lipid accumulation," *Journal of Lipid Research*, vol. 46, no. 7, pp. 1369–1379, 2005.

[28] E. Martella, C. Bellotti, B. Dozza, S. Perrone, D. Donati, and E. Lucarelli, "Secreted adiponectin as a marker to evaluate in vitro the adipogenic differentiation of human mesenchymal stromal cells," *Cytotherapy*, vol. 16, no. 11, pp. 1476–1485, 2014.

[29] L. Sun, A. C. Nicholson, D. P. Hajjar, A. M. Gotto Jr., and J. Han, "Adipogenic differentiating agents regulate expression of fatty acid binding protein and CD36 in the J744 macrophage cell line," *Journal of Lipid Research*, vol. 44, no. 10, pp. 1877–1886, 2003.

[30] K. Maeda, H. Cao, K. Kono et al., "Adipocyte/macrophage fatty acid binding proteins control integrated metabolic responses in obesity and diabetes," *Cell Metabolism*, vol. 1, no. 2, pp. 107–119, 2005.

[31] M. Péterfy, J. Phan, P. Xu, and K. Reue, "Lipodystrophy in the fld mouse results from mutation of a new gene encoding a nuclear protein, lipin," *Nature Genetics*, vol. 27, no. 1, pp. 121–124, 2001.

[32] K. Reue, P. Xu, X.-P. Wang, and B. G. Slavin, "Adipose tissue deficiency, glucose intolerance, and increased atherosclerosis result from mutation in the mouse fatty liver dystrophy (fld) gene," *Journal of Lipid Research*, vol. 41, no. 7, pp. 1067–1076, 2000.

[33] P. Zhang, K. Takeuchi, L. S. Csaki, and K. Reue, "Lipin-1 phosphatidic phosphatase activity modulates phosphatidate levels to promote peroxisome proliferator-activated receptor γ (PPARγ) gene expression during adipogenesis," *The Journal of Biological Chemistry*, vol. 287, no. 5, pp. 3485–3494, 2012.

[34] H. Sembongi, M. Miranda, G.-S. Han et al., "Distinct roles of the phosphatidate phosphatases lipin 1 and 2 during adipogenesis and lipid droplet biogenesis in 3T3-L1 cells," *The Journal of Biological Chemistry*, vol. 288, no. 48, pp. 34502–34513, 2013.

[35] NCD Risk Factor Collaboration, "Worldwide trends in body-mass index, underweight, overweight, and obesity from 1975 to 2016: a pooled analysis of 2416 population-based measurement studies in 128.9 million children, adolescents, and adults," *Lancet*, vol. 390, no. 10113, pp. 2627–2642, 2016.

[36] Y. Liu, M. Sun, H. Yao, Y. Liu, and R. Gao, "Herbal medicine for the treatment of obesity: an overview of scientific evidence from 2007 to 2017," *Evidence-Based Complementary and Alternative Medicine*, vol. 2017, Article ID 8943059, 17 pages, 2017.

[37] J. Park, Y.-D. Jeon, H.-L. Kim et al., "Interaction of *Veratrum nigrum* with *Panax ginseng* against obesity: A Sang-ban relationship," *Evidence-Based Complementary and Alternative Medicine*, vol. 2013, Article ID 732126, 13 pages, 2013.

[38] L. Zhao, F. Cen, F. Tian et al., "Combination treatment with quercetin and resveratrol attenuates high fat diet-induced obesity and associated inflammation in rats via the AMPKα1/SIRT1 signaling pathway," *Experimental and Therapeutic Medicine*, vol. 146, pp. 5942–5948, 2017.

[39] N. Arias, C. Picó, M. Teresa Macarulla et al., "A combination of resveratrol and quercetin induces browning in white adipose tissue of rats fed an obesogenic diet," *Obesity*, vol. 25, no. 1, pp. 111–121, 2017.

[40] H. Koutnikova and J. Auwerx, "Regulation of adipocyte differentiation," *Annals of Medicine*, vol. 33, no. 8, pp. 556–561, 2001.

[41] E. D. Rosen and O. A. MacDougald, "Adipocyte differentiation from the inside out," *Nature Reviews Molecular Cell Biology*, vol. 7, no. 12, pp. 885–896, 2006.

[42] R. F. Morrison and S. R. Farmer, "Hormonal signaling and transcriptional control of adipocyte differentiation," *Journal of Nutrition*, vol. 130, no. 12, pp. 3116S–3121S, 2000.

[43] M. C. Towler and D. G. Hardie, "AMP-activated protein kinase in metabolic control and insulin signaling," *Circulation Research*, vol. 100, no. 3, pp. 328–341, 2007.

[44] D. G. Hardie, F. A. Ross, and S. A. Hawley, "AMPK: a nutrient and energy sensor that maintains energy homeostasis," *Nature Reviews Molecular Cell Biology*, vol. 13, no. 4, pp. 251–262, 2012.

[45] R. B. Ceddia, "The role of AMP-activated protein kinase in regulating white adipose tissue metabolism," *Molecular and Cellular Endocrinology*, vol. 366, no. 2, pp. 194–203, 2013.

[46] Z. Zhen, B. Chang, M. Li et al., "Anti-diabetic effects of a coptis chinensis containing new traditional Chinese medicine formula in type 2 diabetic rats," *American Journal of Chinese Medicine*, vol. 39, no. 1, pp. 53–63, 2011.

[47] T. Wang, H. Jiang, S. Cao et al., "Baicalin and its metabolites suppresses gluconeogenesis through activation of AMPK or AKT in insulin resistant HepG-2 cells," *European Journal of Medicinal Chemistry*, vol. 141, pp. 92–100, 2017.

[48] Q. Chen, M. Liu, H. Yu et al., "Scutellaria baicalensis regulates FFA metabolism to ameliorate NAFLD through the AMPK-mediated SREBP signaling pathway," *Journal of Natural Medicines*, vol. 72, no. 3, pp. 655–666, 2018.

[49] Y. Dagon, Y. Avraham, and E. M. Berry, "AMPK activation regulates apoptosis, adipogenesis, and lipolysis by eIF2α in adipocytes," *Biochemical and Biophysical Research Communications*, vol. 340, no. 1, pp. 43–47, 2006.

Hindawi
Evidence-Based Complementary and Alternative Medicine
Volume 2018, Article ID 7154702, 12 pages
https://doi.org/10.1155/2018/7154702

Research Article

In Vitro Antidiabetic Effects of Isolated Triterpene Glycoside Fraction from *Gymnema sylvestre*

Rashmi S. Shenoy,[1,2] **K. V. Harish Prashanth**,[2,3] **and H. K. Manonmani**[1,2]

[1]*Department of Food Protectants and Infestation Control, CSIR-Central Food Technological Research Institute, Mysore 570020, India*
[2]*Academy of Scientific and Innovative Research, CSIR-Central Food Technological Research Institute, Mysore 570020, India*
[3]*Department of Biochemistry, CSIR-Central Food Technological Research Institute, Mysore 570020, India*

Correspondence should be addressed to H. K. Manonmani; manonmani@cftri.res.in

Received 29 March 2018; Revised 30 May 2018; Accepted 10 June 2018; Published 8 August 2018

Academic Editor: Hilal Zaid

A triterpene glycoside (TG) fraction isolated and purified from ethanolic extract of *Gymnema sylvestre* (EEGS) was investigated for blood glucose control benefit using *in vitro* methods. The HPLC purified active fraction TG was characterized using FTIR, LC-MS, and NMR. The purified fraction (TG) exhibited effective inhibition of yeast α-glucosidase, sucrase, maltase, and pancreatic α-amylase with IC_{50} values 3.16 ± 0.05 μg/mL, 74.07 ± 0.51, 5.69 ± 0.02, and 1.17 ± 0.24 μg/mL, respectively, compared to control. TG was characterized to be a mixture of triterpene glycosides: gymnemic acids I, IV, and VII and gymnemagenin. *In vitro* studies were performed using mouse pancreatic β-cell lines (MIN6). TG did not exhibit any toxic effects on β-cell viability and showed protection against H_2O_2 induced ROS generation. There was up to 1.34-fold increase in glucose stimulated insulin secretion ($p<0.05$) in a dose-dependent manner relative to standard antidiabetic drug glibenclamide. Also, there was further one-fold enhancement in the expression of GLUT2 compared to commercial standard DAG (deacylgymnemic acid). Thus, the present study highlights the effective isolation and therapeutic potential of TG, making it a functional food ingredient and a safe nutraceutical candidate for management of diabetes.

1. Introduction

Type II diabetes is one of the most widespread metabolic disorders in the world, characterized by hyperglycemia and hyperlipidemia. About 190 million people are affected by diabetes, and the number is projected to rise to 642 million by 2040 [1]. It is known that the onset of diabetes is related to many classic risk factors including oxidative stress [2]. The complication associated with diabetes will be enhanced due to the involvement of reactive oxygen species (ROS) [3]. The ROS contributes to oxidative stress and in turn damages pancreatic islets and reduces insulin secretion. Growing evidences show that β-cells are central to the development of type 2 diabetes [4]. Therefore, the functional defects in β-cells are often accompanied by a reduction in expression of glucose transporter-2 (GLUT2) levels, further characterized by increased apoptosis of β-cells [5, 6]. Therefore, therapies for improving the β-cell function have become the potential new strategy to control hyperglycemia [7]. Studies demonstrate that supplementation with natural antioxidant products has shown improvement of hyperglycemic status by reducing the oxidative stress [8]. Also, glucose generation and absorption in the intestine play a vital role in hyperglycemia management [9]. Inhibition of α-glucosidase and α-amylase which digest dietary starch into glucose was studied as a method for controlling blood sugar levels [10]. Although several drugs for type II diabetes are *in vogue*, they have shown side effects such as liver toxicity and gastrointestinal adversity [11]. Thus the quest for safe, economical, and pharmacologically active molecules with multifunctional attributes towards diabetes management is necessary. This can be achieved by screening natural sources such as medicinal plants. Moreover, there is considerable interest in the application of traditional plants due to their natural origin, easily cultivable with minimum or no side effects.

Gymnema sylvestre (GS), a woody vine-like climbing plant, is well known in Indian traditional medicine "Ayurveda". It grows in the tropical forest of central and southern India [12]. The leaves are used mostly as antiviral, diuretic, antiallergic, hypoglycemic, hypolipidemic, antibiotic, antianalgesic, and antirheumatic agents [13]. The leaves of GS contain triterpenoidal saponins belonging to oleanane and dammarane classes [13]. Twenty different saponins and glycosides have been reported in *Gymnema sylvestre* [14]. Several studies suggest that gymnemic acids may act as antidiabetic by promoting regeneration of islet cells and increase insulin secretion [15]. Also, gymnemic acids have been reported to inhibit glucose absorption from the intestine and utilize glucose by enhancing the activities of enzymes in insulin-dependent pathways [15].

The current focus of our study was to isolate and characterize bioactive agents (s) from *Gymnema sylvestre* and evaluate *in vitro* antidiabetic effects to initiate a search for nutraceutical pharmacophores towards inhibition of pancreatic α-amylase and α-glucosidase with improvement in beta cell function.

2. Materials and Methods

2.1. Chemicals. α-Amylase from porcine pancreas, α-glucosidase from *Saccharomyces cerevisiae*, para-nitrophenyl-glucopyranoside (*p*NPG), soluble starch, and 3-4,5-(dimethylthiazol-2-yl)-2,5-diphenyl tetrazolium bromide (MTT) were procured from SRL chemicals (Bangalore, India). Rat intestinal acetone powder (source of α-glucosidase), acarbose, Anti-GLUT2 antibody, anti-insulin antibody, 2′7′-dichlorodihydrofluorescein diacetate (DCFH-DA), acridine orange (AO), and ethidium bromide (EtBr) were from Sigma Chemical Co. (St. Louis, MO, USA). Glucose oxidase kit was purchased from AGAPE diagnostics (India). ELISA kits were purchased from Cytoglow Co. (India). Analytical and HPLC grade solvents were from E. Merck (India). The dried powder of *Gymnema sylvestre* was obtained from Nikhila Karnataka Central Ayurvedic Pharmacy (Mysore, India). Mouse pancreatic β-cell line (MIN6) was purchased from NCCS (Pune, India). Dulbecco's minimal essential medium (DMEM), Fetal Bovine Serum (FBS), and antimycotic solution were purchased from Himedia chemicals (India). All other chemicals used in the study were of analytical grade and purchased from Himedia chemicals (India).

2.2. Preparation of Gymnema sylvestre (GS) Extracts. GS powder was extracted using different solvent systems like methanol, ethanol, acetone, ethyl acetate, chloroform, and water, respectively. The GS powder along with respective solvents were left for 3 h refluxing, and the resulting infusions were filtered. The filtrates were concentrated; solvents were evaporated using rotary evaporator (Cole-Parmer SB 1100, Shanghai, China) at 45°C under reduced pressure and then lyophilized. The greenish-black powder thus obtained was stored at 4°C until used for further assays.

2.3. α-Glucosidase Inhibitory Assay. Extracts of GS were screened for α-glucosidase inhibitory activity according to the method described in [16]. The source of α-glucosidase enzyme was from *Saccharomyces cerevisiae*. The substrate solution *p*NPG (2 mg/mL) was prepared in 50 mM phosphate buffer, pH 6.8. 10 μL of α-glucosidase (1.12 U/mL) was preincubated with 10 μL of known concentrations of GS (extracted from different solvents) for 10 min. *p*NPG (10 μL) was added to start the reaction followed by incubation at 37°C for 20 min. The reaction was stopped by adding 2 mL of 0.1 M Na_2CO_3. The α-glucosidase activity was determined by measuring the yellow-colored para-nitrophenol released from *p*NPG at 405 nm. The results were expressed as percentage of the blank control.

2.4. Preparative HPLC of Ethanolic Extract of Gymnema sylvestre (EEGS). 200 g of dried plant material was extracted using 1 L absolute ethanol under refluxing conditions for 3h. The extracted volume was concentrated using rotary evaporator (Cole-Parmer SB 1100, Shanghai, China) at 45°C at high pressure and brought down to 500 mL. This was further concentrated to ~5 g wet weight and a stock of 1 mg/mL was prepared using HPLC grade methanol solution. The stock solution was filtered using nylon 6 membrane consisting of six multiple filter papers with a pore size of 0.45 μm, degassed by ultrasonic treatment before use. Preparative HPLC (gradient mode) was carried out using ODS C-18 silica column (25 cm X 21.2 mm, 12 μm). The mobile phase was prepared using two solvent systems: solvent A: water (HPLC GRADE) containing 1 % acetic acid; solvent B: acetonitrile containing 1 % acetic acid. The mobile phase was filtered using nylon 6 multiple filter membranes having a pore size of 0.45 μm. The conditions for HPLC [0 min solvent B (5 %), 5 min (8 %), 7 min (12 %), 12 min (18 %), 17 min (22%), 24 min (35 %), 26 min (100 %), 30 min (100 %), 32 min (5 %), 35 min stop] were set; constant flow rate was maintained at 5 mL/min. The detector was set at 254 nm, and fractions were collected. The fractions were made solvent free using a rotary evaporator, freeze-dried and then resuspended in known amount of phosphate buffer (50 mM, pH 6.8), and were analyzed for percentage α-glucosidase inhibitory activity.

2.5. Thin Layer Chromatography (TLC) and High Performance TLC (HPTLC). The purity of the HPLC purified active fraction was tested by thin layer chromatography. Silica gel-G was taken as stationary medium and coated over glass slides. The mobile phase used was toluene:ethylacetate:acetic acid (5:7:1, v/v) [17]. Deacylgymnemic acid (DAG) was used as a standard. The purity of the active fraction was checked by HPTLC. HPTLC system equipped with a Linomat IV sample applicator, a twin-chamber tank, a model III TLC scanner, and CATS 4.0 integration software was employed. Aluminum-backed layers (10 × 10 cm) of silica gel GF254 were used as absorbent. The mobile phase used was chloroform and methanol (8:2, v/v). The spotted plates were developed up to 80 mm under chamber saturation conditions. After air-drying the solvent, the plates were scanned at 205 nm [18].

2.6. Characterization by FTIR, LC-MS, and NMR. The isolated active fraction was characterized by spectroscopic methods. FTIR (Bruker, USA) spectra were recorded in the

range of 4000-400 cm^{-1} by blending samples with KBr. LC-MS (Shimadzu, Japan) was used to detect the molecular weights of the bioactive agents (s) detected in the active fraction. The separation was carried out using C18 column (150 x 4.6 mm ID, 5μ), column temperature maintained at 40°C. Mobile phase consisted of methanol and water both containing methanol and water (80:20) at a flow rate of 1 mL/min over 25 minutes. The electrospray ionisation was carried out in both positive and negative mode. ^{1}H and ^{13}C NMR spectra were recorded in DMSO-d_6 on a Bruker Avance, USA, 400 MHz spectrometer (Bruker, Karlsruhe, Germany). Assignments of ^{13}C signals were based on respective chemical shift values.

2.7. α-Amylase Inhibitory Assay. This assay was carried out using a modified procedure described in [19]. Briefly, a total of 100 μL of different concentration of TG (250 ng–500 μg /mL) was placed in a tube and 100 μL of 50 mM sodium phosphate buffer (pH 6.8) containing α-amylase solution (1.5 mg/mL) was added. This solution was preincubated at 25°C for 20 min, after which 100 μL of 1% soluble starch solution in 50 mM sodium phosphate buffer (pH 6.8) was added and incubated at 25°C for 10 min. The reaction was stopped by adding 500 μL of dinitrosalicylic acid (DNS) reagent followed by incubation in boiling water for 5 min and then cooled to room temperature. The resulting mixture was diluted with 5 mL distilled water and the absorbance was measured at 540 nm. A control was prepared using the same procedure replacing the extract with distilled water. The α-amylase inhibitory activity was calculated as percentage inhibition. Concentrations of extracts resulting in 50% inhibition of enzyme activity (IC_{50}) were determined graphically.

2.8. Rat Intestinal α-Glucosidase Inhibitory Activity (Sucrase and Maltase Inhibitory Activities). The assay was based on the modified method described [20]. 100 mg of rat intestinal acetone powder was dissolved in 3 mL of NaCl (0.9 %) solution and centrifuged at 12,000 g for 30 min and used for the assay. The enzyme solution (30 μL) was incubated with 40 μL of sucrose (400 mM) for sucrase assay. Various concentrations of the extract were taken and made up to final volume of 100 μl with 0.1 M phosphate buffer, pH 6.8. The reaction mixture was incubated at 37°C for 30 min. The reaction was then stopped by suspending mixtures in boiling water for 10 min. The concentrations of glucose released from the reaction mixtures were determined by glucose oxidase method with absorbance at a wavelength of 505 nm. Concentrations of extracts resulting in 50% inhibition of enzyme activity (IC_{50}) were determined graphically.

Similarly, maltase assay was also carried out using the same protocol except that sucrose was replaced with 10 μL maltose (86 mM).

2.9. Cell Culture. MIN6 cells were maintained under 5% CO_2, 37°C in DMEM media supplemented with 10 % FBS, 2 mM L-glutamine, 100 U/mL of penicillin, and 0.1 mg/mL streptomycin.

2.9.1. Cell Viability Assay. 3-4, 5-(Dimethylthiazol-2-yl)-2,5-diphenyl tetrazolium bromide (MTT) assay was based on the protocol described [21]. MIN6 cells were seeded at a density of 2×10^4 cells/well in 96-well plates for 24 h. Then the cells were treated with various concentrations of TG and EEGS (20–650 μg) and incubated for 24 h. After the required period of treatment, MTT solution [10 μL; 5 mg/mL MTT in phosphate-buffered saline (PBS)] was added with continued incubation for 3 h. After that DMSO was added and again incubated for 30 min in the dark. The cell viability was then recorded at 570 nm.

2.9.2. Intracellular ROS. The quantification of the cellular antioxidant activity was determined according to the method described in [22]. To measure ROS levels, 2′7′-dichlorodihydrofluorescein diacetate (DCFH-DA) was used. The cells were seeded in a 96-well microtiter plate at a density of 5 $X10^4$ cells/well. After 24 h, the cells were treated with 50 and 100μg concentration of TG and EEGS and were further incubated for 24 h at 5% CO_2, 37°C. Then 25 μM DCFH-DA was added, and incubation was continued further for 1 h. The intracellular oxidation of DCFH-DA in the wells was measured using fluorescence microplate reader at excitation (488 nm) and emission (525 nm).

2.9.3. Fluorescence Microscopy of MIN6 Cells. MIN6 cells were seeded at a density of 1×10^5 cells/mL on poly-L-Lysine coated cover slips in 6 well plates containing DMEM for 24 h. H_2O_2 treated cells were used as control to show oxidative stress. Subsequently, the cells were treated with 50 and 100 μg concentrations of TG devoid of H_2O_2 for 24 h. Cells were stained by double dye method using acridine orange (AO) and ethidium bromide (1:1). The images were then captured using a fluorescence microscope (Nikon, Tokyo, Japan) [23].

2.9.4. Glucose Stimulated Insulin Secretion Assay. DMEM (Serum-free) without glucose, supplemented with 2 mM L-glutamine and 25 mM HEPES, pH 7.4, was used in this study. Glucose solution was prepared at different concentrations (1, 3, 5, 8, and 25 mM) and incubated at 37°C before use. MIN6 cells were seeded at a density of $1X10^6$ in 96-well plates for 24 h. Subsequently, the cells were treated with 50 and 100 μg concentrations of TG. Prior to the insulin secretion assay, the cells were starved in Krebs-Ringer solution containing 0.1% bovine serum albumin (BSA) with 1 mM glucose for 1h, and the wells were washed twice with the same buffer. The cells were later incubated with Krebs-Ringer solution containing 3, 8, 15, and 25 mM glucose, 10 mM glibenclamide and 8 mM glucose, 30 mM KCl and 8 mM glucose for 1 h). Insulin secreted into the medium was measured using an ELISA kit [23].

2.9.5. Measurement of GLUT 2 Levels. The surface translocation of GLUT2 was measured according to the protocols described [24]. The cells were treated with TG at 50 and 100 μg/mL for 24 h. After treatment, the target GLUT 2 level in the cell lysate was measured using ELISA kit. The primary antibody specific to the target protein GLUT2 was added and allowed to bind to their target epitopes. The secondary antibody tagged with HRP which was specific to the primary

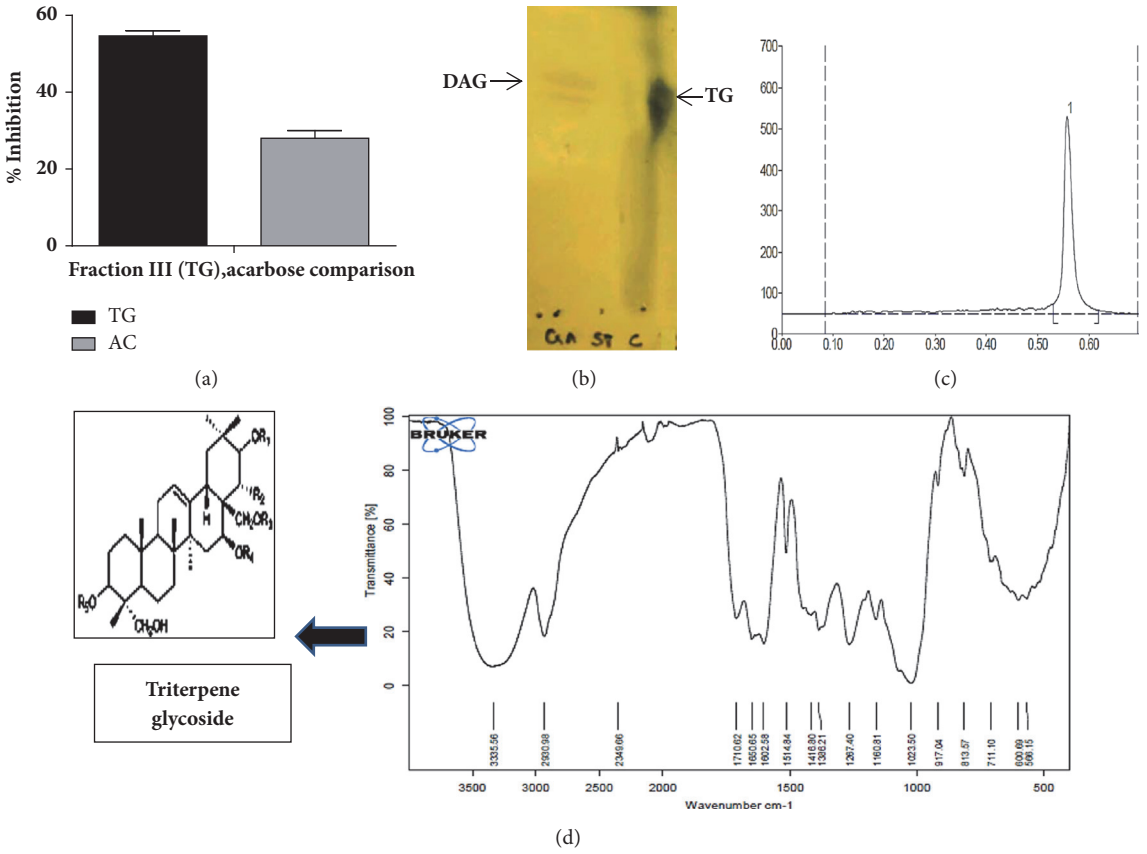

Figure 1: %α-glucosidase inhibition and identification of the active fraction TG. (a) shows the %α-glucosidase inhibition of the active fraction III (TG) relative to the positive control acarbose (AC). Values are expressed as mean ± SD. (b) represents the TLC pattern of the active fraction triterpene glycoside (TG labelled as C) and the available commercial standard deacylgymnemic acid (DAC labelled as GA); (c) represents the HPTLC pattern of triterpene glycoside (TG). The active fraction was checked for purity using TLC and HPTLC. TLC spot indicated the presence of gymnemic acid and HPTLC displayed rf value of 0.56. (d) depicts FTIR spectrum of TG. The characteristic FTIR peaks of TG with ester link 1710 cm-1 revealed presence of triterpene glycoside.

antibody was added, and the detection of GLUT2 was done using TMB-H_2O_2 substrate at 450 nm.

2.10. Statistical Analysis. Results were represented as mean ± SD. Two-way ANOVA was employed to carry out statistical analysis using GraphPad prism, version 5.0. The experiments were conducted in triplicate. A confidence limit of $p<0.05$ was considered statistically significant.

3. Results

3.1. Extraction and Isolation of Bioactive Agents (s) from Gymnema sylvestre. Dried leaf powder of GS (*Gymnema sylvestre*) was extracted using different solvents methanol, ethanol, acetone, ethyl acetate, chloroform, and water. All the solvent extracts were subjected to α-glucosidase inhibitory activity. Ethanolic extract showed maximum inhibition of 97.2 % (Table 1). This fraction was therefore chosen for further studies. The ethanolic extract of *Gymnema sylvestre* (EEGS) was subjected to chromatographic fractionation using preparative gradient HPLC system. The four peaks (fractions) obtained were collected, made solvent free, and resuspended in known amount of phosphate buffer (50mM, pH 6.8). α-Glucosidase inhibitory activity was assayed for all the collected fractions. Fraction III showed the highest inhibitory activity of 53.3% compared to standard acarbose (positive control) which exhibited 26% inhibition against α-glucosidase (Figure 1(a)). The other fractions showed lesser inhibitory activities ranging from 30 to 40% and hence fraction III was used for further

Table 1: % α-glucosidase inhibition for different solvent extracts of GS.

Solvents	% α-glucosidase Inhibition
Methanol	52.2 ± 0.50
Ethanol	**97.24 ± 0.24**
Acetone	80.34 ± 0.63
Ethyl acetate	7.1 ± 0.05
Chloroform	75.24 ± 0.40
Water	-

Known amount of GS powder was extracted using different solvent systems.The experiments were done in triplicate and average values were determined. Values are expressed as mean± SD.

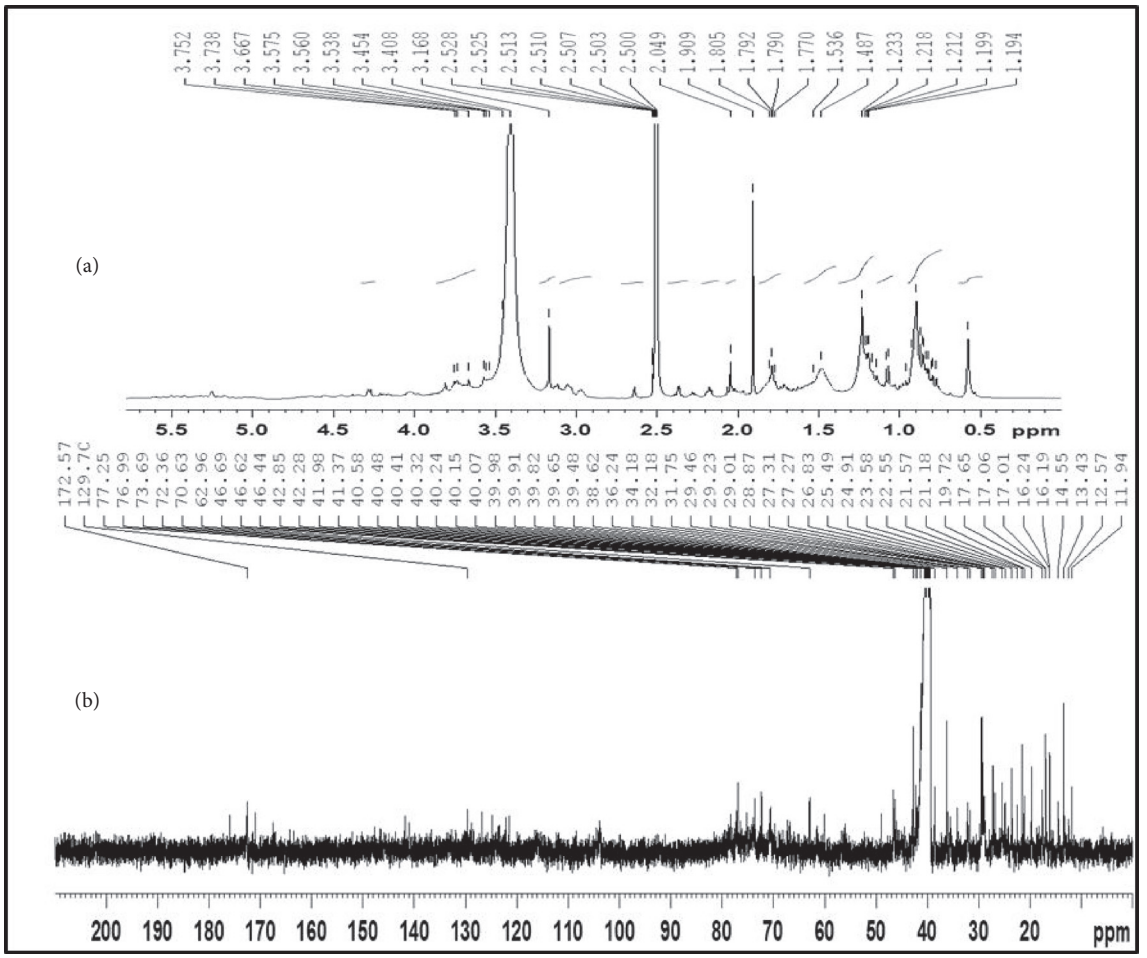

Figure 2: NMR spectrum of the active fraction TG. (a) 1H-NMR; (b) 13C-NMR.

studies. In the subsequent investigation, triterpene glycosides were identified in the active fraction III, after evaluation and characterization by TLC, HPTLC, FTIR, NMR, and LC-MS. This triterpene glycoside active fraction was termed as TG. The presence of gymnemic acid was indicated in TG by TLC (Figure 1(b)), when spotted along with the commercial standard deacylgymnemic acid (DAG). We also observed a single peak when TG was subjected to HPTLC with rf value 0.56 (Figure 1(c)).

FTIR spectrum showed the presence of bands at wavelengths 3335, 2930, and 1710 cm^{-1} corresponding to OH, CH, and C=O functional groups. The characteristic FTIR peaks of TG with ester link 1710 cm^{-1} (Figure 1(d)) revealed presence of typical gymnemic acid. To further elucidate the structure, TG was subjected to NMR assignments (Figure 2). Table 2 gives the details of NMR chemical shifts assigned for TG.

^{1}H NMR spectrum of TG was observed in DMSO–d_6 solvent. The characteristic protons were found in their expected range (Figure 2). Further, the spectroscopic analyses employing chemical carbon (^{13}C) shifts assignments (Table 2) were in good agreement with the MS negative mode data (Figure 3(a)). The spectrum suggested the presence of a tigloyl group at C-21 (Table 2) and acetyl group (172 ppm, –C=O & 23 ppm $-CH_3$) at C-28 suggesting Gymnemic acid I. Saponins are classified as monodesmosides, with a single saccharide chain generally linked to C-3 depending on the number of sugars present. As usual, 77-76 ppm will appear for gymnemic acids due to glycosylation shifts. But we found 70 ppm for C-3 triterpenoids in their free form (sapogenins) indicating the presence of gymnemagenin. The presence of this compound was again reconfirmed with MS data in positive mode (Figure 3(b)). The sugar moiety was found to be 3-O-β-D-glucuronic acid (175ppm, –C=O). Moreover, the pattern gave a peak at NMR sugar region (103 ppm), and they appeared to consist of glucuronic acid alone and no other types of sugar moieties were present. Comparison in relative assignments revealed the presence of a mixture of gymnemagenin and gymnemic acids I, IV and VII, and they differ only in presence/absence of acetyl and tigloyl groups, respectively. These results are in good agreement with literature data with ± 1-2 ppm observed shifts which might be due to complex interactions in the above mixture of saponins in TG. Based on results obtained from ^{1}H, ^{13}C, and FTIR analyses, the structure of TG was proposed as shown in Figure 1(d).

Table 2: ^{13}C NMR spectral data for gymnemagenin and respective gymnemic acids (δ in DMSO-d_6).

Position	Gymnemagenin (δ)	Gymnemic acid I (δ)	Gymnemic acid IV (δ)	Gymnemic acid VII (δ)
C-1	38.6	++	++	38.6
C-2	27.2	26.8	26.8	27.2
C-3	70.6	77.3	76.5	76.5
C-4	42.3	42.9	42.3	42.3
C-5	49.1	--	--	49.1
C-6	17.7	17.6	17.6	17.7
C-7	32.2	--	--	32.2
C-8	40.2	++	++	40.2
C-9	46.7	46.6	46.6	46.7
C-10	36.2	++	++	36.2
C-11	24.9	24.5	23.6	24.9
C-12	121.5	124.8	122.2	121.5
C-13	141.8	--	--	141.8
C-14	41.9	--	--	41.9
C-15	34.2	35.6	35.6	34.2
C-16	67.3	--	--	67.3
C-17	46.0	46.0	46.4	46.0
C-18	42.0	--	--	42.0
C-19	46.4	--	--	46.4
C-20	34.2	36.0	36.0	34.2
C-21	77.0	78.4	78.4	77.0
C-22	73.7	72.5	72.5	73.7
C-23	70.6	62.3	62.3	70.6
C-24	13.4	14.6	14.4	13.4
C-25	16.2	16.3	16.3	16.2
C-26	17.0	17.1	17.1	17.0
C-27	27.2	27.3	27.3	27.2
C-28	60.0	63.0	60.0	60.0
C-29	31.8	29.5	29.2	31.8
C-30	19.7	21.6	21.2	19.7
		Acetyl 1 - 172.6		
		Acetyl 2 – 22.5		
			Tigloyl 1' - 170.9	
			Tigloyl 2' - 129.7	
			Tigloyl 3' - 139.1	
			Tigloyl 4' - 14 .4	
			Tigloyl 5' -12.6	
			3-0-β-D-glucopyranosiduronic acid	
			C1 - 103.9	
			C2 - 74.0	
			C3 - 76.6	
			C4 - 72.4	
			C5 - 75.2	
			C6 - 175.9	

++: overlapped signals; --: not assigned.

Table 3: IC_{50} values for porcine α-amylase, yeast α-glucosidase, and mammalian α-glucosidase inhibitory potential of *TG*.

Enzymes	IC_{50} values for TG (μg/mL)	IC_{50} values for acarbose (μg/mL)
α-glucosidase (yeast source)	3.16 ± 0.05	6.14 ± 0.05
rat Intestinal α-glucosidase (sucrase)	74.07 ± 0.51*	44.30 ± 0.73*
rat Intestinal α-glucosidase (maltase)	5.69 ± 0.02	0.059 ± 0.05
porcine α-amylase	1.17 ± 0.24	0.18 ± 0.02

At different concentrations of TG IC_{50} values for yeast α-glucosidase, sucrase, maltase, and porcine α amylase were studied. Values are expressed as mean± SD of three independent experiments made in duplicate.
*Indicating the significant levels at $p<0.05$.

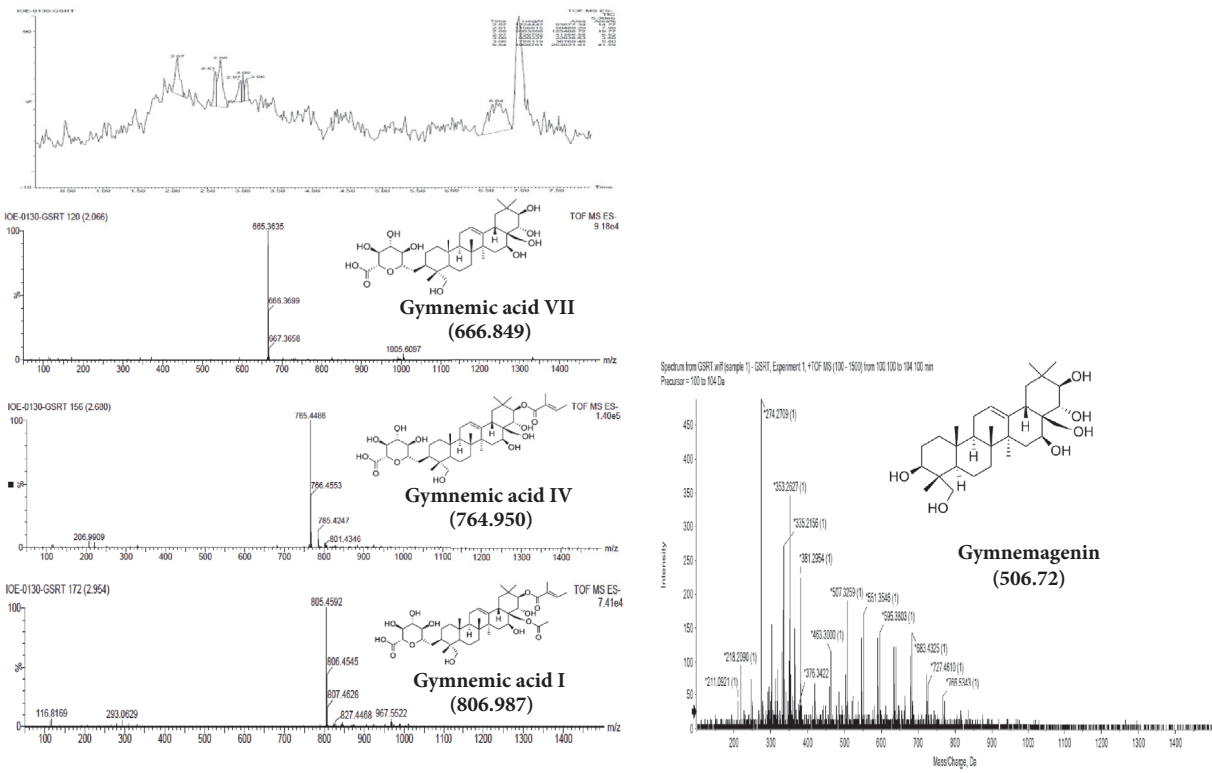

Figure 3: (a) LC chromatogram of TG, ESI -ve mode; (b) LC chromatogram of TG, ESI +ve mode.

In ESI -ve mode, the molecular weights were observed to be 765, 665, and 805, respectively. This indicated that TG contained gymnemic acids I (805), IV (665), and VII (765) all of which have similar triterpene backbone but differ in the positioning of functional groups. Under ESI +ve mode, peaks corresponding to triterpene backbone were observed. This indicated the presence of gymnemagenin, a triterpenoid aglycone of gymnemic acid with a molecular weight of 507 (m/z) (Figures 3(a) and 3(b)). These results correlate very well with the NMR patterns obtained.

3.2. Enzyme Inhibitory Activities. When subjected to different concentrations of TG, the inhibition of α-glucosidase was observed to be concentration dependent. This activity was higher compared to acarbose at their respective similar concentrations (Table 3). TG showed α-glucosidase inhibitory activity with an IC_{50} value of 3.16 ± 0.05 μg/mL. Similarly α-amylase, sucrase, and maltase enzyme activities were inhibited by TG (Table 3) with IC_{50} values of 1.17 ± 0.24 μg/mL, 74.07 ± 5.11 μg/mL, and 5.69 ± 0.02 μg/mL, respectively.

3.3. In Vitro Activity of TG Using MIN6 Cell (Pancreatic β-Cell) Lines. To examine whether the ethanolic extract of Gymnema sylvestre (EEGS) and its active fraction (TG) induced any cytotoxic effects, MTT assay was performed. When extracts were used at concentrations ranging from 20 to 650 μg/mL, the viability retained up to 90% ($p<0.05$), even at highest concentration studied (650 μg) (Figure 4(a)). This demonstrated the nontoxic effects of TG.

To further demonstrate that TG did not induce any cytotoxic effects, MIN6 cells were treated with TG and stained using differential staining method using AO and EtBr.

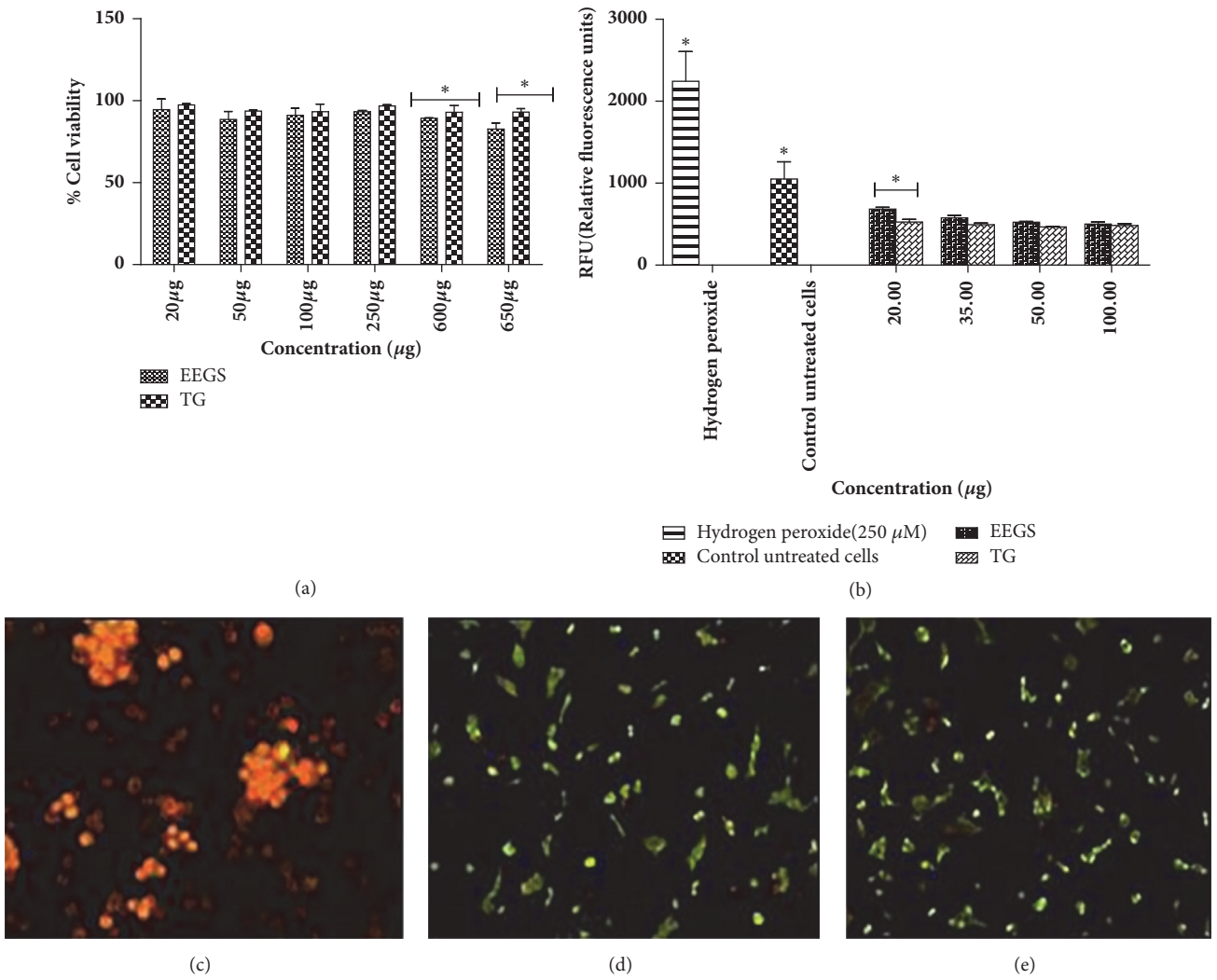

Figure 4: Effects of TG on β-cells viability. (a) MTT was performed to study the cytotoxic effects of TG. MIN6 cells were treated with different concentrations of TG and the cell viability was studied. (b) To study the ROS effect of GS extracts on MIN6 cells, treatment was carried out at concentrations 20, 35, 50, and 100 μg levels. H_2O_2 was used as positive control. Fluorescent microscopy images showing the effect of TG on MIN6 cells, where (c) shows positive control (hydrogen peroxide), (d) shows TG treated cells (50 μg), and (e) shows TG treated cells (100 μg). Green regions indicate uptake of acridine orange, showing live β cells. Orange-red color displays apoptosis/dead cells. All values were represented as mean± SD. Experiments were performed in triplicate. Analysis was performed using two-way ANOVA. *Representing significance at $p<0.05$.

AO/EtBr double staining combines the properties of two dyes to determine the type of cell death. The micrographs clearly indicate noncytotoxic nature of TG (50 and 100 μg). The cells appeared green, and there was no decrease in cell number. H_2O_2 (200 μM) treated cells appeared orange-red, and they were agglomerated indicating cell death due to toxicity (Figures 4(c), 4(d), and 4(e)).

The influence of TG on the generation of reactive oxygen species (ROS) was determined at 20, 35, 50, and 100 μg/mL concentrations. H_2O_2 (200 μM) treatment was used as control. A normal control without any treatment was also used. A significant reduction ($p<0.05$) in the formation of ROS was observed compared to H_2O_2 treated control at all the concentrations studied (Figure 4(b)). But the increase in sample concentration did not show any incremental significance.

3.4. Insulin Secretion by β-Cells. The β-cells displayed dose-dependent response in insulin secretion when stimulated with increasing concentrations of glucose (3-25 mM) in the presence of 50 and 100 μg concentrations of TG. TG at 50 μg level displayed 1.0-fold increase ($p<0.05$) in insulin secretion when cells were exposed to a lower concentration of glucose (3mM and 8mM) compared to the control. The glucose concentrations 5 and 25 mM were considered as normoglycemic and glucotoxic, respectively. But the cells incubated with normoglycemic glucose levels showed a little rise in insulin levels (1.34-fold, $p<0.05$). At glucotoxic conditions,

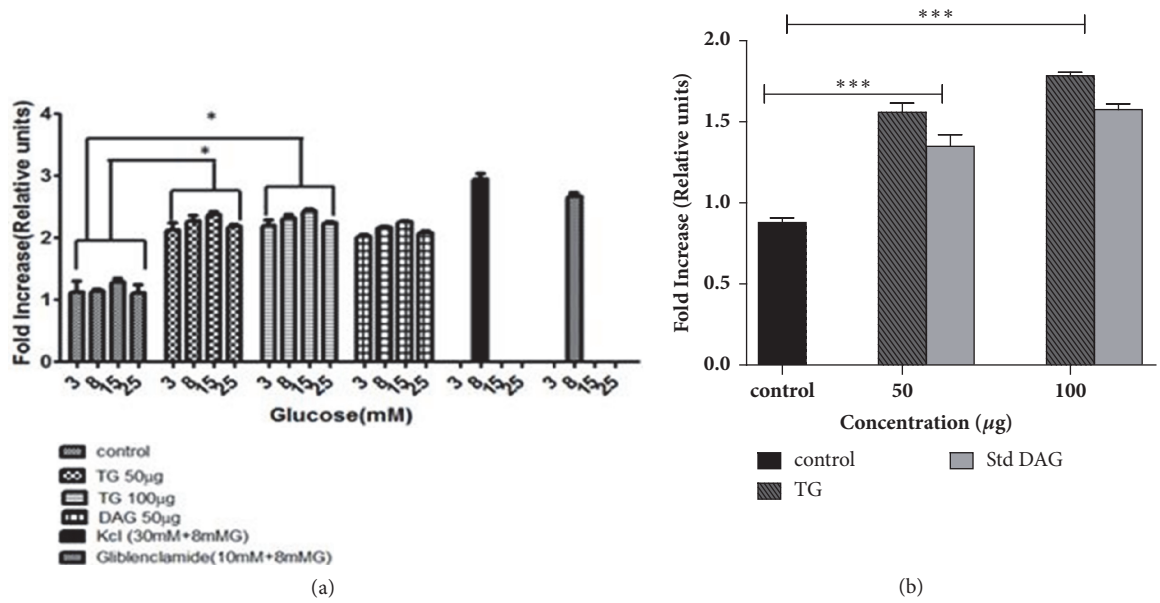

(a) (b)

Figure 5: Effect of TG on *in vitro* antidiabetic activity. (a) MIN6 cells were treated with TG at 50 and 100μg concentrations. Deacylgymnemic acid (DAG), an available commercial standard from GS, and glibenclamide, a commercial drug used for diabetes treatment, were also used for comparison. (b) represents effect of TG on enhancement of GLUT2 levels. Treatment with TG and standard DAG (from GS) was done at 50 and 100 μg concentrations. All experiments were carried out in triplicate and results were represented as mean± SD. Analysis was performed using two-way ANOVA. *Representing significance level at $p<0.05$. ***Representing significance level at $p<0.001$.

the response was quite lower than that of normoglycemic glucose levels yet significant compared to the control, respectively, as illustrated in Figure 5(a) (1.16-fold, $p<0.05$). When cells were treated with TG at 100 μg at low concentrations of glucose (3mM), there was 1.12-fold increase in insulin level ($p<0.05$) compared to control. At normoglycemic and glucotoxic glucose levels, the response of the cells was similar to TG at 50 μg level in insulin secretion as shown in the Figure 5(a). The results obtained were comparable with the positive controls (KCl and glibenclamide) used in this study.

3.5. Effect of TG on GLUT2. We examined the effect of TG on GLUT2 by quantitative ELISA using anti-GLUT2 antibody tagged to HRP (Figure 5(b)). TG treated cells demonstrated better increase in GLUT-2 levels at 50 and 100 μg concentrations compared to commercial standard DAG (deacylgymnemic acid). Preincubation of cells at 50 μg of TG showed a slight increase in GLUT2 levels (0.5 fold), yet it was significant compared to control ($p<0.01$). When cells were treated with TG at 100 μg, a single fold increase in GLUT2 levels was observed when compared to control ($p<0.001$).

4. Discussion

Pancreatic α-amylase breaks down complex carbohydrates into oligosaccharides and disaccharides. Further, the intestinal α-glucosidases digest diet-derived oligosaccharides and disaccharides into monosaccharides, mainly glucose. In previous reports, the ethanolic extract of *Gymnema montanum* leaves demonstrated appreciable α-glucosidase and α-amylase inhibitory activity comparable to that of acarbose, a commercially available drug that inhibits α-glucosidase to decrease postprandial hyperglycemia [25]. In the present study, we have observed that isolated active fraction TG inhibited the activity of pancreatic α-amylase, intestinal α-glucosidases (sucrase and maltase), and yeast α-glucosidase in a concentration-dependent manner as shown in the Table 3. The inhibition effect was significant ($p<0.05$) against intestinal α-glucosidase (sucrase) with an IC_{50} value of 74.07 ± 0.51 μg/mL relative to acarbose, which showed IC_{50} value of 44.30 ± 0.73 μg/mL. We found promising inhibition with IC_{50} value for TG (3.16 ± 0.05 μg/mL) against yeast α-glucosidase compared to acarbose. Similar effects were observed *in vivo,* where inhibition of α-glucosidase and other intestinal enzymes such as maltase and sucrase occurs in polysaccharides and oligosaccharides digestion [26]. α-Amylase and α-glucosidase showed different inhibition patterns probably due to structural differences related to the origins of the enzymes [27]. Gymnemic acid (GA) isolated from GS not only inhibits glucose absorption in the small intestine [27], but also suppresses hyperglycemia and hyperinsulinemia in an oral glucose tolerance test [28]. The efficiency of GA in inhibiting glucose absorption in the small intestine was found to be increased by a combined effect with acarbose and voglibose [28]. Thus we have attempted to study antihyperglycemic effect induced by TG *in vitro,* since it seems to be little more feasible than that *in vivo*. The inhibition of these enzymes could be probably because of the synergistic action of triterpene glycosides present in the active fraction TG as substantiated by *in vitro* antidiabetic studies. Bekzod Khakimov et al. (2016) [29] have shown in their study the mass spectral fragmentation patterns of 49 saponin peaks, detected from plant originating from eight different triterpenoid aglycones with different MW. Further,

they have shown that continuously measured proton NMR data during chromatography separation along with mass spectrometry data revealed significant differences, including contents of saponins, types of aglycones, and numbers of sugar moieties attached to the aglycone. The review [30] has also showed the results about the isolation and chemistry of the triterpenoids and their physicochemical characterization will be better studied using MS, FTIR, and NMR spectral data.

Previous study showed that the aqueous extract of GS decreased blood glucose levels in rats and humans, without improving insulin sensitivity [31]. An insulin secretagogue function was ascribed to GS following observations that its administration led to elevations in serum insulin levels in individuals with type 2 diabetes [32]. However, to identify the mode of action for glucose-lowering agents, we have carried out experiments *in vitro* for potential effects of GS extracts to stimulate insulin secretion by direct action at β-cells. Pretreatment with (50–100 μg) of TG for 2 h triggered a significant increase of glucose-induced insulin secretion in a dose-dependent manner. This may be mainly attributed to the effect of TG on the insulin secretion enhancement capacity of MIN6 cells. The ability of TG to further stimulate insulin secretion at 15 mM glucose demonstrated that TG acts by enhancing glucose metabolism within the β-cells. TG was also an efficient amplifier of insulin secretion, thus assisting in sustained amplification of insulin secretion at 15 and 25 mM glucose concentrations, respectively. The ability of TG to stimulate insulin secretion at substimulatory glucose concentrations was comparable to glibenclamide, a standard drug for stimulating insulin secretion used in our study. GS has been widely utilized in Indian medicine (Ayurveda) for the treatment of diabetes and other disorders [33]. GS extracts contain various biologically active compounds that exert antidiabetic effects [34]. GS leaves contain numerous saponin components, some of which may solubilize mammalian cell membrane proteins in much the same way as digitonin, which was used experimentally to permeabilize plasma membranes [35]. The major saponins present in the isolated active fraction TG showed the stimulatory effect on insulin release from MIN6 β-cells at 50 and 100μg, accompanied by 90-95% cell viability as revealed by staining with 1:1 mixture of ethidium bromide (EtBr) and acridine orange (AO). In one of the studies, novel isolate of GS termed OSA (named after Om Santal Adivasi) showed insulinotropic activities on β-cell lines and isolated human islets *in vitro* had beneficial effects on glycemic control in patients with type 2 diabetes [36]. OSA at around 0.25 mg/mL stimulated insulin secretion *in vitro* without adverse effects on cell viability. Similarly, in our study, TG at 50 μg/mL level stimulated insulin secretion *in vitro* without hostile effects on cell viability. Even at 650 μg/mL concentration tested, 90 % of β-cells were viable. These investigations suggested that membrane damaging components in TG or their concentrations might be much lower. Differential staining with ethidium bromide and acridine orange was an established test of cell viability that paves the way for rapid visual readout of compromised plasma membrane integrity. In this study increased dye uptake of acridine orange to give green fluorescence indicated the nontoxic effects of TG on β-cells.

The pancreatic islet includes the most vulnerable cells for the attack after ROS generation in human as it has less antioxidant enzymes as compared to other organs [8]. The damage of pancreatic islet leads to decrease in insulin secretion, resulting in hyperglycemic conditions and regeneration of ROS. *In vitro,* GS alcoholic leaf extract showed antioxidant ability by inhibiting 1,1-diphenyl-2-picrylhydrazyl (DPPH) and scavenging superoxide and hydrogen peroxide [37]. In the present study, H_2O_2 was chosen as known model biological ROS. A significant reduction in the formation of ROS was observed compared to control at all the concentrations of TG studied.

Many medicinal plants are used in the traditional medicine to enhance the translocation of GLUT, and this could lead to a new approach for treating type 2 diabetes. GLUT2 is a facilitative glucose transporter located in the plasma membrane of pancreas, liver, intestinal, kidney cells, and the hypothalamus areas [38]. Due to its high capacity and low affinity, GLUT2 transports dietary sugars, glucose, fructose, and galactose in a broad range of physiological concentrations. GLUT2 has the highest capacity and the lowest affinity for glucose, which allows glucose uptake in the beta cells only when the glucose level is high and insulin secretion is necessary [38]. According to literature, ethanolic extract of *Catharanthus roseus* enhanced GLUT2 levels in streptozotocin-induced diabetic Wistar rats. In our studies, at 50 μg concentration of TG, there was 0.5-fold increase of GLUT2 compared to control. At 100μg concentration, the increase was 1-fold ($p<0.05$). In a similar previous study conducted, methanolic leaf extract of *Gymnema sylvestre* (MLGS) demonstrated a significant and dose-dependent increase in glucose uptake in all the concentrations of MLGS studied [39]. TG at 50 and 100 μg elevated GLUT2 levels comparable to standard DAG (deacylgymnemic acid). Renewal of glucose transport induction would, therefore, enhance the uptake of glucose and thus help to combat hyperglycemic conditions.

5. Conclusion

In conclusion, the present study exhibited an evidence that isolated active fraction, triterpene glycoside, TG from *Gymnema sylvestre*, could inhibit the activity of pancreatic α-amylase, α-glucosidase, sucrase, and maltase. Further, it was shown to enhance the GLUT2 protein levels and ameliorate impaired insulin secretion of MIN6 cells. However, the underlying molecular mechanism remains to be understood. The isolated and characterized active fraction, triterpene glycoside (TG), gives insight into dietary antidiabetic benefits by reducing antinutritional factors of saponins in *Gymnema sylvestre*.

Abbreviations

GS: *Gymnema sylvestre*
EEGS: Ethanolic extract of *Gymnema sylvestre*
*p*NPG: Para-nitrophenyl-glucopyranoside
TLC: Thin layer chromatography
HPTLC: High performance thin layer chromatography
HPLC: High performance liquid chromatography

FTIR:	Fourier transform infrared spectrum
LC-MS/MS:	Liquid chromatography mass spectrometry
NMR:	Nuclear magnetic resonance
TG:	Active fraction III, mixture of triterpenoid glycosides
MIN6:	Pancreatic β-cell lines from mouse
MTT:	3-4,5-(Dimethylthiazol-2-yl)-2,5-diphenyl tetrazolium bromide
ROS:	Reactive oxygen species
DCFH-DA:	$2'7'$-dichlorodihydrofluorescein diacetate$''''$
GLUT2:	Glucose transporter 2.

Data Availability

All the data used to support the findings of this study are included in the manuscript.

Conflicts of Interest

The authors declare that there are no conflicts of interest regarding the publication of this paper.

Acknowledgments

The authors thank Director, Central Food Technological Research Institute, Mysore, for providing the necessary facilities to carry out this work and CSIR-Delhi for providing CSIR-GATE fellowship for Rashmi S. Shenoy.

Supplementary Materials

The graphical representation depicts the gist of entire manuscript. In this work, we have attempted to evaluate the antidiabetic potential of Gymnema sylvestre. The active fraction "TG" has been characterized and explored for its antidiabetic effects. The active fraction TG showed inhibition of the disaccharidase activity, owing to its glucose control benefits. TG also improved insulin secretion and glucose transporter protein levels in beta cells in vitro. *(Supplementary Materials)*

References

[1] T. Kawai, I. Takei, A. Shimada et al., "Effects of olmesartan medoxomil, an angiotensin II type 1 receptor antagonist, on plasma concentration of B-type natriuretic peptide, in hypertensive patients with type 2 diabetes mellitus: A preliminary, observational, open-label study," *Clinical Drug Investigation*, vol. 31, no. 4, pp. 237–245, 2011.

[2] H. Sakuraba, H. Mizukami, N. Yagihashi, R. Wada, C. Hanyu, and S. Yagihashi, "Reduced beta-cell mass and expression of oxidative stress-related DNA damage in the islet of Japanese Type II diabetic patients," *Diabetologia*, vol. 45, no. 1, pp. 85–96, 2002.

[3] R. Kakkar, S. V. Mantha, J. Radhi, K. Prasad, and J. Kalra, "Increased oxidative stress in rat liver and pancreas during progression of streptozotocin-induced diabetes," *Clinical Science*, vol. 94, no. 6, pp. 623–632, 1998.

[4] P. Marchetti, S. Del Prato, R. Lupi, and S. Del Guerra, "The pancreatic beta-cell in human Type 2 diabetes," *Nutrition, Metabolism & Cardiovascular Diseases*, vol. 16, pp. S3–S6, 2006.

[5] W.-H. Kim, J. W. Lee, Y. H. Suh et al., "AICAR potentiates ROS production induced by chronic high glucose: Roles of AMPK in pancreatic β-cell apoptosis," *Cellular Signalling*, vol. 19, no. 4, pp. 791–805, 2007.

[6] S. R. Sampson, E. Bucris, M. Horovitz-Fried et al., "Insulin increases H_2O_2-induced pancreatic beta cell death," *Apoptosis*, vol. 15, no. 10, pp. 1165–1176, 2010.

[7] E. Bonora, "Protection of pancreatic beta-cells: Is it feasible?" *Nutrition, Metabolism & Cardiovascular Diseases*, vol. 18, no. 1, pp. 74–83, 2008.

[8] R. Robertson, H. Zhou, T. Zhang, and J. S. Harmon, "Chronic oxidative stress as a mechanism for glucose toxicity of the beta cell in type 2 diabetes," *Cell Biochemistry and Biophysics*, vol. 48, no. 2-3, pp. 139–146, 2007.

[9] W. F. Caspary, "Physiology and pathophysiology of intestinal absorption," *American Journal of Clinical Nutrition*, vol. 55, no. 1, pp. 299S–308S, 1992.

[10] F. Zhao, Y. Watanabe, H. Nozawa, A. Daikonnya, K. Kondo, and S. Kitanaka, "Prenylflavonoids and phloroglucinol derivatives from hops (Humulus lupulus)," *Journal of Natural Products*, vol. 68, no. 1, pp. 43–49, 2005.

[11] N. Tewari, V. Tiwari, R. Mishra et al., "Synthesis and bioevaluation of glycosyl ureas as α-glucosidase inhibitors and their effect on mycobacterium," *Bioorganic & Medicinal Chemistry*, vol. 11, no. 13, pp. 2911–2922, 2003.

[12] S. Najafi and S. S. Deokule, "Studies on Gymnema sylvestre- a medicinally important plant of the family Asclepiadaceae," *TGS*, vol. 9, pp. 26–32, 2011.

[13] V. A. Khramov, A. A. Spasov, and M. P. Samokhina, "Chemical composition of dry extracts of Gymnema sylvestre leaves," *Pharmaceutical Chemistry Journal*, vol. 42, no. 1, pp. 29–31, 2008.

[14] P. D. Trivedi and K. Pundarikakshudu, "A validated high performance thin-layer chromatographic method for the estimation of gymnemic acids through gymnemagenin in Gymnema sylvestre, materials, extracts and formulations," *International Journal of Applied Sciences*, vol. 6, p. 19, 2008.

[15] P. V. Kanetkar, K. S. Laddha, and M. Y. Kamat, *Gymnemic acids: A molecular perspective of its action on carbohydrate. Poster presented at the 16th ICFOST meet organized by CFTRI and DFRL*, India, Mysore, 2004.

[16] Y.-M. Kim, Y.-K. Jeong, M.-H. Wang, W.-Y. Lee, and H.-I. Rhee, "Inhibitory effect of pine extract on α-glucosidase activity and postprandial hyperglycemia," *Nutrition Journal* , vol. 21, no. 6, pp. 756–761, 2005.

[17] K. Y. Kim, K. A. Nam, H. Kurihara, and S. M. Kim, "Potent α-glucosidase inhibitors purified from the red alga Grateloupia elliptica," *Phytochemistry*, vol. 69, no. 16, pp. 2820–2825, 2008.

[18] P. V. Kanetkar, R. S. Singhal, K. S. Laddha, and M. Y. Kamat, "Extraction and quantification of gymnemic acids through gymnemagenin from callus cultures of Gymnema sylverstre," *Phytochemical Analysis*, vol. 17, no. 6, pp. 409–413, 2006.

[19] Y.-M. Kim, M.-H. Wang, and H.-I. Rhee, "A novel α-glucosidase inhibitor from pine bark," *Carbohydrate Research*, vol. 339, no. 3, pp. 715–717, 2004.

[20] S. Adisakwattana and B. Chanathong, "α-glucosidase inhibitory activity and lipid-lowering mechanisms of Moringa oleifera leaf extract," *European Review for Medical and Pharmacological Sciences*, vol. 15, no. 7, pp. 803–808, 2011.

[21] T. Mosmann, "Rapid colorimetric assay for cellular growth and survival: application to proliferation and cytotoxicity assays," *Journal of Immunological Methods*, vol. 65, no. 1-2, pp. 55–63, 1983.

[22] C.-L. Hsu, B. O.-H. Hong, Y. S. Yu, and G.-C. Yen, "Antioxidant and Anti-Inflammatory effects of *Orthosiphon aristatus* and its bioactive compounds," *Journal of Agricultural and Food Chemistry*, vol. 58, no. 4, pp. 2150–2156, 2010.

[23] K. Cheng, K. Ho, R. Stokes, C. Scott, and S. M. Lau, "Hypoxia-inducible factor-1alpha regulates beta cell function in mouse and human islets," *The Journal of Clinical Investigation*, vol. 120, pp. 2171–2183, 2010.

[24] S. Kadan, B. Saad, Y. Sasson, and H. Zaid, "In vitro evaluation of anti-diabetic activity and cytotoxicity of chemically analysed Ocimum basilicum extracts," *Food Chemistry*, vol. 196, pp. 1066–1074, 2016.

[25] A. A. F. Sima and S. Chakrabarti, "Long-term suppression of postprandial hyperglycaemia with acarbose retards the development of neuropathies in the BB/W-rat," *Diabetologia*, vol. 35, no. 4, pp. 325–330, 1992.

[26] T. Matsui, T. Tanaka, S. Tamura et al., "α-glucosidase inhibitory profile of catechins and theaflavins," *Journal of Agricultural and Food Chemistry*, vol. 55, no. 1, pp. 99–105, 2007.

[27] M. Yoshikawa, N. Nishida, H. Shimoda, M. Takada, Y. Kawahara, and H. Matsuda, "Polyphenol constituents from salacia species: Quantitative analysis of mangiferin with α-glucosidase and aldose reductase inhibitory activities," *Yakugaku Zasshi*, vol. 121, no. 5, pp. 371–378, 2001.

[28] H. Luo, T. Imoto, and Y. Hiji, "Inhibitory effect of voglibose and gymnemic acid on maltose absorption in vivo," *World Journal of Gastroenterology*, vol. 7, no. 2, pp. 270–274, 2001.

[29] B. Khakimov, L. H. Tseng, M. Godejohann, S. Bak, and S. B. Engelsen, "Screening for triterpenoid saponins in plants using hyphenated analytical platforms," *Molecules*, vol. 21, no. 12, Article ID 21121614, 2016.

[30] G. Di Fabio, V. Romanucci, A. De Marco, and A. Zarrelli, "Triterpenoids from Gymnema sylvestre and their pharmacological activities," *Molecules*, vol. 19, no. 8, pp. 10956–10981, 2014.

[31] M. Tominaga, M. Kimura, K. Sugiyama et al., "Effects of Seishin-renshi-in and Gymnema sylvestre on insulin resistance in streptozotocin-induced diabetic rats," *Diabetes Research and Clinical Practice*, vol. 29, no. 1, pp. 11–17, 1995.

[32] K. Baskaran, B. Kizar Ahamath, K. Radha Shanmugasundaram, and E. R. B. Shanmugasundaram, "Antidiabetic effect of a leaf extract from *Gymnema sylvestre* in non-insulin-dependent diabetes mellitus patients," *Journal of Ethnopharmacology*, vol. 30, no. 3, pp. 295–305, 1990.

[33] R. Bradley, E. B. Oberg, C. Calabrese, and L. J. Standish, "Algorithm for complementary and alternative medicine practice and research in type 2 diabetes," *The Journal of Alternative and Complementary Medicine*, vol. 13, no. 1, pp. 159–175, 2007.

[34] Y. Sugihara, H. Nojima, H. Matsuda, T. Murakami, M. Yoshikawa, and I. Kimura, "Antihyperglycemic effects of gymnemic acid IV, a compound derived from *Gymnema sylvestre* leaves in streptozotocin-diabetic mice," *Journal of Asian Natural Products Research*, vol. 2, no. 4, pp. 321–327, 2000.

[35] A. Varadi, A. Grant, M. McCormack et al., "Intracellular ATP-sensitive K+ channels in mouse pancreatic beta cells: Against a role in organelle cation homeostasis," *Diabetologia*, vol. 49, no. 7, pp. 1567–1577, 2006.

[36] A. Al-Romaiyan, B. Liu, H. Asare-Anane et al., "A novel *Gymnema sylvestre* extract stimulates insulin secretion from human islets in vivo and in vitro," *Phytotherapy Research*, vol. 24, no. 9, pp. 1370–1376, 2010.

[37] S. R. Rachh, H. V. Patel, M. T. Hirpara, M. R. Rupareliya, A. S. Rachh, and N. M. Bhargava, "In vitro evaluation of antioxidant activity of Gymnema sylvestre," *In vitro evaluation of antioxidant activity of Gymnema sylvestre*, vol. 54, no. 2, pp. 141–148, 2009.

[38] A. Leturque, E. Brot-Laroche, M. Le Gall, E. Stolarczyk, and V. Tobin, "The role of GLUT2 in dietary sugar handling," *Journal of Physiology and Biochemistry*, vol. 61, no. 4, pp. 529–538, 2005.

[39] P. M. Kumar, M. V. Venkataranganna, K. Manjunath, G. L. Viswanatha, and G. Ashok, "Methanolic leaf extract of Gymnema sylvestre augments glucose uptake and ameliorates insulin resistance by upregulating glucose transporter-4, peroxisome proliferator-activated receptor-gamma, adiponectin, and leptin levels in vitro," *Journal of Intercultural Ethnopharmacology*, vol. 5, no. 2, pp. 146–152, 2016.

Hindawi
Evidence-Based Complementary and Alternative Medicine
Volume 2018, Article ID 3565427, 10 pages
https://doi.org/10.1155/2018/3565427

Research Article

The Effect of *Morinda citrifolia* L. Fruit Juice on the Blood Sugar Level and Other Serum Parameters in Patients with Diabetes Type 2

Petra Algenstaedt,[1] **Alexandra Stumpenhagen**,[1] **and Johannes Westendorf**[2]

[1]*Department for Endocrinology and Diabetology, University Clinic Hamburg-Eppendorf, Martinistraße 52, D-20246 Hamburg, Germany*
[2]*Institute of Experimental Pharmacology and Toxicology, University Clinic Hamburg-Eppendorf, Martinistraße 52, D-20246 Hamburg, Germany*

Correspondence should be addressed to Petra Algenstaedt; algensta@gmail.com

Received 28 February 2018; Revised 21 May 2018; Accepted 13 June 2018; Published 6 August 2018

Academic Editor: Thomas Efferth

Background. The effect of the daily consumption of *Morinda citrifolia* (Noni) fruit juice on the physiological status of patients with diabetes type 2 (DT2) was tested over a period of two months. *Methods*. *Morinda citrifolia* (Noni) fruit juice (NFJ), 2 ml per kg bw per day, was consumed by twenty patients with DT2 after they underwent a standard treatment regimen including carbohydrate reduced diet and treatment with an antidiabetic drug and/or insulin. NFJ consumption started only after no further improvement was achieved. The intake of NFJ was terminated after eight weeks. The fasting blood sugar level was monitored every morning during the entire treatment period. Blood samples were taken before, at, and four and eight weeks after the start of NFJ intake. The analysis of the blood samples included the concentration of blood glucose, HbA1c, C-peptide, hs-CRP, triglycerides, total cholesterol, LDL, and HDL. *Results*. The consumption of NFJ by 20 patients with DT2 resulted in a significant mean decrease of the morning blood sugar level monitored over a period of eight weeks. While NFJ reduced the blood glucose level in several but not all hyperglycemic patients, it did not cause hypoglycemia in normoglycemic patients. NFJ consumption also reduced the mean HbA1c value significantly ($p = 0.033$). Significant decreases ($p = 0.01$) were also achieved for high sensitive CRP values in patients starting with high levels (>2 mg/L), whereas no change was observed in patients with normal values (< 2 mg/L). The level of C-peptide showed a significant mean increase after four weeks of NFJ consumption in those patients who started with low levels (<3 μg/l, $p=0.004$, N=11) but not in patients with higher levels (> 3 μg/L). *Conclusion*. The daily consumption of NFJ has the potential to regulate elevated blood sugar levels and some other pathological parameters in patients with DT2. NFJ therefore serves as a suitable additive to the diet of diabetic patients.

1. Background

Diabetes type 2 (DT2) is a metabolic disorder characterized by high blood glucose levels, insulin resistance, and a relative lack of insulin. The global number of patients diagnosed with DT2 has increased from 30 million in 1985 to 392 million in 2015 [1]. Obesity and lack of exercise significantly enhance the risk of developing DT2, which shows a higher incidence in industrial compared to underdeveloped countries [2]. DT2 is associated with increased incidences of secondary diseases, such as arteriosclerosis leading to strokes, ischemic heart disease and lower limb amputations, reduction of glomerular filtration and kidney failure, and retinopathy leading to blindness [1, 3].

The primary goal of DT2 management is to reduce the fasting blood sugar level to < 130 mg/dl. Because of the high uncertainty of the daily fasting blood glucose level, the HbA1c value is preferentially used to characterize the glycemic status of patients with diabetes [4]. This value represents the percentage of glycosylated hemoglobin accumulated during the previous 8-12 weeks and is less sensitive to deviations. Healthy patients have values around 5%. A goal of the

clinical diabetes management is to keep the HbA1c level below 7%. This is facilitated by weight reduction, a diet poor in carbohydrates, and regular exercise. Additionally, antidiabetic drugs or insulin may be necessary to adjust the blood glucose and HbA1c level. These drugs act on either the intestinal glucose absorption, biliary gluconeogenesis, insulin production and secretion, or the transcellular glucose transport. Antidiabetic drugs have several side effects, like gastrointestinal and metabolic disturbances, hypoglycemic sensations, increased risk of cardiovascular disease, and others [5].

Long before the availability of synthetic drugs, plants and their products have been used to treat diabetes. Today treatment of diabetes with phytomedicine is mostly used in underdeveloped countries, where access to synthetic drugs and insulin is limited, or in industrialized countries with tradition in the use of alternative medicine, such as China and India [6–10]. Although alternative treatment of diabetes is rarely taught in medical schools or practiced in hospitals, an increasing number of patients in Europe, USA, and Canada use nonprescribed remedies to treat their disease, mostly in addition to the conventional therapy [11–14]. Although hundreds of plants and plant products have been identified as useful in the treatment of diabetes in traditional medicine, only a few have undergone systematic investigation to demonstrate effectiveness [15]. Mechanisms of improving insulin resistance, enhancement of β-cell function, suppression of appetite, stimulation of energy expenditure, and regulation of lipid and carbohydrate metabolism have been shown for some plant derived antidiabetic remedies mainly from animal experiments [15–18]. Clinical trials to support the findings obtained from animal experiments are rare.

The fruits and leaves of the tropical plant *Morinda citrifolia* L. (Noni) have been used as a food and medicine by indigenous people of South East Asia and the Polynesian Triangle for hundreds of years. Noni was one of the most important medicinal plants for Polynesian people, who used it for multiple reasons, among which was also the treatment of diabetes [19, 20]. In the last twenty years, Noni fruit juice (NFJ) became popular worldwide as a wellness drink with the European Union authorizing the sale of NFJ in 2003 under the Novel Food Regulation [21]. Although among the benefits reported by consumers an improvement in the management of diabetes is included [22], systematic clinical trials to support the consumer testimonies are lacking. Our knowledge about the antidiabetic activity of extracts of Noni fruits and leaves comes from investigations in animal and tissue culture models for diabetes, which demonstrated an insulin-like enhancement of glucose uptake in fat and muscle cells [23].

The present clinical investigation was performed to demonstrate a possible antidiabetic action of NFJ in patients with DT2.

2. Methods

2.1. Patients. Twenty patients of the Endocrinological Department of the University Clinic Hamburg-Eppendorf diagnosed with DT2 participated in the investigation. Age, gender, fasting blood glucose level, HbA1c-value at the start of the observation period, and medication are listed in Table 1. All patients had undergone a standard management program for their condition independently from the study in order to optimize their glycemic status, before entering the study. This included adaptation of the diet, physical exercise, and medication where necessary. Patients were given the opportunity to participate in the investigation after no further improvement by the standard treatment was achieved. Patients with a poor overall health status or those with doubt about compliance were not selected to participate in the study.

2.2. Intake of NFJ and Collection of Data. NFJ is an authorized novel food in the *European Union* that confirmed that its consumption is not associated with a health risk. The clinical management of the patients attending the study did not differ from the regular schedule of patients with diabetes in the facility, which excluded any additional risk caused by the participation in the study. The data taken were a normal part of the clinical management of patients with diabetes. A special authorization by an ethical committee was not needed, because the law of the State of Hamburg, Germany, allows the use of anonymized data of patients for research purposes [24]. Nevertheless, the protocol strictly followed the principles laid down in the declaration of Helsinki [25]. All patients involved in the study were informed about the scientific background of the study, the procedure of collecting data, the anonymization, and the use of the data. A written agreement of the patients was obtained prior to participation.

NFJ (Tahitian Noni™ Juice) was kindly provided by the Company Morinda Inc., Provo, Utah, USA. The juice consisted of 89% fermented Noni fruit puree harvested in French Polynesia, blended with 11% of blueberry and red grape juice, to mask the unpleasant taste of the Noni fruits. Patients were asked to drink 2 ml NFJ/kg bw per day over a period of eight weeks. Blood samples were taken before and four and eight weeks after the start of NFJ consumption. The blood was analyzed by a routine screening protocol used in the facility for 67 different parameters like blood cells, electrolytes, liver and kidney parameters, hormones, and others (e.g., HbA1c, ferritin, and interleukins). Fasting blood glucose levels were monitored by the patients daily or every second day during the period of the NFJ consumption.

2.3. Statistical Analysis. All calculations of means and standard deviations, p values, and linear regression curves were performed by using the OriginPro® 9.1 Data Analysis and Graphing Software of Origin Lab® Corporation, Northampton, MA, USA, as well as Microsoft Excel®, 2010. p values of changes in HbA1c, C-peptide, and hs-CRP blood levels were calculated from paired t-test (values of day 0 against values after four or eight weeks). The p value of the slope of linear regression curves of fasting blood sugar values of patients between days 1 and 50 of the intake of NFJ was calculated by the one sample t-test.

Table 1: Basic data of patients, participating in the study.

No. of patients	Age (years)	Gender	Initial blood Glucose level (mg/dl)	Initial HbA1c-blood level (%)	Medication[a]
1	52	F	96	6,3	MF
2	64	M	190	6,0	MF
3	29	M	164	6,9	MF, DPI, IN
4	66	M	100	6,4	MF, DPI
5	62	F	119	6,7	
6	62	F	134	6,5	
7	69	F	138	7,6	
8	61	M	136	7,6	MET, GLP
9	65	M	118	6,3	MET
10	72	M	178	7,0	IN
11	67	M	170	7,1	MET, IN
12	52	M	193	7,1	GLP, IN
13	60	M	179	7,2	IN
14	57	M	135	7,3	MET
15	49	F	158	6,5	DPI, IN
16	43	M	134	6,9	MET
17	77	M	147	7,4	MET
18	60	M	141	6,3	MET
19	62	F	94	5,8	MET
20	69	M	186	7,2	MET, GLP, IN

[a]MET = metformin; DPI= DPP4-inhibitor, GLP1= receptor antagonist; IN= insulin

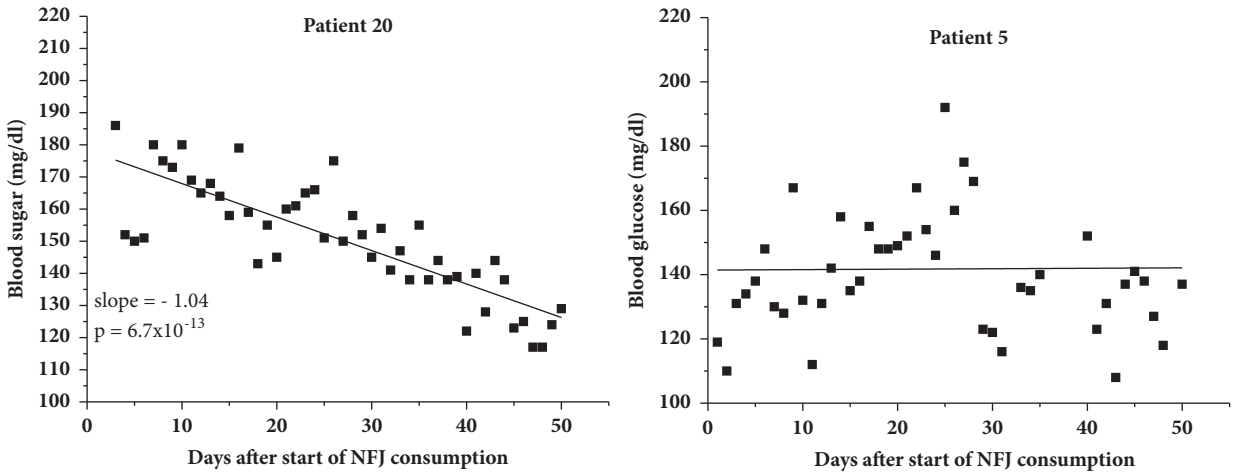

Figure 1: Fasting blood sugar level of two patients during 50 days of NFJ intake (2 ml/kg bw per day). p value for patient 20 was calculated from t-test of the linear regression coefficient.

3. Results

Fasting blood sugar profiles monitored over the entire period of NFJ consumption were available for 19 out of 20 patients. One patient (no. 16) reported only a limited number of blood sugar values and was excluded from the calculation. As expected, the daily blood sugar values showed considerable variation, which made statistical calculations difficult. Linear regression curves were therefore calculated for each individual blood sugar profile between the start and termination of the NFJ consumption. Two examples are shown in Figure 1. Patient 20 experienced a continual decrease of his fasting blood sugar value after the start of the NFJ consumption of about 50 mg/dl although the triple medication before was not able to reduce the blood sugar level below approx. 180 mg/dl. In contrast, patient 5 did not respond at all. The results of all

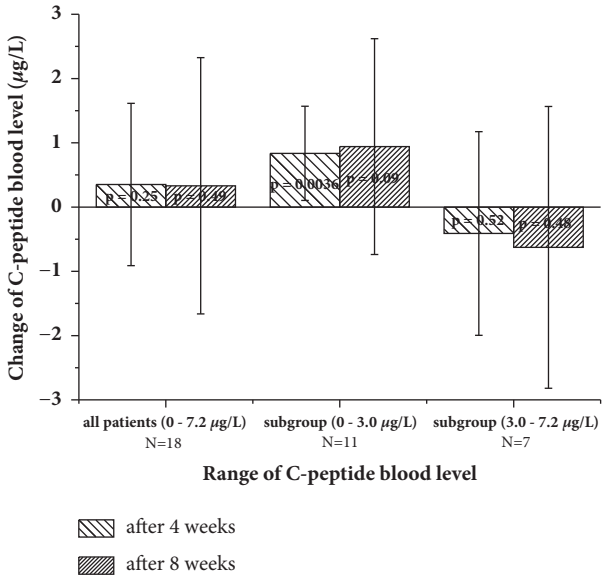

Figure 2: Changes in C-peptide blood level after four and eight weeks of NFJ consumption (2 ml/kg bw and day). p values were calculated from paired t-test (values at start against values after 4 or 8 weeks).

patients are shown in Table 2. The "*intersection with ordinate*" at day zero and day 50 represents the values of the blood sugar levels at the beginning and termination of the NFJ consumption, extrapolated from the linear regression of the blood sugar curves. This procedure reduces the spontaneous daily deviations in the blood sugar level. Negative slopes of the linear regression curves of the blood sugar level, indicating a decrease after NFJ consumption, were observed in 14 out of 20 patients. The mean and SD of the initial blood sugar value calculated from the regression curves were 139 ± 23. The corresponding values for the final blood sugar values were 125 ± 22 mg/dl. A paired t-test performed with the individual differences between the initial and final blood sugar values revealed a significant result with a p value of 0.0024. The mean and SD of the slopes of the linear regression of the blood sugar curves of the patients were -0.28 ± 0.34 mg/dl per day with a p value of 0.002, calculated from a one sample t-test. HbA1c levels of the patients under consideration at the start of the NFJ intake are shown in Table 3. All patients underwent a diabetes management program prior to the start of NFJ intake which resulted in HbA1c levels in the range of 5.8–7.9% for those recruited in the study. A significant reduction (p= 0.033) of the mean HbA1c-value of 0.27 ± 0.5% was achieved after 8 weeks of NFJ consumption on top of the routine clinical diabetes management of the patients.

The blood concentration of C-peptide is used as an indicator of the ability of pancreatic beta-cells to excrete insulin. C-peptide is liberated during transformation of proinsulin to insulin and excreted together with insulin in equimolar amounts. Its concentration is considerably more stable in blood compared to insulin, which makes it a preferable parameter for monitoring insulin secretion. Data of C-peptide blood concentrations were available for 18 patients. Because consumption of carbohydrates will cause an elevation of the C-peptide level lasting up to two hours, all patients agreed not to eat for two hours prior to the blood collection. Eleven out of 18 patients had normal or reduced ranges of C-peptide between 0.7 and 3.0 μg/L at the start of the NFJ consumption. Seven patients had elevated levels of 3.1-7.2 μg/L. Of the 11 patients with normal or reduced ranges of C-peptide, 10 showed an increase and six of the seven patients with elevated levels > 3 μg/L showed a decrease after four weeks of NFJ consumption. Considering all patients, the mean increase after four and eight weeks was 0.35 ± 1.26 (p=0.25) and 0.33 ± 1.99 (p=0.49) μg/L, respectively, and thus not significant. Different results were achieved if the patients are split into groups with normal or reduced C-peptide levels (0.7 – 3.0 μg/L) and those with elevated levels (3.1–7.2 μg/L). The results are demonstrated in Figure 2. Significant increases were obtained at normal or reduced C-peptide range between 0.7 and 3.0 μg/L (p= 0.0036) after four weeks of NFJ consumption. Although the absolute values of the increases in C-peptide levels are greater after eight compared to four weeks, the statistical significance is lower because of an increased variation within this group. DT2 is associated with an elevated risk of complications in the cardiac circulatory system. Control of the blood lipid values is therefore an important part of the clinical management of the disease. We therefore analyzed the blood concentrations of triglycerides and total cholesterol as well as HDL and LDL concentrations during the observation period. The level of triglycerides of the patients before the intake of NFJ showed considerable variation (254 ± 172 mg/dl). The lowest concentration (patient 3) was 60 and the highest (patient 14) was 580 mg/dl. Eleven out of 20 patients had values > 200 mg/dl. Independently of the starting level, some patients showed an increase and others a decrease of the triglyceride blood level after four and eight weeks of NFJ consumption. A clear trend was not observable.

Five out of 19 patients had total cholesterol levels >200 mg/dl at the start of the NFJ consumption. After eight weeks the mean blood level of these patients was reduced from 258 ± 50 mg/dl to 248 ± 43 mg/dl (p= 0.07).

Calculations of statistics for LDL-levels interfered with high triglyceride levels. There were ten triglyceride levels > 400 mg/dl in five patients, which did not allow estimation of LDL-levels. Another six vales were between 300 and 400 mg/dl, making the estimated LDL values questionable. Because of the reduced available LDL blood levels, no statistical calculation was performed.

The mean of HDL-levels of the patients at the start of the NFJ intake was 41.0 ± 10.6 mg/dl. The corresponding values after four and eight weeks of NFJ intake were 42.3 ± 10.3 mg/dl and 41.75 mg/dl, respectively. The differences were not statistically significant.

The blood level of high sensitive C-reactive protein (hs-CRP) is used as a marker for the risk of complications arising from CVD, like heart attack, strokes, and others. There was a consensus that values > 5 mg/L indicate a high risk; however, more recent studies suggest that this might be the case already with levels > 2 mg/L [26]. hs-CRP levels were available for 18 out of 20 patients. Of these, four had values > 5 (5.2–6.7) mg/L

Table 2: Linear regression data of fasting blood sugar values of patients between days 1 and 50 of the intake of NFJ (2ml/kg bw per day).

No. of patients	Intersection with Ordinate at day 0 (mg/dl)	Intersection with Ordinate at day 50 (mg/dl)	Slope (mg/dl and day)
1	103	105	0.032
2	147	160	0.26
3	133	115	-0.36
4	138	116	-0.45
5	141	142	0.014
6	114	101	-0.26
7	122	130	0.15
8	141	126	-0.30
9	125	120	-0.11
10	181	151	-0.61
11	170	164	-0.12
12	162	155	-0.14
13	154	128	-0.52
14	114	106	-0.17
15	136	90	-0.76
17	142	143	0.012
18	145	107	-0.77
19	100	90	-0.21
20	178	126	-1.04
Mean ± SD	139 ± 23	125 ± 22	-0.28 ±0.34
p-value		0.0024[a]	0.002[b]

[a]Calculated from paired t-test (values of day 0 against values of day 50).
[b]Calculated from one sample t-test.

and eleven had values > 2 (2.5–6.7) mg/L. The development of the hs-CRP values during the consumption period of NFJ is shown in Figure 3. No significant changes of the mean values after eight weeks of NFJ consumption are seen, if all patients are included in the calculation; however, if only patients with values > 2 mg/L are considered, a highly significant decrease occurs after eight weeks (p=0.01).

4. Discussion

DT2 is one of the greatest health threats in modern societies, potentially leading to morbidity and early death. The disease is closely related to excess nutrition and lack of physical exercise. Consequently, control of nutrition and enhancement of physical exercise are primary mechanisms of diabetes management; however these actions are not sufficient in many cases, especially for those in advanced stages of the disease. Most patients with DT2 receive additionally an oral medication and/or injection of insulin [27]. A variety of synthetic drugs with hypoglycemic activities are used. The drug categories include sulfonylureas, biguanides, alpha-glucosidase inhibitors, thiazolidinediones, and meglitinides. Their mechanisms of action involve the enhancement of insulin secretion, the improvement of insulin sensitivity in muscle and liver cells, the inhibition of hepatic glucose formation, enhancement of muscle glucose uptake, and the inhibition of carbohydrate digestion [15]. Each of the different mechanisms has its own side effects, which can be mild, such as gastrointestinal disturbances, or severe, such as liver and kidney toxicity.

Phytotherapy is an alternative to the treatment of diabetes with synthetic drugs, mainly used in countries like China and India; however, its acceptance in Europe and North America is increasing. Although several hundred plants have been reported to be useful in the treatment of diabetes, in most cases a systematic scientific evaluation of their effects is lacking [15]. Further investigation of traditional medicinal herbs useful in diabetes treatment is recommended by the WHO Expert Committee on diabetes [13].

Similar to synthetic drugs, plants with hypoglycemic properties act also via different mechanisms, among which are the inhibition of carbohydrate digestion and glucose absorption, enhancement of glucose uptake into liver and muscle cells via upregulation of glucose transporters, regulation of fatty acid, carbohydrate, and glucose metabolism via activation of nuclear receptor PPAR-γ, and insulinomimetic and insulinotropic effects [19]. Most of the plants used for the treatment of DT2 do not have the side effects of synthetic drugs. Moreover, antidiabetic phytomedicines often have additional activities, which are directed against the long term collateral damage caused by DT2 [15]. This is possible, because plants and herbal extracts contain a variety

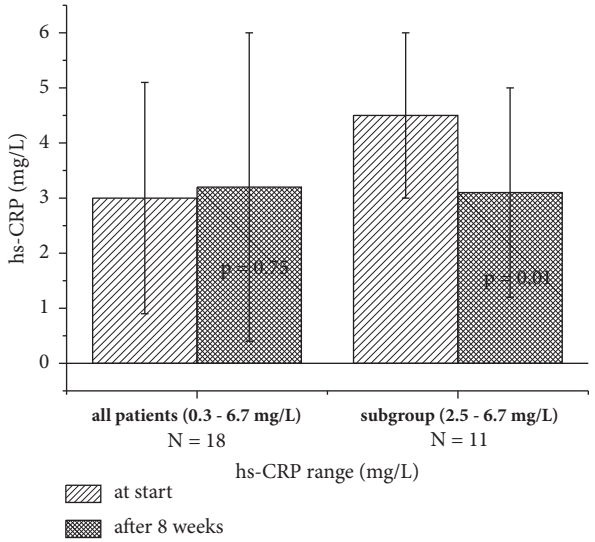

Figure 3: hs-CRP values of patients at the start and after consumption of NFJ (2 ml/kg BW per day). p values were calculated from paired t-test (p values at start against values after 4 or 8 weeks).

of compounds with antioxidative, anti-inflammatory, wound healing, antimicrobial, and hormone regulating properties, which act on the complex clinical symptoms associated with diabetes mellitus.

Noni plants have been used by indigenous Polynesian people for the treatment of diabetes for hundreds of years [20, 21]. After 1996, NFJ became very popular as a wellness drink worldwide, but also for relief of inflammatory pain, to improve the immune defense system and physical endurance and also to lower the blood glucose level and adverse symptoms associated with diabetes [23]. Our knowledge about the antidiabetic activity of NFJ comes mainly from preclinical investigations [28–31]. Nayak et al. [28] have shown that a NFJ dose of 2 ml/kg bw twice a day decreased the fasting blood glucose level in streptozotocin induced diabetic rats to 150 mg/dl compared to 300 mg/dl in controls. A marked decrease of the blood glucose and HbA1c levels was also observed in diabetic mice fed with fermented Noni fruit juice [30]. The authors of this study also demonstrated that fermented NFJ stimulated the glucose uptake into cultured C2C12 cells via stimulation of AMP-activated protein kinase.

In our clinical study, 20 patients consumed 2 ml/kg bw of NFJ once a day. In contrast to the rat experiment, NFJ was taken by the patients additionally to the standard therapy including adaptation of the diet, enforcement of physical exercise, and application of antidiabetic drugs. Nevertheless, significant decreases of the blood glucose levels and HbA1c were observed. Patient 20, who received a triple medication with metformin, insulin, and a GLP1-receptor antagonist, experienced an additional decrease of the blood sugar level of about 50 mg/dl during the intake of NFJ. The mean and SD of the slopes of the blood sugar curves of the patients between start and termination of NFJ consumption after eight weeks were -0.28 ± 0.34 mg/dl per day with a p value of 0.002. Thus, the decrease of the blood sugar values was highly

Table 3: Changes in the HbA1c (%) blood level of patients with DT2 during 50 days of NFJ intake (2ml/kg bw per day).

No. of patients	at start	after 4 weeks	after 8 weeks
1	6.2	6.1	5.6
2	6.4	6.6	6.6
3	6.9	6.5	6.3
4	6.4	6.7	6.6
5	6.6	6.6	6.3
6	6.9	5.9	5.6
7	6.9	6.5	6.8
8	7.6	7.0	6.6
9	5.4	5.6	5.6
10	7.0	7.2	6.7
11	7.9	8.0	8.3
12	7.2	7.6	7.3
13	7.2	7.4	6.9
14	7.3	6.9	6.9
15	6.5	5.9	5.9
16	6.9	6.9	7.4
17	7.4	7.3	7.3
18	6.3	6.5	6.5
19	5.5	5.4	no data
20	7.2	6.7	6.3
Mean (range)	6.80 (5.5-7.9)	6.67 (5.4-8.0)	6.61 (5.6-8.3)
SD	0.64	0.67	0.69
p-value		0.17[a]	0.044[b]

[a]Calculated from paired t-test (values at start against values after 4 weeks; N=20).
[b]Calculated from paired t-test (values at start against values after 8 weeks; N=19).

significant. This was also confirmed by the comparison of the HbA1c values between start and termination of the NFJ consumption. A mean decrease of 0.2 ± 0.7% was achieved after eight weeks (p value = 0.03). Although this decrease was only small, it should be noted that it is significant and on top of a standard management of diabetes. Moreover, the observation time of eight weeks is the minimum duration for changes of the HbA1c-value to be detectable. Thus, the clinical data from the present investigation are in line with the experimental data obtained previously with laboratory animals.

Mechanistic experiments regarding the hypoglycemic effects of NFJ have been performed in animals and with tissue culture [28–31]. Such results demonstrated that NFJ exerts an insulin mimetic activity. Applied together with insulin, NFJ synergistically improved the hypoglycemic effect of insulin in alloxan-induced diabetic rats [31]. Insulin mimetic effects of NFJ were also demonstrated in 3T3-L1 adipocytes; however, no synergistic activity with insulin was observed [30]. Activation of AMP-kinase (AMPK) via phosphorylation leads to an increased uptake of glucose in adipocytes and

muscle cells [32]. Lee et al. [30] demonstrated that fermented NFJ increased the phosphorylation of AMPK in C2C12-derived myotubes in culture in a dose dependent manner. Furthermore, the authors showed that NFJ also enhanced the activity of PPAR-γ, a transcription factor that regulates gene expression in the liver, adipose tissue, vascular endothelium, and muscle. Activation of PPAR-γ increases the expression of the glucose transporter GLUT-4 and its translocation into the cell membrane of adipocytes [33]. It also decreases the output of glucose from liver cells [34]. It is therefore likely that the improvement of the glucose homeostasis observed in our study with DT2 patients is at least partly attributed to an increase of an insulin-independent uptake of glucose into energy storage cells and a decrease of the output from liver cells. Our finding that the C-peptide secretion is increased after consumption of NFJ in patients with a low blood level ($< 3\,\mu$g/L) but not in patients with higher levels (3-7 μg/L) additionally indicates that NFJ may also be able to restore the feedback of the glucose blood level on the insulin synthesis in and/or secretion from pancreatic β-cells. Thus, patients with DT2 may benefit from two different mechanisms of NFJ, one of which is directed to the glucose storage cells and the other to insulin supply.

Diabetes is associated with a variety of secondary consequences, which increase the morbidity and reduce the life expectancy. Most critical ones are micro- and macrovascular damage, leading to ischemic heart disease, stroke, kidney failure, blindness, and lower limp amputations [1]. Disturbances of the lipid metabolism with elevated cholesterol levels and inflammatory processes are involved in the damage of vascular tissue [33]. Synthetic drugs used for the treatment of DT2 reduce the blood sugar level; however, they have no or little influence on the complications associated with the disease. Plant derived preparations are complex in composition and often contain compounds with multiple benefits for patients with diabetes [6, 10, 16, 17, 19, 20]. This is also the case for NFJ, which is known to stabilize and restore the homeostasis. Epidemiological surveys among consumers have shown that regular consumption of NFJ is able to enhance the energy and physical endurance, improve inflammatory pain in joints and back, and strengthen the immune system [23, 35]. A double-blind placebo controlled clinical trial among heavy smokers has shown that NFJ is able to reduce the cholesterol level significantly [36]. A differential analysis of the serum lipid fraction made in this trial showed a decrease of triglycerides and LDL and an increase of HDL. An improvement of the blood cholesterol status of patients with DT2 was also observed in our study. A small nonsignificant reduction of 3 and 4 mg/dl total cholesterol was observed after four and eight weeks of NFJ consumption, respectively. If only patients with elevated cholesterol levels (> 200 mg/dl) were considered (N=5) the reduction after four and eight weeks was 15 and 17 mg/dl. Statistical calculations of LDL-levels were not possible, because several patients had triglyceride levels of $>$ 400 mg/dl, which made monitoring of the LDL-levels difficult or impossible. Triglyceride levels of patients were reduced by NFJ intake in some cases and elevated in others. A clear trend was not observable.

Inflammatory processes are involved in obesity and DT2. Reduction of inflammation markers, such as cytokines (IL6, TNF-α) and CRP may lead to an improvement of glycaemia and cardiovascular prognosis [37]. One of the most beneficial properties of NFJ is its anti-inflammatory activity, which has been proven in epidemiological investigations [23, 35] and preclinical studies in tissue culture [38] and animal models [39, 40]. Recently we observed anti-inflammatory effects in dentistry patients with gingivitis after mouth wash with NFJ followed by swallowing [41]. In the present study we investigated the effect of NFJ on the inflammation marker hs-CRP of patients with DT2. Eleven out of 19 patients had elevated blood levels > 2 mg/L. After eight weeks, the mean hs-CRP values of these patients were reduced from 4.5 ± 1.5 to 3.1 ± 1.9 mg/L. This change was highly significant ($p = 0.01$).

NFJ contains numerous compounds with beneficial health effects. Among these are flavonoids (quercetin, kaempferol), coumarins (scopoletin), iridoids (deacetylasperulosidic acid, asperulosidic acid, and asperuloside), and others [42–45], which have been demonstrated to exert antioxidative and anti-inflammatory properties [46–49]. Special attention has been given to the iridoid fraction in NFJ because of the biological activity profile of this group of compounds [50]. The most abundant iridoid in NFJ is deacetylasperulosidic acid (DAA) [45]. This compound has been shown to exert antioxidative and anti-inflammatory properties in rats [51]. Monotropein, an iridoid which is closely structurally related to DAA, also showed antinociceptive and anti-inflammatory activity in rats [52]. We have recently demonstrated that DAA is absorbed and excreted unchanged after oral application to mice [53]. This finding was unexpected because DAA is an iridoid glucoside, which is expected to be hydrolyzed by intestinal and/or liver glucosidases. Plants synthesize iridoid glycosides for defense purposes against herbivorous predators [54]. The aglycones released after hydrolysis are highly reactive and bind to bioactive functional proteins of the intestinal wall and liver, which are inactivated. The lack of sensitivity of murine (and other mammalian) glucosidases towards DAA is most probably an evolutionary adaptation of the animals to bypass the toxicity of DAA and similar compounds. We also found that some other iridoids, structurally related to DAA (monotropein, geniposidic acid, and asperulosidic acid), appeared unchanged in the urine after oral application to mice (unpublished results). The systemic appearance of iridoid glycosides, which are bitter in taste, could nevertheless be recognized as potential toxic via bitter taste receptors [55]. Such receptors (i.e., T2Rs) are distributed in several organs and initiate a cascade of defense mechanisms in order to combat with the impact of the expected toxicity [56]. T2R16 has been demonstrated to be sensitive to β-glucopyranosides, the chemical group to which DAA and other iridoids belong [57]. Properties of iridoids, such as an enhancement of the antioxidative potential, decrease of inflammatory processes, pain perception, and metabolic effects, could be interpreted as an adaptogenic response to potential toxic compounds with bitter taste. T2Rs present in some gastrointestinal cells have been shown to secrete the peptide hormones ghrelin and

glucagon-like peptide-1 (GLP-1) in response to stimulation by bitter tasting compounds [56]. GLP-1 stimulates the excretion of insulin in response to an increase of the blood glucose level [58]. This mechanism could also be involved in the observed effects of NFJ on the blood glucose level of patients with DT2 involved in our study. The fact that some of the patients showed a response of the blood glucose level after NFJ consumption, while others did not, is possibly due to individual differences in the expression of extraoral bitter taste receptors, which show an extensive polymorphism within the human population [59]. The widespread distribution of iridoids in plants used as food and spices could open new strategies in the treatment of diabetes and other diseases; however, the validity of this hypothesis has to be confirmed by further investigations.

5. Conclusion

The present pilot study showed that the consumption of 2 ml/kg bw of NFJ over a period of eight weeks caused a significant decrease in fasting blood glucose levels and HbA1c values in twenty patients with diabetes type 2. All patients had followed a standard diabetes treatment schedule before recruitment and during the study. The NFJ consumption also increased the insulin excretion (monitored via C-peptide), improved the blood cholesterol status, and reduced the inflammation parameter hs-CRP. The study showed that NFJ can serve as a suitable addition to the diet of patients with diabetes type 2. Further trials with an increased number of participants are warranted to confirm the findings of the present study.

Abbreviations

AMPK: Adenosine monophosphatase kinase
bw: Body weight
CRP: C-reactive protein
DAA: Deacetylasperulosidic acid
DT-1 (2): Diabetes type 1 (2)
GLP-1: Glucagon-like peptide 1
HDL: High density lipoprotein
HbA1c: Glycated hemoglobin
hs-CRP: High sensitive C-reactive protein
LDL: Low density lipoprotein
NFJ: Noni fruit juice
SD: Standard deviation
T2Rs: Mammalian taste receptors.

Data Availability

The data used to support the findings of this study are available from the corresponding author upon request.

Additional Points

Author's Information. Petra Algenstaedt is the leading physician of the Department of Endocrinology and Diabetology of the University Clinic Hamburg-Eppendorf and supervisor of the present study. Alexandra Stumpenhagen is physician and doctoral student of Petra Algenstaedt. Johannes Westendorf is professor emeritus of the Institute of Experimental Pharmacology and Toxicology of the University Clinic Hamburg-Eppendorf.

Ethical Approval

The present study is not a comparative intervention study. All patients underwent a normal clinical management for diabetes and consumed NFJ (an EU-approved novel food) voluntarily over a time of eight weeks. The hospital law of the state of Hamburg, Germany, allows the use of data collected from patients during their normal clinical management in anonymized form for research purposes without approval by an ethical committee (see reference [22]). Nevertheless, the principles laid down in the declaration of Helsinki were strictly followed.

Consent

All patients signed a written agreement to allow the use of their data for research purposes in an anonymized form.

Disclosure

The study was not funded by a third party.

Conflicts of Interest

The authors declare that they have no conflicts of interest.

Authors' Contributions

Petra Algenstaedt supervised this work and was responsible for the management of the diabetic patients. She also provided the anonymized data of her patients to the other authors. Alexandra Stumpenhagen collected the data and performed the calculations together with Johannes Westendorf, who also wrote the manuscript.

Acknowledgments

The help of Marlies John during the recruitment of the patients is gratefully acknowledged. The authors thank Dr. Andrew Chesson for the revision of the language of the manuscript. They also acknowledge the Company Morinda Inc., Provo, Utah, USA, for providing them with Noni fruit juice.

References

[1] S. Melmed, K. S. Polonsky, P. R. Larsen, and H. M. Kronenberg, Eds., *Williams Textbook of Endocrinology*, Elsevier/Saunders, Philadelphia, PA, USA, 12 edition, 2011.

[2] L. Carulli, S. Rondinella, S. Lombardini, I. CanedI, P. Loria, and N. Carulli, "Review article: diabetes, genetics and ethnicity,"

Alimentary Pharmacology and Therapeutics, vol. 22, no. 2, pp. 16–19, 2005.

[3] C. M. Ripsin, H. Kang, and R. J. Urban, "Management of blood glucose in type diabetes mellitus," *American Family Physician Journal*, vol. 79, no. 1, pp. 29–36, 2009.

[4] D. M. Nathan, D. E. Singer, K. Hurxthal, and J. D. Goodson, "The clinical information value of the glycosylated hemoglobin assay," *The New England Journal of Medicine*, vol. 310, no. 6, pp. 341–346, 1984.

[5] A. Chaudhury, C. Duvoor, and V. S. Reddy Dendi, "Clinical review of antidiabetic drugs: implications for type 2 diabetes mellitus management," *Frontiers in Endocrinology*, vol. 8, no. 6, 2017.

[6] M. F. Mahomoodally, A. Mootoosamy, and S. Wambugu, "Traditional therapies used to manage diabetes and related complications in mauritius: a comparative ethnoreligious study," *Evidence-Based Complementary and Alternative Medicine*, vol. 2016, 2016.

[7] R. J. Marles and N. R. Farnsworth, "Antidiabetic plants and their active constituents," *Phytomedicine*, vol. 2, no. 2, pp. 137–189, 1995.

[8] S. K. Marwat, F. Rehman, E. A. Khan et al., "Useful ethnomedicinal recepies of angiosperms used against diabetes in South East Asian countries (India, Pakistan and Sri Lanka)," *Pakistan Journal of Pharmaceutical Sciences*, vol. 27, no. 5, pp. 1333–1358, 2014.

[9] U. F. Ezuruike and J. M. Prieto, "The use of plants in the traditional management of diabetes in Nigeria: pharmacological and toxicological considerations," *Journal of Ethnopharmacology*, vol. 155, no. 2, pp. 857–924, 2014.

[10] A. Pandey, P. Tripathi, R. Pandey, R. Srivatava, and S. Goswami, "Alternative therapies useful in the management of diabetes: A systematic review," *Journal of Pharmacy and Bioallied Sciences*, vol. 3, no. 4, pp. 504–512, 2011.

[11] E. A. Ryan, M. E. Pick, and C. Marceau, "Use of alternative medicines in diabetes mellitus," *Diabetic Medicine*, vol. 18, no. 3, pp. 242–245, 2001.

[12] J. A. Astin, "Why patients use alternative medicine: results of a national study," *Journal of the American Medical Association*, vol. 279, no. 19, pp. 1548–1553, 1998.

[13] C. J. Bailey and C. Day, "Traditional plant medicines as treatments for diabetes," *Diabetes Care*, vol. 12, no. 8, pp. 553–564, 1989.

[14] S. A. Kouzi, S. Yang, D. S. Nuzum, and A. J. Dirks-Naylor, "Natural supplements for improving insulin sensitivity and glucose uptake in skeletal muscle," *Frontiers in Bioscience (Elite edition)*, vol. 7, pp. 94–106, 2015.

[15] L. Dey, A. S. Attele, and C. S. Yuan, "Alternative therapies for type 2 diabetes," *Alternative Medicine Review*, vol. 7, no. 1, pp. 45–58, 2002.

[16] H. Jung, Y. Lim, and E. Kim, "Therapeutic Phytogenic compounds for obesity and diabetes," *International Journal of Molecular Sciences*, vol. 15, no. 11, pp. 21505–21537, 2014.

[17] N. G. Jambocus, A. Ismail, A. Khatib et al., "Morinda citrifolia L. leaf extract prevent weight gain in sprague-dawley rats fed a high fat diet," *Food and Nutrition Research*, vol. 61, no. 1, p. 1338919, 2017.

[18] N. G. S. Jambocus, N. Saari, A. Ismail, A. Khatib, M. F. Mahomoodally, and A. J. Abdul Hamid, "An investigation into the antiobesity effects of morinda citrifolia L. leaf extract in high fat diet induced obese rats using a 1H NMR metabolomics approach," *Journal of Diabetes Research*, vol. 2016, Article ID 2391592, 14 pages, 2016.

[19] H. S. El-Abhar and M. F. Schaalan, "Phytotherapy in diabetes: Review on potential mechanistic perspectives," *World Journal of Diabetes*, vol. 5, no. 2, pp. 176–197, 2014.

[20] W. McClatchey, "From Polynesian healers to health food stores: changing perspectives of *Morinda citrifolia* (Rubiaceae)," *Integrative Cancer Therapies*, vol. 1, no. 2, pp. 110–120, 2003.

[21] L. McBride, *Practical Folk Medicine of Hawaii*, The Petroglyph Press, Hilo, HI, USA, 1975.

[22] European Commission, "Commission Decision of 5 June 2003 authorising the placement on the market of "Noni juice" (juice of the fruit of Morinda citrifolia L.) as a novel food ingredient under the regulation (EC) No. 258/97 of the European Parliament and of the Council," *Official Journal of the European Union*, vol. 12, no. 12.6, p. L144, 2003.

[23] J. Westendorf and C. Mettlich, "The benefits of Noni juice: an epidemiological evaluation in Europe," *Medical Food Plants*, vol. 1, no. 2, pp. 64–79, 2009.

[24] *Hamburgisches Krankenhausgesetz (HmbKHG) vom 17*, Hospital Law of the state of Hamburg, Germany, 1991.

[25] World Medical Association Declaration of Helsinki, *Ethical Principles for Medical Research Involving Human Subjects*, vol. 79, Bulletin of the World Health Organization, 4th edition, 2001.

[26] T. A. Pearson, G. A. Mensah, R. W. Alexander et al., "Markers of inflammation and cardiovascular disease: application to clinical and public health practice: A statement for healthcare professionals from the centers for disease control and prevention and the American Heart Association," *Circulation*, vol. 107, no. 3, pp. 499–511, 2003.

[27] R. A. DeFronzo, "Pharmacologic therapy for type 2 diabetes mellitus," *Annals of Internal Medicine*, vol. 131, no. 4, pp. 281–303, 1999.

[28] B. S. Nayak, J. R. Marshall, G. Isitor, and A. Adogwa, "Hypoglycemic and hepatoprotective activity of fermented fruit juice of Morinda citrifolia (noni) in diabetic rats," *Evidence-Based Complementary and Alternative Medicine*, vol. 2011, 2011.

[29] P. V. Nerurkar, A. Nishioka, P. O. Eck, L. M. Johns, E. Volper, and V. R. Nerurkar, "Regulation of glucose metabolism via hepatic forkhead transcription factor 1 (FoxO1) by Morinda citrifolia (noni) in high-fat diet-induced obese mice," *British Journal of Nutrition*, vol. 108, no. 2, pp. 218–228, 2012.

[30] S. Y. Lee, S. L. Park, J. T. Hwang, S. H. Yi, Y. D. Nam, and S. I. Lim, "Antidiabetic effect of morinda citrifolia (Noni) fermented by cheonggukjang in KK-Ay diabetic mice," *Evidence-Based Complementary and Alternative Medicine*, vol. 2012, Article ID 163280, 8 pages, 2012.

[31] A. U. Horsfall, O. Olabiyi, A. Aiyegbusi, C. C. Noronha, and A. O. Okanlawon, "Morinda citrifolia fruit juice augments insulin action in Sprague-Dawley rats with experimentally induced diabetes.," *Nigerian Quarterly Journal of Hospital Medicine*, vol. 18, no. 3, pp. 162–165, 2008.

[32] M. Zang, A. Zuccollo, X. Hou et al., "AMP-activated protein kinase is required for the lipid-lowering effect of metformin in insulin-resistant human HepG2 cells," *The Journal of Biological Chemistry*, vol. 279, no. 46, pp. 47898–47905, 2004.

[33] M. Armoni, N. Kritz, C. Harel et al., "Peroxisome proliferator-activated receptor-γ represses GLUT4 promoter activity in primary adipocytes, and rosiglitazone alleviates this effect," *The Journal of Biological Chemistry*, vol. 278, no. 33, pp. 30614–30623, 2003.

[34] K. Nagashima, C. Lopez, D. Donovan et al., "Effects of the PPARγ agonist pioglitazone on lipoprotein metabolism in patients with type 2 diabetes mellitus," *The Journal of Clinical Investigation*, vol. 115, no. 5, pp. 1323–1332, 2005.

[35] M. Pande, M. Naiker, G. Mills, N. Singh, and T. Voro, "The Kura files: qualitative social survey," *Pacific Health Surveillance and Response*, vol. 12, no. 2, pp. 85–93, 2005.

[36] M. Wang, L. Peng, V. Weidenbacher-Hoper, S. Deng, G. Anderson, and B. J. West, "Noni juice improves serum lipid profiles and other risk markers in cigarette smokers," *The Scientific World Journal*, vol. 2012, Article ID 594657, 8 pages, 2012.

[37] C. Garcia, B. Feve, P. Ferré et al., "Diabetes and inflammation: Fundamental aspects and clinical implications," *Diabetes & Metabolism*, vol. 36, no. 5, pp. 327–338, 2010.

[38] E. Dussossoy, P. Brat, E. Bony et al., "Characterization, anti-oxidative and anti-inflammatory effects of Costa Rican noni juice (Morinda citrifolia L.)," *Journal of Ethnopharmacology*, vol. 133, no. 1, pp. 108–115, 2011.

[39] N. Yilmazer, C. Coskun, E. Gurel-Gurevin, I. Yaylim, E. H. Eraltan, and E. I. Ikitimur-Armutak, "Antioxidant and anti-inflammatory activities of a commercial noni juice revealed by carrageenan-induced paw edema," *Polish Journal of Veterinary Science*, vol. 19, no. 3, pp. 589–595, 2016.

[40] S. Basar, K. Uhlenhut, P. Högger, F. Schöne, and J. Westendorf, "Analgesic and antiinflammatory activity of Morinda citrifolia L. (Noni) fruit," *Phytotherapy Research*, vol. 24, no. 1, pp. 38–42, 2010.

[41] J. Glang, W. Falk, and J. Westendorf, "Effect of Morinda citrifolia L. fruit juice on gingivitis/periodontitis," *Modern Research in Inflammation*, vol. 02, no. 02, pp. 21–27, 2013.

[42] A. D. Pawlus and A. D. Kinghorn, "Review of the ethnobotany, chemistry, biological activity and safety of the botanical dietary supplement *Morinda citrifolia* (noni)," *Journal of Pharmacy and Pharmacology*, vol. 59, no. 12, pp. 1587–1609, 2007.

[43] B.-N. Su, A. D. Pawlus, H.-A. Jung, W. J. Keller, J. L. McLaughlin, and A. D. Kinghorn, "Chemical constituents of the fruits of Morinda citrifolia (Noni) and their antioxidant activity," *Journal of Natural Products*, vol. 68, no. 4, pp. 592–595, 2005.

[44] O. Potterat and M. Hamburger, "*Morinda citrifolia* (Noni) fruit—Phytochemistry, pharmacology, safety," *Planta Medica*, vol. 73, no. 3, pp. 191–199, 2007.

[45] S. Deng, B. J. West, A. K. Palu, and C. J. Jensen, "Determination and comparative analysis of major iridoids in different parts and cultivation sources of *Morinda citrifolia*," *Phytochemical Analysis*, vol. 22, no. 1, pp. 26–30, 2011.

[46] U. J. Youn, E.-J. Park, T. P. Kondratyuk et al., "Anti-inflammatory and quinone reductase inducing compounds from fermented noni (morinda citrifolia) juice exudates," *Journal of Natural Products*, vol. 79, no. 6, pp. 1508–1513, 2016.

[47] J. V. Formica, "Review of the biology of quercetin and related bioflavonoids," *Food and Chemical Toxicology*, vol. 33, no. 12, pp. 1061–1080, 1995.

[48] H.-J. Kim, S. I. Jang, Y.-J. Kim et al., "Scopoletin suppresses pro-inflammatory cytokines and PGE2 from LPS-stimulated cell line, RAW 264.7 cells," *Fitoterapia*, vol. 75, no. 3-4, pp. 261–266, 2004.

[49] K. S. Park, B. H. Kim, and I. M. Chang, "Inhibitory potencies of several iridoids on cyclooxygenase-1, cyclooxygnase-2 enzymes activities, tumor necrosis factor-α and nitric oxide production in vitro," *Evidence-Based Complementary and Alternative Medicine*, vol. 7, Article ID 598084, pp. 41–45, 2010.

[50] R. Tundis, M. R. Loizzo, F. Menichini, and G. A. Statti, "Biological and pharmacological activities of iridoids: recent developments," *Mini-Reviews in Medicinal Chemistry*, vol. 8, no. 4, pp. 399–420, 2008.

[51] D. L. Ma, M. Chen, C. X. Su, and B. J. West, "In vivo antioxidant activity of deacetylasperulosidic acid in noni," *Journal of Analytical Methods in Chemistry*, vol. 2013, Article ID 804504, 5 pages, 2013.

[52] J. Choi, K.-T. Lee, M.-Y. Choi et al., "Antinociceptive anti-inflammatory effect of monotropein isolated from the root of Morinda officinalis," *Biological & Pharmaceutical Bulletin*, vol. 28, no. 10, pp. 1915–1918, 2005.

[53] S. Basar-Maurer, T. Hackl, E. Schwedhelm, and J. Westendorf, "Pharmacokinetic of 3H-deacetylasperulosidic acid in mice," *Funct Foods Health Disease*, vol. 6, no. 8, pp. 478–492, 2016.

[54] S. Dobler, G. Petschenka, and H. Pankoke, "Coping with toxic plant compounds - The insect's perspective on iridoid glycosides and cardenolides," *Phytochemistry*, vol. 72, no. 13, pp. 1593–1604, 2011.

[55] M. Behrens and W. Meyerhof, "Mammalian bitter taste perception," *Results and Problems in Cell Differentiation*, vol. 47, pp. 203–220, 2009.

[56] A. A. Clark, S. B. Liggett, and S. D. Munger, "Extraoral bitter taste receptors as mediators of off-target drug effects," *The FASEB Journal*, vol. 26, no. 12, pp. 4827–4831, 2012.

[57] B. Bufe, T. Hofmann, D. Krautwurst, J.-D. Raguse, and W. Meyerhof, "The human TAS2R16 receptor mediates bitter taste in response to β-glucopyranosides," *Nature Genetics*, vol. 32, no. 3, pp. 397–401, 2002.

[58] Z. Wang, R. M. Wang, A. A. Owji, D. M. Smith, M. A. Ghatei, and S. R. Bloom, "Glucagon-like peptide-1 is a physiological incretin in rat," *The Journal of Clinical Investigation*, vol. 95, no. 1, pp. 417–421, 1995.

[59] A. A. Bachmanov and G. K. Beauchamp, "Taste receptor genes," *Annual Review of Nutrition*, vol. 27, pp. 389–414, 2007.

Hindawi
Evidence-Based Complementary and Alternative Medicine
Volume 2018, Article ID 5490491, 11 pages
https://doi.org/10.1155/2018/5490491

Research Article

Metabolomics-Based Clinical Efficacy and Effect on the Endogenous Metabolites of Tangzhiqing Tablet, a Chinese Patent Medicine for Type 2 Diabetes Mellitus with Hypertriglyceridemia

Jia Liu,[1] Ziqiang Li,[1] Hua Liu,[2] Xianhua Wang,[3] Chunxiao Lv,[1] Ruihua Wang,[1] Deqin Zhang,[2] Yan Li,[4] Xi Du,[1] Yanfen Li,[1] Baohe Wang,[1] and Yuhong Huang[1]

[1]*Second Affiliated Hospital of Tianjin University of Traditional Chinese Medicine, Tianjin, China*
[2]*Tianjin University of Traditional Chinese Medicine, Tianjin, China*
[3]*Tianjin Medical University, Tianjin, China*
[4]*Tianjin International Joint Academy of Biomedicine, Tianjin, China*

Correspondence should be addressed to Yuhong Huang; hyh101@126.com

Jia Liu and Ziqiang Li contributed equally to this work.

Received 25 January 2018; Revised 29 May 2018; Accepted 27 June 2018; Published 24 July 2018

Academic Editor: Akhilesh K. Tamrakar

Tangzhiqing tablet (TZQ) is derived from Tangzhiqing formula, which has been used to regulate glucose and lipid metabolism in China for hundreds of years. However, as a new Chinese patent medicine, its clinical indication is not clear. To explore the clinical indication and effect on the patients with type 2 diabetes mellitus (T2DM), a pilot clinical trial and metabolomics study were carried out. In the clinical study, T2DM patients were divided into three groups and treated with TZQ, placebo, or acarbose for 12 weeks, respectively. The metabolomic study based on UPLC Q-TOF MS was performed including patients with hypertriglyceridemia in TZQ and placebo groups and healthy volunteers. The clinical results showed that TZQ could reduce glycosylated hemoglobin (HbA1c) and fasting insulin. For patients with hypertriglyceridemia in TZQ group, the levels of HbA1c all decreased and were correlated with the baseline level of triglyceride. Metabonomics data showed a significant difference between patients and healthy volunteers, and 17 biomarkers were identified. After 12-week treatment with TZQ, 11 biomarkers decreased significantly ($p<0.05$), suggesting that TZQ could improve the metabolomic abnormalities in these participants. In conclusion, the clinical indication of TZQ was T2DM with hypertriglyceridemia, and its target was related to glycerophospholipid metabolism.

1. Introduction

Diabetes is a global health concern causing increasing morbidity, mortality, and social and economic burdens annually. According to the newly released Diabetes Atlas from the International Diabetes Federation (IDF), a total of 425 million adults had diabetes globally in 2017, and the number is expected to rise to 642 million by 2040 (www.diabetesatlas.org). During the past few years, the number of people with diabetes, especially type 2 diabetes mellitus (T2DM), is growing rapidly worldwide. Hypertriglyceridemia, which is tightly relevant to unhealthy lifestyle, is a common comorbidity in diabetes. Epidemiological studies in Asia and Europe found that hypertriglyceridemia is commonly associated with diabetes [1, 2]. Both of these two symbiotic disorders are recognized as independent risk factors for cardiovascular disease [3].

Traditional Chinese Medicine (TCM) has a long history in treating diabetes and hypertriglyceridemia, because of early intervention, multiple targets, and treatment based on syndrome differentiation. TCM can significantly retard diseases progression and improve quality of life. Tangzhiqing tablet (TZQ) is a Chinese patent medicine derived from Tangzhiqing formula which consists of five herbs, *Paeonia*

lactiflora Pall., root, *Morus alba* L., leaf, *Nelumbo nucifera* Gaertn., leaf, *Salvia miltiorrhiza bge*., roots, and *Crataegus pinnatifida bge*., leaf [4]. The preclinical studies have shown that TZQ could significantly regulate the abnormal glucose and lipid levels in genetic type 2 diabetic KK-A^y mice [5–8] and high-carbohydrate/high-fat diet rats [9]. These effects are related to glucose and lipid absorption inhibition and free radical scavenging. The effects on glucose and lipid homeostasis are mediated through regulating adipocyte differentiation and insulin action by AMPK signaling pathway and PI3K/AKT signaling pathway [5–9]. Besides, TZQ can improve glucose metabolism by reducing α-glycosidase activity [5].

Metabolomics is used to evaluate the characteristics and interactions of low molecular weight metabolites under a specific set of conditions. It is a powerful analytical strategy to identify the metabolites *in vivo* and clarify metabolic pathways. Especially for metabolic disease, such as T2DM, metabolomics offers an opportunity to test multiple metabolic markers in large settings. Wang et al. found five branched-chain and aromatic amino acids had highly significant associations with future diabetes by the prospective Framingham Heart Study (FHS) using a 12-year follow-up [10]. Lu et al. found three branched-chain amino acids and four nonesterified fatty acids (NEFA) were potent predictors of diabetes development in Chinese adults [11]. Other metabolites, including phospholipids [11–14], acylcarnitines [12, 13], amino acids [11–15], triglycerides [16], and small molecular weight compounds [11, 12, 14–16] have been defined as biomarkers for predicting T2DM, covering the glucose and phospholipid metabolism.

As a new Chinese patent medicine, the clinical indication of TZQ is still undefined, and the regulating effect on patients is not clear yet. In this study, we carried out a pilot clinical trial on T2DM patients to tentatively evaluate the clinical efficacy and determine clinical indication of TZQ. Moreover, the metabolomics strategy based on the ultraperformance liquid chromatography combined with quadrupole time-of-flight tandem mass spectrometry (UPLC Q-TOF MS) method combining with pattern recognition techniques was performed to investigate the changes in endogenous metabolites in serum between T2DM patients with hypertriglyceridemia and healthy volunteers.

2. Materials and Methods

2.1. Drugs and Reagents. TZQ (0.64 g), TZQ simulation agent (0.64 g), and acarbose simulation agent (50 mg) were obtained from Shandong Buchang Shenzhou Pharmaceutical Co., Ltd., which conducted Investigational New Drug Application (IND) study in November 2010 by CFDA (China Food and Drug Administration). Acarbose (50 mg) was produced by Bayer Healthcare Pharmaceuticals.

HPLC-grade acetonitrile was purchased from Merck (Merck, Germany). HPLC-grade formic acid was bought from ROE (ROE, USA). Deionized water was produced by Milli-Q ultrapure water system (Millipore, USA). Leucine-enkephalin was obtained from Sigma-Aldrich (MO, USA).

2.2. Study Subjects and Clinical Trial Design. The study subjects were recruited as part of a project entitled "Clinical trial to evaluate the efficacy and safety of TZQ on T2DM". (The registration number from the international clinical trial net is ChiCTR-TTRCC-12002866.) All participants were adults in Tianjin region without renal or liver dysfunction. The study protocol was in accordance with the Helsinki declaration and approved by the Ethics Committee of the Second Affiliated Hospital of Tianjin University of Traditional Chinese Medicine. Written informed consent was obtained from all participants.

Diabetic patients (with glycosylated hemoglobin (HbA1c) of 7.0%-9.0%) without any previous history of drug use and with ages between 18 and 75 were selected as subjects. Figure 1 showed the flow diagram of this pilot clinical trial. The subjects who met the inclusion criteria were introduced to run-in period (TZQ simulation agent 1.92 g, TID) for 2 weeks and then entered the trial period for 12 weeks. The subjects were divided into three groups randomly: (1) TZQ group (TZQ 1.92 g, TID; acarbose simulation 50 mg, TID), (2) placebo group (TZQ simulation agent 1.92 g, TID; acarbose simulation 50 mg, TID), and (3) acarbose group (TZQ simulation agent 1.92 g, TID; acarbose 50 mg, TID). During the 12-week study period, a total of three visits (on the 4th, 8th, and 12th weeks) would be performed. During the process of the trial, the low fat diet was performed, including the fact that the calories from fat were no more than 30% of total calories, and the acceptable intake of saturated fatty acid was no more than 10%. The use of any other T2DM or hyperlipidemia treatment including oral medication, TCM therapy, and health care products was prohibited.

To investigate pharmacologic effects, the body mass index (BMI), waistline, glycosylated hemoglobin (HbA1c), fasting insulin (FINS), fasting blood glucose (FBG), oral glucose tolerance test at 2 h after oral ingestion of 75 g of glucose (OGTT2hBG), triglycerides (TG), total cholesterol (TC), low-density lipoprotein cholesterol (LDL-C), and high-density lipoproteins cholesterol (HDL-C) were measured at the beginning and the end of the study. To evaluate the safety of TZQ, routine clinical laboratory tests and electrocardiogram (ECG) were also measured.

2.3. Samples Collection and Preparation for Metabolomics. For metabolomics, each five subjects with hypertriglyceridemia (TG>1.70) in TZQ group and placebo group were selected. In addition, five healthy volunteers matched by age and sex were included in the normal group. They were screened by medical history, physical examination, and routine laboratory investigations. Their body mass index ranged between 19.67 and 21.84 kg/m^2 (mean ± SD, 20.82±0.92 kg/m^2). All of them signed the informed consent form. For TZQ group and placebo group, human blood samples were collected at the beginning and the end of the study. For normal group, blood samples were collected just once. Venous blood of every subject was collected in the morning before breakfast and was immediately centrifuged at 3500 rpm for 10 min and serum was transferred into a clean eppendorf tube. The serum samples were stored at -80°C until analysis.

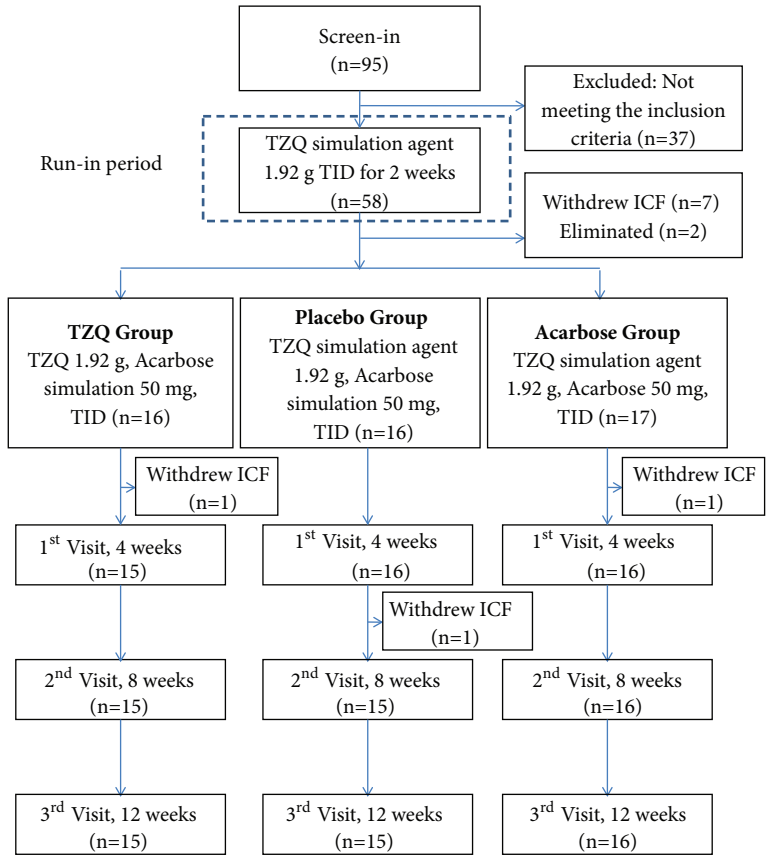

Figure 1: Flow diagram of the clinical trial.

Prior to analysis, the samples were thawed at room temperature and 100 μL of serum samples was mixed with 300 μL of acetonitrile. After being vortexed for 1 min and incubated for 10 min at 4°C, the mixture was centrifuged for 10 min at 13,000 rpm. The supernatant was transferred to a new eppendorf tube, followed by evaporation to dryness in a speedvac concentrator. Subsequently, the residue was resuspended in 100 μL mobile phase prior to instrument analysis. Quality-control (QC) samples were prepared by mixing equal amount of serum from each sample and the metabolites were extracted using the same procedures as the test samples. One QC was inserted regularly before and after running every five samples.

2.4. Instrument Analysis. The ultraperformance liquid chromatography combined with quadrupole time-of-flight tandem mass spectrometry (UPLC Q-TOF MS) analysis was performed on Nexera X2 system (Shimadzu, Japan) coupled with a TripleTOF 5600 quadrupole-time-of-flight mass spectrometer (SCIEX, USA). Samples were separated on an Agilent ZORBAX Eclipse Plus C18 column (2.1×100 mm, 1.8 μm). The column temperature was maintained at 40°C, and the flow rate was 0.25 mL/min. The mobile phase consisted of water (A) and acetonitrile (B) both containing 0.1% (v/v) formic acid. The gradient was initiated with 2% B for 1 min and then linearly increased to 90% B within 13 min. The gradient was kept at 90% B for 2 min and then back to 2% B within 0.1 min and held at 2 % B for another 4 min. The total run was 20 min. The Q-TOF mass spectrometer was run in positive mode. The data of m/z were collected for each test sample from 50 Da to 1500 Da. Parameters of MS were set as follows: capillary voltage: 3.0 kV; curtain gas: 35 psi; declustering potential: 100 V; collision energy: 10 V; interface heater temperature: 550°C.

2.5. Metabolomics Data Analysis. The raw data acquired by UPLC Q-TOF MS were imported to MarkerView software (version 1.2.1, SCIEX, USA) to conduct data pretreatment procedures, such as retention time alignment, peak discrimination, filtering, alignment, matching, and identification. After the algorithm operation of the software, a peak table with retention time (t_R), m/z value, and corresponding peak intensity was generated. MetaboAnalyst 3.0 (http://www.metaboanalyst.ca/) was used for chemometrics analysis, such as principal components analysis (PCA) and partial least squares discriminate analysis (PLS-DA). To identify potential biomarkers, the accurate mass, retention time, and the fragmentation pattern from MS/MS had to be used. Besides, Human Metabolome Database (http://www.hmdb.ca/) was used to screen the potential biomarkers through m/z acquired by UPLC Q-TOF MS with molecular weight tolerance ±10 ppm. Open database sources, including MetaboAnalyst 3.0

Table 1: The comparison of baseline characteristics among three groups (mean ± S.D.).

Variable	TZQ-F Group (n=15)	Placebo Group (n=15)	Acarbose Group (n=16)
Sex (M/F)	8/7	12/3	9/7
Age (year)	62.93±6.11	57.40±9.74	58.07±5.23
BMI (kg/m2)	26.99±3.17	28.56±3.87	25.90±2.27
Waistline (cm)	95.43±11.24	100.23±8.36	94.87±8.44
HbA1c (%)	7.64±0.81	7.59±1.03	7.25±0.79
FINS (mIU/L)	16.64±8.65	15.00±7.07	15.10±14.57
FBG (mmol/L)	7.44±1.17	7.75±1.07	7.62±1.17
OGTT2hBG (mmol/L)	13.96±4.02	13.76±3.15	13.91±4.68
TG (mmol/L)	1.52±0.61	2.06±1.05	2.35±1.38
TC (mmol/L)	4.92±0.70	4.87±0.82	4.74±0.78
LDL-C (mmol/L)	2.86±0.52	2.87±0.61	2.59±0.63
HDL-C (mmol/L)	1.38±0.39	1.17±0.25	1.22±0.35

Note: data were analyzed using ANOVA. $p>0.05$ (among three groups). FBG: fasting blood glucose; OGTT 2hBG: oral glucose tolerance test 2 h blood glucose; HbA1c: glycosylated hemoglobin; BMI: body mass index; TC: total cholesterol; TG: triglyceride; HDL: high-density lipoprotein cholesterol; LDL: low-density lipoprotein cholesterol.

(http://www.metaboanalyst.ca/) and KEGG (http://www.kegg.jp/), were used to identify the metabolic pathways.

2.6. Statistical Analysis. For clinical trial, all data were presented as mean ± SD and performed using SPSS 20.0 software. Paired t-test was used to assess the effects of each subject before and after the treatment. One-way analysis of variance (ANOVA) and covariance analysis were carried out to analyze the differences among the groups. Independent sample t-test was used to compare the baseline characteristics between case group and normal group. For metabolomics data, the mass and charge features of metabolites were log-transformed and auto scaled before PCA and PLS-DA. Besides, the univariate analysis, including fold change (FC) analysis and Student's *t*-tests, was also performed in MetaboAnalyst 3.0. Paired t-test was used to compare the changes of the peak intensity of the potential biomarkers before and after treatment in TZQ group and placebo group. All tests were two-tailed, and the level of significance was set at 0.05.

3. Results

3.1. Comparison of Baseline Characteristics among Three Groups. A total of 95 subjects were recruited for the study, and 58 subjects were suitable for inclusion criteria mentioned above. Except for 10 who withdrew due to personal reasons and 2 eliminated because of unstable (changes >15%) FBG or TG levels observed during the run-in period, 46 subjects completed the clinical trial, aged from 39 to 75. There were no adverse events in this study. The comparison of baseline characteristics among three groups was summarized in Table 1. The baseline characteristics of gender, age, BMI, waistline, HbA1c, FINs, FBG, OGTT2hBG, and blood lipids showed no statistically significant difference among three groups by ANOVA ($p > 0.05$).

3.2. Comparisons of Clinical Characteristics among Different Groups before and after Treatment. After the 12-week treatment, a significant decrease of OGTT2hBG (p=0.020) and TG (p=0.044) from baseline was observed in acarbose group using paired t-test. Compared with placebo group, FINS (p=0.019) and OGTT2hBG (p=0.041) decreased significantly in acarbose group using covariance analysis. The decrease of HbA1c, FINs, and OGTT2hBG from baseline in TZQ group, although not statistically significant, was also observed (Table 2). For HbA1c, a decreasing tendency was observed in TZQ group (n=5) as TG>1.70 mmol/L (n=5). Interestingly, the decrease of HbA1c was positively correlated with the baseline level of TG (Figure 2).

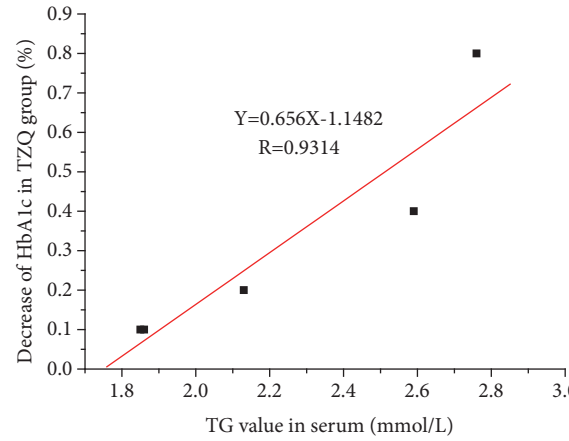

Figure 2: The relationship between the decrease of HbA1c and the corresponding TG baseline value (TG>1.7 mmol/L) in TZQ group (n=5).

3.3. Clinical Subjects in Metabolomics. To demonstrate that TZQ had more dramatic hypoglycemic effect on T2DM patients with hypertriglyceridemia, each five subjects with TG>1.70 mmol/L from TZQ group and placebo group were selected to metabolomics (case group). In addition, five healthy volunteers matched by age and sex were admitted into

Table 2: The changes comparison of clinical characteristics before and after treatment in three groups (mean ± S.D.).

Variable	TZQ Group (n=15)		Placebo Group (n=15)		Acarbose Group (n=16)	
	Before treatment	After treatment	Before treatment	After treatment	Before treatment	After treatment
BMI (kg/m2)	26.99±3.17	25.41±3.44	28.56±3.87	28.53±3.44	25.90±2.27	25.69±2.33
Waistline (cm)	95.43±11.24	92.77±10.29	100.23±8.36	100.60±8.29	94.87±8.44	93.63±7.74
HbA1c (%)	7.64±0.81	7.52±1.18	7.59±1.03	7.67±0.74	7.25±0.79	7.16±0.92
FINS (mIU/L)	16.64±8.65	14.28±8.29	15.00±7.07	15.73±7.77	15.10±14.57	$10.42\pm4.97^{\triangle}$
FBG (mmol/L)	7.44±1.17	7.85±2.11	7.75±1.07	7.98±1.43	7.62±1.17	7.27±1.22
OGTT2hBG (mmol/L)	13.96±4.02	13.72±4.89	13.76±3.15	13.90±4.65	13.91±4.68	$12.03\pm4.30^{*\triangle}$
TG (mmol/L)	1.52±0.61	1.88±1.51	2.06±1.05	2.17±1.24	2.35±1.38	$1.81\pm1.18^{*}$
TC (mmol/L)	4.92±0.70	4.99±0.93	4.87±0.82	4.95±1.05	4.74±0.78	4.56±0.90
LDL (mmol/L)	2.86±0.52	2.91±0.70	2.87±0.61	2.85±0.79	2.59±0.63	2.52±0.73
HDL (mmol/L)	1.38±0.39	1.30±0.40	1.17±0.25	1.17±0.30	1.22±0.35	1.24±0.40

Note: data were analyzed using paired t-test or covariance analysis. $^{*}p< 0.05$ (compared with the same group before treatment, paired t-test), $^{\triangle}p < 0.05$ (compared with placebo group, covariance analysis). FBG: fasting blood glucose; OGTT 2hBG: oral glucose tolerance test 2 h blood glucose; HbA1c: glycosylated hemoglobin; BMI: body mass index; TC: total cholesterol; TG: triglyceride; HDL: high-density lipoprotein cholesterol; LDL: low-density lipoprotein cholesterol.

Table 3: The comparison of baseline characteristics between case group and normal group in metabolomics (mean ± SD).

Variable	Normal group (n=5)	Case group (n=10)			
		TZQ group (n=5)		placebo group (n=5)	
	mean ± SD	mean ± SD	p	mean±SD	p
Sex (M/F)	2/3	2/3		4/1	
Age (year)	60.60±1.95	62.60±6.43	0.524	49.80±8.76	0.027
BMI (kg/m2)	20.82±0.92	24.92±3.80	0.047	29.32±4.37	0.003
Waistline (cm)	73.60±4.72	93.30±16.10	0.031	98.40±7.27	<0.001
HbA1c (%)	4.66±0.92	7.84±0.75	<0.001	7.96±0.71	<0.001
FINS (mIU/L)	9.50±4.29	16.71±8.87	0.140	14.66±5.90	0.153
FBG (mmol/L)	4.66±0.50	6.89±1.30	0.007	8.29±1.34	<0.001
OGTT2hBG (mmol/L)	9.26±0.92	12.38±1.32	0.002	14.42±1.46	<0.001
TG (mmol/L)	1.04±0.06	2.24±0.42	<0.001	2.61±0.47	<0.001
TC (mmol/L)	3.47±0.68	5.29±0.64	0.002	4.88±0.39	0.004
LDL-C (mmol/L)	1.88±0.61	3.06±0.41	0.007	2.88±0.36	0.013
HDL-C (mmol/L)	1.50±0.22	1.21±0.26	0.087	0.95±0.28	0.009

Note: data were analyzed using independent sample t test. FBG: fasting blood glucose; OGTT2hBG: oral glucose tolerance test 2 h blood glucose; HbA1c: glycosylated hemoglobin; BMI: body mass index; TC: total cholesterol; TG: triglyceride; HDL: high-density lipoprotein cholesterol; LDL: low-density lipoprotein cholesterol.

normal group. Demographic and clinical parameters of these groups were shown in Table 3.

3.4. The Detection Analysis of the Metabolomics by UPLC Q-TOF MS. UPLC Q-TOF MS analysis was carried out to acquire metabolic profiles. Operation conditions were optimized to elute as many metabolites as possible in a single injection. Finally, a total of 4859 positive ion mode features were extracted from the UPLC Q-TOF MS data. QC data showed that the RSD of retention time and peak intensity of m/z 132.1 (1.94 min), m/z 302.3 (8.48 min), and m/z 496.3 (4.16 min) were 0.21%, 0.47%, 0.85%, and 9.76%, 8.64%, 8.98%, respectively. The results indicated the good stability and reproducibility during the whole analysis procedure.

3.5. Metabolomics and Pathway Analysis. To distinguish case group and normal group based on UPLC Q-TOF MS spectra and understand their endogenous metabolic differences, principal components analysis (PCA) was carried out. Case group and normal group contained 10 and 5 samples, respectively. The results of PCA scores plot showed that the two groups were separated with no overlap (Figure 3(a)), indicating that the serum metabolic pattern was significantly different between the case group and normal group.

The variable importance in the projection (VIP) in partial least square discriminate analysis (PLS-DA) and t-test analysis identified metabolites that were significantly different between case group and normal group. The potential biomarkers were identified by the fragmentation pattern from MS/MS and ions with VIP>1 and $p<0.05$. Table 4 showed the potential biomarkers and possible metabolite pathways. The levels of diacylglycerol (DG(22:0/20:5), DG(15:0/18:3)), phosphatidylcholine (PC(15:0/20:2), PC(16:0/22:4), PC(14:0/14:1)), phosphatidylethanolamine (PE(14:0/18:4), PE (14:0/20:4)), lysophosphatidylcholine (LysoPC(16:0), LysoPC

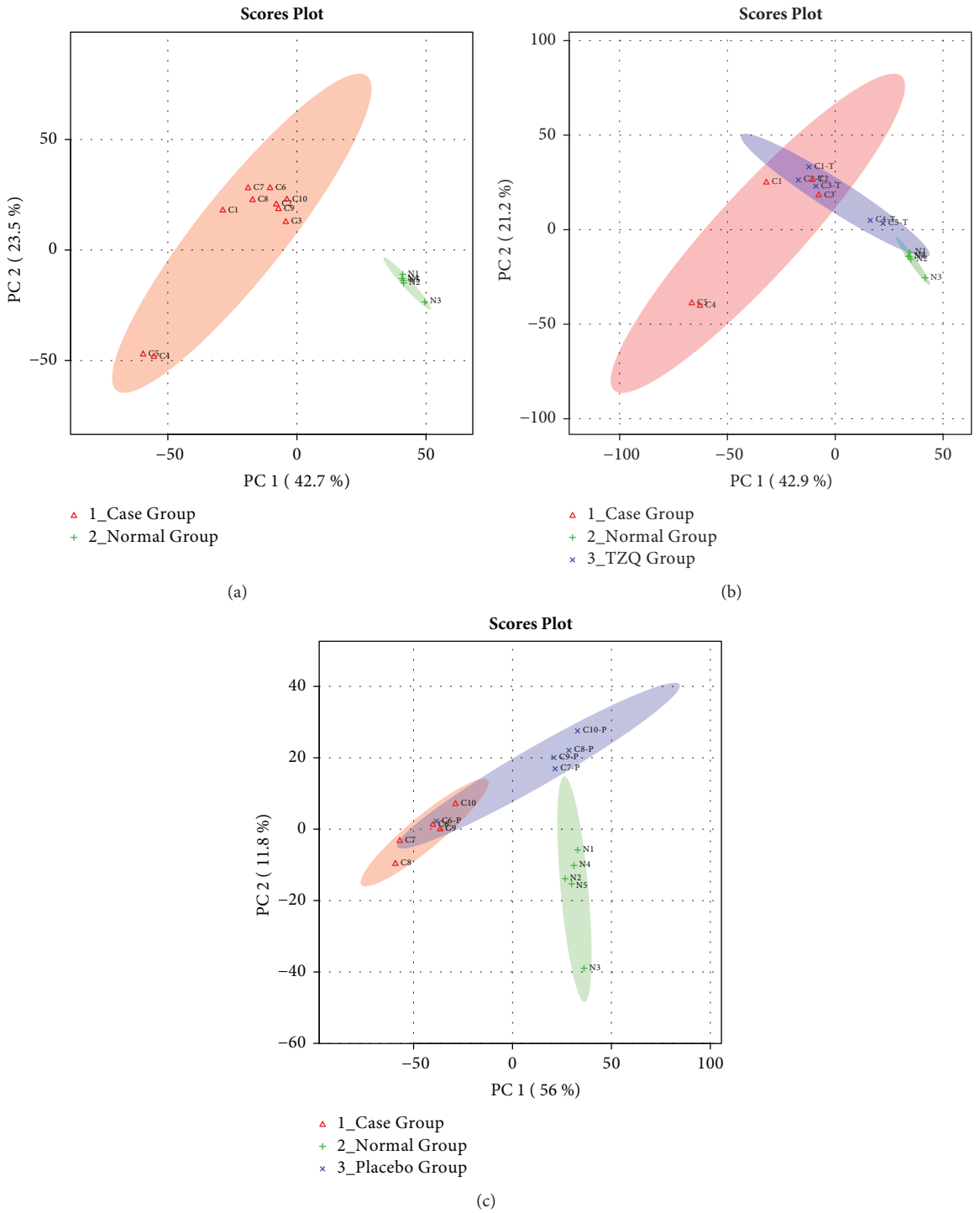

Figure 3: Principal components analysis (PCA) scores plot of case group and normal group (a); case group, normal group, and TZQ group (b); and case group, normal group, and placebo group (c).

(18:0), LysoPC(18:3), LysoPC(14:1)), D-galactose, uridine diphosphate glucose (UDP-glucose), L-leucine, and L-tyrosine in patients were significantly higher than that in healthy volunteers, whereas sphinganine and cholest-5-ene were significantly lower.

To determine whether TZQ affected the metabolic pattern of patients and to find the metabolites with significant changes, PCA was used. The results of scores plot showed that the case group and normal group were separated clearly, and the five cases with TZQ treated for 12 weeks (Figure 3(b)) were mainly located between the case group and the normal group. While the other five cases with placebo treated (Figure 3(c)) were much closer to the case group. Combined with the result of clinical effect, this change of serum

Table 4: The potential biomarkers and possible metabolite pathways.

m/z	t_R	Metabolite	Class	HMDB	VIP	p value	Trend*	Metabolic pathways
181.1559	1.52	D-Galactose	Carbohydrate	00143	1.5497	<0.001	up	Galactose metabolism
567.3018	2.13	UDP-glucose		00286	1.3043	0.002	up	
132.1018	1.94	L-Leucine	amino acid	00687	1.4244	<0.001	up	Aminoacyl-tRNA biosynthesis
182.0809	1.85	L-Tyrosine		00158	1.1778	0.002	up	
496.3386	4.16	LysoPC(16:0)	Glycerophospholipid	10382	1.4823	<0.001	up	Glycerophospholipid metabolism
524.3685	5.15	LysoPC(18:0)		10384	1.0618	0.008	up	
518.3238	4.79	LysoPC(18:3)		10387	1.5689	0.007	up	
466.2898	3.83	LysoPC(14:1)		10380	1.3510	<0.001	up	
772.5782	8.97	PC(15:0/20:2)		07946	1.1258	0.004	up	
810.6019	9.38	PC(16:0/22:4)		07988	1.0647	0.008	up	
676.4853	8.26	PC(14:0/14:1)		07867	1.5373	<0.001	up	
684.4608	9.54	PE(14:0/18:4)		08832	1.4224	<0.001	up	
712.4935	9.99	PE(14:0/20:4)		08838	1.5114	<0.001	up	
699.5945	11.93	DG(22:0/20:5)	glyceride	07607	1.4373	<0.001	up	
577.4806	11.03	DG(15:0/18:3)		07076	1.005	0.014	up	
302.3058	8.48	Sphinganine	Sphingolipid	00269	1.4622	<0.001	down	Sphingolipid metabolism
371.3699	9.81	Cholest-5-ene	Cholestene	00941	1.3602	<0.001	down	- - -

Note: Data were analyzed by Student's t-tests. *Trend: Case group versus Normal group.

metabolic pattern showed that the patients were exhibiting a tendency to recovering to normal group after TZQ treatment, which agreed with the change of HbA1c. Table 5 indicated that LysoPC(16:0), LysoPC(18:3), LysoPC(14:1), PC(15:0/20:2), PC(16:0/22:4), PC(14:0/14:1), PE(14:0/20:4), DG(22:0/20:5), and DG(15:0/18:3) decreased significantly ($p<0.05$) after the treatment of TZQ. These results indicated that some metabolites had tendency to come back from the case group to the normal group after TZQ treatment.

On the basis of 17 potential biomarkers between the case group and normal group, the pathway analysis based on MetaboAnalyst 3.0 was carried out. As shown in Figure 4, the main pathways between T2DM patients with hypertriglyceridemia and healthy volunteers were glycerophospholipid metabolism, galactose metabolism, aminoacyl-tRNA biosynthesis, and amino sugar and nucleotide sugar metabolism ($p<0.05$). Compared with the peak intensity in the different groups, TZQ treatment drove glycerophospholipid metabolism in patients to return to normal gradually.

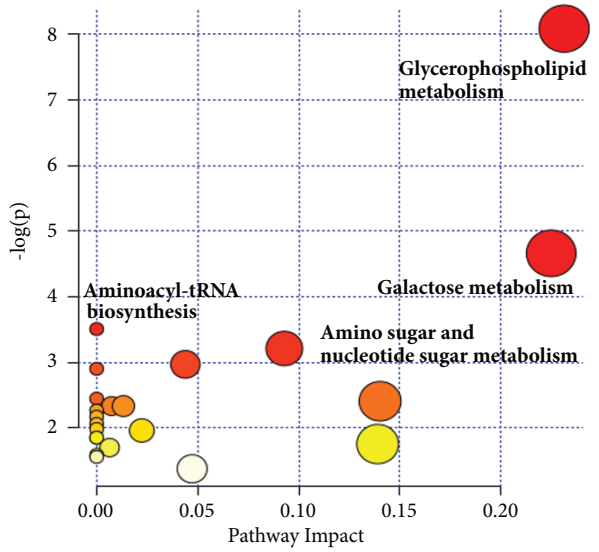

Figure 4: The main metabolic pathways based on potential biomarkers.

4. Discussion

In this study, a pilot clinical trial on T2DM patients for evaluating the clinical efficacy and determining clinical indication of TZQ was carried out. The results showed that TZQ was beneficial for T2DM with hypertriglyceridemia. Metabolomics revealed that TZQ regulated the disorder of glycerophospholipid metabolism in T2DM patients with hypertriglyceridemia.

4.1. Clinical Trials. Patients with TZQ treatment (1.92g, TID) for 12 weeks had a trend to lower the values of FINS, OGTT2h, HbA1c, waistline, and BMI based on this pilot clinical trial. Compared with other diagnostic criteria for diabetes, HbA1c level is correlated with blood glucose level and can represent the average blood glucose level within 4 to 12 weeks. While FBG, OGTT2hBG, and random blood glucose can only represent transient blood glucose and be impacted by nervousness. This trial indicated that TZQ could decrease the level of HbA1c for the patients with TG>1.70. Moreover, the decrease of HbA1c was positive correlation with the baseline level of TG. The results of HbA1c demonstrated that TZQ treatment for 12 weeks continuously had an effective hypoglycemic activity on T2DM patients with hypertriglyceridemia. Besides, the sample size could be estimated through this pilot clinical trial as follows [17, 18]:

Table 5: The changes comparison of the peak intensity of the potential biomarkers before and after treatment in two groups (mean ± S.D.).

Biomarkers	TZQ Group (n=15)			Placebo Group (n=15)		
	Before treatment	After treatment	p	Before treatment	After treatment	p
D-Galactose	2097.23±555.64	1796.80±1050.53	0.610	2217.10±464.44	2486.60±1038.89	0.579
UDP-glucose	1220.75±685.75	468.26±308.37	0.155	682.36±217.58	882.12±213.60	0.086
L-Leucine	3490.38±274.78	3397.90±76.80	0.470	3505.53±239.78	4093.26±1029.48	0.331
L-Tyrosine	1667.88±208.55	1573.02±135.06	0.276	1579.23±185.80	1847.48±480.83	0.237
LysoPC(16:0)	9833.36±1318.86	3633.52±1197.10	<0.001	6021.73±1873.12	5961.09±4533.85	0.969
LysoPC(18:0)	751.23±118.43	742.64±381.31	0.958	863.39±81.89	850.71±315.53	0.926
LysoPC(18:3)	18365.49±1468.24	8804.01±1598.84	<0.001	16399.05±1399.12	15440.55±4240.13	0.513
LysoPC(14:1)	626.84±296.06	157.11±18.67	0.026	517.33±293.07	299.37±381.13	0.294
PC(15:0/20:2)	781.42±142.81	489.05±169.67	0.001	840.39±64.15	893.06±417.55	0.778
PC(16:0/22:4)	7471.85±2200.75	3462.13±407.02	0.015	6396.02±2356.44	4846.48±1015.19	0.222
PC(14:0/14:1)	1081.27±366.46	186.24±47.03	0.005	1062.27±340.92	1141.66±292.78	0.665
PE(14:0/18:4)	816.29±661.96	226.31±196.64	0.198	360.05±91.35	511.65±125.01	0.124
PE(14:0/20:4)	1659.73±611.85	642.14±142.21	0.026	1867.68±441.45	1896.16±1102.87	0.966
DG(22:0/20:5)	1171.63±515.18	365.11±60.69	0.017	935.65±219.09	916.33±549.78	0.952
DG(15:0/18:3)	1549.78±708.90	415.63±292.41	0.007	779.78±508.12	835.61±482.38	0.860
Sphinganine	3594.59±5522.04	1203.80±287.44	0.396	1302.85±151.44	1205.19±355.10	0.451
Cholest-5-ene	28.69±29.76	37.82±34.07	0.341	7.89±4.14	17.73±18.12	0.326

Note: data were analyzed using paired t-test.

$$m = \frac{\left(Z_{1-\alpha/2} + Z_{1-\beta}\right)^2 2\sigma^2}{\delta^2} \quad (1)$$

$$\sigma^2 = \frac{\left(n_1 - 1\right) S_1^{\ 2} + \left(n_2 - 1\right) S_2^{\ 2}}{n_1 + n_2 - 2} \quad (2)$$

where m is the sample size required in each group; α is the significance level; $Z_{1-\alpha/2}$ is the 100(1-α/2)th percentile of the standard normal distribution and depends on level of significance, $Z_{1-\alpha/2}$=1.960 for α=0.05; 1-β is the power; $Z_{1-\beta}$ is the 100(1-β)th percentile of the standard normal distribution and depends on power, $Z_{1-\beta}$=0.845 for 1-β=0.8; n is the number of every group of the pilot clinical trial; S^2 is the variance in the change of outcome in every group; δ is the margin based upon a combination of statistical reasoning and clinical importance, generally ranged from 1/5 to 1/2 of σ^2, here, δ=0.4 for both noninferiority trial and superiority trial.

According to the equations above, a significant difference (p<0.05) would be detected for the primary outcome HbA1c between TZQ group and acarbose group (noninferiority trial) or between TZQ group and placebo group (superiority trial) if the sample size increased to 92 or 108.

4.2. Metabolomics Study. Compared with healthy volunteers, 17 potential biomarkers were identified as risk of T2DM, including increased levels of D-galactose, UDP-glucose, L-leucine, L-tyrosine, LysoPC species, PC species, PE species, and DG species, and decreased levels of sphinganine and cholest-5-ene. These potential biomarkers refer to glucose, amino acid, and lipid metabolism, and the relationship to insulin resistance was illuminated in Figure 5.

After the 12-week treatment with TZQ, a serial of PC, PE, lysoPC, and DG was decreased, while other metabolites were not changed significantly. Briefly, TZQ influenced the glycerophospholipid metabolism directly and regulated the glucose and lipid metabolism to treat T2DM with hypertriglyceridemia.

4.3. Glycerophospholipid Metabolism. In this study, TZQ had strong impact on glycerophospholipids, including LysoPC, PC, PE, and DG, which were significantly elevated in case group (VIP>1 and p<0.05). PC and PE are the largest amount of glycerophospholipid in mammals. They are classes of important constituents in the biomembranes and provide the majority of membrane lipids within cells. In most types of cells, the synthesis of PC and PE is both through DG, which is related to insulin resistance [19]. Glycerophospholipid species, which are synthesized downstream of DG, are probable contributors to metabolic diseases. In fact, the increase of PC and PE was related strongly to obesity, diabetes, and other metabolic syndromes [20, 21].

PC plays an important role in the lipid storage to form lipid droplets and lipoproteins, which are both increased in obesity. Some researchers indicated that the increase of PC to liver-derived microsomes *in vitro* or the additional PC content in the membrane inhibited the calcium transport activity of sarcoendoplasmic reticulum Ca^{2+}-ATPase (SERCA), which maintained calcium homeostasis in this organelle principally [22, 23]. This contributed to protein misfolding and endoplasmic reticulum (ER) stress and resulted in insulin resistance finally [24]. Selathurai et al. verified that phospholipids were the probable modulators of muscle insulin resistance rather than diacylglycerol or triacylglycerol, through muscle-specific knocking out of ethanolamine-phosphate cytidylyltransferase in mice, which retained insulin sensitivity and showed marked increases in mitochondrial biogenesis

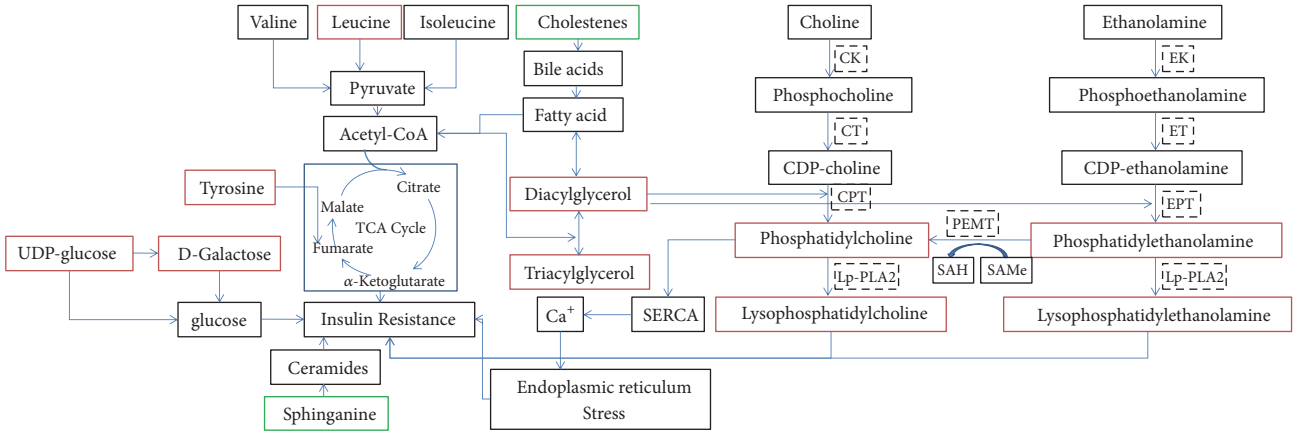

Figure 5: The relationship between insulin resistance and 17 potential biomarkers. Red represented the biomarkers whose peak intensity rose in case group, and green represented the biomarkers whose peak intensity reduced in case group (CK, choline kinase; CT, CTP phosphocholine cytidylyltransferase; CPT, CDP-choline:1,2-diacylglycerol cholinephos-photransferase; lp-PLA2: phospholipase A2; EK, Ethanolamine kinase; ET, phosphoethanolamine cytidylyltransferase; EPT, CDP-ethanolamine:1,2-diacylglycerol ethanolaminephosphotransferase; PEMT, phosphatidylethanolamine N-methyltransferase; SAH, S-adenosylhomocysteine; SAMe, S-adenosylmethionine).

and muscle oxidative capacity compared with wild-type mice [25].

LysoPC belongs to the class of glycerophospholipids and is generated by PC hydrolysis through phospholipase catalyzing. Because of the high activity of phospholipase in diabetes, the hydrolysis of the sn-2 position of glycerophospholipids increased. Therefore, LysoPC in patients is much more than normal. Han et al. used various pharmacological inhibitors to find evidence favoring the role of LysoPC produced from FFA in insulin resistance *in vitro* and *in vivo* [26].They implicated LysoPC as an important lipid intermediate that links saturated fatty acids to insulin resistance.

4.4. Other Metabolisms. In this study, the differences between the case group and normal group in carbohydrate metabolism, amino acid metabolism, and other lipid metabolism were also found. These metabolisms were implicated in T2DM, but they were not the main targets for TZQ. This could be the reason that TZQ had no influence on patients with isolated disorder of glucose metabolism.

The level of D-galactose and UDP-glucose was higher in patients and was significantly associated with T2DM. D-Galactose is an aldohexose, which occurs naturally in the D-form in lactose, cerebrosides, gangliosides, and mucoproteins. Galactose is an isomeride of glucose and can be rapidly converted to glucose through the Leloir pathway [27]. Similar to glucose, D-galactose is an energy-providing metabolite and also a necessary basic substrate for the biosynthesis of many macromolecules in the body. Increased galactose metabolism may lead to long-term, gradual increases in serum glucose and may result in insulin resistance. UDP-glucose is a key intermediate in carbohydrate metabolism. Served as a precursor of glycogen, UDP-glucose can be metabolized into UDP-galactose and UDP-glucuronic acid, which can be incorporated into polysaccharides as galactose and glucuronic acid. UDP-glucose also serves as a precursor of sucrose lipopolysaccharides and glycosphingolipids [28].

L-leucine belongs to branched-chain amino acid (BCAAs) along with isoleucine and valine, which play an essential role in the insulin secretion, regulation of protein turnover, and protein synthesis [12]. The additional fasting concentrations of circulating BCAAs are associated with an elevated risk of T2DM, insulin resistance, and other metabolic diseases in humans because of the decreased activity of branched-chain α-keto acid dehydrogenase [29]. L-tyrosine, as one part of aromatic amino acid (AAAs), is a glucogenic and ketogenic amino acid. Some studies revealed that L-tyrosine has positive effects on the development of diabetes, as well as BCAAs [30]. In 2011, the Framingham Offspring Study reported that increased BCAAs (isoleucine, leucine, and valine) and AAAs (tyrosine and phenylalanine) were able to predict the risk of diabetes up to 12 years prior to disease onset [10].

Sphinganine belongs to sphingolipids and is a key precursor on ceramide de novo synthesis pathway [31]. Several studies have suggested that ceramides and other sphingolipids in cells play a direct role in reducing insulin sensitivity [32]. However, sphinganine in serum of patients was lower than healthy volunteers in this study. Cholestenes are derivatives of cholestanes which have a double bond. They are principally responsible for the synthetic process of bile acids. Some studies showed that the activation of bile acid–responsive G protein–coupled receptor TGR5 may promote pathways that were protective against diet-induced diabetes [33]. Therefore, the reduction of cholestenes would be related to the development of T2DM.

5. Conclusions

In this study, the clinical trial indicated that TZQ was appropriate for T2DM patients with hypertriglyceridemia. The decrease of HbA1c was positive correlation with the baseline level of TG. Metabolomics study based on UPLC Q-TOF MS and chemometrics analysis illustrated that TZQ

influenced glycerophospholipid metabolism to regulate the disorder of glucose and lipid metabolism.

This was a pilot clinical trial to explore the clinical efficacy and effect on endogenous metabolites for T2DM of TZQ because of the small sample size. If we enlarge the sample size and eliminate the difference of genetic background, with uniform diets and living habits, the results will be more meaningful. Based on this study, a multicenter clinical trial will be carried out by our team to evaluate the safety and efficacy of TZQ on the T2DM with hypertriglyceridemia in the near future.

Data Availability

The data used to support the findings of this study are available from the corresponding author upon request.

Conflicts of Interest

The authors declare that there are no conflicts of interest regarding the publication of this paper.

Authors' Contributions

Jia Liu and Ziqiang Li contributed equally.

Acknowledgments

This study is supported by the National Natural Science Foundation of China (nos. 81673751, 81303141) and National Science and Technology Major Project of China (nos. 2017ZX09304008, 2015ZX09101043-009).

References

[1] L. Zhang, Q. Qiao, J. Tuomilehto et al., "Blood lipid levels in relation to glucose status in seven populations of Asian origin without a prior history of diabetes: The DECODA study," *Diabetes/Metabolism Research and Reviews*, vol. 25, no. 6, pp. 549–557, 2009.

[2] L. Zhang, Q. Qiao, J. Tuomilehto et al., "Blood lipid levels in relation to glucose status in European men and women without a prior history of diabetes: The DECODE Study," *Diabetes Research and Clinical Practice*, vol. 82, no. 3, pp. 364–377, 2008.

[3] A. Tenenbaum, R. Klempfner, and E. Z. Fisman, "Hypertriglyceridemia: A too long unfairly neglected major cardiovascular risk factor," *Cardiovascular Diabetology*, vol. 13, no. 1, article no. 159, 2014.

[4] H. Yuhong, F. Wenxu, L. Yanfen et al., "Comparison of the effects of acarbose and TZQ-F, a new kind of traditional Chinese medicine to treat diabetes, Chinese healthy volunteers," *Evidence-Based Complementary and Alternative Medicine*, vol. 2014, Article ID 308126, 9 pages, 2014.

[5] W. Wang, T. Miura, H. Shi et al., "Effect of Tangzhiqing on Glucose and Lipid Metabolism in Genetically Type 2 Diabetes KK-Ay Mice," *Journal of Health Science*, vol. 54, no. 2, pp. 203–206, 2008.

[6] J. N. Xia, D. Q. Zhang, J. Du, and J. Wen, "Regulation effects of TZQ-F on adipocyte differentiation and insulin action," *Journal of Ethnopharmacology*, vol. 150, no. 2, pp. 692–699, 2013.

[7] Y. An, X. Liu, Q. Qian et al., "Triglyceride accumulation: Inhibitory effects of Tangzhiqing formula," *Alternative Therapies in Health and Medicine*, vol. 19, no. 5, pp. 20–29, 2013.

[8] J. Gao, J. Li, Y. An et al., "Increasing effect of Tangzhiqing formula on IRS-1-dependent PI3K/AKT signaling in muscle," *BMC Complementary and Alternative Medicine*, vol. 14, article no. 198, 2014.

[9] W. Tao, Z. Deqin, L. Yuhong et al., "Regulation effects on abnormal glucose and lipid metabolism of TZQ-F, a new kind of Traditional Chinese Medicine," *Journal of Ethnopharmacology*, vol. 128, no. 3, pp. 575–582, 2010.

[10] T. J. Wang, M. G. Larson, R. S. Vasan et al., "Metabolite profiles and the risk of developing diabetes," *Nature Medicine*, vol. 17, no. 4, pp. 448–453, 2011.

[11] Y. Lu, Y. Wang, C.-N. Ong et al., "Metabolic signatures and risk of type 2 diabetes in a Chinese population: an untargeted metabolomics study using both LC-MS and GC-MS," *Diabetologia*, vol. 59, no. 11, pp. 2349–2359, 2016.

[12] A. Floegel, N. Stefan, and Z. Yu, "Identification of serum metabolites associated with risk of type 2 diabetes using a targeted metabolomic approach," *Diabetes*, vol. 62, no. 2, pp. 639–648, 2013.

[13] R. Wang-Sattler, Z. Yu, C. Herder et al., "Novel biomarkers for pre-diabetes identified by metabolomics," *Molecular Systems Biology*, vol. 8, article 615, 2012.

[14] D. Yu, S. C. Moore, C. E. Matthews et al., "Plasma metabolomic profiles in association with type 2 diabetes risk and prevalence in Chinese adults," *Metabolomics*, vol. 12, no. 1, 2016.

[15] K. Suhre, C. Meisinger, A. Döring et al., "Metabolic footprint of diabetes: a multiplatform metabolomics study in an epidemiological setting," *PLoS ONE*, vol. 5, no. 11, Article ID e13953, 2010.

[16] J. Liu, S. Semiz, S. J. van der Lee et al., "Metabolomics based markers predict type 2 diabetes in a 14-year follow-up study," *Metabolomics*, vol. 13, no. 9, 2017.

[17] U. K. Rao, "Concepts in sample size determination," *Indian Journal of Dental Research*, vol. 23, no. 5, pp. 660–664, 2012.

[18] C. Rutterford, A. Copas, and S. Eldridge, "Methods for sample size determination in cluster randomized trials," *International Journal of Epidemiology*, vol. 44, no. 3, Article ID dyv113, pp. 1051–1067, 2015.

[19] R. J. Perry, V. T. Samuel, K. F. Petersen, and G. I. Shulman, "The role of hepatic lipids in hepatic insulin resistance and type 2 diabetes," *Nature*, vol. 510, no. 7503, pp. 84–91, 2014.

[20] S. Park, K. C. Sadanala, and E.-K. Kim, "A metabolomic approach to understanding the metabolic link between obesity and diabetes," *Molecules and Cells*, vol. 38, no. 7, pp. 587–596, 2014.

[21] K. Srikanthan, A. Feyh, H. Visweshwar, J. I. Shapiro, and K. Sodhi, "Systematic review of metabolic syndrome biomarkers: a panel for early detection, management, and risk stratification in the West Virginian population," *International Journal of Medical Sciences*, vol. 13, no. 1, pp. 25–38, 2016.

[22] Y. Li, M. Ge, L. Ciani et al., "Enrichment of endoplasmic reticulum with cholesterol inhibits sarcoplasmic-endoplasmic reticulum calcium ATPase-2b activity in parallel with increased order of membrane lipids: Implications for depletion of endoplasmic reticulum calcium stores and apoptosis in cholesterol-loaded macrophages," *The Journal of Biological Chemistry*, vol. 279, no. 35, pp. 37030–37039, 2004.

[23] K.-H. Cheng, J. R. Lepock, S. W. Hui, and P. L. Yeagle, "The role of cholesterol in the activity of reconstituted Ca-ATPase vesicles

containing unsaturated phosphatidylethanolamine," *The Journal of Biological Chemistry*, vol. 261, no. 11, pp. 5081–5087, 1986.

[24] S. Fu, L. Yang, P. Li et al., "Aberrant lipid metabolism disrupts calcium homeostasis causing liver endoplasmic reticulum stress in obesity," *Nature*, vol. 473, no. 7348, pp. 528–531, 2011.

[25] A. Selathurai, G. M. Kowalski, M. L. Burch et al., "The CDP-Ethanolamine Pathway Regulates Skeletal Muscle Diacylglycerol Content and Mitochondrial Biogenesis without Altering Insulin Sensitivity," *Cell Metabolism*, vol. 21, no. 5, pp. 718–730, 2015.

[26] M. S. Han, Y.-M. Lim, W. Quan et al., "Lysophosphatidylcholine as an effector of fatty acid-induced insulin resistance," *Journal of Lipid Research*, vol. 52, no. 6, pp. 1234–1246, 2011.

[27] H. M. Holden, I. Rayment, and J. B. Thoden, "Structure and Function of Enzymes of the Leloir Pathway for Galactose Metabolism," *The Journal of Biological Chemistry*, vol. 278, no. 45, pp. 43885–43888, 2003.

[28] H. Dreyfus, P. F. Urban, S. Edel-Harth, N. M. Neskovic, and P. Mandel, "Enzymatic synthesis of glucocerebroside by UDP-glucose: Ceramide glucosyltransferase during ontogenesis of chicken retina," *Lipids*, vol. 10, no. 9, pp. 545–547, 1975.

[29] G. Bajotto, T. Murakami, M. Nagasaki, Y. Sato, and Y. Shimomura, "Decreased enzyme activity and contents of hepatic branched-chain α-keto acid dehydrogenase complex subunits in a rat model for type 2 diabetes mellitus," *Metabolism - Clinical and Experimental*, vol. 58, no. 10, pp. 1489–1495, 2009.

[30] A. Stančáková, M. Civelek, N. K. Saleem et al., "Hyperglycemia and a common variant of GCKR are associated with the levels of eight amino acids in 9,369 finnish men," *Diabetes*, vol. 61, no. 7, pp. 1895–1902, 2012.

[31] M. Górska, A. Dobrzyń, and M. Baranowski, "Concentrations of sphingosine and sphinganine in plasma of patients with type 2 diabetes," *Medical Science Monitor*, vol. 11, no. 1, pp. CR35–CR38, 2005.

[32] J. A. Chavez and S. A. Summers, "A ceramide-centric view of insulin resistance," *Cell Metabolism*, vol. 15, no. 5, pp. 585–594, 2012.

[33] A. Perino, T. W. H. Pols, M. Nomura, S. Stein, R. Pellicciari, and K. Schoonjans, "TGR5 reduces macrophage migration through mTOR-induced C/EBPβ differential translation," *The Journal of Clinical Investigation*, vol. 124, no. 12, pp. 5424–5436, 2014.

Hindawi
Evidence-Based Complementary and Alternative Medicine
Volume 2018, Article ID 8781352, 11 pages
https://doi.org/10.1155/2018/8781352

Research Article

Identification of Digestive Enzyme Inhibitors from *Ludwigia octovalvis* (Jacq.) P.H.Raven

Dulce Morales,[1,2] **Guillermo Ramirez**,[2] **Armando Herrera-Arellano**,[1] **Jaime Tortoriello**,[2] **Miguel Zavala**,[3] **and Alejandro Zamilpa**[2]

[1]*Facultad de Medicina, Universidad Autónoma del Estado de Morelos, Cuernavaca 62350, Mexico*
[2]*Centro de Investigación Biomédica del Sur, Instituto Mexicano del Seguro Social, Xochitepec 62790, Mexico*
[3]*Departamento de Sistemas Biológicos, UAM–Xochimilco, Mexico City 04960, Mexico*

Correspondence should be addressed to Alejandro Zamilpa; azamilpa_2000@yahoo.com.mx

Received 10 April 2018; Revised 6 June 2018; Accepted 26 June 2018; Published 16 July 2018

Academic Editor: Mohammed S. Razzaque

Current antiobesity and antidiabetic tools have been insufficient to curb these diseases and frequently cause side effects; therefore, new pancreatic lipase and α–glucosidase inhibitors could be excellent aids for the prevention and treatment of these diseases. The aim of this study was to identify, quantify, and characterize the chemical compounds with the highest degree of inhibitory activity of these enzymes, contained in a *Ludwigia octovalvis* hydroalcoholic extract. Chemical purification was performed by liquid–liquid separation and column chromatography. Inhibitory activities were measured *in vitro*, employing acarbose, orlistat, and a *Camellia sinensis* hydroalcoholic extract as references. For structural elucidation, Nuclear Magnetic Resonance was carried out, and High Performance Liquid Chromatography was used to quantify the compounds. For α–glucosidases, *L. octovalvis* hydroalcoholic extract and its ethyl acetate fraction showed half–maximal Inhibitory Concentration (IC_{50}) values of 700 and 250 μg/mL, for lipase, 480 and 718 μg/mL, while *C. sinensis* showed 260 and 587 μg/mL. The most active compounds were identified as ethyl gallate (**1**, IC_{50} 832 μM) and gallic acid (**2**, IC_{50} 969 μM); both displayed competitive inhibition of α–glucosidases and isoorientin (**3**, IC_{50} 201 μM), which displayed uncompetitive inhibition of lipase. These data could be useful in the development of a novel phytopharmaceutical drug.

1. Introduction

Although α–glucosidase inhibitors such as acarbose and pancreatic lipase inhibitors such as orlistat are one of the safest antiobesity and antidiabetic drugs for weight loss and regulation of several metabolic and cardiovascular parameters in adults [1–3], these drugs have unpleasant gastrointestinal side effects that frequently result in therapy abandonment [4]. Therefore, it is necessary to continue the search for new alternatives to α–glucosidase and pancreatic lipase inhibitors, with milder side effects and which contribute to the treatment of obesity and type 2 diabetes mellitus, in conjunction with current therapies.

Treatment with acarbose brings forth benefits in the regulation of HbA1c, blood pressure, coagulation factors, thickness of the intimal layer of the carotid, endothelial dysfunction, serum glucose, and postprandial insulin [2], being especially useful in the treatment of diabetic patients with adequate baseline control but persistent postprandial hyperglycaemia [1]. While orlistat treatment not only produces a reduction in body weight and waist diameter, it also decreases HbA1c, blood pressure, and cholesterol [5], reducing the incidence of type 2 diabetes mellitus. In addition, orlistat is currently the only drug approved by the Food and Drug Administration (FDA) for the treatment of obesity in children [3].

Ludwigia octovalvis (Jacq.) P.H.Raven (Onagraceae) [syn: *Jussiaea suffruticosa* L., *Jussiaea pubescens* L., and *Jussiaea angustifolia* Lamk] is an helophyte, erect, herb with oblong–lanceolate leaves and solitary flowers of four yellow petals [6]. According to Mexican data, this species is not on a protection status [7]. Almost all parts of the plant

have been reported as having several medicinal uses [8, 9], among them, the antidiabetic use by Mexican and Indian healers [10, 11], in which the boiled extract or the juice of the whole plant is used. Previous phytochemical studies have described the presence of flavonoids, phenolic acids, polyphenols, saponins, sterols, tannins, and triterpenoids [12–15] in different organs of this medicinal plant. Several pharmacological effects such as hypoglycaemic [8], anti-hyperglycaemic [16, 17], and antiproliferative, in 3T3–L1 adipocytes [18], have been described through various models. Moreover, the hydroalcoholic extract of *L. octovalvis* leaves was the most effective in the inhibition of α–glucosidases and pancreatic lipase in a screening of 23 extracts of medicinal plants reported as traditional treatments for type 2 diabetes mellitus [10]. In addition, a report also exists on *L. octovalvis* antidiarrheal activity, probably mediated by regulation of gastrointestinal motility [19]; this activity could help reduce some of the side effects of intestinal enzyme inhibition, such as faecal urgency or abdominal pain.

The aim of this work was to isolate, identify, quantify, and characterize the compounds with the greatest inhibitory activity of α–glucosidases and pancreatic lipase, in the hydroalcoholic extract of *L. octovalvis* leaves, through its bioassay–guided fractionation.

2. Materials and Methods

2.1. General. All chemicals were of analytical–reagent grade. Corn starch (S4126); 2,3–dimercapto–1–propanol tributyrate (DMPTB 97%, 282413); 5,5′–dithiobis(2–nitrobenzoic acid) (DTNB ≥98%, D8130); lipase from porcine pancreas (PPL type II, 100–500 units/mg, L3126); Triton X–100 (X100); SDS (≥98.5%, L3771); glycerol (≥99.5%, GE17–1325–01); DMSO (≥99.9%, 547239); polyethylene glycol (PEG, 1546580); 2–aminoethyl diphenylborinate (97%, D9754); isoorientin (≥98%; I1536); and gallic acid (≥97%, 27645) were purchased from Sigma–Aldrich (St. Louis, MO). Miscellaneous solvents were purchased from Merck KGaA (Darmstadt, Germany).

Orlistat (Lysthin, PsicoFarma, Mexico City) and acarbose (Sincrosa, Alpharma, Mexico City) were purified by silica chromatography and crystallized, to be used as positive controls for enzyme inhibition assays.

Thin layer chromatography (TLC) was performed using silica gel 60 RP–18 F254s aluminium sheets (105560, Merck KGaA). TLC plates were analysed under UV light at 254 and 360 nm, using the Natural Products–PEG reagent (NP–PEG; 1% methanolic solution of diphenylboryloxyethylamine followed by 5% ethanolic PEG) as chemical detection system [20].

Melting points were obtained on a Thermo Scientific IA9000 series melting point apparatus (Electrothermal, Essex, UK).

Nuclear Magnetic Resonance (NMR) ^{1}H (400 MHz) and NMR ^{13}C (100 MHz) spectra were obtained with Varian INOVA–400 equipment (Varian Co., Palo Alto, CA) using tetramethylsilane as internal standard.

2.2. Plant Material and Preparation of Extracts. Leaves of *L. octovalvis* were collected at Xochitepec, Morelos, Mexico (18°47′40.70″ N, 99°11′49.27″ W), between September and October of 2012. A voucher of plant material was deposited under code number 34667 at the HUMO Herbarium in the *Centro de Investigación en Biodiversidad y Conservación* of the Autonomous University of the State of Morelos (*Universidad Autónoma del Estado de Morelos–CIByC–UAEM*, Morelos, Mexico).

Camellia sinensis (L.) Kuntze (Theaceae) commercial ground leaves, purchased at a Japanese specialty store (Yamamotoyama, Pomona, CA), was used as a positive vegetal control. Plant names were checked and updated with the online website http://www.theplantlist.org. [21].

Fresh leaves of *L. octovalvis* were washed and dried under dark conditions at room temperature and then milled to 4–6 mm. Ground material (1 kg) was extracted (1:10 ratio, w/v) with a 60% ethanol aqueous solution at 25°C for 24 h. The liquid extract was paper-filtered, concentrated in a rotary evaporator Laborota 4000 (Heidolph, Schwabach, Germany) under reduced pressure at 50°C, and freeze-dried to obtain 337 g of brown powder (32.4% yield). This dry extract (LoHAE) was stored at 4°C until its pharmacological and phytochemical analysis. *C. sinensis* hydroalcoholic extract (CsHAE) was identically prepared.

2.3. Fractionation of LoHAE and Purification of Active Fractions. One hundred and ninety grams of LoHAE was subjected to a liquid–liquid separation process using water and ethyl acetate. The solvent of both fractions was eliminated by low pressure distillation to obtain an organic fraction (LoEAF) and an aqueous fraction (LoAqF).

The less polar fraction (LoEAF, 25 g) was subjected to a chromatographic silica gel 60 column (109385, Merck KGaA) using dichloromethane/methanol gradient system as mobile phase, to give 69 samples of 150 mL each. The separation process was monitored by TLC and all the samples were grouped into 20 final fractions. The most representative fractions (yields ≥5%; C1F1–C1F6) were subjected to both assays.

The active fractions C1F4 and C1F6 were fractionated using column chromatography with silica gel LiChroprep® RP–18 (113900, Merck KGaA) and a mixture of water/acetonitrile. All the fractions were analysed by TLC and the samples with similar chemical composition were grouped.

From C1F4 (186 mg), 10 final fractions were obtained, of which C2F1 produced a white precipitate, which was found to be a pure compound by TLC and High Performance Liquid Chromatography (HPLC).

From C1F6 (1.1 g), 19 final fractions were obtained; the most representative (yields ≥5%) were C3F1, C3F2, C3F3, and C3F4. Fraction C3F3 was purified, obtaining fractions C4F1, C4F2, C4F3, C4F4, C4F5, and C4F6. Fraction C4F4 produced an orange/yellow precipitate (C4F4–P, 12 mg). All these fractions (see Scheme 1) were subjected to the pharmacological assay.

2.4. HPLC Analysis. HPLC analysis was performed on a chromatographic system equipped with a Waters Alliance Separation Module (2695, Waters Corporation, Milford, MA)

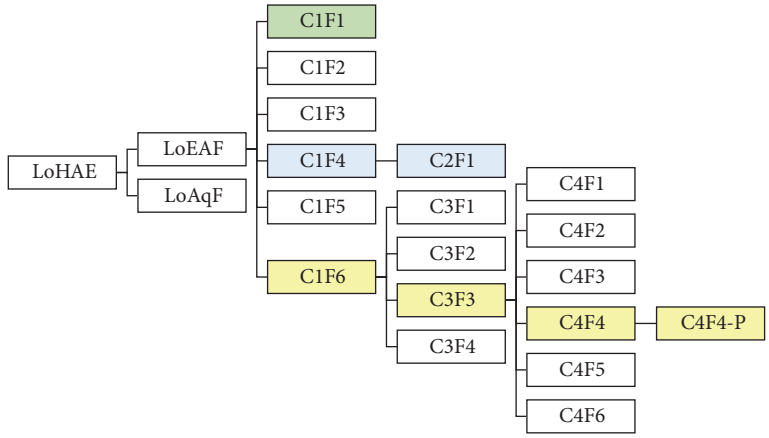

Scheme 1: Fractionation of *L. octovalvis* hydroalcoholic extract (LoHAE). The isolation process of the active compounds is illustrated by colors: green for ethyl gallate, blue for gallic acid, and yellow for isoorientin.

and a photodiode array detector (2996, Waters Corporation), employing Empower Pro software (Waters Corporation). Separation was carried out using a Supelcosil LC–F HPLC column (59158, Supelco, Bellefonte, PA). The mobile phase consisted of a mixture of trifluoroacetic acid solution (solvent A, 0.5%) and acetonitrile (solvent B) with the following ratios: A:B = 100:0 (0–1 min); 95:5 (2–3 min); 70:30 (4–7 min); 50:50 (8–22 min); 20:80 (23 min); 0:100 (24–26 min); 100:0 (27–30 min). The sample injection volume was 10 mL with a 0.9 mL/min flow rate during 30 min. The detection wavelength was 190–600 nm.

Quantification of the isolated compounds was achieved using calibration curves and LoHAE or LoEAF HPLC analysis. The calibration curve was made using ascendant concentrations (25, 50, 100, and 200 μg/mL) of the isolated compounds, which were injected by triplicate at 10 μL in the previously described HPLC method. A chromatographic profile of each concentration was obtained at 254 or 360 nm wavelength and data on area under curve peak were used to obtain the respective straight–line equations.

2.5. Enzymatic Inhibition Assays. Pancreatic lipase inhibition assay was previously reported [22]. Briefly, the absorbance of a mixture of DTNB 0.2 mM, DMPTB 0.8 mM, NaCl 0.1M, CaCl2 2 mM, Triton X–100 0.04%, porcine lipase 65 μg/mL, and the sample (dissolved in DMSO and water) at 0.25 mg/mL was followed with a Thermo Scientific Genesys 20 Visible Spectrophotometer (Fisher Scientific, 4001000, Hampton, NH) at 412 nm every 20 s for five minutes and plotted (Excel, Microsoft) to obtain initial velocity value. The lipase was prepared as a stock at 10 mg/mL in Tris–HCl 25 mM pH 6.2 with 0.1 M NaCl, SDS 2 mM, and 250 μL/mL of glycerol. A control assay without substrate was carried out to discard nonspecific reactions with DTMB. All reactions were tested by triplicate.

The α–glucosidase assay was previously reported [10]. In brief, corn starch (4 mg/mL) was digested by crude enzyme at 37°C during 10 minutes in a phosphate buffer pH 7 solution at a sample concentration of 0.6 mg/mL (dissolved in DMSO and water). Subsequently, released glucose was quantified by a glucose oxidase-based clinical reagent with the GOD–POD Trinder kit (Spinreact, Girona, Spain) following manufacturer's directions. All tests were performed in quadruplicate. Crude enzyme was obtained directly from healthy Wistar rats (12 h fasting). The small intestine was flushed several times with ice-cold isotonic buffer pH 7 and after the scraping of the mucosa, it was homogenized and stored at -20°C. Animal care and management were carried out under the guidelines of Mexican Official Standard NOM–062–ZOO–1999.

For both assays, percentage of inhibitions was calculated as the residual enzymatic activity of the negative control (DMSO and water) by using

$$\%\, inhibition = 100 - \left(\frac{Absorbance_{sample}}{Absorbance_{control}} \times 100 \right) \quad (1)$$

Concentrations of extracts resulting in 50% inhibition of enzyme activity (IC_{50} values) were determined graphically, quantifying enzymatic activities at ascendant concentrations of each sample (6–3600 μg/mL for α–glucosidases and 5–2500 μg/mL for pancreatic lipase). The logarithm of the concentration was plotted on the x-axis and the percentage of enzymatic inhibitory activity on the y-axis to obtain a semilogarithmic graphic.

The type of inhibition was determined quantifying the activity with and without inhibitor at different substrate concentrations (5–0.35 mg/mL for α–glucosidases and 0.05–0.2 μg/mL for pancreatic lipase) and comparing Lineweaver–Burk plots (inverse substrate concentration [S] and inverse reaction velocity V). In the case of the determination of α–glucosidase type of inhibition, the substrate was changed from corn starch to maltodextrin (MD100, Luzhou Bio–Chem Technology Co., Shandong, China), in order to have greater uniformity in the reaction.

Michaelis–Menten constant (K_m) and apparent K_m (K_m^{app}) were obtained analysing the Lineweaver–Burk plots. These values allowed to obtain the inhibition constant (K_i)

Table 1: Enzyme inhibition of hydroalcoholic extract, fractions, and compounds isolated from *L. octovalvis* leaves.

Sample	Inhibition percentage	
	α–glucosidases 0.6 mg/mL	Pancreatic lipase 0.25 mg/mL
Acarbose	50.0 ± 1.6∗	N.A.
Orlistat	N.A.	50.0 ± 2.6∗∗
CsHAE	80.8 ± 1.1	34.8 ± 2.5
LoHAE	58.9 ± 5.7	23.6 ± 2.5
LoEAF	**82.8 ± 3.6**	**31.2 ± 1.9**
LoAqF	76.8 ± 1.9	15.6 ± 2.5
C1F1 (ethyl gallate)	**98.4 ± 2.0**	23.2 ± 3.0
C1F2	60.1 ± 5.5	22.5 ± 3.6
C1F3	39.9 ± 5.6	4.3 ± 3.5
C1F4	**98.9 ± 1.6**	20.0 ± 2.3
C1F5	84.2 ± 5.3	28.2 ± 2.7
C1F6	79.8 ± 3.8	**45.3 ± 0.6**
C2F1 (gallic acid)	**98.9 ± 0.6**	N.A.
C3F1	N.A.	10.9 ± 0.3
C3F2	N.A.	29.3 ± 3.6
C3F3	N.A.	43.5 ± 4.3
C3F4	N.A.	36.4 ± 4.0
C4F1	N.A.	41.4 ± 3.2
C4F2	N.A.	16.6 ± 4.5
C4F3	N.A.	45.8 ± 5.1
C4F4–P (isoorientin)	N.A.	**55.1 ± 3.1**
C4F5	N.A.	53.5 ± 3.7
C4F6	N.A.	49.1 ± 3.8
Luteolin	66.3 ± 5.6	N.A.

The data is indicated as the mean ± standard deviation.
N.A. = not analysed; ∗ evaluated at 5.8 μM; ∗∗ evaluated at 1.6 μM.

for competitive inhibitors using (2), where [I] represents inhibitor concentration.

$$K_m{}^{app} = K_m\left(1 + \frac{[I]}{K_i}\right) \quad (2)$$

2.6. Statistical Analysis. Experimental enzymatic inhibition activity values are expressed as the percentage of inhibition. All biological assays were analysed by ANOVA followed by a Tukey post–test, with statistical differences established at $p<0.05$, using the SPSS10.0 program.

3. Results

3.1. Fractionation of Hydroalcoholic Extract. The liquid–liquid separation of LoHAE produced LoAqF (82.3% yield; 156 g) and LoEAF (17.1%; 32 g). Samples of these materials and CsHAE were analysed in the *in vitro* models of enzyme inhibition at 0.6 mg/mL in the case of α–glucosidases and at 0.25 mg/mL in the case of pancreatic lipase (see Table 1).

LoHAE inhibited the α–glucosidases by 58.9% and the pancreatic lipase by 23.6%, while CsHAE produced an 80.8% inhibition of α–glucosidases and 34.8% of pancreatic lipase. The organic fraction, LoEAF, had more inhibitory activity than LoAqF fraction or LoHAE extract in both assays, with an 82.8% inhibition of α–glucosidases and 31.2% inhibition of pancreatic lipase.

High Performance Liquid Chromatography spectra analysis of LoEAF (see Figure 1(a)) indicated the presence of flavonoids and organic acids [20, 23]. The first chromatography separation of LoEAF afforded 60 fractions, which were grouped in six (C1F1–C1F6), where C1F1 and C1F4 fractions displayed the highest inhibitory effect on α–glucosidases, while C1F6 was the most active for lipase (see Table 1).

3.2. Identification of α–Glucosidase Inhibitors. Fraction C1F1 produced a white precipitate (melting point = 160°C) that was analysed by HPLC (see Figure 1(b)) and its chemical structure was corroborated by comparison of spectroscopic ^{1}H and ^{13}C NMR data (see Table 2 and Figures S1–S2 in the Supplementary Material) indicating that this compound corresponds to ethyl gallate [24] (see Figure 2).

Fraction C1F4 produced Fraction C2F1, which also produced a white precipitate (melting point= 260°C). HPLC, UV spectra (see Figures 1(c)–1(d)), and spectroscopic ^{1}H

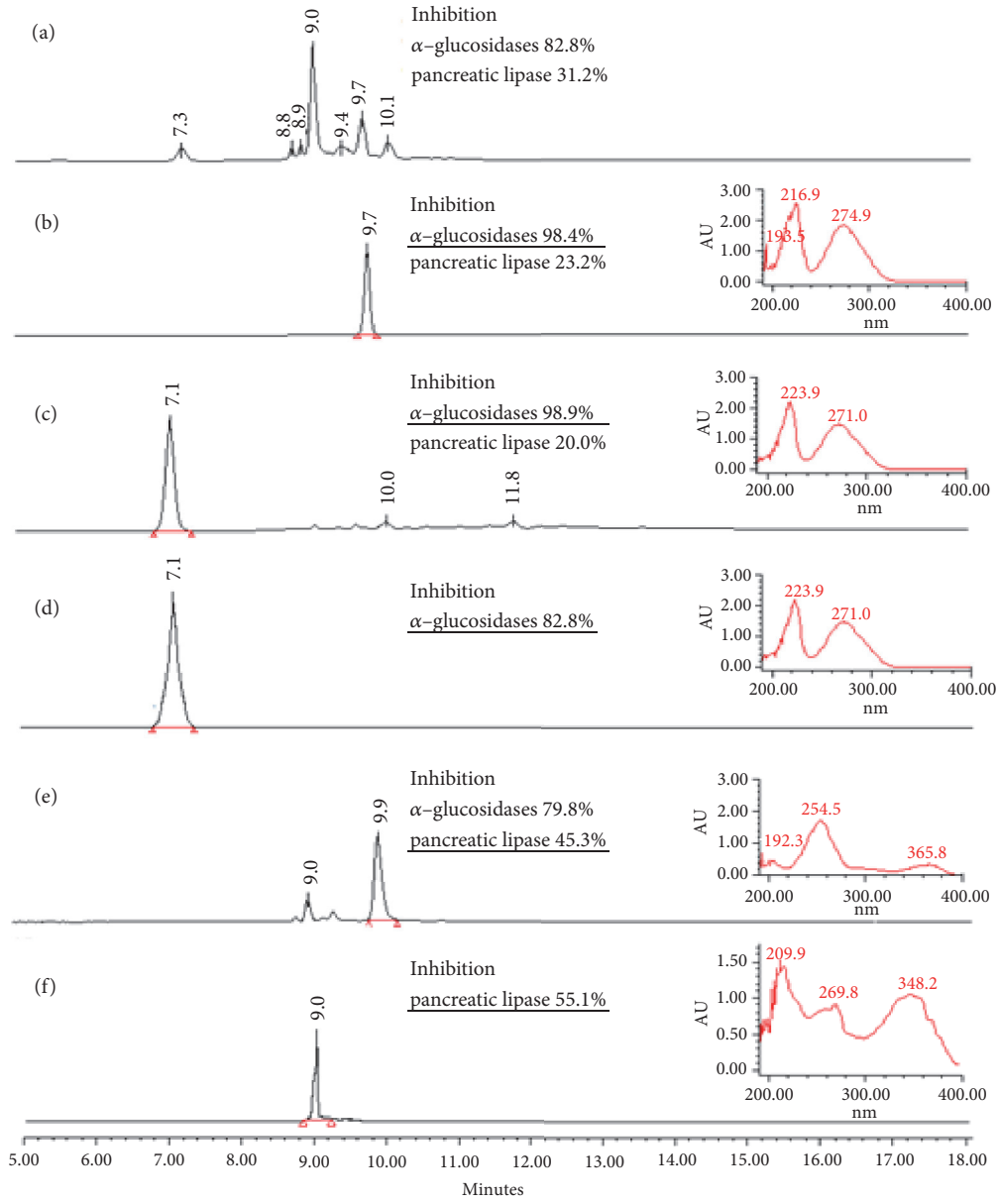

Figure 1: High Performance Liquid Chromatography chromatograms, UV spectra (at 270 nm), and enzymatic inhibition percentage of different *L. octovalvis* fractions. (a) Ethyl acetate fraction LoEAF. (b) Fraction C1F1. (c) Fraction C1F4. (d) Fraction C2F1. (e) Fraction C1F6. (f) Fraction C4F4–P.

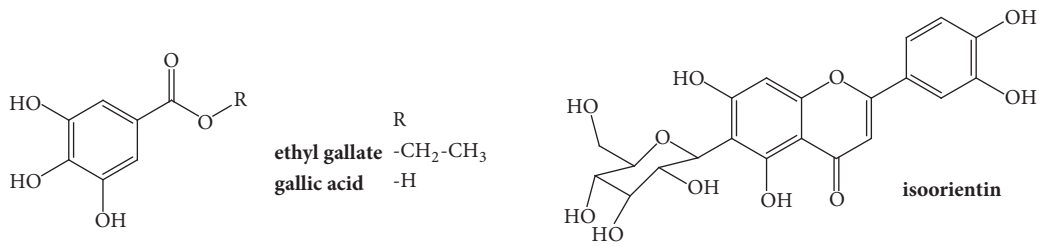

Figure 2: Chemical structure of the most active compounds identified in *L. octovalvis* hydroalcoholic extract.

Table 2: Nuclear Magnetic Resonance (NMR) ^{13}C data of the compounds contained in C1F1 and C4F4–P fractions and previously reported data for ethyl gallate and isoorientin.

Carbon position	Chemical shifts (ppm)			
	Ethyl gallate	C1F1	Isoorientin	C4F4–P
1	121.9	121.95	–	–
2	110.1	110.18	163.44	163.61
3	146.4	146.57	102.38	102.78
4	139.6	139.79	181.45	181.84
5	146.4	146.57	160.59	160.67
6	110.1	110.18	108.88	108.86
7	168.6	168.69	163.44	163.23
8	61.6	61.81	93.73	93.46
9	14.6	14.73	156.27	156.16
10	–	–	102.79	103.38
1′	–	–	121.56	121.4
2′	–	–	118.82	118.95
3′	–	–	116.00	116.02
4′	–	–	150.44	149.68
5′	–	–	145.95	145.72
6′	–	–	112.92	113.29
1″	–	–	73.18	73.02
2″	–	–	70.50	70.60
3″	–	–	78.95	78.93
4″	–	–	70.19	70.17
5″	–	–	81.35	81.56
6″	–	–	61.34	61.48

NMR analysis (see Figure S3 in the Supplementary Material) indicated that this fraction corresponds to gallic acid [24] (see Figure 2).

According to HPLC analysis (see Figure S4 in the Supplementary Material), LoHAE and LoEAF contained, respectively, 0.7% and 4.6% of ethyl gallate and 1.9% and 2.5% of gallic acid.

3.3. Identification of Pancreatic Lipase Inhibitors. Fraction C1F6 was analysed by HPLC where several kinds of organic constituents were observed (see Figure 1(e)). Subsequent chromatographic separations of this fraction, followed by inhibitory activity evaluation (see Table 1), allowed us to obtain 11 fractions (see Scheme 1) with different chemical profiles but similar inhibitory activities. The most active fraction, C4F4–P (melting point = 245°C), was evaluated by HPLC (see Figure 1(f)) and elucidated by ^{1}H NMR, ^{13}C NMR, and two–dimensional NMR spectroscopy experiments (see Table 2 and Figures S5–S9 in the Supplementary Material) and corresponded to isoorientin [25] (see Figure 2). The other active fractions are constituted mainly by flavonoids and other nonidentified compounds.

According to HPLC analysis (see Figure S4 in the Supplementary Material), LoHAE and LoEAF contained 0.2% and 0.1% of isoorientin, respectively.

3.4. Calculating Half–Maximal Inhibitory Concentration and Determining Type of Inhibition

3.4.1. α–Glucosidases. All graphs corresponding to concentration–response curves in the α–glucosidase inhibition model are shown (see Figure 3). CsHAE displayed a value of half–maximal Inhibitory Concentration (IC_{50}) 260 μg/mL, while LoHAE produced IC_{50} 700 μg/mL. Ethyl gallate (C1F1) and gallic acid (C2F1) IC_{50} values were 832 μM and 969 μM, respectively. Luteolin (Sigma, L9283) was used as a naturally occurring reference displaying an IC_{50} = 1257.7 μM.

Both compounds, ethyl gallate and gallic acid, make K_m (intersection x-axis) increase, but maximal velocity (V_{max}; intersection y-axis) remains the same, as expected for a competitive enzymatic inhibition (see Figures 4(a)–4(b)).

For the particular conditions of this assay, the calculated K_m was 460 ± 3 μM. In the case of K_i constants, for ethyl gallate at 625 μM, K_i = 636μM and at 1250 μM, K_i = 315 μM; for gallic acid at 625 μM, K_i = 436 μM and at 1250 μM, K_i = 208 μM.

3.4.2. Pancreatic Lipase. The positive vegetal control, *C. sinensis,* displayed an IC_{50} value of 587 μg/mL, while LoHAE displayed 480 μg/mL, LoEAF 718 μg/mL, and isoorientin 201 μM (see Figure 5).

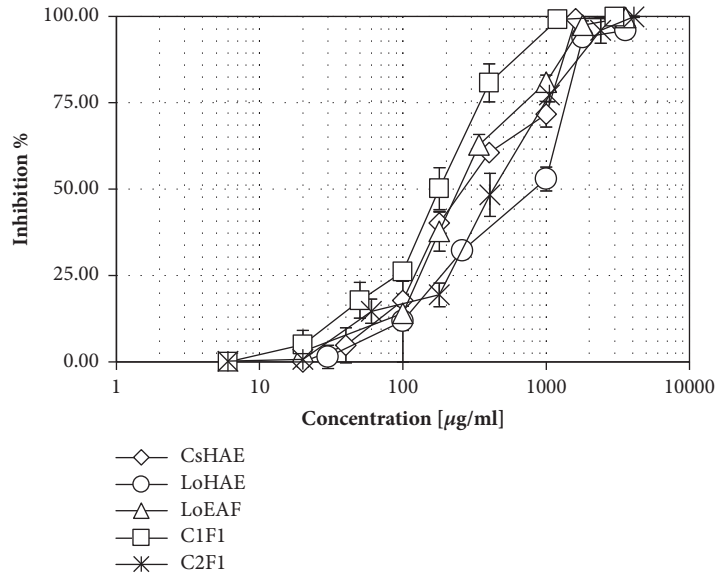

Figure 3: Concentration–response graphics for half–maximal Inhibitory Concentration (IC_{50}) determination of CsHAE, LoHAE, LoEAF, C1F1 (isolated ethyl gallate), and C2F1 (isolated gallic acid), in the inhibition model of α–glucosidases. X-axis values are presented in μg/mL (real values are logarithmic). The error bars represent the standard deviation of 2 measurements in four separate sample runs (n = 8).

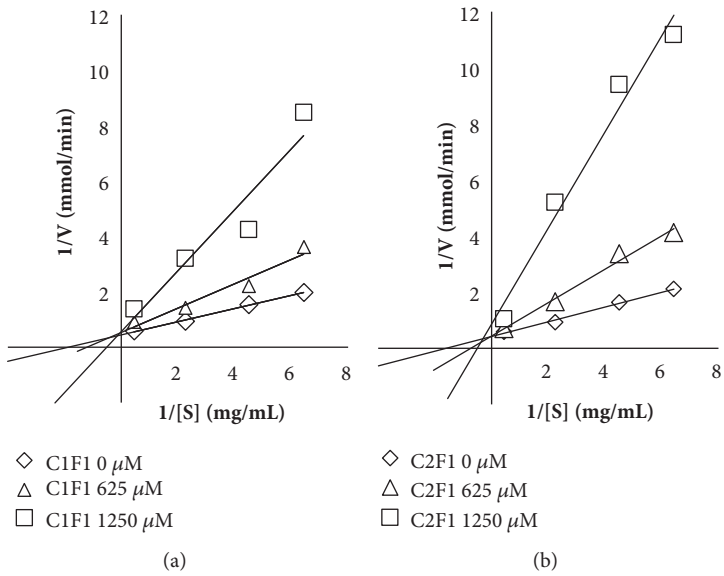

Figure 4: Determination of enzymatic inhibition type by Lineweaver–Burk plots curves in the α–glucosidase inhibition model. (a) C1F1 (isolated ethyl gallate). (b) C2F1 (isolated gallic acid).

As observed in the graph (see Figure 6), isoorientin changed both V_{max} and K_m (both intersection axes), so it produced uncompetitive enzymatic inhibition of pancreatic lipase [26].

4. Discussion

According to several studies, postprandial hyperglycaemia periods, even the relative short–lasting ones, contribute to the development of chronic diabetes complications even more than basal hyperglycaemia [27]. Moreover, the management of postprandial hyperglycaemia is more difficult to achieve than basal glucose control, even with a satisfactory HbA1c control [28], making it one of the main problems in diabetes treatment [1]. Of all the available antidiabetic drugs, α–glucosidase inhibitors are currently the most effective and safest for postprandial glycaemia control as well as intraday and interday glucose fluctuation [29]. On the other hand, changes have also been found in postprandial lipaemia and plasma free fatty acids (fasting and postprandial) in patients with type 2 diabetes mellitus, which increase macrovascular damage [30] and also may cause β–cell dysfunction [31].

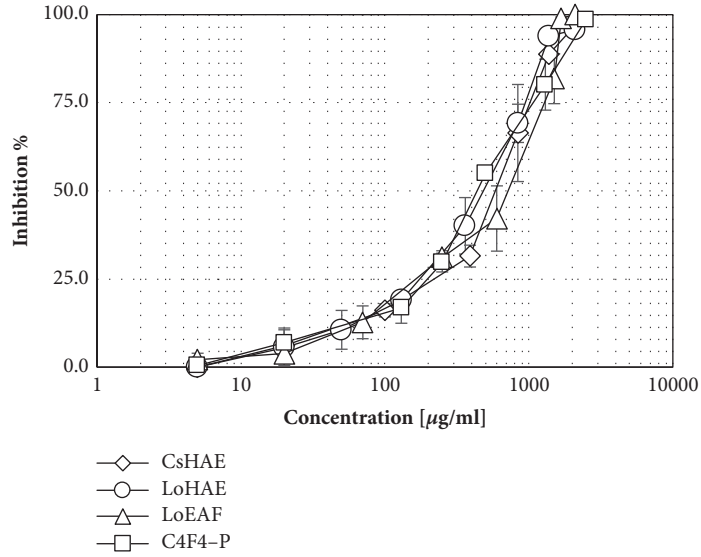

Figure 5: Concentration–response graphics for half–maximal Inhibitory Concentration (IC_{50}) determination of CsHAE, LoHAE, LoEAF, and C4F4–P (isolated isoorientin) in the inhibition model of pancreatic lipase. x-axis values are represented in μg/mL (real values are logarithmic). The error bars represent the standard deviation of 2 measurements in three separate sample runs (n = 6).

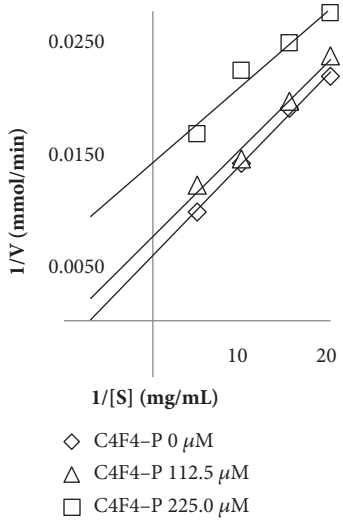

Figure 6: Determination of enzymatic inhibition type of C4F4–P (isolated isoorientin) by Lineweaver–Burk plots curves in the pancreatic lipase inhibition model.

What is worse, when high levels of free fatty acids couple with glycaemic fluctuations, they not only cause endothelium damage [32], but also have a prooxidant effect on pancreatic β cells, leading to β–cell exhaustion [33]; this phenomenon has been called glucolipotoxicity. However, it has been shown that orlistat, a lipase inhibitor, significantly improves postprandial lipaemia and free fatty acid levels in nondiabetic hyperlipidemic subjects and also in overweight type 2 diabetic patients [34, 35].

L. octovalvis hydroalcoholic extract has the advantage of displaying both α–glucosidase and pancreatic lipase inhibition activities. This is the first time that these mechanism modes are described for this species. Besides *L. octovalvis* is an interesting option as antidiabetic because it was described as innocuous according to the OECD [12].

In this study, the concentration of low and intermediate polarity compounds contained in LoEAF considerably increased the inhibition of both digestive enzymes, although an increase of α–glucosidase inhibition was also observed in LoAqF, indicating the presence of other polar compounds with high inhibitory activity of these enzymes. Nevertheless, according to HPLC quantitative analysis, the bipartition process successfully increased the concentration of the two α–glucosidase inhibitors in the organic fraction. Therefore, it would be proper to design an extraction or separation method that concentrates these polyhydroxy benzoic acid derivatives. Although gallic acid has been previously described for *L. octovalvis* [15], this is the first time that its ethyl ester derivative (ethyl gallate) is identified and related to the biological activity. The inhibition of these compounds using intestinal rat enzyme and starch as substrate was found higher than that produced by the natural product reference luteolin ($IC_{50} \approx 1257.7$ μM) which has been described as good inhibitor of α–glucosidases [36–38].

The inhibitory activity of carbohydrate degrading enzymes by gallic acid and its esters, such as ethyl gallate, has been described with inconsistent results. According to some authors, gallic acid showed very low or no inhibitory activity on porcine and Bacillus sp. α–amylase on rat and *Saccharomyces* sp. α–glucosidases on rat maltase [39–43]. However, other studies report that this compound shows high inhibitory activity on rat [42, 44] and yeast α–glucosidases [45] and on porcine α–amylase [43]. Moreover it was found that gallic acid was able to inhibit mouse, rabbit, and rat sucrose as well as rat maltase and trehalase [46]. Furthermore, the IC_{50} values of gallic acid and ethyl gallate in the inhibition of maltase (390 μM, 415 μM) and sucrase

(130 μM, 660 μM) in rat were considered significantly high values [40].

This inconsistency of results could be due in part to the diversity of enzymes and substrates used for these tests; it has been shown that the effect of α–glucosidase inhibitors varies according to the origin of the enzymes and the type of substrate used. According to Oki *et al.* [47], to perform the best evaluation of possible α–glucosidase inhibitors for clinical use, mammalian enzymes and natural substrates of each type of enzyme should be used. Results of this work strengthen the hypothesis that these phenolic compounds (gallic acid and ethyl gallate) could be active in the inhibition of human α–glucosidases.

In this study, ethyl gallate and gallic acid displayed a competitive enzymatic inhibition, in which the inhibitor competes directly with the substrate for the binding site in the active site of the enzyme [27]. This is one of few studies in which the enzymatic inhibition type and K_i of naturally occurring compounds are described on digestive enzymes [48].

In the case of lipase inhibition, the most active compounds were enriched in the organic LoEAF fraction. Further purification by silica chromatography allowed us to obtain a C–glycosylated flavone: isoorientin [13]. This flavonoid displayed the best inhibitory effect and most of the fractions that produced significant activity (C1F6, C4F3, C4F5, and C4F6) contain high levels of isoorientin.

These kinds of C–glycosylated flavonoids have shown high inhibition of pancreatic lipase and according to some authors, glycosylation in position C–8 seems to significantly increase this biological activity [42–44].

Considering that it is desirable to have reference compounds to standardize a phytopharmaceutical drug, isoorientin could fulfil this purpose in *L. octovalvis* extracts with pancreatic lipase inhibitory action.

According to a toxicity analysis of this plant, an alcoholic extract from *L. octovalvis* did not display acute toxicity in mice when it was tested at 5000 mg/kg nor subacute toxicity at 400 mg/kg during 28 days [12], which is essential in the development of new phytomedicines. Furthermore, it is worth mentioning that the findings of the present study validate the traditional use of this plant species in the treatment of diabetes and also as an alternative to synthetic drugs such as acarbose and orlistat, since *L. octovalvis* displayed at least two mechanisms of antidiabetic and antiobesity action, which are synergistic and complementary.

Although none of the *L. octovalvis* treatments were as potent as the reference drugs, there are reports where *in vitro* digestive enzyme inhibition of naturally occurring compounds is lower than acarbose or orlistat but when tested on *in vivo* models, they produced similar pharmacological activities [49, 50].

5. Conclusions

The chemical separation of *L. octovalvis* hydroalcoholic extract which is bioactive in α–glucosidase and pancreatic lipase inhibition allowed the identification and pharmacological characterization of one flavone (isoorientin) with considerable inhibitory effect of pancreatic lipase and two isolated compounds with high inhibitory effect of the α–glucosidases (ethyl gallate and gallic acid). These findings bear out one of the possible mechanisms of action by which this medicinal plant could help in the prevention and treatment of type 2 diabetes and obesity; therefore, these data will be useful in the development of a potential novel phytomedicine.

Data Availability

The data used to support the findings of this study are available from the corresponding author upon request.

Conflicts of Interest

The authors declare that there are no conflicts of interest regarding the publication of this paper.

Acknowledgments

The authors are indebted to Gabriel Flores, curator of HUMO Herbarium, for his support identifying *L. octovalvis* and also to Ernesto Sánchez for his technical spectroscopic support of NMR. The technical assistance of Arturo Pérez and Jonathan Orduño is also acknowledged. This work was supported by the Consejo Nacional de Ciencia y Tecnología (CONACYT) [Grant no. 598815] and CIS–IMSS [(FIS/IMSS/PROT/MD17/1693); Grant no. 99187804]. Alejandro Zamilpa thanks Fundación IMSS.

Supplementary Materials

Figure S1: Nuclear Magnetic Resonance (NMR) 1H spectrum of C1F1 and structure of the identified compound, ethyl gallate. Figure S2: Nuclear Magnetic Resonance (NMR) 13C spectrum of C1F1 and structure of the identified compound, ethyl gallate. Figure S3: Nuclear Magnetic Resonance (NMR) 1H spectrum of C2F1 and structure of the identified compound, gallic acid. Figure S4: calibration curves of the HPLC analysis of the isolated compounds and their straight–line equations. Figure S5: Nuclear Magnetic Resonance (NMR) 1H spectrum of C4F4–P and structure of the identified compound, isoorientin. Figure S6: Nuclear Magnetic Resonance (NMR) 13C spectrum of C4F4–P and structure of the identified compound, isoorientin. Figure S7: Correlation Spectroscopy (COSY) of C4F4–P. Figure S8: Heteronuclear Single Quantum Coherence Spectroscopy (HSQC) of C4F4–P. Figure S9: Heteronuclear Multiple Bond Correlation Spectroscopy (HMBC) of C4F4–P. *(Supplementary Materials)*

References

[1] M. C. Riddle, "Basal glucose can be controlled, but the prandial problem persistsdit's thenext target," *Diabetes Care*, vol. 40, no. 3, pp. 291–300, 2017.

[2] M. A. Esquivel and M. C. Lansang, "Optimizing diabetes treatment in the presence of obesity," *Cleveland Clinic Journal of Medicine*, vol. 84, no. 1, pp. S22–S29, 2017.

[3] V. Shettar, S. Patel, and S. Kidambi, "Epidemiology of Obesity and Pharmacologic Treatment Options," *Nutrition in Clinical Practice*, vol. 32, no. 4, pp. 441–462, 2017.

[4] U. Ghani, "Re-exploring promising α-glucosidase inhibitors for potential development into oral anti-diabetic drugs: finding needle in the haystack," *European Journal of Medicinal Chemistry*, vol. 103, pp. 133–162, 2015.

[5] R. S. Padwal and S. R. Majumdar, "Drug treatments for obesity: orlistat, sibutramine, and rimonabant," *The Lancet*, vol. 369, no. 9555, pp. 71–77, 2007.

[6] L. J. Cumana-Campos, "Clave para especies de Ludwigia L. (Onagraceae) de la regi≤n nor-oriental e insular de Venezuela depositadas en el herbario IRBR," *Acta Bot. Venez*, vol. 33, no. 2, pp. 299–327, 2010.

[7] "SEMARNAT, 'Norma Oficial Mexicana NOM-059-SEMARNAT-2010, Protección ambiental-Especies nativas de México de flora y fauna silvestres-Categorías de riesgo y especificaciones para su inclusión, exclusión o cambio-Lista de especies en riesgo', Diario Oficial de la Federación. Mexico, pp. 1–78, 2006".

[8] T. Murugesan, S. Sinha, M. Pal, and B. Saha, "Review on Phytochemical and Medicinal Aspects of Jussiaea Suferuticosa Linn," *Ancient Science of Life*, vol. 21, no. 3, pp. 205–207, 2002.

[9] "UNAM, Atlas de las Plantas de la Medicina Tradicional Mexicana', Biblioteca Digital de la Medicina Tradicional Mexicana," http://www.medicinatradicionalmexicana.unam.mx/atlas.php.

[10] G. Ramírez, M. Zavala, J. Pérez, and A. Zamilpa, "In vitro screening of medicinal plants used in Mexico as antidiabetics with glucosidase and lipase inhibitory activities," *Evidence-Based Complementary and Alternative Medicine*, vol. 2012, pp. 1–6, 2012.

[11] M. H. Khan and P. S. Yadava, "Antidiabetic plants used in Thoubal district of Manipur, Northeast India," *Indian Journal of Traditional Knowledge*, vol. 9, no. 3, pp. 510–514, 2010.

[12] H. Kadum Yakob, A. Manaf Uyub, and S. Fariza Sulaiman, "Toxicological evaluation of 80% methanol extract of Ludwigia octovalvis (Jacq.) P.H. Raven leaves (Onagraceae) in BALB/c mice," *Journal of Ethnopharmacology*, vol. 142, no. 3, pp. 663–668, 2012.

[13] J. E. Averett, E. M. Zardini, and P. C. Hoch, "Flavonoid systematics of ten sections of Ludwigia (Onagraceae)," *Biochemical Systematics and Ecology*, vol. 18, no. 7-8, pp. 529–532, 1990.

[14] C.-I. Chang, C.-C. Kuo, J.-Y. Chang, and Y.-H. Kuo, "Three New Oleanane-Type Triterpenes from Ludwigia octovalvis with Cytotoxic Activity against Two Human Cancer Cell Lines," *Journal of Natural Products*, vol. 67, no. 1, pp. 91–93, 2004.

[15] J. Yan and X. W. Yang, "Studies on the chemical constituents in herb of Ludwigia octovalvis," *China Journal of Chinese Materia Medica*, vol. 30, no. 24, pp. 1923–1926, 2005.

[16] W.-S. Lin, J.-Y. Chen, J.-C. Wang et al., "The anti-aging effects of Ludwigia octovalvis on Drosophila melanogaster and SAMP8 mice," *AGE*, vol. 36, no. 2, pp. 689–703, 2014.

[17] W.-S. Lin, J.-H. Lo, J.-H. Yang et al., "Ludwigia octovalvis extract improves glycemic control and memory performance in diabetic mice," *Journal of Ethnopharmacology*, vol. 207, pp. 211–219, 2017.

[18] S.-J. Wu, L.-T. Ng, G.-H. Wang, Y.-J. Huang, J.-L. Chen, and F.-M. Sun, "Chlorophyll a, an active anti-proliferative compound of Ludwigia octovalvis, activates the CD95 (APO-1/CD95) system and AMPK pathway in 3T3-L1 cells," *Food and Chemical Toxicology*, vol. 48, no. 2, pp. 716–721, 2010.

[19] T. Murugesan, L. Ghosh, K. Mukherjee, J. Das, M. Pal, and B. P. Saha, "Evaluation of antidiarrhoeal profile of Jussiaea suffruticosa Linn. extract in rats," *Phytotherapy Research*, vol. 14, no. 5, pp. 381–383, 2000.

[20] H. Wagner and S. Bladt, '*Flavonoid Drugs', in Plant drug analysis: A Thin Layer Chromatography Atlas*, Springer-Verlag, Berlin, Germany, 2nd edition, 1996.

[21] "The Plant List," http://www.theplantlist.org/.

[22] G. Ramirez, A. Zamilpa, M. Zavala, J. Perez, D. Morales, and J. Tortoriello, "Chrysoeriol and other polyphenols from Tecoma stans with lipase inhibitory activity," *Journal of Ethnopharmacology*, vol. 185, pp. 1–8, 2016.

[23] T. J. Mabry, K. R. Markham, and M. B. Thomas, *Reagents and procedures for the Ultraviolet Spectral Analysis of Flavonoids*, Springer Berlin Heidelberg, Heidelberg, Germany, 1st edition, 1970.

[24] S. Uzuner and D. Cekmecelioglu, "A rapid screening approach to factors affecting dilute acid hydrolysis of hazelnut shells," *International Proceedings of Chemical, Biological & Environmental Engineering*, vol. 50, pp. 180–185, 2013.

[25] J. Peng, G. Fan, Z. Hong, Y. Chai, and Y. Wu, "Preparative separation of isovitexin and isoorientin from Patrinia villosa Juss by high-speed counter-current chromatography," *Journal of Chromatography A*, vol. 1074, no. 1-2, pp. 111–115, 2005.

[26] H. Bisswanger, '*Enzyme Kinetics', in Enzyme kinetics: Principles and Methods*, Ringgold Inc, Portland, Ore, USA, 2nd edition, 2008.

[27] D. S. H. Bell, J. H. O'Keefe, and P. Jellinger, "Postprandial dysmetabolism: the missing link between diabetes and cardiovascular events?" *Endocrine Practice*, vol. 14, no. 1, pp. 112–124, 2008.

[28] T. Shiraiwa, H. Kaneto, T. Miyatsuka et al., "Postprandial hyperglycemia is a better predictor of the progression," *Diabetes Care*, vol. 28, no. 11, pp. 2806-2807, 2005.

[29] G. Derosa and P. Maffioli, "α-Glucosidase inhibitors and their use in clinical practice," *Archives of Medical Science*, vol. 8, no. 5, pp. 899–906, 2012.

[30] M. P. Hermans, "Diabetes and the endothelium," *Acta clinica Belgica*, vol. 62, no. 2, pp. 97–101, 2007.

[31] A. Gastaldelli, M. Gaggini, and R. A. DeFronzo, "Role of adipose tissue insulin resistance in the natural history of type 2 diabetes: Results from the san antonio metabolism study," *Diabetes*, vol. 66, no. 4, pp. 815–822, 2017.

[32] M. Brownlee, "The pathobiology of diabetic complications: a unifying mechanism," *Diabetes*, vol. 54, no. 6, pp. 1615–1625, 2005.

[33] J. Kim and K. Yoon, "Glucolipotoxicity in Pancreatic β-Cells," *Diabetes & Metabolism Journal*, vol. 35, no. 5, pp. 444–450, 2011.

[34] K. C. B. Tan, A. W. K. Tso, S. C. F. Tam, R. W. C. Pang, and K. S. L. Lam, "Acute effect of orlistat on post-prandial lipaemia and free fatty acids in overweight patients with Type 2 diabetes mellitus," *Diabetic Medicine*, vol. 19, no. 11, pp. 944–948, 2002.

[35] J. B. Reitsma, M. C. Cabezas, T. W. A. de Bruin, and D. W. Erkelens, "Relationship between improved postprandial lipemia and low-density lipoprotein metabolism during treatment with tetrahydrolipstatin, a pancreatic lipase inhibitor," *Metabolism*, vol. 43, no. 3, pp. 293–298, 1994.

[36] K. Tadera, Y. Minami, K. Takamatsu, and T. Matsuoka, "Inhibition of α-glucosidase and α-amylase by flavonoids," *Journal of Nutritional Science and Vitaminology*, vol. 52, no. 2, pp. 149–153, 2006.

[37] H. Li, F. Song, J. Xing, R. Tsao, Z. Liu, and S. Liu, "Screening and Structural Characterization of α-Glucosidase Inhibitors from Hawthorn Leaf Flavonoids Extract by Ultrafiltration LC-DAD-MSn and SORI-CID FTICR MS," *Journal of The American Society for Mass Spectrometry*, vol. 20, no. 8, pp. 1496–1503, 2009.

[38] S. V. Reddy, A. K. Tiwari, U. S. Kumar, R. J. Rao, and J. M. Rao, "Free radical scavenging, enzyme inhibitory constituents from antidiabetic ayurvedic medicinal plant Hydnocarpus wightiana blume," *Phytotherapy Research*, vol. 19, no. 4, pp. 277–281, 2005.

[39] S. Ochir, M. Nishizawa, B. Jae Park et al., "Inhibitory effects of Rosa gallica on the digestive enzymes," *Journal of Natural Medicines*, vol. 64, no. 3, pp. 275–280, 2010.

[40] O. Kamiyama, F. Sanae, K. Ikeda et al., "In vitro inhibition of α-glucosidases and glycogen phosphorylase by catechin gallates in green tea," *Food Chemistry*, vol. 122, no. 4, pp. 1061–1066, 2010.

[41] A. Ishikawa, H. Yamashita, M. Hiemori et al., "Characterization of inhibitors of postprandial hyperglycemia from the leaves of Nerium indicum," *Journal of Nutritional Science and Vitaminology*, vol. 53, no. 2, pp. 166–173, 2007.

[42] A. Kam, K. M. Li, V. Razmovski-Naumovski et al., "A comparative study on the inhibitory effects of different parts and chemical constituents of pomegranate on α-amylase and α-glucosidase," *Phytotherapy Research*, vol. 27, no. 11, pp. 1614–1620, 2013.

[43] L. Kakarla, S. Katragadda, A. Tiwari et al., "Free radical scavenging, α-glucosidase inhibitory and anti-inflammatory constituents from Indian sedges, Cyperus scariosus R.Br and Cyperus rotundus L," *Pharmacognosy Magazine*, vol. 12, supplement 4, no. 47, pp. S488–S496, 2016.

[44] J. Li, Y. Lu, X. Su et al., "A norsesquiterpene lactone and a benzoic acid derivative from the leaves of Cyclocarya paliurus and their glucosidase and glycogen phosphorylase inhibiting activities," *Planta Medica*, vol. 74, no. 3, pp. 287–289, 2008.

[45] J. D. Wansi, M.-C. Lallemand, D. D. Chiozem et al., "α-Glucosidase inhibitory constituents from stem bark of Terminalia superba (Combretaceae)," *Phytochemistry*, vol. 68, no. 15, pp. 2096–2100, 2007.

[46] N. Gupta, S. Gupta, and A. Mahmood, "Gallic acid inhibits brush border disaccharidases in mammalian intestine," *Nutrition Research*, vol. 27, no. 4, pp. 230–235, 2007.

[47] T. Oki, T. Matsui, and Y. Osajima, "Inhibitory effect of α-glucosidase inhibitors varies according to its origin," *Journal of Agricultural and Food Chemistry*, vol. 47, no. 2, pp. 550–553, 1999.

[48] A. I. Martinez-Gonzalez, Á. G. Díaz-Sánchez, L. A. De La Rosa et al., "Polyphenolic compounds and digestive enzymes: In vitro non-covalent interactions," *Molecules*, vol. 22, no. 4, article no. 669, 2017.

[49] G.-N. Kim, M.-R. Shin, S. H. Shin et al., "Study of Antiobesity Effect through Inhibition of Pancreatic Lipase Activity of *Diospyros kaki* Fruit and *Citrus unshiu* Peel," *BioMed Research International*, vol. 2016, Article ID 1723042, pp. 1–7, 2016.

[50] L. Liu, Y.-L. Yu, J.-S. Yang et al., "Berberine suppresses intestinal disaccharidases with beneficial metabolic effects in diabetic states, evidences from in vivo and in vitro study," *Naunyn-Schmiedeberg's Archives of Pharmacology*, vol. 381, no. 4, pp. 371–381, 2010.

Hindawi
Evidence-Based Complementary and Alternative Medicine
Volume 2018, Article ID 2409471, 11 pages
https://doi.org/10.1155/2018/2409471

Research Article

Zuo Gui Wan Alters Expression of Energy Metabolism Genes and Prevents Cell Death in High-Glucose Loaded Mouse Embryos

Qi Liang,[1] **Zhipeng Qu**,[2] **Yu Liang**,[1] **QianJin Feng**,[1] **Xin Niu**,[3] **Temaka Bai**,[3] **Yingli Wang**,[1] **Qiang Song**,[1] **and David L. Adelson**[2]

[1]*Shanxi University of Chinese Medicine, Taiyuan 030619, China*
[2]*School of Biological Sciences, University of Adelaide, Adelaide, SA 5005, Australia*
[3]*Beijing University of Chinese Medicine, Beijing 100029, China*

Correspondence should be addressed to Qiang Song; 13834648844@163.com and David L. Adelson; david.adelson@adelaide.edu.au

Received 7 December 2017; Revised 15 March 2018; Accepted 3 April 2018; Published 25 June 2018

Academic Editor: Mohammed S. Razzaque

Background. *Zuo Gui Wan* (ZGW) is a classic formula in traditional chinese medicine (TCM). Previous studies have shown that it is beneficial for impaired glucose tolerance (IGT) of adults and the offspring as well. This study aimed to understand the molecular mechanisms of the efficacy of ZGW on IGT. *Methods*. We used high-glucose loaded 2-cell stage mouse embryos as a model and took advantage of single-cell RNA sequencing technology to analyze the transcriptome of the model with or without ZGW. Differential gene expression analysis was performed with DESeq2. *Results*. High glucose can downregulate genes in the ribosome pathway, while ZGW can reverse this inhibition and as a result prevent embryo cell death caused by high glucose. Furthermore, high glucose can affect sugar metabolism and influence mitochondrial function, but ZGW can promote sugar metabolism via the tricarboxylic acid cycle mainly through upregulating the genes in the respiratory chain and oxidative phosphorylation. *Conclusions*. ZGW had a protective effect on embryonic cell death caused by glucose loading. The reversion of inhibition of ribosome pathway and regulation of mitochondrial energy metabolism are main effects of ZGW on high-glucose loaded embryos. This research not only revealed the global gene regulation changes of high glucose affecting 2-cell stage embryos but also provided insight into the potential molecular mechanisms of ZGW on the IGT model.

1. Background

Impaired glucose tolerance (IGT) is a sugar metabolism disorder between normal glucose tolerance (NGT) and diabetes mellitus [1]. It is estimated that there are 308 million people with IGT in the world [2], many more than those diagnosed with diabetes. People with IGT can progress to DM and are predisposed to cardiocerebrovascular disease [3–8], microvascular disease [9], lipid metabolism disorders [10], and chronic kidney disease [11, 12]. Therefore, it is becoming more and more important to understand how to prevent IGT. Currently, drugs such as Metformin, Acarbose, and Rosiglitazone are used to treat IGT and can postpone the occurrence of diabetes; however, they cannot prevent corresponding complications [13–18]. Many reports have shown that TCM might be one of the resources to develop new methods for preventing IGT [19–25].

In a previous report, three different Chinese formulas, *Zuo Gui Wan* (ZGW), *You Gui Wan* (YGW), and *Ba Zhen Tang* (BZD), were separately used to treat pregnant Wistar rats. After drugs were administered for three weeks, offspring from different groups were then fed with a high-fat diet for 12 weeks. Many indices, such as fasting blood glucose (FBG), 2-hour blood glucose (2hBG), blood lipid, fasting serum insulin (FINS), and leptin and adiponectin (APN), were measured. Results showed that rats on a high-fat diet developed IGT with abnormal blood lipid, insulin resistance, leptin resistance, and fatty liver. However, ZGW could prevent IGT in these offspring. Compared to YGW and BZD, which only reversed part of above indexes, ZGW

was the most effective formula [26]. Another recent report has also found that giving ZGW to Gestational Diabetes Mellitus (GDM) rats can have a preventive effect on the IGT of offspring induced by a high-fat and high-sugar diet [27]. ZGW is a classic traditional Chinese medicine (TCM) formula with extract from 8 traditional Chinese medicines, which are *Rehmannia glutinosa* (Shu Di Huang), *Cuscuta chinensis* (Tu Si Zi), *Cornus officinalis* (Shan Zhu Yu), *Lycium barbarum* (Gou Qi Zi), *Dioscorea opposita* (Shan Yao), *Cyathula officinalis* (Chuan Niu Xi), *Cervi cornus Colla* (Lu Jiao Jiao), and *Chinemys reevesii* (Gui Ban Jiao). 12 main metabolites were detected in ZGW rat serum with UPLC/MS: β-D-ribofuranuronic acid methyl ester triacetate, 5-hydroxymethyl-2-furfural glucuronide, dihydro-5-hydroxymethyl-2-furfural glucuronide, 8-epiloganic acid, loganic acid, morroniside, coumaric acid, loganin, sweroside, 3-hydroxy-2,6,6-trimethyl-1-cyclohexene-1-carboxylic acid, kaempferol-3-glucuronide, and cuscutamine. Of these, morroniside and loganin could regulate rat mesangial cell growth by reducing oxidative stress and could be used at the early stages of diabetic nephropathy [28]. Studies have shown that dietary kaempferol may reduce the risk of chronic diseases, especially cancers, by augmenting antioxidants to combat free radicals [29].

Previous studies have shown that ZGW is an effective treatment in the IGT rat model, and it is beneficial not only to the mother but also to the offspring [26, 27, 30]. But the molecular mechanisms of ZGW on IGT, particularly at the transcriptome level, are still unclear. Therefore, in this study, we used mouse embryos loaded with high glucose as an IGT model to study the effect of ZGW. By analyzing the transcriptome of our IGT model treated with ZGW, we identified ribosome pathway and oxidative phosphorylation as the potential target molecular pathways of ZGW on IGT. A list of potential response genes to ZGW on IGT was also identified, and these genes provide a good resource for further functional studies.

2. Methods

All chemicals used in this study were purchased from Sigma-Aldrich Corporation (St. Louis, MO, USA) unless otherwise indicated. The Institutional Animal Care and Use Committee at the China Agricultural University (Beijing, China) approved the protocols used in this study.

2.1. Preparation of ZGW. ZGW is a classic formula in TCM and includes the extract from 8 traditional Chinese medicines. First, these 8 medicines were immersed in 800 ml water at 50°C and then decocted for 1.5 hours and filtered. The decoction and filtration were repeated two times. The filtrates were combined and concentrated to 1 g/ml crude drug.

2.2. ZGW Serum Preparation. Rats from National Institutes for Food and Drug Control, China (license number: SCXK-(JING) 2009- 0017), were fed with 20 g/kg/d ZGW for 7 days. Blood was collected directly from their hearts and incubated at 4°C for 30 min, followed by centrifugation at 4000 rpm for 15 min at 4°C. The serum, denoted as ZGW-containing rat serum, was collected immediately and stored at −75°C before use. The concentration of ZGW rat serum used in this research was 0.01% v/v ZGW.

2.3. Super Ovulation. For timed pregnancy, pregnant mare's serum gonadotropin (PMSG) (5 IU) was intraperitoneally injected into ICR female mice aged 6 to 8 weeks. Next, human chorionic gonadotropin (hCG) (5 IU) was intraperitoneally injected after 48 h; on the evening of hCG injection, male mice and the female mice (2 : 1) were housed together in a cage for one night. The next morning, females were checked for a vaginal plug to determine if they were pregnant.

2.4. Drug Administration and Grouping. Pregnant mice were cervically dislocated and zygotes were washed out from the vagina. All zygotes were randomly assigned to three groups: control group, model group, and drug group. Each group contained 9 zygotes. Zygotes in different groups were cultured with media as follows: control group with cell-culture medium, model group with cell culture medium supplemented with high glucose 15.6 mmol/L, and drug group similar to the model group but with the addition of rat serum containing 0.01% v/v ZGW.

2.5. Determination of Blastocyst Embryo Cell Number. Zygotes in the three groups were cultured *in vitro* for five days (blastocyst stage) and then incubated separately in M2 medium [NaCl (5.533 g/L), KCl (0.356 g/L), $CaCl_2{\cdot}2H_2O$ (0.252 g/L), KH_2PO_4 (0.162 g/L), $MgSO_4{\cdot}7H_2O$ (0.293 g/L), $NaHCO_3$ (0.349 g/L), Hepes (4.969 g/L), sodium lactate (2.610 g/L), sodium pyruvate (0.036 g/L), glucose (1.000 g/L), BSA (4.000 g/L), penicillin (0.060 g/L), and streptomycin (0.050 g/L)] containing Hoechst 33342 (10 μg/mL) for 15 minutes at 37°C. After washing three times with M2 medium, blastocysts from the three groups were separately mounted on microscope slides and examined on an epifluorescence microscope to count the number of embryo cell nuclei.

2.6. Sample Preparation for Single-Cell RNA Sequencing. Zygotes from the three groups were cultured in vitro to 2-cell stage, and three zygotes were randomly selected as a sample from each group and stored in liquid nitrogen. Each group was replicated three times for biological replication. Zygotes were resuspended in freshly prepared lysis buffer [total volume 100 μl, containing 93 μl nuclease-free water, 2 μl Triton X-100, and 5 μl RNaseOUT (20 U/μl)]; each zygote was lysed with a micropipette to yield more than 7 μl of lysate and the lysate stored at −80°C.

2.7. Single-Cell RNA Sequencing and Bioinformatic Analysis. RNA amplification was performed according to SMARTer Ultra Low Input RNA for Illumina Kit (Clontech Laboratories). Quantity and quality of amplified cDNAs were measured with Qubit and Agilent Bioanalyzer 2100 (Agilent Technologies, Santa Clara, CA, USA). RNA sequencing was performed using Illumina HiSeq 2500 (Shanghai Biotechnology Corporation, Shanghai, China). Adaptors and low-quality sequences from raw reads were filtered using Trim Galore! with the following parameter: stringency 6. Trimmed

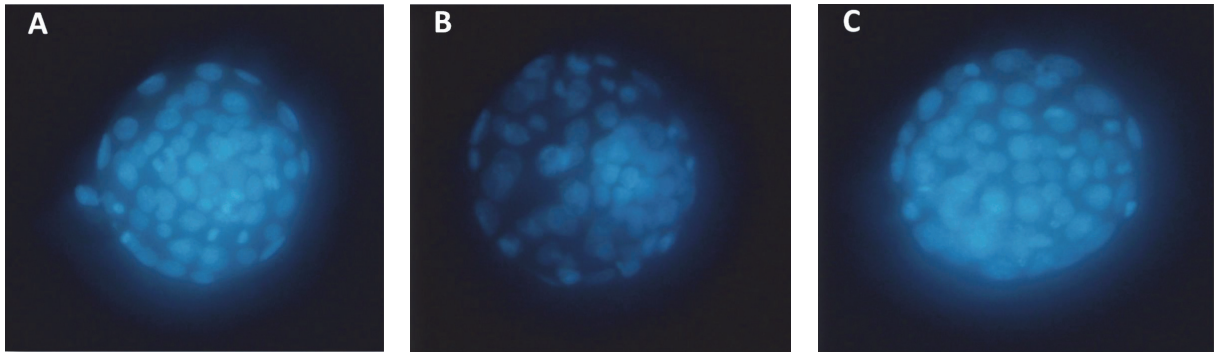

(a) (b) (c)

Figure 1: Fluorescence photomicrographs of blastocyst cells stained with Hoechst 33342. (a) Stained blastocyst cells in control group. (b) Stained blastocyst cells in model group. (c) Stained blastocyst cells in drug group.

Table 1: Effects of ZGW rat serum on blastocyst cell number.

Group	Blastocyst cell number (n)
Control	$68.4^{a} \pm 2.4$
Model	$57.2^{a,b} \pm 1.6$
Drug	$63.2^{b} \pm 2.2$

Values are mean ± SEM. Means in column with different superscripts indicate significant differences ($P < 0.05$).

reads were mapped to the mouse reference genome (mm10) using STAR v2.5 with the following parameters: out Filter Mismatch Nover L max 0.05 and seed Search Start L max 30 [31]. Raw counts of mouse RefSeq genes were acquired with R package "Genomic Alignments" [32]. Differential gene expression analysis was performed with DESeq2 [33]. Gene Ontology (GO) and Kyoto Encyclopedia of Genes and Genomes (KEGG) enrichment analyses were performed using Clue GO based on significantly differentially expressed genes (false discovery rate < 0.05) from DESeq2 [1]. Enriched GO terms or KEGG pathways were visualized with Cytoscape V3 [34].

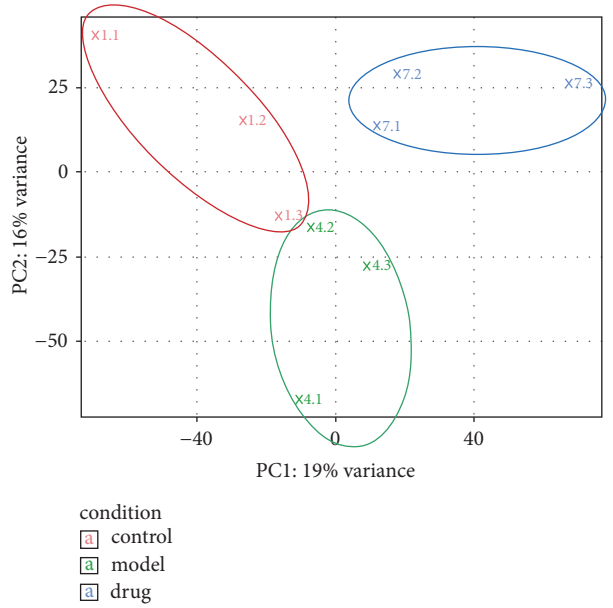

Figure 2: PCA of gene expression patterns for 2-cell stage embryos. Different colors identify different groups as indicated in the legend.

3. Results

3.1. Blastocyst Cell Number. In the control group (Figure 1(a)), the cells in blastocyst showed bright nuclear fluorescence. But in the model group (Figure 1(b)), blastocysts showed decreases in both nuclear fluorescence and the number of nuclei. In contrast to this, in the drug group (Figure 1(b)), both nuclear fluorescence and the number of nuclei in blastocysts increased compared to the model group. There were significant differences in the blastocyst cell number between the control group and the model group ($P < 0.05$) and between the model group and the drug group ($P < 0.05$) (Table 1).

3.2. Summary of Transcriptome Analysis. Principal component analysis (PCA) was able to resolve and separate the three groups (Figure 2), indicating overall differences in the patterns of gene expression in these treatments. The *MA*-plot ("M" is for log ratios and "A" is for mean average) (Figure 3) demonstrates that most of the points were clustered tightly around the horizontal line, indicating that RNA-Seq data were of good quality. There were differently expressed genes between these three groups (red dots), indicating that expression of some genes was changed after the control group was loaded with high glucose (Figure 3(a)) and after the model group was treated with ZGW rat serum (Figure 3(b)). Furthermore, by comparing the global gene expression changes between model group and control group, we identified 71 upregulated and 100 downregulated genes, respectively. We then also compared the drug group to the model group, and 115 upregulated and 174 downregulated genes were detected (Table 2).

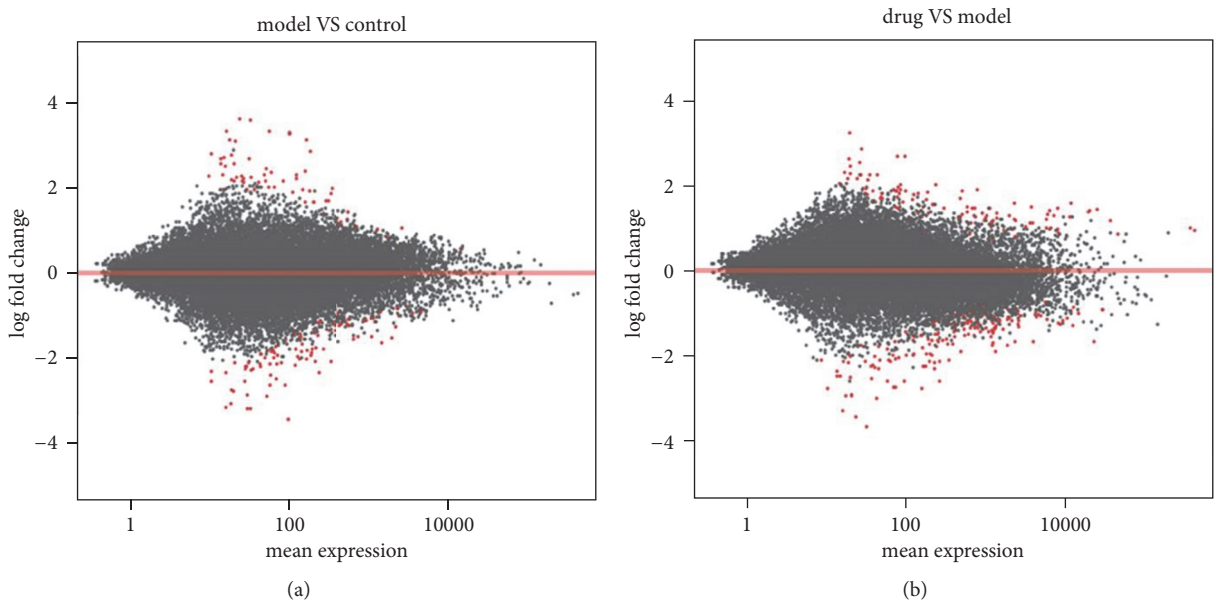

Figure 3: *MA*-plot of the log 2 fold changes over the mean of RNA-Seq read counts. The log 2 fold change for a particular comparison is plotted on y-axis and the average of the counts normalized by size factor is shown on x-axis. Each gene is represented with a dot, and genes with FDR < 0.05 are shown in red. (a) Comparison of model group with control group. (b) Comparison of drug group with model group.

Table 2: Summary of differentially regulated gene numbers among the three groups (FDR < 0.05).

	Control	Model	Drug
Control	N/A	**100**	**N/A**
Model	*71*	N/A	**174**
Drug	*N/A*	*115*	N/A

Numbers in italic are upregulated genes, while those in bold are downregulated (DOCX).

3.3. Pathway Analysis of Embryos Treated with High Glucose. To identify the gene regulatory pathways potentially affected when embryos were treated with high glucose, two gene enrichment analyses were carried out for the differentially expressed genes between the model and control groups. For the Gene Ontology (GO) enrichment analysis (Table 3), we found 6 enriched biological process GO terms, including *"gluconeogenesis"* (GO: 0006094). For cellular components, we found *ribosome* (GO: 0022625, GO: 0015934, and GO: 0022626) and *mitochondrial respiratory chain* (GO: 0005746) as overrepresented terms. The *insulin-like growth factor binding* (GO: 0005520) was identified as the most significant overrepresented GO term in the molecular function category. Based on KEGG enrichment analysis, ribosome was identified as the only significantly overrepresented pathway with differentially expressed genes enriched in 2-cell stage of mouse embryo treated with high glucose (Figure 4).

3.4. Gene Expression Changes in High-Glucose Loaded Embryos Treated with ZGW Rat Serum. We used the same enrichment analysis to analyze the potential molecular

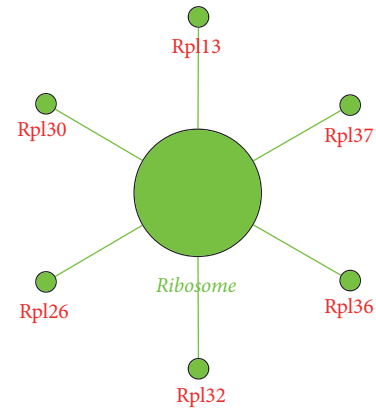

Figure 4: KEGG pathway (FDR < 0.05) enriched by the 171 differentially expressed genes in model group compared to control group. Green colored dots are downregulated. The big dot is a sign of the enriched pathway and the big green word is the name of the pathway. Small green dots show the genes that are downregulated, and the red words are the names of downregulated genes.

pathways affected by ZGW in high-glucose loaded embryos. Based on differentially expressed genes in the drug group compared to the model group, 22 overrepresented GO terms were observed and 13 of them were in the molecular function category (Table 4). These terms included *hydrogen ion transmembrane transporter activity* (GO: 0015078), *cytochrome-c oxidase activity* (GO: 0004129), *heme-copper terminal oxidase activity* (GO: 0015002), and *oxidoreductase activity* (GO: 0016676, GO: 0016675). For cellular component terms, we found two main locations, the ribosome and mitochondria, with terms such as *ribosomal subunit* (GO:

Table 3: Summary of GO terms for differentially expressed genes between model and control groups.

Ontology source	GO ID	GO term	Term P value
Biological process	GO: 0034616	Response to laminar fluid shear stress	$1.07E-04$
	GO: 0006525	Arginine metabolic process	$4.12E-04$
	GO: 0034405	Response to fluid shear stress	$2.18E-03$
	GO: 0021885	Forebrain cell migration	$1.63E-02$
	GO: 0035914	Skeletal muscle cell differentiation	$1.75E-02$
	GO: 0006094	Gluconeogenesis	$1.81E-02$
Cellular component	GO: 0022625	Cytosolic large ribosomal subunit	$1.19E-05$
	GO: 0015934	Large ribosomal subunit	$1.53E-04$
	GO: 0022626	Sytosolic ribosome	$2.36E-04$
	GO: 0031941	Filamentous actin	$1.19E-03$
	GO: 0005881	Cytoplasmic microtubule	$8.66E-03$
	GO: 0005746	Mitochondrial respiratory chain	$1.18E-02$
Molecular function	GO: 0005520	Insulin-like growth factor binding	$6.88E-04$
	GO: 0016879	Ligase activity, forming carbon-nitrogen bonds	$7.94E-03$
	GO: 0033613	Activating transcription factor binding	$9.60E-03$

15 GO terms are significantly enriched by the 171 changed genes after control group loaded by high glucose.

Table 4: Summary of GO terms for differentially expressed genes between drug and model groups.

Ontology source	GO ID	GO term	Term P value
Biological process	GO: 1902600	Hydrogen ion transmembrane transport	$2.60E-04$
	GO: 0070646	Protein modification by small protein removal	$6.99E-04$
Cellular component	GO: 0005732	Small nucleolar ribonucleoprotein complex	$3.34E-06$
	GO: 0005685	U1 snRNP	$1.47E-03$
	GO: 0044391	Ribosomal subunit	$1.52E-03$
	GO: 0005753	Mitochondrial proton-transporting ATP synthase complex	$1.70E-03$
	GO: 0045259	Proton-transporting ATP synthase complex	$2.52E-03$
	GO: 0016469	Proton-transporting two-sector ATPase complex	$2.57E-03$
	GO: 0044455	Mitochondrial membrane part	$3.11E-03$
Molecular function	GO: 0015078	Hydrogen ion transmembrane transporter activity	$1.90E-04$
	GO: 0004129	Cytochrome-c oxidase activity	$4.00E-04$
	GO: 0015002	Heme-copper terminal oxidase activity	$4.00E-04$
	GO: 0016676	Oxidoreductase activity, acting on a heme group of donors, oxygen as acceptor	$4.00E-04$
	GO: 0008553	Hydrogen-exporting ATPase activity, phosphorylative mechanism	$4.19E-04$
	GO: 0016675	Oxidoreductase activity, acting on a heme group of donors	$4.55E-04$
	GO: 0030515	snoRNA binding	$3.03E-03$
	GO: 0036442	Hydrogen-exporting ATPase activity	$3.79E-03$
	GO: 0016830	Carbon-carbon lyase activity	$3.95E-03$
	GO: 0016814	Hydrolase activity, acting on carbon-nitrogen (but not peptide) bonds, in cyclic amidines	$4.66E-03$
	GO: 0000062	Fatty-acyl-CoA binding	$6.17E-03$
	GO: 0019783	Ubiquitin-like protein-specific protease activity	$6.26E-03$
	GO: 0019843	rRNA binding	$3.21E-02$

22 GO terms are significantly enriched by the 289 changed genes after model group treated with ZGW rat serum.

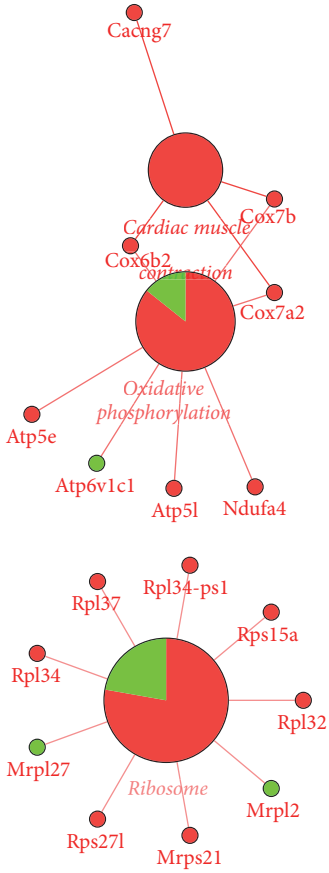

Figure 5: KEGG pathway (FDR < 0.05) enriched by the 289 differentially expressed genes in drug group compared to model group. Red means upregulated, while green means downregulated. Big dots represent the enriched pathways and big red words are the names of these pathways. Small red dots show the upregulated genes and the related red words are downregulated gene names. Small green dots show the downregulated genes and the related green words are downregulated gene names.

0044391), *small nucleolar ribonucleoprotein complex* (GO: 0005732), *mitochondrial proton-transporting ATP synthase complex* (GO: 0005753), and *mitochondrial membrane part* (GO: 0044455). Results of KEGG enrichment analysis showed that genes in the ribosome pathway were upregulated, and some genes in the oxidative phosphorylation pathway were also upregulated by ZGW (Figure 5).

3.5. Identification of Potential Response Genes for ZGW. Among the 71 upregulated genes in the model group compared to the control group, 14 genes were downregulated in embryos treated with ZGW (Figure 6). These genes were *Irf6, H2afy, Smarca1, Fmr1os, Ifi27, Fam46c, Cym, Caps2, Rassf8, Xkr4, Plac1, Xrra1, 3110001I22Rik,* and *A230056J06Rik* (Figure 7). No GO terms could be enriched based on these 14 genes. In the 100 downregulated genes from the model group compared to the control group, 14 genes were upregulated in embryos treated with ZGW (Figure 6). They were *Krt27, Deb1, Myg1, Pmvk, Rpl37, Snord72, Gpalpp1, Zscan26, Rpl32, Adh1, Slc17a1, Aurkaip1, Nop10,* and *Cox7b* (Figure 8). These 14 genes were enriched for GO terms highly related to mitochondrial energy metabolism (Table 5).

4. Discussion

4.1. Effects of High Glucose on Mice Embryo Development. Ample studies have shown that high glucose can affect embryos and block embryo development [35–37]. Research on the mechanism of this embryo development block has shown that high glucose can induce reactive oxygen species and cause damage to the embryo through oxidative stress [37, 38]. In this study, we found that high glucose downregulated several genes in the ribosome pathway (Figure 4), and three GO terms of *ribosome* have been enriched based on the differentially expressed genes between the model and control groups. Ribosome mediates protein synthesis and the downregulation of genes involved in the ribosome pathway in high-glucose loaded embryos indicated that protein synthesis might be affected. Furthermore, 2-cell stage is a key stage between maternal regulation and zygotic regulation in mouse [39]. Downregulation of ribosomal genes at this stage could affect the regulation of this transition.

We also found that genes involved in gluconeogenesis, including *crtc2*, *Ppara*, and *Sds*, were all downregulated in the model group. Molecular function of "insulin-like growth factor binding (GO:0005520)" was also affected by high glucose (Table 3). Insulin growth factors (IGFs) are important proteins in the regulation of embryo development, and a study showed that IGFs were main endocrine factors in the regulation of embryo development [40]; IGF-I has effects on metabolic regulation in embryos [41, 42]. The gluconeogenesis process is one of the pathways regulated by sugar in the uterus [40].

All these indicated that downregulating genes in ribosome pathway and affecting the sugar metabolism of mice embryo at 2-cell stage are two of the main causes of embryo developmental block induced by high glucose.

4.2. Efficacy of ZGW on High-Glucose Loaded Mice Embryo. Previous studies showed that ZGW rat serum could induce cell proliferation and differentiation [43, 44], inhibit cell apoptosis [45], and promote germ cell and embryo development [30, 46]. Furthermore, it has also been shown that the administration of ZGW to GDM rats has a preventive effect on the offspring's IGT caused by a high-fat and high-sugar diet [27]. In our study, we found that ZGW could upregulate several genes in the ribosome pathway, which were downregulated in embryos loaded with high glucose (Figure 5). The ribosomal subunit (GO: 0044391) was also one of the terms that been affected by ZGW (Table 4). In addition, among the 14 downregulated genes in the model group but upregulated in the drug group (Figure 8), *Rpl32* and *Rpl37* are both involved in the ribosome pathway.

Furthermore, we found that some pathways associated with energy metabolism were altered in high-glucose loaded embryos after treatment with ZGW. ZGW upregulated genes in the oxidative phosphorylation pathway (Figure 5), consistent with activate energy metabolism and sugar metabolism

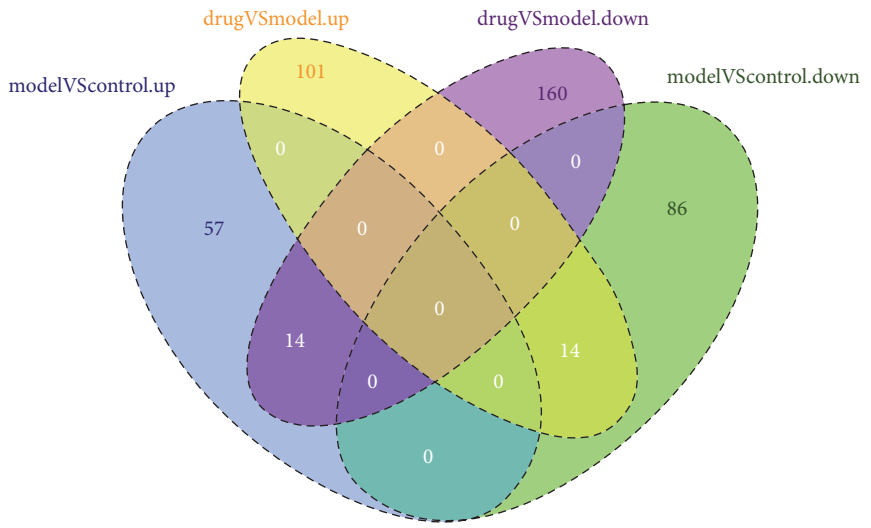

Figure 6: Venn diagram of pairwise gene expression changes between the three groups. Numbers in ovals represent different gene numbers between two groups.

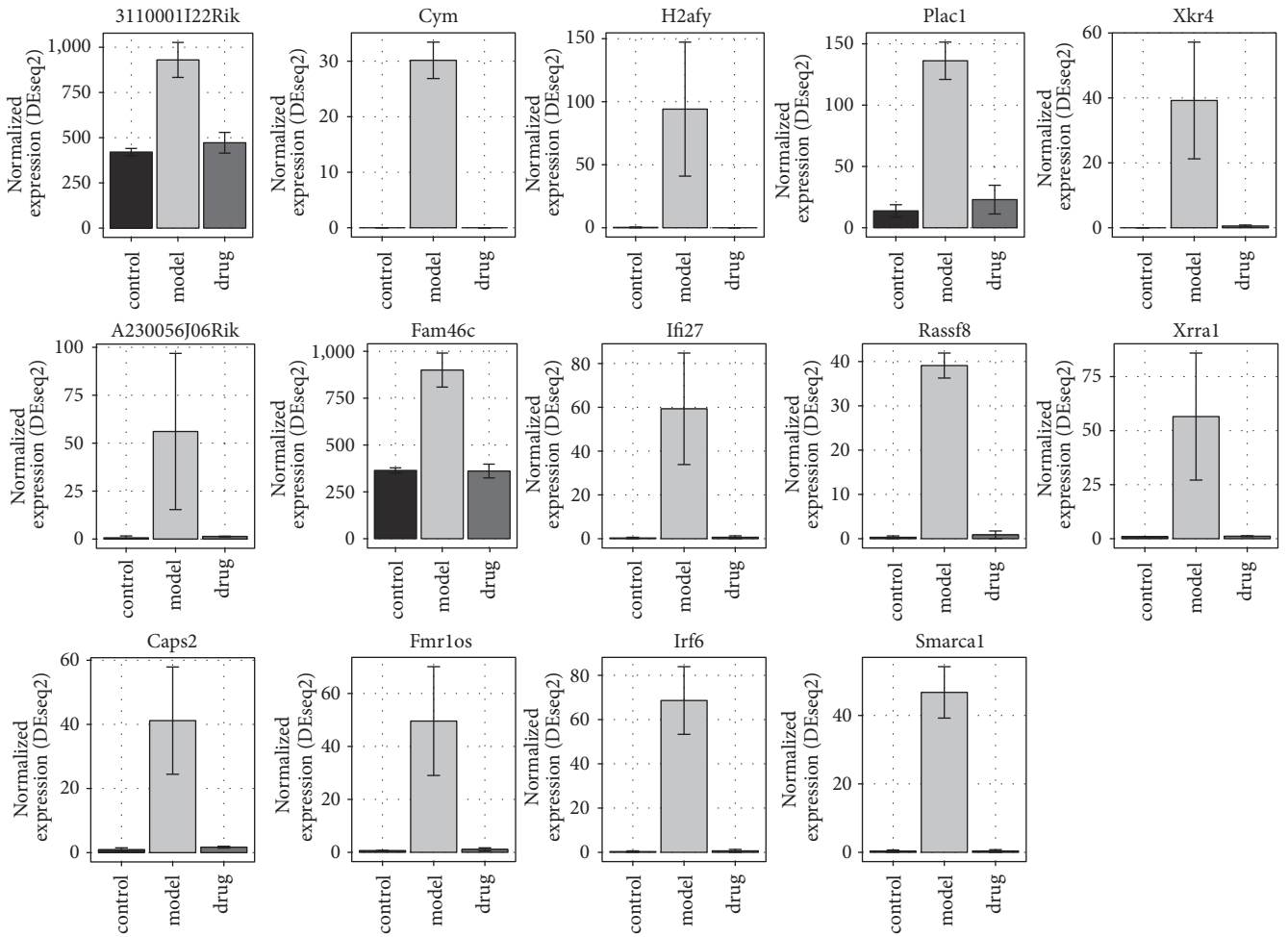

Figure 7: 14 genes upregulated in model group and downregulated in drug group. Read counts normalized by library size according to DESeq2 are shown on y-axis.

Table 5: Summary of GO terms of 14 genes downregulated in model group and upregulated in drug group.

GO ID	Description	q-value
GO: 0005743	Mitochondrial inner membrane	$1.92E-06$
GO: 0019866	Organelle inner membrane	$2.07E-06$
GO: 0005746	Mitochondrial respiratory chain	$2.19E-05$
GO: 0070469	Respiratory chain	$2.19E-05$
GO: 0044455	Mitochondrial membrane part	$6.72E-05$
GO: 1990204	Oxidoreductase complex	$1.54E-04$
GO: 0030964	NADH dehydrogenase complex	$4.25E-04$
GO: 0005747	Mitochondrial respiratory chain complex I	$4.25E-04$
GO: 0045271	Respiratory chain complex I	$4.25E-04$

9 GO terms are significantly enriched by the 14 reversed genes in drug group.

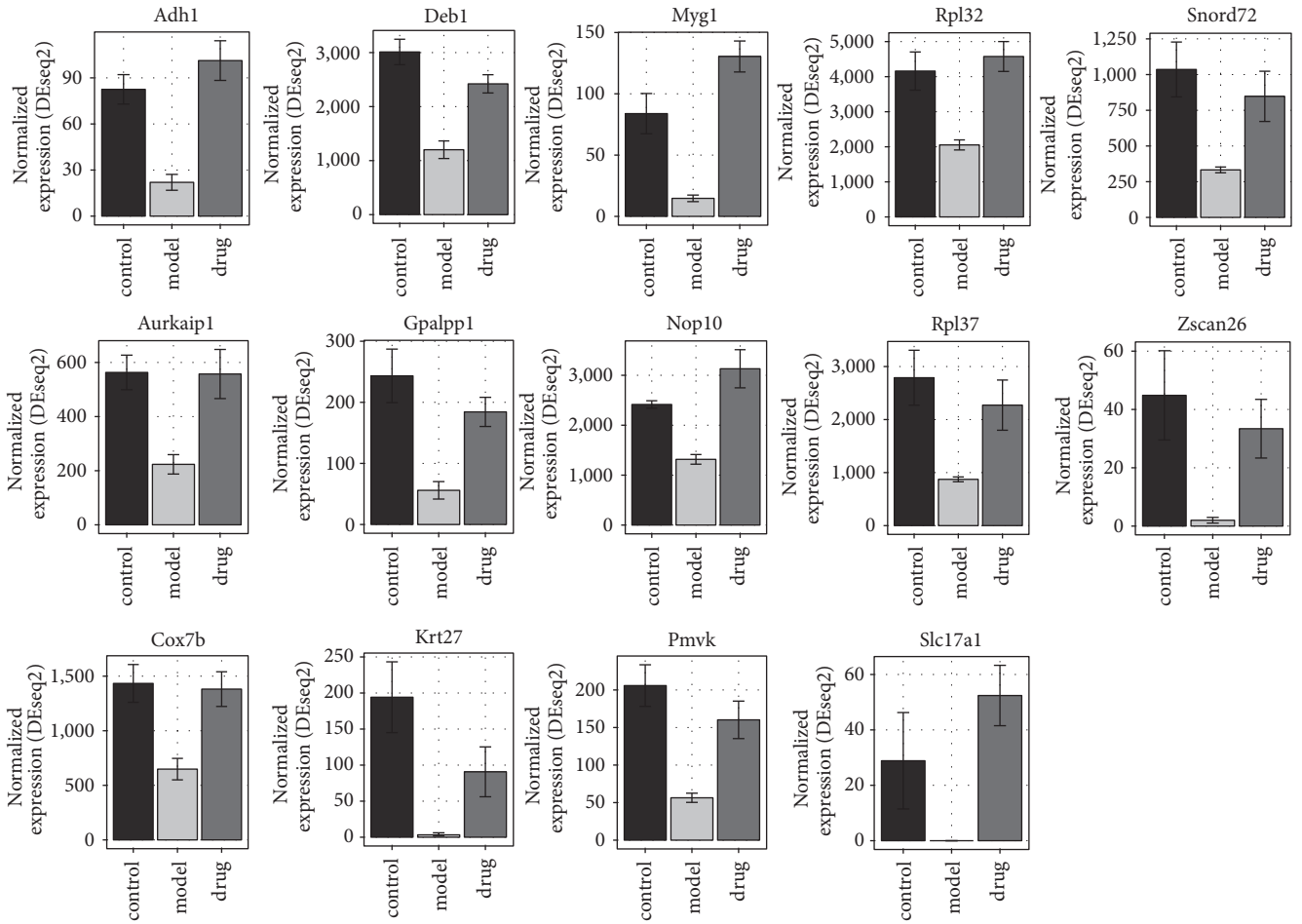

Figure 8: 14 genes downregulated in model group and upregulated in drug group. Read counts normalized by library size according to DESeq2 are shown on y-axis.

in embryos. *Oxidoreductase activity* (GO: 0016676 and GO: 0016675), *mitochondrial proton-transporting ATP synthase complex* (GO: 0005753), and *mitochondrial membrane part* (GO: 0044455) were also enriched based on the differentially expressed genes between the drug and model groups (Table 4). The GO annotation and coexpression network of 14 genes downregulated in the model group but upregulated by ZGW in the drug group (Table 5) showed that some of them were associated with the mitochondrial energy metabolism.

By these results, taken together with the result showing that ZGW prevented the embryo cell death caused by high glucose and promotes the blastocyst formation rate and total cell numbers in blastocysts, we conclude that ZGW may reverse the inhibition of the ribosome pathway and increase

mitochondrial energy metabolism, which were inhibited by high glucose, and prevent the mouse embryo cell death caused by high glucose.

5. Conclusions

IGT can be effectively modeled using mouse embryos loaded with high glucose, providing an effective means to explore its pathogenesis and molecular mechanisms. By analyzing the transcriptome of this IGT model treated with ZGW, we found that high glucose might affect sugar metabolism and influence the mitochondrial function of mouse embryos at the 2-cell stage and that ZGW can counteract this by upregulating genes in the respiratory chain and oxidative phosphorylation. Furthermore, ZGW can prevent the embryo cell death caused by high glucose through upregulating genes inhibited by high glucose in ribosome pathway.

Abbreviations

ZGW: *Zuo Gui Wan*
TCM: Traditional Chinese medicine
IGT: Impaired glucose tolerance
NGT: Normal glucose tolerance
DM: Diabetes mellitus
YGW: *You Gui Wan*
BZD: *Ba Zhen Tang*
FBG: Fasting blood glucose
2hBG: 2-hour blood glucose
FINS: Fasting serum insulin
APN: Leptin and adiponectin
GDM: Gestational Diabetes Mellitus
PMSG: Pregnant mare's serum gonadotropin
hCG: Human chorionic gonadotropin
PCA: Principal component analysis
GO: Gene Ontology enrichment analysis
KEGG: Kyoto Encyclopedia of Genes and Genomes.

Data Availability

All data are contained within the article. Raw data and material are available at https://www.ncbi.nlm.nih.gov/geo/query/acc.cgi?acc=GSE85477.

Ethical Approval

The Institutional Animal Care and Use Committee at the China Agricultural University (Beijing, China) approved the protocols used in this study.

Conflicts of Interest

The authors declare that they have no conflicts of interest.

Authors' Contributions

Qi Liang, QianJin Feng, David L. Adelson, Qiang Song, and Xin Niu conceived and designed the experiments. Qi Liang, Zhipeng Qu, and David L. Adelson performed the experiments and analyzed the transcriptome data. Qi Liang, Zhipeng Qu, Yu Liang, and David L. Adelson wrote the paper. Temaka Bai cultured the embryos and quantified blastocyst cells. Yingli Wang helped with the extraction of serum containing ZGW and the analysis of main metabolites in ZGW rat serum.

Acknowledgments

This study was funded by the Shanxi Province Key Research and Development Project (International Cooperation): the regulatory function of tonifying SHEN formula in TCM on the early development of mouse embryo at transcriptome level (no. 201703D421017). The authors wish to thank Zhu Shien of the National Engineering Laboratory for Animal Breeding of China Agricultural University (Beijing, China) for providing embryo culture technology.

References

[1] G. Bindea, B. Mlecnik, H. Hackl et al., "ClueGO: a Cytoscape plug-in to decipher functionally grouped gene ontology and pathway annotation networks," *Bioinformatics*, vol. 25, no. 8, pp. 1091–1093, 2009.

[2] S. J. Grant, A. Bensoussan, D. Chang, H. Kiat, N. L. Klupp, J. P. Liu et al., "Chinese herbal medicines for people with impaired glucose tolerance or impaired fasting blood glucose," *The Cochrane Database of Systematic Reviews*, Article ID CD006690, 2009.

[3] E. S. Ford, G. Zhao, and C. Li, "Pre-diabetes and the risk for cardiovascular disease: a systematic review of the evidence," *Journal of the American College of Cardiology*, vol. 55, no. 13, pp. 1310–1317, 2010.

[4] Q. Jia, H. Zheng, X. Zhao et al., "Abnormal glucose regulation in patients with acute stroke across China: Prevalence and baseline patient characteristics," *Stroke*, vol. 43, no. 3, pp. 650–657, 2012.

[5] A. Karasik, "Glycaemic control is essential for effective cardiovascular risk reduction across the type 2 diabetes continuum," *Annals of Medicine*, vol. 37, no. 4, pp. 250–258, 2005.

[6] M. Alssema, J. M. Dekker, G. Nijpels, C. D. A. Stehouwer, L. M. Bouter, and R. J. Heine, "Proinsulin concentration is an independent predictor of all-cause and cardiovascular mortality: An 11-year follow-up of the Hoorn study," *Diabetes Care*, vol. 28, no. 4, pp. 860–865, 2005.

[7] Y.-X. Meng, E. S. Ford, C. Li et al., "Association of C-reactive protein with surrogate measures of insulin resistance among nondiabetic US from National Health and Nutrition Examination Survey 1999–2002," *Clinical Chemistry*, vol. 53, no. 12, pp. 2152–2159, 2007.

[8] S. E. Vermeer, W. Sandee, A. Algra, P. J. Koudstaal, L. J. Kappelle, and D. W. J. Dippel, "Impaired glucose tolerance increases stroke risk in nondiabetic patients with transient ischemic attack or minor ischemic stroke," *Stroke*, vol. 37, no. 6, pp. 1413–1417, 2006.

[9] M. M. Gabir, R. L. Hanson, D. Dabelea et al., "Plasma glucose and prediction of microvascular disease and mortality: evaluation of 1997 American Diabetes Association and 1999 World Health Organization criteria for diagnosis of diabets," *Diabetes Care*, vol. 23, no. 8, pp. 1113–1118, 2000.

[10] Y. Mori, K. Hoshino, K. Yokota, T. Yokose, and N. Tajima, "Increased visceral fat and impaired glucose tolerance predict the increased risk of metabolic syndrome in Japanese middle-aged men," *Experimental and Clinical Endocrinology & Diabetes: Official Journal, German Society of Endocrinology [and] German Diabetes Association*, vol. 113, no. 6, pp. 334–339, 2005.

[11] T. Basturk and A. Unsal, "What is the frequency of carbohydrate metabolism disorder in CKD?" *Journal of Renal Care*, vol. 38, no. 1, pp. 15–21, 2012.

[12] Y. I. Kim, C.-H. Kim, C. S. Choi et al., "Microalbuminuria is associated with the insulin resistance syndrome independent of hypertension and type 2 diabetes in the Korean population," *Diabetes Research and Clinical Practice*, vol. 52, no. 2, pp. 145–152, 2001.

[13] A. H. Xiang, R. K. Peters, S. L. Kjos et al., "Effect of pioglitazone on pancreatic β-cell function and diabetes risk in Hispanic women with prior gestational diabetes," *Diabetes*, vol. 55, no. 2, pp. 517–522, 2006.

[14] J.-L. Chiasson, R. G. Josse, R. Gomis, M. Hanefeld, A. Karasik, and M. Laakso, "Acarbose for prevention of type 2 diabetes mellitus: the STOP-NIDDM randomised trial," *The Lancet*, vol. 359, no. 9323, pp. 2072–2077, 2002.

[15] W. C. Knowler, E. Barrett-Connor, S. E. Fowler et al., "Reduction in the incidence of type 2 diabetes with lifestyle intervention or metformin," *The New England Journal of Medicine*, vol. 346, no. 6, pp. 393–403, 2002.

[16] Investigators TDT, "Effect of ramipril on the incidence of diabetes," *The New England Journal of Medicine*, vol. 35, no. 15, pp. 1551–1562, 2006.

[17] A. J. Scheen, "Drug treatment of non-insulin-dependent diabetes mellitus in the 1990s," *Drugs*, vol. 54, pp. 355–368, 1997.

[18] S. E. Nissen and K. Wolski, "Effect of rosiglitazone on the risk of myocardial infarction and death from cardiovascular causes," *The New England Journal of Medicine*, vol. 356, no. 24, pp. 2457–2471, 2007.

[19] H. J. H. Ai-zhen, L. Zhe-Feng, and C. Yuan, "Observation of clinical efficacy of Xiao-ke-hua-Yu-pian on impaired glucose tolerance," *Medical Journal of Chinese People's Liberation Army*, vol. 29, pp. 993-994, 2004.

[20] P. Shan-Yu, "Prevention and treating impaired glucose tolerance with Traditional Chinese Medicine," *ZheJiang Journal of Integrated Traditional Chinese and Western Medicine*, vol. 16, article 354, 2006.

[21] D.-H. D.-B. Wang and Z. Qi, "Observation of clinical efficacy of Traditional Chinese medicine on impaired glucose tolerance," *Journal of Si Chuan of Traditional Chinese Medicine*, vol. 24, pp. 63-64, 2006.

[22] X. Z. Wang, "Traditional Chinese medicine experience of professor TONG Xiao-lin in the treatment of steroid diabetes," *Chinese Archives of Traditional Chinese Medicine*, vol. 23, pp. 1764-1765, 2005.

[23] W.-Q. W.-H. Yu, "Observation of clinical efficacy of Jia-Wei-Yu-Ye-Tang on impaired glucose tolerance," *Journal of ZheJiang University of Traditional Chinese Medicine*, vol. 33, pp. 402-403, 2009.

[24] W. Yue-Xin, "Preventive effect of Jin-qi-jiang-tang-pian on impaired glucose tolerance," *TianJin Medicial Journal*, vol. 33, pp. 793-794, 2005.

[25] H. Shu-Ling, H. Shu-Fang, M. Ming, and Z. Yu-Qing, "Observation of Clinical Therapeutic Effects of Xiaodan Decoction on 32 Cases of Impaired Glucose Tolerance," *World Journal of Integrated Traditional and Western Medicine*, vol. 2, article 016, 2009.

[26] X. Kai-Xia, *Experimental study on preventive effect of tonifying kidney formulas fed during embryonic period on offspring rats' IGT which induced by high-fat diet Beijing University of Traditional Chinese Medicine*, 2012.

[27] Y. Wang, Q. Feng, X. Niu et al., "The preventive effect of Zuogui wan on offspring rats' impaired glucose tolerance whose mothers had gestational diabetes mellitus," *Evidence-Based Complementary and Alternative Medicine*, vol. 2016, Article ID 9417362, 8 pages, 2016.

[28] H. Xu, J. Shen, H. Liu, Y. Shi, H. Li, and M. Wei, "Morroniside and loganin extracted from *Cornus officinalis* have protective effects on rat mesangial cell proliferation exposed to advanced glycation end products by preventing oxidative stress," *Canadian Journal of Physiology and Pharmacology*, vol. 84, no. 12, pp. 1267–1273, 2006.

[29] A. Y. Chen and Y. C. Chen, "A review of the dietary flavonoid, kaempferol on human health and cancer chemoprevention," *Food Chemistry*, vol. 138, no. 4, pp. 2099–2107, 2013.

[30] Q. J. Feng, M. L. Feng, and Y. L. Wang, "Effect of zuoguiwan on early embryonic development of mice," *Zhongguo Zhong xi yi jie he za zhi Zhongguo Zhongxiyi jiehe zazhi= Chinese journal of integrated traditional and Western medicine/Zhongguo Zhong xi yi jie he xue hui, Zhongguo Zhong yi yan jiu yuan zhu ban*, vol. 16, no. 11, pp. 673–675, 1996.

[31] A. Dobin, C. A. Davis, F. Schlesinger et al., "STAR: ultrafast universal RNA-seq aligner," *Bioinformatics*, vol. 29, no. 1, pp. 15–21, 2013.

[32] M. Lawrence, W. Huber, H. Pags, P. Aboyoun, and M. Carlson, "Software for computing and annotating genomic ranges," *PLoS Computational Biology*, vol. 9, no. 8, Article ID e1003118, 2013.

[33] M. I. Love, W. Huber, and S. Anders, "Moderated estimation of fold change and dispersion for RNA-seq data with DESeq2," *Genome Biology*, vol. 15, no. 12, article 550, 2014.

[34] P. Shannon, A. Markiel, O. Ozier et al., "Cytoscape: a software Environment for integrated models of biomolecular interaction networks," *Genome Research*, vol. 13, no. 11, pp. 2498–2504, 2003.

[35] K. H. Moley, W. K. Vaughn, A. H. DeCherney, and M. P. Diamond, "Effect of diabetes mellitus on mouse pre-implantation embryo development," *Journal of Reproduction and Fertility*, vol. 93, no. 2, pp. 325–332, 1991.

[36] X.-M. Z.-Y. Luo, F. Yin, Y. Chen et al., "The effect of hyperglycemia on early mouse embryo development," *Life Science Research*, vol. 12, pp. 347–350, 2008.

[37] Z. Hong, *Study on relationship between reactive oxygen, p66~(shc) and development block of mouse embryos induced by high glucose*, Zhengzhou University, 2013.

[38] L. Zhang, Z.-S. Li, and N.-Z. Fang, "Glucose-induced ROS inhibits mouse early embryo development at late 2-cell stage in vitro," *Academic Journal of Second Military Medical University*, vol. 30, no. 8, pp. 888–891, 2009.

[39] K. D. Taylor and L. Pikó, "Expression of ribosomal protein genes in mouse oocytes and early embryos," *Molecular Reproduction and Development*, vol. 31, no. 3, pp. 182–188, 1992.

[40] M. Li-Li, *Epigenetics research of abnormal glucose metabolism in uterus*, Peking Union Medical College, 2011.

[41] C. E. H. Stewart and P. Rotwein, "Growth, differentiation, and survival: multiple physiological functions for insulin-like growth factors," *Physiological Reviews*, vol. 76, no. 4, pp. 1005–1026, 1996.

[42] V. Rouiller-Fabre, L. Lecerf, C. Gautier, J. M. Saez, and R. Habert, "Expression and effect of insulin-like growth factor I on rat fetal Leydig cell function and differentiation," *Endocrinology*, vol. 139, no. 6, pp. 2926–2934, 1998.

[43] L. P. Liu, Y. L. Ren, and R. Li, "Effects of p38 signal pathway on osteoblastic cell differentiation by Zuogui pill medicated serum in MC3T3-E1 cell," *Chinese Journal of Gerontology*, vol. 7, article 042, 2013.

[44] C.-Y. Hao, Y.-L. Ren, and J.-R. Zhao, "Effects of Zuogui pill medicated serum via ERK/samds dependent pathway on MC3T3-E1 cell gene expression," *Chinese Pharmacological Bulletin*, vol. 28, no. 6, pp. 872–876, 2012.

[45] Z.-B. X.-C. Gong and G.-Q. Jin, "The study of modulating effect of zuogui pill on rat thymocytes apoptosis and expression of Bcl-2 and Bax," *Chinese Journal of Gerontology*, vol. 30, pp. 3290–3292, 2010.

[46] X.-F. Sun, L. Luo, Q.-C. Sun et al., "Experimental study of zuogui pills in stimulation of mouse immature oocytes nuclear maturation in vitro," *Progress in Modern Biomedicine*, vol. 3, article 015, 2011.

Hindawi
Evidence-Based Complementary and Alternative Medicine
Volume 2018, Article ID 8294320, 8 pages
https://doi.org/10.1155/2018/8294320

Research Article

Gundelia tournefortii Antidiabetic Efficacy: Chemical Composition and GLUT4 Translocation

Sleman Kadan,[1,2] Yoel Sasson,[2] Bashar Saad,[1,3] and Hilal Zaid [1,3]

[1] *Qasemi Research Center, Al-Qasemi Academic College, P.O. Box 124, 30100 Baqa Al-Gharbiyye, Israel*
[2] *Casali Center for Applied Chemistry, Institute of Chemistry, The Hebrew University of Jerusalem, Givat Ram, 91904 Jerusalem, Israel*
[3] *Faculty of Sciences, Arab American University, P.O. Box 240, Jenin, State of Palestine*

Correspondence should be addressed to Hilal Zaid; hilal.zaid@gmail.com

Received 8 August 2017; Revised 27 November 2017; Accepted 1 March 2018; Published 26 April 2018

Academic Editor: Cecilia C. Maramba-Lazarte

In the present *in vitro* study, we tested the chemical composition, cytotoxicity and antidiabetic activity of two distinct extracts of wild Artichoke-like vegetable, *Gundelia tournefortii*: methanol and hexane. GC/MS phytochemical analysis of *G. tournefortii* methanol and hexane extracts revealed 39 compounds reported here for the first time in *G. tournefortii* out of the 45 detected compounds. Only Stigmasterol was present in both extracts. The efficacy of *G. tournefortii* extracts in enhancing glucose transporter 4 (GLUT4) translocation to the plasma membrane (PM) was tested in L6 muscle cells stably expressing myc-tagged GLUT4 (L6-GLUT4myc) using cell-ELISA test. Results obtained here indicate that methanol and hexane extracts were safe up to 250 μg/ml as measured with MTT and the LDH leakage assays. The methanol extract was the most efficient in GLUT4 translocation enhancement. It increased GLUT4 translocation at 63 μg/ml 1.5- and 2-fold relative to the control in the absence and presence of insulin, respectively. These findings indicate that *G. tournefortii* possesses antidiabetic activity in part by enhancing GLUT4 translocation to the PM in skeletal muscle.

1. Introduction

Plants produce a remarkably diverse array of thousands of secondary metabolites. In addition to their roles in the defense of plants against changing environmental conditions, they were reported to be beneficial in treating animals and human being diseases [1–4]. The phytochemicals, polysaccharides, flavonoids [5], terpenoids, tannins and steroids [6], and others, were reported to possess antidiabetic activity [2]. Metformin and resveratrol, two main antidiabetic drugs, were derived from medicinal plants [7].

Circulating glucose levels can be balanced through controlling glucose production and utilization or through increasing insulin secretion and effectiveness as well as through increasing energy expenditure or reduction of energy intake [8, 9]. The natural herbs for diabetes treatment focus on lowering blood sugar and minimizing the damaging effects of the disease. The action mechanism(s) of antidiabetic plants are usually insulin mimics, sensitizer, and secretagogues as well as inhibitors of intestinal carbohydrate digestion and absorption [2, 3, 10, 11].

Insulin sensitizers include plants that increase glucose uptake and disposal by muscle, fat, and hepatic cells and those that regulate hepatic glycogen metabolism. For instance, garlic *(Allium sativum)* and onion *(Allium cepa)* were reported to decrease blood glucose levels by normalizing liver glucose-6-phosphatase and hexokinase activity [12]. Black cumin *(Nigella sativa)* and cinnamon *(Cinnamomum officinalis)* were suggested to have insulin mimetic properties, through enhancing insulin signaling pathway independently of insulin [13, 14]. We had recently tested several medicinal plants extracts mechanisms in increasing glucose uptake and found that *Trigonella foenum-graecum*, *Urtica dioica*, *Atriplex halimus*, *Cinnamomum officianalis*, and *Ocimum basilicum* increase glucose disposal by enhancing the glucose transporter 4 (GLUT4) translocation to the plasma membrane [9, 10].

Glucose uptake into skeletal muscle is mediated by the facilitative glucose transporter-4 (GLUT4), a membrane protein that continuously recycles between intracellular vessels and the plasma membrane (PM). Insulin primarily enhances the rate of GLUT4 exocytosis towards and fusion with the PM, a process termed GLUT4 translocation that results in a gain in PM GLUT4 [8].

Wild Artichoke-like vegetable, *Gundelia tournefortii*, is one of the traditional used antidiabetic herbs. *G. tournefortii* is an edible spiny, thistle-like plant native to the Middle East and other areas of Western Asia [15]. It is considered as one of the highest cultural importance valuable eatable wild species in Palestine [16]. In the Greco-Arab medicine, *G. tournefortii* has been used for different pathological conditions including inflammation and antibiotic resistant inhibitor [17], hepatoprotective and blood purifier [18], and hypolipidemic and antioxidant agent [15], as well as antidiabetes herb [19, 20]. *G. tournefortii* antidiabetic activity was evaluated in dexamethasone induced diabetic mice. Oral administration of *G. tournefortii* to the dexamethasone induced diabetic mice led to a significant decrease in serum glucose levels (as well as triglyceride and cholesterol) [21].

The aim of the present study was to evaluate the chemical composition of *G. tournefortii* extracts by GC/MS and determine if GLUT4 translocation plays a role in its antidiabetic effect.

2. Materials and Methods

2.1. Materials. All tissue culture reagents including fetal bovine serum and standard culture medium α-MEM (modified Eagle's medium) were purchased from Biological Industries (Beit Haemek, Israel). Horseradish peroxidase (HRP)-conjugated goat anti-rabbit antibodies were obtained from Promega (Madison, WI, USA). Polyclonal anti-myc (A-14) and other standard chemicals were purchased from Sigma.

2.2. Plant Extract Preparation. *Gundelia tournefortii* (aerial parts) were collected from the Galil area in Israel in March 2016. Forty grams of the air-dried aerial parts of *G. tournefortii* were powdered and packed in an Erlenmeyer. The Erlenmeyers were then sonicated for 2 hours at 50°C and left in dark glass bottles for 24 h for complete extraction hours to give a dark green extract. The hexane extract was filtered and evaporated to dryness under pressure at 50°C and dissolved in DMSO for *in vitro* studies. Rotary vacuum evaporator was used to concentrate the methanol extract. The yield of the extracts was found to be 3.2% and 1.8% for the methanol and hexane extracts, respectively. The stock extracts were kept at −20°C in airtight glass container.

2.3. Silylation Derivatization. One milliliter of each extract was transferred to a 2 mL glass vial, and the solvents were evaporated under a stream of nitrogen at room temperature. A 150 μL of *N,O*-Bis(trimethylsilyl)trifluoroacetamide (BSTFA) containing 1% trimethylchlorosilane reagent used for GC silylation derivatization (>99%, Sigma-Aldrich) was added to each dry *Gundelia tournefortii* crude extract followed by heating up to 70°C for 20 minutes [10, 22]. One microliter of each derivatized sample was injected into the gas chromatograph coupled with mass selective detector (GC/MS).

2.4. Gas Chromatography-Mass Spectrometry Analysis. Solutions of *Gundelia tournefortii* from methanol and hexane extracts were ran and identified using HP5890 Series II GC equipped with a Hewlett-Packard MS Engine (HP5989A) single quadrupole MS, HP7673 autosampler, HP MS-DOS Chemstation, and HP-5MS capillary column (0.25 μm × 15 m × 0.25 mm) with Triple-Axis Detector. The GC was operated on an Agilent J&W GC column HP-5 column (30 m × 0.32 mm, i.d. with 0.25 μm film thickness). The injection port temperature was 180°C and the initial temperature was 40°C for 6 min, followed by gradient 20°C/min until 140°C and then gradient 10°C/min until 200°C, and hold on to this temperature for 3 min. The MS parameters were 180°C for the source temperature and 280°C for the transfer line, positive ion monitoring, and EI-MS (70 eV)[10].

2.5. Identification of Components. The percentages of the phytochemical components were calculated from the GC peak areas by normalization. Library searches were carried out using the Mass Spectral Library of the National Institute of Standards and Technology (NIST, Gaithersburg, USA) or with mass spectra extracted from the literature [10].

2.6. Cell Culture. Rat L6 muscle cell lines genetically modified to express myc-tagged GLUT4 (L6-GLUT4myc) stably were maintained in myoblast monolayer culture [7]. Cells were grown under 95% air and 5% CO_2 atmosphere in α-MEM accompanied with 10% fetal bovine serum (FBS), 0.1 mg/ml streptomycin, and 0.1 mU/ml penicillin.

2.7. MTT Assay. MTT (3-[4,5-dimethylthiazol-2-yl]-2,5-diphenyltetrazoliumbromide) is a water soluble tetrazolium salt. Once delivered to the mitochondria, it is converted to an insoluble purple formazan by succinate dehydrogenase. As such, the formazan product accumulates only in healthy cells [23]. The assay was optimized for the L6-GLUT4myc cell line as described previously [10]. Cells (2×10^4/well) were plated in 200 μl of medium/well in 96-well plates and were allowed to attach to the plate for 24 h. The cells were incubated then with the *Gundelia tournefortii* extracts (0-1 mg/mL) for additional 24 h. The cell medium was then replaced with 100 μl fresh medium/well containing 0.5 mg/mL MTT and cultivated for 4 h darkened in the cells incubator. The supernatant was removed and 100 μl isopropanol/HCl (2% HCl (0.1 M) in isopropanol) was added per well. The absorbance at 620 nm was measured with microtiter plate reader (Anthos). Two wells per plate without cells served as blank. All experiments were repeated three times in triplicate. The effect of the plants extracts on cell viability was expressed using the following formula:

$$\text{Percent viability} = \left(\frac{\text{A620 nm of plant extract treated sample}}{\text{A620 nm of none treated sample}}\right) * 100. \quad (1)$$

2.8. Lactate Dehydrogenase Assay (LDH). LDH, a cytoplasmic enzyme, release is the consequence of cell membrane breach. The activity of LDH released to the cell culture medium was monitored following the formation of formazan at 492 nm according to the manufacture kit (Promega) and was described earlier [10]. Cell membrane breach was defined as the ratio of LDH activity in the cell culture medium of treated cells relative to the LDH activity released in the control cells. L6-GLUT4myc cells (2×10^4/well) were plated in 200 μl of medium/well in 96-well plates and were allowed to attach to the plate for 24 h. The cells were incubated then with the *Gundelia tournefortii* extracts (0-1 mg/mL) for additional 24 h and the LDH activity in the medium was then measured. 50 μl from each well was transferred to a new 96-well plate and the enzyme reaction was carried out according to the manufacture kit (CytoTox 96, Promega). The experiments were performed in triplicate. The following formula effect was used to calculate the plant extracts effect on cell viability:

$$\text{Percent viability} = \left(\frac{\text{A492 nm of plant extract treated sample}}{\text{A492 nm of control}}\right) * 100. \quad (2)$$

2.9. Determination of Surface GLUT4myc. Surface myc-tagged GLUT4 was measured in intact cells as described previously [10, 24] using anti-myc antibody followed by horseradish peroxidase conjugated secondary antibody. L6-GLUT4myc cells grown in 24-well plates for 24 h followed by addition of the plant extracts for 20 h and serum-starvation for 3 h (including the plant extracts) were treated with or without 1 μM insulin for 20 min. The cells were washed twice with ice-cold PBS and immediately fixed with 3% paraformaldehyde for 15 min, blocked with 3% (v/v) goat serum for 10 min, incubated with polyclonal anti-*myc* antibody (1 : 200) for 1 h at 4°C, washed 10 times with PBS and incubated with goat anti-rabbit-secondary antibody conjugated with horseradish peroxidase (1 : 1000) for 1 h at 4°C, and then washed 10 times with PBS at room temperature. One milliliter of *o*-phenylenediamine dihydrochloride reagent was added to each well and incubated in the dark at room temperature for 20–30 min. 0.5 ml of 3 M HCl was added to each well to stop the reaction. 100 μl from each well was transferred to 96 well plates and the absorbance was measured at 492 nm. Background absorbance obtained from 3 wells in each 24-well plate untreated with anti-*myc* antibody was subtracted from all values.

3. Results and Discussion

Glucose transporter 4 (GLUT4) continuously recycles between intracellular stores (vesicles) and the plasma membrane (PM). Insulin shifts GLUT4 translocation towards the PM while glucagon shifts GLUT4 translocation towards the intracellular stores [8, 25, 26]. Several traditional used antidiabetic medicinal plants were reported to exert their hypoglycemic effects through increasing glucose transporter

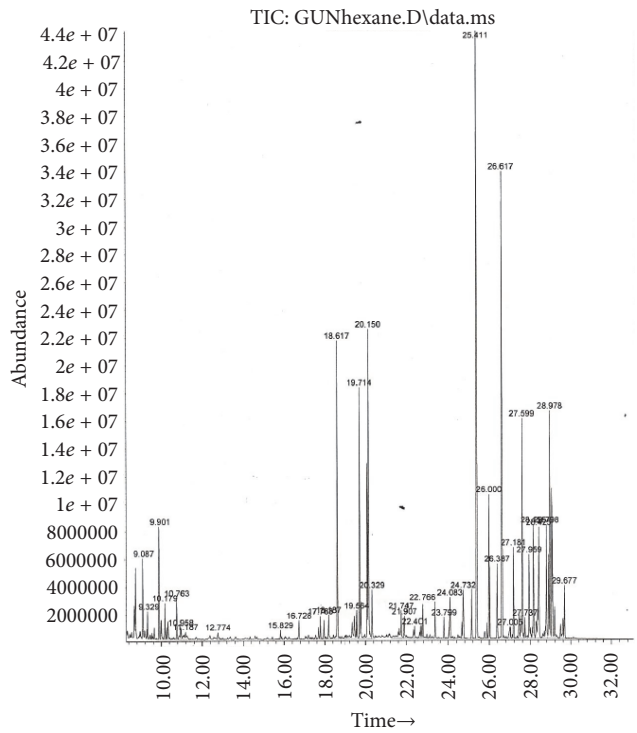

Figure 1: Total ion chromatogram (TIC) of *G. tournefortii* hexane extract.

(GLUT) translocation to the plasma membrane in muscle, liver, and hepatic tissue [25, 26]. Although, *G. tournefortii* is recommended by herbal and integrative practitioners for the treatment of diabetes [19, 20] the action mechanism whereby *G. tournefortii* exerts its hypoglycemic effects is still unknown. Therefore, the present study was conducted to evaluate the role of GLUT4 translocation in the observed antidiabetic *G. tournefortii* effects. Two *G. tournefortii* extracts (methanol and hexane) were prepared and their effects on GLUT4 translocation were measured in L6 skeletal muscle cell line, in the present and absence of insulin. Moreover, the chemical composition of *G. tournefortii* extracts was analyzed via GC/MS, highlighting potential antidiabetic compounds in *G. tournefortii* extracts.

3.1. G. tournefortii Chemical Composition. Resolution, selectivity, and elution time were obtained on the capillary GC HP-5 column. We noticed sharp peaks culminated. The derivatization of the secondary metabolites of *G. tournefortii* seemed to be helpful due to presence of polar phytochemicals. Typically, upon derivatization, volatile and stable compounds are generated with amenable properties to GC/MS analysis. Figures 1 and 2 show the total ion chromatograms (TICs) of the hexane and methanol extracts.

Phytochemical screening using GC/MS in the electron impact mode (EI) revealed 46 compounds in *G. tournefortii* methanolic (Table 1) and hexane extracts (Table 2), including sterols, esters, phenolic, saturated and unsaturated fatty acids, and aromatic compounds. 39 out of the 45 detected compounds are reported for the first time in *G. tournefortii*

Table 1: Phytochemicals of *Gundelia tournefortii* from methanol extract verified by GC/MS.

#	Compound name	RT (minute)	Peak area%	% of similarity*
(1)	Aminoethanol	9.87	0.93%	91
(2)	Glycerol	9.99	3.59%	76
(3)	L-Isoleucine	10.255	0.45%	91
(4)	Succinic acid	10.6	2.2%	72
(5)	Glyceric acid	10.75	0.68%	91
(6)	Fumaric acid	11.05	0.46%	86
(7)	DL-serine	11.15	0.95%	94
(8)	2-Piperidine carboxylic acid	11.198	0.58%	94
(9)	Threonine	11.46	0.52%	90
(10)	Malic acid	12.79	7.58%	91
(11)	Asparagine	14.94	6.15%	99
(12)	Xylitol	15.05	0.28%	83
(13)	Arabitol	15.32	1.12%	94
(14)	D-Ribofuranose	16.23	3.96%	74
(15)	D-Galactofuranose	16.625	0.45%	80
(16)	Lyxose	17.1	6.88%	80
(17)	Sorbitol	17.42	1.36%	91
(18)	Inositol	17.7	5.09%	93
(19)	Glucopyranose	18.00	5.01%	89
(20)	D-Gluconic acid	18.15	2.61%	70
(21)	Palmitic acid	18.61	0.95%	70
(22)	Linoleic acid	20.069	0.66%	91
(23)	L-Tryptophan	20.135	1.22%	87
(24)	Methyl α-D-glucopyranoside	23.23	7.04%	72
(25)	D-Xylonic acid	24.17	0.33%	83
(26)	*Stigmasterol*	27.58	0.24%	99

* % of similarity relative to the reference library in the GC/MS.

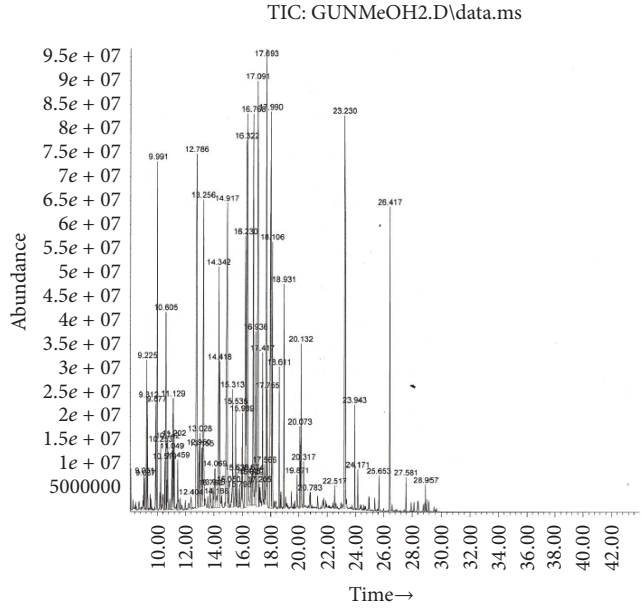

Figure 2: Total ion chromatogram (TIC) of *G. tournefortii* methanol extract.

Table 2: Phytochemicals of *Gundelia tournefortii* from hexane extract verified by GC/MS.

Number	Component name	RT (minutes)	Peak area%	% of similarity*
(1)	Propanoic acid	12.77	0.34%	64
(2)	Cetanol	17.78	1.48%	94
(3)	Ethyl icosanoate	18.18	0.58%	87
(4)	Tetradecanoic acid	18.613	5.06%	64
(5)	Octadecan-1-ol	19.556	2.2%	97
(6)	(E)-3,7,11,15-Tetramethylhexadec-2-en-1-ol	19.714	4.68%	86
(7)	α-Linolenic acid	20.152	9.38%	99
(8)	Stearic acid	20.317	0.95%	80
(9)	Oleamide	21.74	1.37%	94
(10)	Eicosanoic acid	21.906	0.71%	72
(11)	5-Octadecene	22.402	0.51%	87
(12)	Di-n-Octyl Phtalate	22.76	1.99%	72
(13)	Tetracosan-1-ol	24.09	1.09%	90
(14)	Hexacosan-1-ol	25.414	15.07%	81
(15)	Heptacosane	26.39	1.05%	91
(16)	Octacosan-1-ol	26.623	9.15%	97
(17)	*Stigmasterol*	27.599	4.73%	96
(18)	β-sitosterol	27.95	1.91%	66
(19)	12-Oleanen-3-yl acetate	28.791	2.69%	94
(20)	Hop-22(29)-en-3beta-ol	29.67	1.97%	80

*% of similarity relative to the reference library in the GC/MS.

(Tables 1 and 2). Six components, namely, Stigmasterol (PubChem CID: 5280794), β-Sitosterol (PubChem CID: 222284), Palmitic acid, Linoleic acid, α-Linolenic acid, and Stearic acid were reported elsewhere [19]. Only one mutual compound, Stigmasterol, was mutual in the two extracts (Table 1). The GC/MS analysis revealed seven major components in each extract of the hexane and methanol (Figures 3 and 4).

3.2. G. tournefortii Extracts Toxicity. MTT and LDH leakage assays were used to evaluate the nontoxic concentrations of the methanol and hexane *G. tournefortii* extracts. The plant extracts toxicity was tested *in vitro* in L6-GLUT4myc cells. Cells were seeded in 96 well plates and were subjected to increasing concentrations of the extracts (0-1 mg/ml) for 24 hours. Extracts concentrations that led to less than 5% cell death were considered safe. Hexane (Figure 5) and methanol (Figure 6) extracts were found to be safe up to 250 μg/ml. The efficacy studies were performed at concentrations less than the safe concentration for each extract.

3.3. Effects of G. tournefortii Extracts on GLUT4 Translocation. Skeletal muscle and liver are the primary tissues responsible for dietary glucose uptake and disposal. In muscle and adipose tissues, insulin promotes the exocytic traffic of intracellular GLUT4 vessels towards the plasma membrane to elicit a rapid increase in glucose uptake [8, 25, 26]. In insulin resistance and diabetes type II, insulin fails to promote GLUT4 translocation to the PM. Some of the antidiabetic synthetic drugs and medicinal plant-based products bypass the insulin resistance by increasing GLUT4 translocation in insulin dependent or independent pathway [4].

The involvement of glucose transporter (GLUT4) in the observed antidiabetic effects of *G. tournefortii* extracts was evaluated here by applying the GLUT4 translocation assay. Insulin increases GLUT4 translocation to the surface of myoblasts, where it mediates the increase in glucose uptake [8, 26]. L6 skeletal muscle cell lines expressing myc epitope at the exofacial loop of the glucose transporter 4 (GLUT4), named L6-GLUT4myc, were used as a model to follow GLUT4 translocation to the plasma membrane [8]. The extracts were added to the L6-GLUT4myc cells in the presence or absence of insulin and GLUT4myc translocation to the plasma membrane was assessed as described in Methods. Results obtained indicate that, in muscle L6-GLUT4myc cells, insulin-independent (basal) as well as insulin dependent GLUT4 translocation to the PM is significantly increased in response to *G. tournefortii.* extracts (especially the methanol extract). Insulin enhanced GLUT4 translocation about 150% (Figures 7 and 8) as reported elsewhere [8].

The hexane extract was found to have the lowest effects on GLUT4 translocation, and only 16% increase of GLUT4 translocation was obtained at 32 μg/ml and 63 μg/ml *G. tournefortii* hexane extracts in the absence of insulin. A similar effect was appreciated in the presence of insulin (Figure 7). Methanol extract (63 μg/ml) increased GLUT4 translocation to the PM by about 1.5 and 2 times in the absence and presence of insulin, respectively (Figure 8).

One of the detected compounds in *G. tournefortii* was palmitic acid. Intestinally, palmitic acid was recently reported

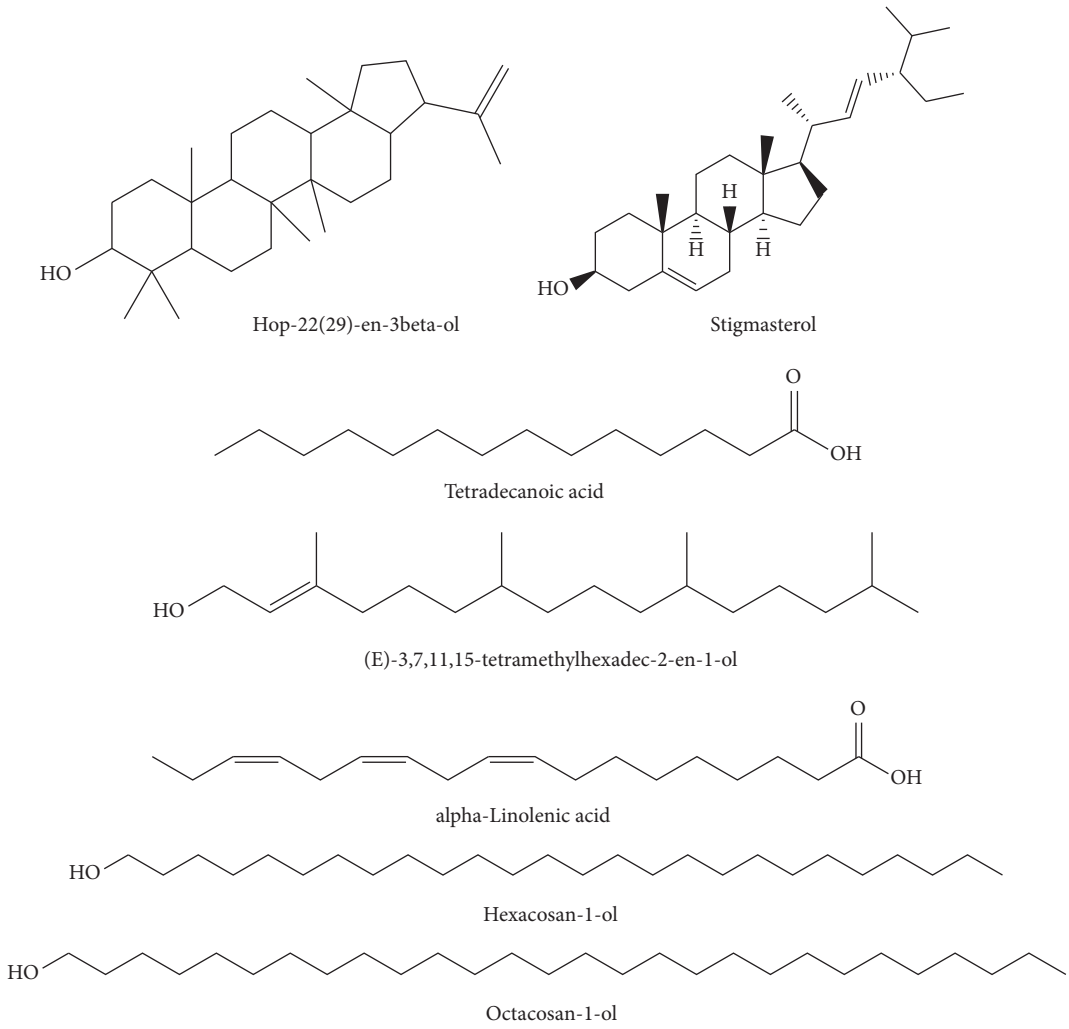

Figure 3: Chemical structure of major components in *G. tournefortii* hexane extract.

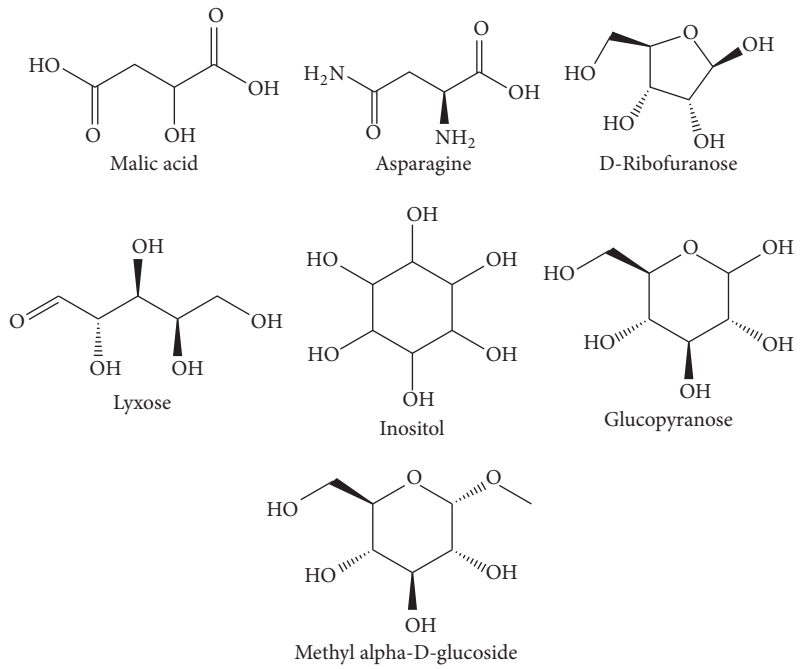

Figure 4: Chemical structure of major components in *G. tournefortii* methanol extract.

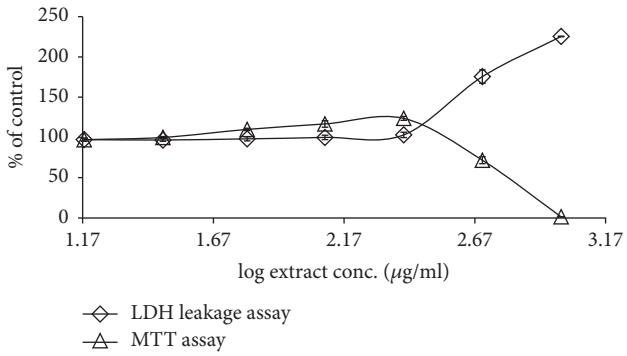

Figure 5: Effect of *G. tournefortii* hexane extract on cell viability by MTT and LDH leakage assays. L6-GLUT4myc cells (20,000 cell/well) exposed to methanol extract for 20 h. Values given represent means ± SEM (% of untreated control cells) of three independent experiments carried out in triplicate.

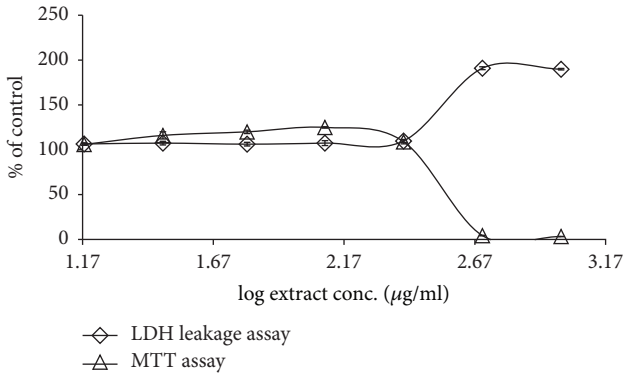

Figure 6: Effect of *G. tournefortii* methanol extract on cell viability by MTT and LDH leakage assays. L6-GLUT4myc cells (20,000 cell/well) exposed to hexane extract for 20 h. Values given represent means ± SEM (relative to untreated control cells) of three independent experiments carried out in triplicate.

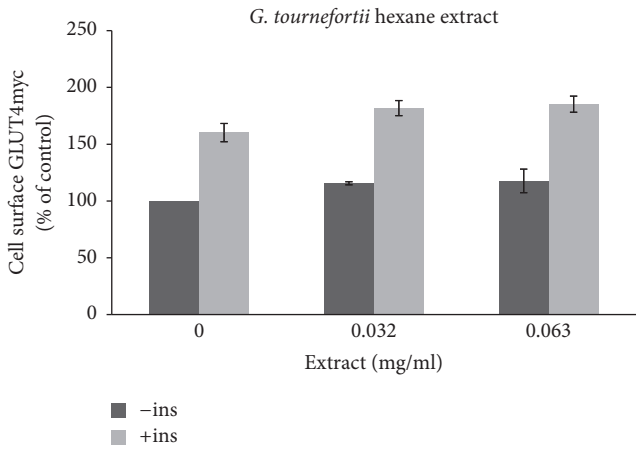

Figure 7: GLUT4 translocation to the plasma membrane. For the evaluation of the GLUT4 L6-GLUT4myc, cells (150,000 cell/well) were exposed to hexane extract for 20 h. Serum depleted cells were treated without (−) or with (+) 1 μM insulin for 20 min at 37°C and surface *myc*-tagged GLUT4 density was quantified using the antibody coupled colorimetric assay. Values given represent means ± SEM (relative to untreated control cells) of three independent experiments carried out in triplicate.

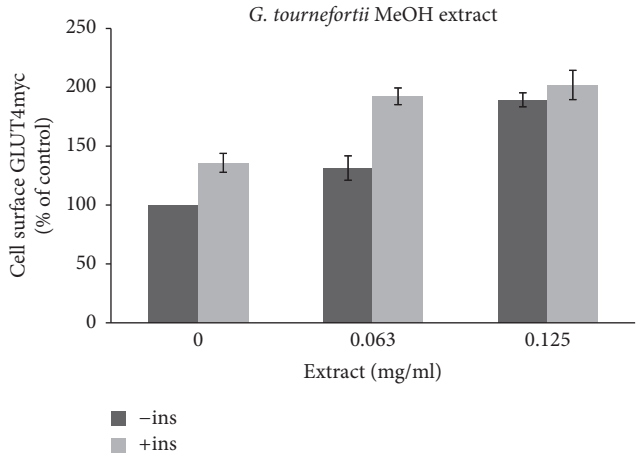

Figure 8: GLUT4 translocation to the plasma membrane. For the evaluation of the GLUT4 L6-GLUT4myc, cells (150,000 cell/well) were exposed to MeOH extract for 20 h. Serum depleted cells were treated without (−) or with (+) 1 μM insulin for 20 min at 37°C and surface *myc*-tagged GLUT4 density was quantified using the antibody coupled colorimetric assay. Values given represent means ± SEM (relative to untreated control cells) of three independent experiments carried out in triplicate.

by our group to be found in three deferent *Ocimum basilicum* L. extracts (methanol, hexane and dichloromethane). Ocimum *basilicum* was reported as antidiabetic herb and palmitic acid was suggested to take an essential role in the plant extracts antidiabetic activity [10]. Concomitant with our previous reported results, palmitic acid was detected only in the MeOH extract of *G. tournefortii*, that enhanced GLUT4 translocation much more than the hexane extract.

4. Conclusion

The extent of increase in insulin-stimulated GLUT4 translocation was additive to that of basal GLUT4 translocation in *G. tournefortii*-exposed cells, suggesting a possible synergistic effect between *G. tournefortii* active ingredients and insulin. Alternately, *G. tournefortii* active ingredients might activate GLUT4 translocation in noninsulin dependent pathway, such as AMPK pathway. It is possible then that *G. tournefortii* active ingredients might possess "insulin-like" or "insulin-sensitizing" activity/compounds. It is essential to dissect *G. tournefortii* active compounds in order to identify its cellular molecular target and point out its specific antidiabetic mechanism and cellular pathway(s).

Disclosure

The abstract was presented in the 9th World Congress on Pharmacology in Paris, France (Sep. 5, 2017).

Conflicts of Interest

The authors declare no conflicts of interest. The mentioned received funding did not lead to any conflicts of interest regarding the publication of this manuscript.

Acknowledgments

The authors would like to acknowledge Al-Qasemi and AAUJ Research Foundations and CA15129 COST Action for providing their financial support. Sleman Kadan highly appreciates the "Ministry of Science Technology and Space" for the scholarship.

References

[1] B. Saad, H. Zaid, S. Shanak, and S. Kadan, *Anti-Diabetes and Anti-Obesity Medicinal Plants and Phytochemicals: Safety, Efficacy, and Action Mechanisms*, Springer International Publishing AG, 2017, Chapter 2.

[2] H. Zaid, A. A. Mahdi, A. K. Tamrakar, B. Saad, M. S. Razzaque, and A. Dasgupta, "Natural active ingredients for diabetes and metabolism disorders treatment," *Evidence-Based Complementary and Alternative Medicine*, vol. 2016, Article ID 2965214, 2 pages, 2016.

[3] H. Zaid, B. Saad, A. A. Mahdi, A. K. Tamrakar, P. S. Haddad, and F. U. Afifi, "Medicinal plants and natural active compounds for diabetes and/or obesity treatment," *Evidence-Based Complementary and Alternative Medicine*, vol. 2015, Article ID 469762, 2 pages, 2015.

[4] H. Zaid, M. Silbermann, E. Ben-Arye, and B. Saad, "Greco-Arab and Islamic herbal-derived anticancer modalities: from tradition to molecular mechanisms," *Evidence-Based Complementary and Alternative Medicine*, vol. 2012, Article ID 349040, 13 pages, 2012.

[5] R. Testa, A. R. Bonfigli, S. Genovese, V. De Nigris, and A. Ceriello, "The possible role of flavonoids in the prevention of diabetic complications," *Nutrients*, vol. 8, no. 5, Article ID 310, 2016.

[6] E. A. Omara, A. Kam, A. Alqahtania et al., "Herbal medicines and nutraceuticals for diabetic vascular complications: mechanisms of action and bioactive phytochemicals," *Current Pharmaceutical Design*, vol. 16, no. 34, pp. 3776–3807, 2010.

[7] B. Saad, H. Zaid, S. Shanak, and S. Kadan, *Anti-diabetes and Anti-obesity Medicinal Plants and Phytochemicals: Safety, Efficacy, and Action Mechanisms*, Springer International Publishing AG, 2017, Chapters 6 and 7.

[8] H. Zaid, C. N. Antonescu, V. K. Randhawa, and A. Klip, "Insulin action on glucose transporters through molecular switches, tracks and tethers," *Biochemical Journal*, vol. 413, no. 2, pp. 201–215, 2008.

[9] S. Kadan, B. Saad, Y. Sasson, and H. Zaid, "In vitro evaluations of cytotoxicity of eight antidiabetic medicinal plants and their effect on GLUT4 translocation," *Evidence-Based Complementary and Alternative Medicine*, vol. 2013, Article ID 549345, 9 pages, 2013.

[10] S. Kadan, B. Saad, Y. Sasson, and H. Zaid, "In vitro evaluation of anti-diabetic activity and cytotoxicity of chemically analysed Ocimum basilicum extracts," *Food Chemistry*, vol. 196, pp. 1066–1074, 2016.

[11] J. L. Ríos, F. Francini, and G. R. Schinella, "Natural products for the treatment of type 2 diabetes mellitus," *Planta Medica*, vol. 81, no. 12-13, pp. 975–994, 2015.

[12] C. G. Sheela, K. Kumud, and K. T. Augusti, "Anti-diabetic effects of onion and garlic sulfoxide amino acids in rats," *Planta Medica*, vol. 61, no. 4, pp. 356-357, 1995.

[13] A. Benhaddou-Andaloussi, L. C. Martineau, D. Vallerand et al., "Multiple molecular targets underlie the antidiabetic effect of Nigella sativa seed extract in skeletal muscle, adipocyte and liver cells," *Diabetes, Obesity and Metabolism*, vol. 12, no. 2, pp. 148–157, 2010.

[14] H. Zaid and B. Saad, "State of the art of diabetes treatment in greco-arab and islamic medicine," in *Bioactive Food as Dietary Interventions for Diabetes*, R. R. Watson and V. R. Preedy, Eds., pp. 327–337, Academic Press, San Diego, CA, USA, 2013.

[15] F. Hajizadeh-Sharafabad, M. Alizadeh, M. H. S. Mohammadzadeh, S. Alizadeh-Salteh, and S. Kheirouri, "Effect of Gundelia tournefortii L. extract on lipid profile and TAC in patients with coronary artery disease: a double-blind randomized placebo controlled clinical trial," *Journal of Herbal Medicine*, vol. 6, no. 2, pp. 59–66, 2016.

[16] M. S. Ali-Shtayeh, R. M. Jamous, J. H. Al-Shafie' et al., "Traditional knowledge of wild edible plants used in Palestine (Northern West Bank): a comparative study," *Journal of Ethnobiology and Ethnomedicine*, vol. 4, Article ID 13, 2008.

[17] R. M. Darwish and T. A. Aburjai, "Effect of ethnomedicinal plants used in folklore medicine in Jordan as antibiotic resistant inhibitors on Escherichia coli," *BMC Complementary and Alternative Medicine*, vol. 10, Article ID 9, 2010.

[18] A. Jamshidzadeh, F. Fereidooni, Z. Salehi, and H. Niknahad, "Hepatoprotective activity of Gundelia tourenfortii," *Journal of Ethnopharmacology*, vol. 101, no. 1-3, pp. 233–237, 2005.

[19] M. A. Samani, M.-K. Rafieian, and N. Azimi, "Gundelia: a systematic review of medicinal and molecular perspective," *Pakistan Journal of Biological Sciences*, vol. 16, no. 21, pp. 1238–1247, 2013.

[20] A. Subramoniam, *Plants with Anti-Diabetes Mellitus Properties*, CRC Press, 2016.

[21] O. H. Azeez and A. E. Kheder, "Effect of Gundelia tournefortii on some biochemical parameters in dexamethasone-induced hyperglycemic and hyperlipidemic mice," *Iraqi Journal of Veterinary Sciences*, vol. 26, no. 2, pp. 73–79, 2012.

[22] D. L. Stalling, C. W. Gehrke, and R. W. Zumwalt, "A new silylation reagent for amino acids bis (trimethylsilyl)trifluoroacetamide (BSTFA)," *Biochemical and Biophysical Research Communications*, vol. 31, no. 4, pp. 616–622, 1968.

[23] T. Mosmann, "Rapid colorimetric assay for cellular growth and survival: application to proliferation and cytotoxicity assays," *Journal of Immunological Methods*, vol. 65, no. 1-2, pp. 55–63, 1983.

[24] H. Zaid, I. Talior-Volodarsky, C. Antonescu, Z. Liu, and A. Klip, "GAPDH binds GLUT4 reciprocally to hexokinase-II and regulates glucose transport activity," *Biochemical Journal*, vol. 419, no. 2, pp. 475–484, 2009.

[25] J. R. Zierath, L. He, A. Gumà, E. O. Wahlström, A. Klip, and H. Wallberg-Henriksson, "Insulin action on glucose transport and plasma membrane GLUT4 content in skeletal muscle from patients with NIDDM," *Diabetologia*, vol. 39, no. 10, pp. 1180–1189, 1996.

[26] C. Osorio-Fuentealba and A. Klip, "Dissecting signalling by individual Akt/PKB isoforms, three steps at once," *Biochemical Journal*, vol. 470, no. 2, pp. e13–e16, 2015.

Hindawi
Evidence-Based Complementary and Alternative Medicine
Volume 2018, Article ID 5101656, 10 pages
https://doi.org/10.1155/2018/5101656

Research Article

Potential Hypoglycaemic and Antiobesity Effects of *Senna italica* Leaf Acetone Extract

R. O. Malematja, V. P. Bagla, I. Njanje, V. Mbazima, K. W. Poopedi, L. Mampuru, and M. P. Mokgotho

Department of Biochemistry, Microbiology and Biotechnology, Faculty of Science and Agriculture, University of Limpopo, Turfloop Campus, Private Bag X1106, Sovenga, Limpopo 0727, South Africa

Correspondence should be addressed to R. O. Malematja; 201531170@keyaka.ul.ac.za

Received 20 September 2017; Accepted 22 January 2018; Published 19 February 2018

Academic Editor: Hilal Zaid

Background. Type II diabetes is on the rise while obesity is one of the strongest risk factors of type II diabetes. The search for a drug for type II that can equally mitigate obesity related complication is desired. *Methods*. The acetone leaf extract of *Senna italica* was evaluated for its cytotoxic, antiglycation, and lipolytic effect, glucose uptake, and GLUT4 translocation and expression using published methods, while that for adipogenesis and protein expression levels of obesity related adipokines was assessed using adipogenesis assay and mouse adipokine proteome profiler kit, respectively. The possible mechanism of glucose uptake was assessed through the inhibition of PI3K pathway. *Results*. The extract had no adverse effect on 3T3-L1 cell viability (CC50 > 1000 μg/ml). High antiglycation effect was attained at 10 mg/ml, while at 25–200 μg/ml it showed no significant increase in adipogenesis and lipolysis. The extract at 100 μg/ml was shown to decrease the expression levels of various adipokines and minimal glucose uptake at 50–100 μg/ml with a nonsignificant antagonistic effect when used in combination with insulin. GLUT4 translocation and expression were attained at 50–100 μg/ml with an increase in GLUT4 expression when in combination with insulin. *Conclusion*. The acetone leaf extract of *S. italica* stimulates glucose uptake through the PI3K-dependent pathway and can serve as a source of therapeutic agent for the downregulation of obesity-associated adipokines in obesity and antiglycation agents.

1. Introduction

Diabetes mellitus (DM) is a group of metabolic disorders characterised by a hyperglycaemic condition resulting from defects in insulin secretion, insulin action, or both [1]. The condition occurs in three forms, namely, types I and II and gestational diabetes. Type II diabetes is on the rise as a global health problem. Several pathogenic processes are involved in the development of diabetes. These range from autoimmune destruction of the β-cells of the pancreas with consequent insulin deficiency, to abnormalities that result in resistance to insulin action in major target organs such as the liver, muscle, and adipose tissue [2, 3].

Obesity on the other hand is associated with type II diabetes, due to its link with induced insulin resistance [4]. The incidence of insulin resistance is on the rise worldwide, hand-in-hand with the rise in obesity [5]. However, the relationship between obesity and insulin resistance is not completely understood. Diabetes is associated with serious long-term complications which can lead to chronic morbidities and mortality [6]. A nonenzymatic process known as glycation on the other hand becomes accelerated as a result of persistent elevated plasma glucose levels which occur in diabetic patients.

The use of natural medicines appears to offer better means of managing diseases at lower cost [7, 8]. *Senna italica*, with synonyms *Cassia italica* and *Acacia obovata* belongs to the family of Fabaceae. *Senna* species have been of extreme interest in phytochemical and pharmacological research due to their excellent medicinal values. They are well known in folk medicine for their laxative and purgative effect. Besides, they have been found to exhibit anti-inflammatory, antioxidant, hypoglycemic, antiplasmodial, larvicidal, antimutagenic, and anticancer activities [9]. Furthermore, antioxidant constituents in plants were shown to play a critical role in the management of diabetes mellitus [10]. This study was

therefore aimed at evaluating the potential effect of *S. italica* on GLUT4 translocation, expression, and adipogenesis in 3T3-L1 preadipocyte cells.

2. Materials and Methods

2.1. Plant Collection and Preparation. The leaves of *S. italica* were collected from Zebediela region, Limpopo Province, South Africa. The plant material with Voucher specimen number UNIN11129 is deposited at the Larry Leach Herbarium of the University of Limpopo. Dried plant material was ground into a fine powder using a commercial electric blender and stored in air-tight bottles. Twenty grams of leaf material was extracted with 200 ml acetone (Sigma-Aldrich, Germany). The mixture was shaken overnight at room temperature using a Series 25 shaking incubator machine (New Brunswick Scientific Co. Inc., USA) set at 200 rpm. The extraction procedure was repeated three times in order to extract as much components as possible. The extract was filtered using Whatman no. 1 filter paper and dried under a stream of cold air. The dried extract material was stored in preweighed vials for further use.

2.2. Determination of Anti-Glycation Activity. Antiglycation activity of *S. italica* acetone leaf extract was determined using bovine serum albumin (BSA) assay according to [11] with minor modifications. Briefly, BSA (1 mg/ml) was incubated with fructose (500 mM) in phosphate buffer (PB) containing 0.02% of sodium azide at pH 7.4 for 30 days at 37°C. The incubation was conducted in the presence and absence of the plant extract (1.25–10 mg/ml). Incubations without plant extract served as a negative control and arbutin was used as a standard inhibitor. Corresponding blanks were prepared in the absence of fructose. The reaction was terminated by adding 10 μl of 100% trichloroacetic acid (TCA) and centrifuged (13,000 rpm) at 4°C for 4 min. The supernatant was then discarded and the pellet was redissolved in 500 μl of alkaline phosphate buffer saline (PBS) (Thermo-Fisher Scientific, USA) at pH 10. Fluorescence was measured using Glomax Microtiter Plate Reader (Promega, USA).

2.3. Cytotoxicity Assay. The effect of *S. italica* acetone leaf extract on viability of 3T3-L1 preadipocyte cells was evaluated using the 3-(4,5-dimethylthiazol-2-yl)-2,5-diphenyltetrazolium bromide (MTT) assay [12]. The cells were plated at a density of 5×10^3 cells/well in Dulbecco's minimum-eagle's medium (DMEM) (Thermo-Fisher Scientific, USA) supplemented with 10% foetal bovine serum, FBS (Thermo-Fisher Scientific, USA). The plated cells were treated with various concentrations (25–800 μg/ml) of *S. italica* acetone leaf extract in 96-well microtiter plates (Whitehead Scientific, RSA) and incubated at 37°C in a humidified incubator (5% CO_2) for 24 and 48 h. Thereafter, the treatment media was removed. Two mg/ml of MTT (Sigma-Aldrich, Germany) solution was added to each well and incubated for 4 h. The MTT solution was removed from the wells and 100 μl of dimethyl sulfoxide (DMSO) was added to each well and agitated to dissolve the formazan deposit. The absorbance was recorded using a Glomax Microtiter Plate Reader (Promega, USA) at 560 nm.

2.4. Differentiation of 3T3-L1 Preadipocytes. 3T3-L1 preadipocytes were differentiated as described by [13]. The cells were treated with adipocyte differentiation media containing 10% FBS (Thermo-Fisher Scientific), 1 μM dexamethasone (DEX) (Sigma-Aldrich, Germany), 0.5 mM 3-isobutyl-1-methylxanthine (Sigma-Aldrich, Germany), and 1 μg/ml insulin (Sigma-Aldrich, Germany) for 3 days. Thereafter, the differentiation media was substituted with adipocyte maintenance media (DMEM, 10% FBS, and 1 μg/ml insulin) for a further 2 days. On day 5 the adipocyte maintenance medium was substituted with DMEM containing 10% FBS and cells were cultured until day 8. On day 8 the cells were fully differentiated to mature adipocytes.

2.5. Lipolysis Assay. Cells were seeded in a 96-well plate (20,000 cells/ml) and differentiated. After differentiation, the cells were washed twice with lipolysis wash buffer (Sigma-Aldrich, Germany) and then treated with various concentrations (25–200 μg/ml) of *S. italica* acetone leaf extract. Hundred micromolar isoproterenol was used as a positive control and untreated cells as negative control. Plates were incubated at 37°C in a 5% CO_2 atmosphere for 3 h. Fifty microliters of the treatment from each well was aspirated and transferred to a new 96-well assay plate and mixed with lipolysis assay reaction mix (Sigma-Aldrich, Germany) and further incubated for 30 min at room temperature. To measure the amount of glycerol released, absorbance was recorded using Glomax Microtiter Plate Reader (Promega, USA) at 560 nm.

2.6. Adipogenesis. Cells were seeded in a 96-well plate (20,000 cells/ml) and incubated to form a confluent monolayer. The cells were thereafter treated with different concentrations of *S. italica* acetone leaf extract for 48 h. Adipocyte differentiation medium (ADM) was used as a positive control and untreated cells as negative control. After 48 h treatment, the medium was removed and cells were washed once with PBS. Hundred microliters of lipid extraction buffer was added in each well, plate sealed, and incubated for 30 min at 90°C. The plate was cooled and agitated to homogenise the solution. Fifty microliters of each treatment was added to a new 96-well assay plate and 2 μl of lipase solution (Sigma-Aldrich, Germany) was added to each well and incubated for 10 min at room temperature. Thereafter, 50 μl of adipogenesis master mix was added to each well and further incubated for 30 min. In order to measure the amount of accumulated triglycerides, absorbance was recorded using Glomax Microtiter Plate Reader (Promega, USA) at 560 nm.

2.7. Mouse Adipokine Array Dot Blot. Cells were grown in 75 cm^2 flasks (White Scientific, RSA) and differentiated. After differentiation, cells were treated for 24 h with *S. italica* acetone leaf extract (100 μg/ml) with or without 100 ng/ml lipopolysaccharide (LPS). Lipopolysaccharide alone was used as a positive control and untreated cells used as a negative control. Cells were washed with PBS and lysed with lysis buffer (1% Igepal CA-630, 20 Mm Tris-HCl (pH 8.8),

137 mM NaCl, 10% glycerol, and complete EDTA-free protease inhibitor cocktail) using tissue lyser (Retsch., Germany) for 5 min and centrifuged at 13,000 rpm for 10 min at 4°C (Whitehead Scientific, RSA). The expression of adipokines in the cells was determined using the mouse adipokine profiler assay kit according to the manufacturer's instructions (R&D Systems). Briefly, membranes were blocked for 1 h on a rocking platform shaker. Protein samples (500 μg) were prepared and 15 μl of reconstituted mouse adipokine detection antibody cocktail was added to each prepared sample, mixed, and incubated at room temperature for 1 h. Sample/antibody mixtures were then added and incubated overnight at 2–8°C on a rocking platform shaker. After incubation, membranes were washed with wash buffer and 2 ml of streptavidin-HRP in Array Buffer 6 (1 : 2000) was added into each membrane and incubated for 30 min at room temperature on a rocking platform shaker. Each membrane was then washed and removed from its wash container allowing excess wash buffer to drain from the membrane. The membranes were detected using ChemiDoc XRS Image Analyser (Bio-Rad, USA).

2.8. Glucose Uptake Assay. Glucose uptake assay was measured using the method of [14] with slight modification. Briefly, 3T3-L1 preadipocytes cells were cultured and differentiated, after which they were untreated/pretreated with 50 μM of LY294-002 for 30 min to inhibit PI3K. The cells were further incubated in Krebs-Ringer bicarbonate buffer (110 mM NaCl, 4.4 mM KCl, 1.45 mM KH_2PO_4, 1.2 $MgCl_2$, 2.3 $CaCl_2$, 4.8 mM $NaHCO_3$, 10 mM HEPPES, and 0.3% BSA) containing 50 μg/ml and 100 μg/ml *S. italica* acetone extract with and without insulin for 4 h. Insulin (1 μM) was used as a positive control and untreated cells as a negative control. Glucose oxidase (ITinder-GOD/PAP) (KAT Medical, RSA) was thereafter added and incubated for 20 min at 37°C. The absorbance was recorded using Glomax Microtiter Plate reader (Promega, USA) at 560 nm.

2.9. GLUT4 Translocation Assay. Cells were seeded in a corning cell bind 24-well plate (20,000 cells/ml) and differentiated. After differentiation, the cells were treated with 50 μg/ml and 100 μg/ml of *S. italica* acetone leaf extract in the presence or absence of 1 μM insulin for 4 h. Untreated cells were used as negative control and 1 μM insulin as positive control. After treatment, cells were washed and blocked with 0.5% bovine serum albumin (BSA) and incubated with rabbit polyclonal GLUT4 primary antibody (1 : 200) (Santa Cruz Biotechnology, USA) for 30 min at 37°C. After 30 min, cells were washed and further incubated with goat anti-rabbit IgG FITC (conjugated) (Santa Cruz Biotechnology, USA) for 30 min in the dark at room temperature. Cells were then washed with PBS and images were captured by fluorescence microscope (Nikon, Japan) at 40x magnification.

2.10. Western Blotting. 3T3-L1 preadipocytes were seeded at a density of 2×10^4 cells/ml in a 25 cm^2 cell culture flask (Whitehead Scientific, RSA). Cells were then treated for 24 h (5% CO_2, 37°C) with 50 μg/ml and 100 μg/ml of *S. italica* acetone leaf extract in the presence and absence of 1 μM insulin. Insulin (1 μM) was used as a positive control. After treatment, cells were then washed with PBS and lysed with lysis buffer (1% N-P40, 50 mM Tris-HCl (pH 8.8), 150 mM NaCl, 0.5% sodium deoxycholate, 0.1% sodium dodecyl sulphate (SDS), and complete EDTA-free protease inhibitor cocktail) using tissue lyser (Retsch., Germany) for 5 min and centrifuged at 13,000 rpm for 10 min at 4°C (Whitehead Scientific, RSA). The supernatant was transferred into a clean 2 ml tube and protein concentration was determined using the detergent compatible (DC) protein assay (Bio-Rad, USA). This was followed by separating 30 μg of the total protein using 12% SDS-PAGE (Bio-Rad, USA) before transferring the gels onto the membrane. Membranes were immersed in transfer buffer (Bio-Rad, USA) and 100% methanol for 2 min. The gel was then transferred to the membranes using trans-blot turbo transfer system (Bio-Rad, USA). After transferring, the bands were visualised using ponceau stain (Sigma-Aldrich, Germany). Then membrane was washed and blocked with 5% skimmed milk for 90 min followed by incubation with GLUT4 mouse monoclonal antibody (Cell Signaling, RSA) 1 : 500 dilutions at 4°C overnight. After incubation the membrane was washed with TBST followed by incubation with goat anti-rabbit antibodies (Santa Cruz Biotechnology, USA) 1 : 4000 dilutions for 90 min at room temperature. The membrane was washed and substrate was added. Antigen antibody complex was visualised by photo-detection using the Syne-Gene Image Analyser (Bio-Rad, USA).

2.11. Statistical Analysis. GraphPad Instat Software was used for statistical analysis. The results were obtained from three independent replicate experiments and expressed as means ± SEM. The statistical significance of the results was tested using one-way ANOVA employing the Tukey-Kramer Multiple Comparisons Test. Statistical significance was considered at $p < 0.05$.

3. Results

3.1. Antiglycation Effect of S. italica Acetone Leaf Extract. The ability of the extract and arbutin to inhibit glycation was comparable to the control and was significantly high at all concentrations ($p < 0.001$). Antiglycation was concentration-dependent for both arbutin and the plant extract. The extract exhibited a significantly high glycation ability compared to arbutin (Figure 1).

3.2. Effect of S. italica Acetone Leaf Extract on Viability of 3T3-L1. The plant extract at both 24 and 48 h of treatment was not cytotoxic on 3T3-L1 cells at the concentrations used in the study. However, prolonged incubation with increased concentration of the extract affected cell viability. The CC_{50} values of the extract at 24 and 48 h were >1000 μg/ml, Figure 2.

3.3. Effect of S. italica Acetone Leaf Extract on Lipolysis. The results show that lipolytic activity of the extract decreases with increase in concentration in comparison with the control (Figure 3). Isoproterenol resulted in significant lipolytic activity compared to the control ($p < 0.01$).

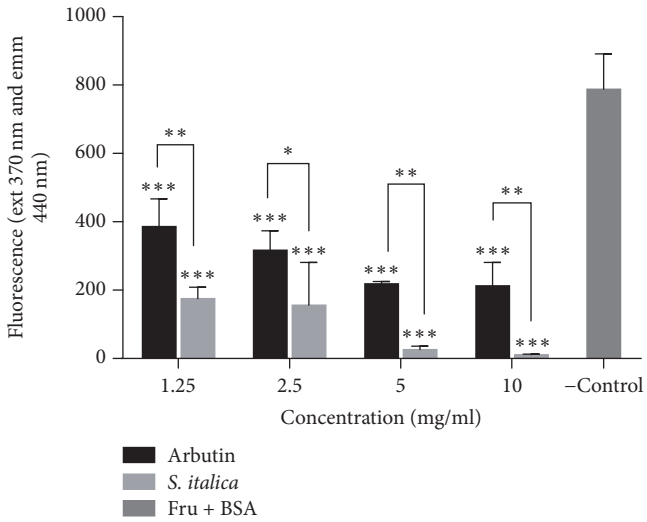

Figure 1: Effect of *S. italica* on fluorescence intensity of glycated BSA. Fructose and BSA were incubated with various concentrations of *S. italica* 1.25–10 mg/ml. The experiment was carried out for 30 days. Arbutin was used as a positive control and fructose + BSA as a negative control. Data represents the ± SEM of 3 independent experiments, $^{***}p < 0.001$, $^{**}p < 0.01$, and $^{*}p < 0.05$.

3.4. Effect of S. italica Acetone Leaf Extract on Adipogenesis. Figure 4 shows the effect of the extract on adipogenesis. The extract at 100 μg/ml compared to other concentrations exhibits adipogenesis activity. The positive control (ADM) significantly increase adipogenesis compared to all treatment groups.

3.5. Effect of S. italica Acetone Leaf Extract on Expression Levels of Obesity Related Adipokines. Results show no significant effect on the expression levels of adiponectin, resistin, and lipocalin-2 after treatment with LPS. The extract shows a slight and significant decrease in expression level of adiponectin and lipocalin-2, respectively, in adipocytes that were not treated with LPS (Figure 5(a)).

Figure 5(b) shows no significant effect on the expression levels of leptin, RBP4, DPPIV, TNF-α, and IL-6 after treatment with LPS. The plant extract alone on the other hand shows a significant decrease in the expression levels of the above-mentioned proteins in both LPS treated and LPS untreated adipocytes except for that of TNF-α.

3.6. Effect of S. italica Acetone Leaf Extract on Glucose Uptake. Glucose uptake analysis of 3T3-L1 adipocytes following treatment with 50 and 100 μg/ml of *S. italica* acetone leaf extract in the presence and absence of insulin for 4 h was evaluated. In order to identify the pathway through which *S. italica* stimulate glucose uptake, 3T3-L1 were pretreated with PI3K inhibitor (LY294-002). The extract shows the ability of inducing glucose uptake although there was no significant difference as compared to the control. The inhibitor at 50 μM shows a decrease in insulin stimulated glucose uptake (Figure 6).

3.7. Effect of S. italica Acetone Leaf Extract on GLUT4 Translocation. The potential effects of different concentrations of

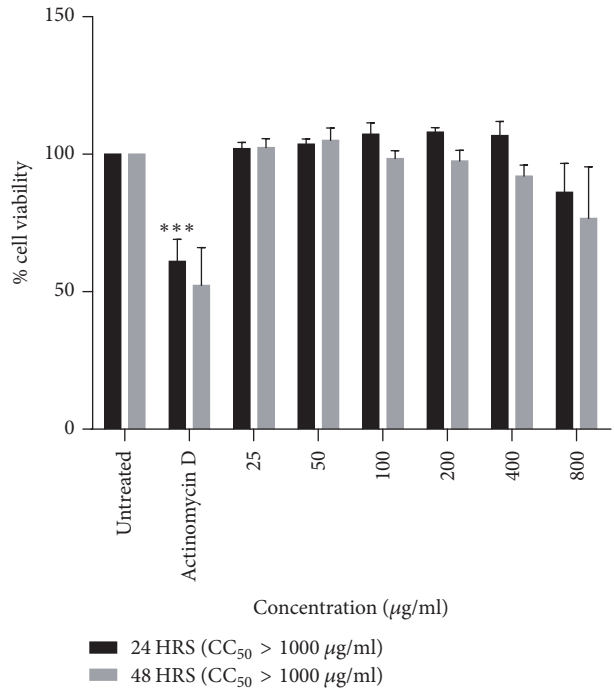

Figure 2: The effect of *S. italica* acetone leaf extract on 3T3-L1 preadipocytes cells treated with various concentrations (25–800 μg/ml). The experiment was carried out for 24 and 48 h using MTT assay. Untreated cells and Actinomycin D were used as negative and positive controls, respectively. Data represents the ± SEM of 3 independent replicate experiments, $^{***}p < 0.001$.

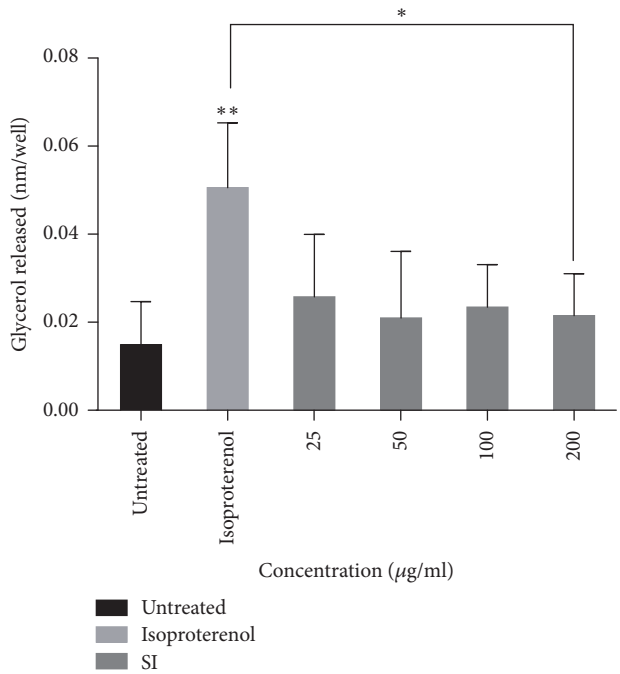

Figure 3: Effect of *S. italica* acetone leaf extract on lipolysis. Differentiated 3T3-L1 cells were treated with various concentrations (25–200 μg/ml) of *S. italica* extract. Isoproterenol was used as a positive control and untreated cells as negative control. The experiment was carried out for 3 h. Data represents the ± SEM of 3 independent replicate experiments, $^{**}p < 0.01$ and $^{*}p < 0.05$.

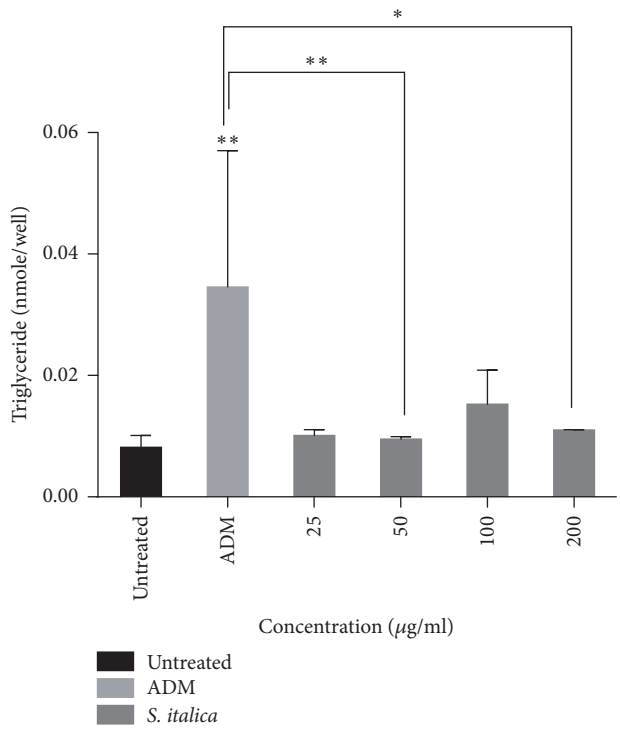

Figure 4: Effect of *S. italica* acetone leaf extract on adipogenesis. Cells were treated with various concentrations (25–200 μg/ml) of *S. italica*. The amount of accumulated triglycerides was extracted and quantified. Adipocyte differentiation medium was used as a positive control. The experiment was carried out for 48 h. Data represents the ± SEM of 3 independent replicate experiments, $^{**}P < 0.01$ and $^{*}P < 0.05$.

acetone leaf extracts on translocation of GLUT4 to the plasma membrane of 3T3-L1 adipocytes are presented in Figure 7. The extract concentrations tested show a slight increase in GLUT4 translocation. The extract at a concentration of 100 μg/ml in combination with insulin shows a significant increase in GLUT4 translocation ($p < 0.05$). The green fluorescence on the cell membrane indicates that GLUT4 has been effectively translocated (Figure 7(a)) and the FITC was also quantified (Figure 7(b)).

3.8. Effect of S. italica Acetone Leaf Extract on GLUT4 Expression. The cells were treated with concentrations of 50 μg/ml and 100 μg/ml of acetone leaf extracts of *S. italica* in the presence and absence of 1 μM insulin. The extract is shown to nonsignificantly increase protein expression of GLUT4 in 3T3-L1 preadipocyte cells when in combination with insulin. Different bands in Figure 8(a) show the expression levels of different treatments and the bands were quantified (Figure 8(b)).

4. Discussion and Conclusion

Diabetes mellitus and obesity remain a global health problem and the use of currently available therapeutics in managing the conditions remains a huge challenge, coupled with their availability and cost to the rural poor in developing countries [15, 16]. Glucose transporter 4 (GLUT4) plays a crucial role in maintaining whole body glucose homeostasis. This is achieved through translocation of GLUT4 from an intracellular pool to the cell surface [17]. Hence, compounds facilitating GLUT4 translocation can be potentially beneficial for the treatment of diabetes [18]. Furthermore, altered balance between energy intake and expenditure can result in excess storage of triglycerides. Research in the identification of medicinal plants with potent antidiabetic and antiobesity agents with less or no side effects and readily available remains less explored [19]. The current study was aimed at determining the antidiabetic and antiobesity potential of *S. italica* through its effect on GLUT4 translocation, expression, and adipogenesis in 3T3-L1 adipocytes.

Toxicity testing plays an essential role in determining the toxic effect and characterisation of test substance. It is thus important in the development of new drugs and for the improvement of therapeutic potential of existing molecules [20, 21]. In this study, the cytotoxic effect of *S. italica* acetone leaf extract on 3T3-L1 preadipocytes was assessed. The cells were exposed to the extract for 24 and 48 h and the results show that the extract was not toxic to 3T3-L1 preadipocytes at both time intervals. The higher the CC_{50} value, the higher the concentration that is needed to kill 50% of the cells. The CC_{50} values were shown to be >1000 μg/ml at both time intervals which suggests that the plant extract is not toxic. This finding could validate the safety use of the plant in clinical settings.

Glycation is identified as a key molecular mechanism of chronic diabetic complications. Identification of medicinal plants with protein glycation inhibitory potential will enhance the therapeutic strategies to delay or inhibit diabetic complications with minimum side effects [8]. Reference [22] has shown that BSA glycation is much faster in the presence of fructose. The observed decrease in fluorescence intensity during coincubation with the plant extract might suggest that the extract contains compounds that prevent or decrease the formation of advanced glycation end products (AGEs). Although there are no studies that have been reported on the antiglycation potential of *S. italica*, other authors in another study have also shown the effect of *Murraya koenigii* inhibition of glycation to be greater than that of aminoguanidine (AG), which was used as the standard inhibitor [8]. According to [23] polyphenolic compound in plants may play a major role in the inhibition AGEs. Resveratrol which has been reported to be present in *S. italica* extract [24] might have played a role in the ability of the extract to inhibit protein glycation. Recent studies have also revealed that resveratrol has beneficial effects on the liver by extenuating oxidative stress and downregulation of receptor for AGE (RAGE) expression in the liver of rats with type 2 diabetes [25].

Dysregulation of lipid metabolism is a key feature of some pathological conditions including diabetes mellitus, insulin resistance, and obesity [19]. In this study, the effect of *S. italica* on adipogenesis and lipolysis in mouse 3T3-L1 adipocyte cells was also evaluated. The lipid accumulation was measured based on the triglycerides content of the cells differentiated at various conditions. Furthermore, lipolysis was assessed

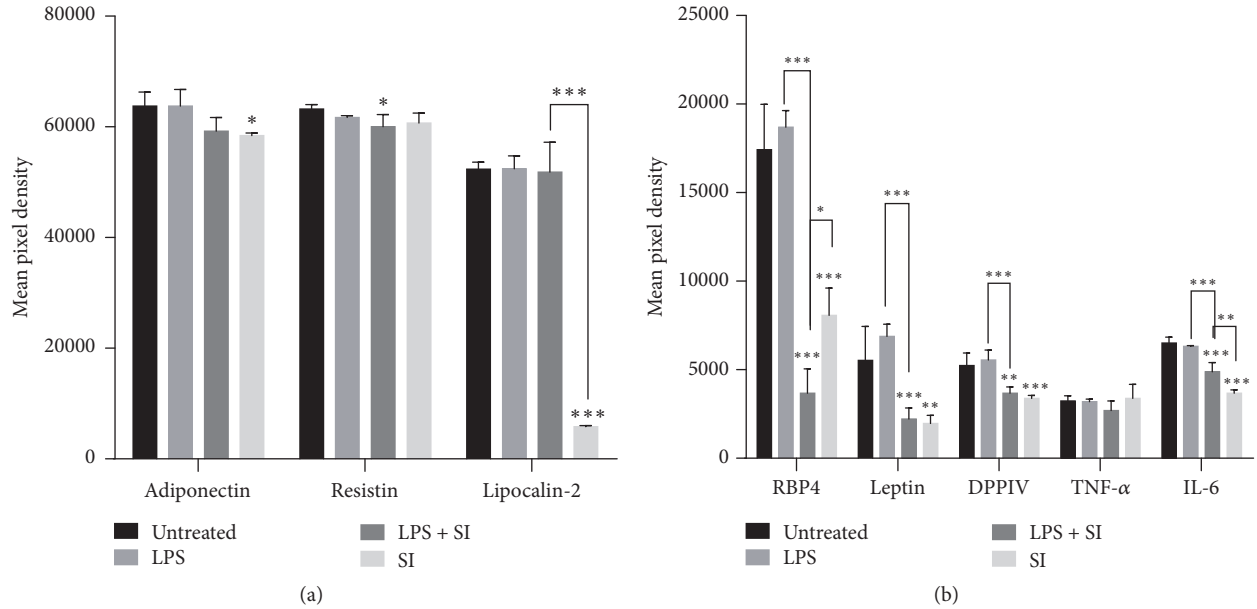

Figure 5: Effect of *S. italica* on the protein expression of obesity-associated adipokines. 3T3-L1 adipocytes were untreated or treated with 100 ng/ml LPS, 100 μg/ml SI, and LPS in combination with SI for 24 h. Untreated cells were considered as standard control and LPS as a positive control. Data represents the ± SEM of 3 independent replicate experiments, $^{***}p < 0.001$, $^{**}p < 0.001$, and $^{*}p < 0.05$.

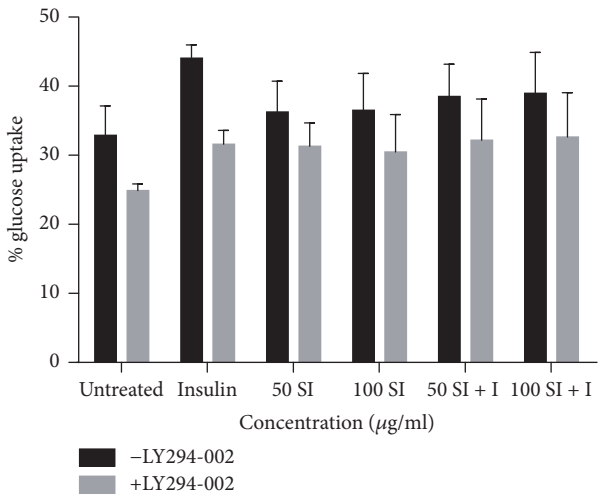

Figure 6: Effect of *S. italica* acetone leaf extract on glucose uptake in 3T3-L1 adipocytes. Cells were treated with various concentrations (50–100 μg/ml) in the absence and presence of insulin for 4 h. LY294-002 was used to inhibit PI3K. Data represents the ± SEM of 3 independent replicate experiments.

through the measurements of glycerol released in the culture medium.

The current findings revealed the extract does not bring about a significant increase in adipogenesis and lipolysis when compared to the untreated control. Triglycerides accumulation during treatment with the extract was significantly lower than that of adipocyte differentiation medium which was used as a positive control for adipogenesis. Furthermore, glycerol released during treatment with the extract was also significantly lower than that of isoproterenol which was used as a positive control for lipolysis. Since resveratrol has been isolated from *S. italica* [24] and other authors [26] have observed low triacylglycerol accumulation in 3T3-L1 adipocytes treated with 100 μM of resveratrol for 12, 24, and 48 h, the possibility that the presence of this compound in the extract that is responsible for the minimal induction of lipolysis in this study is high. A way of evading this is to isolate the pure compound in this extract that elicits the desired function which may not have negative effect on lipolysis. Some authors have also found resveratrol to reduce lipid accumulation in 3T3-L1 preadipocytes in a dose-dependent manner [27].

Furthermore, adipose tissues have a major endocrine function secreting multiple adipokines; many of the adipokines are involved in energy homeostasis. In obese state, adipocytes are integral to the development of obesity-induced inflammation by increasing secretion of various adipokines (including leptin, resistin, lipocalin-2, RBP4, IL-6, TNF-α, and DPPIV). On the other hand, adiponectin has been found to be lower in obese individuals [4]. Hence, the effect of *S. italica* acetone leaf extract on the expression levels of obesity-associated adipokines became pertinent and was thus evaluated. The results show that *S. italica* acetone leaf extract significantly decreased the expression levels of leptin, lipocalin-2, RBP4, IL-6, and DPPIV. Decrease in the expression levels of these adipokines can play a vital role in the management of insulin resistance, since these molecules are modulators of insulin resistance. However, the extract did not show any significant effect on the expression levels of resistin and TNF-α but rather a slight decrease which may serve as a positive indicator in the management of obesity. Furthermore, the extract is shown to slightly decrease the expression level of adiponectin which is known to be one

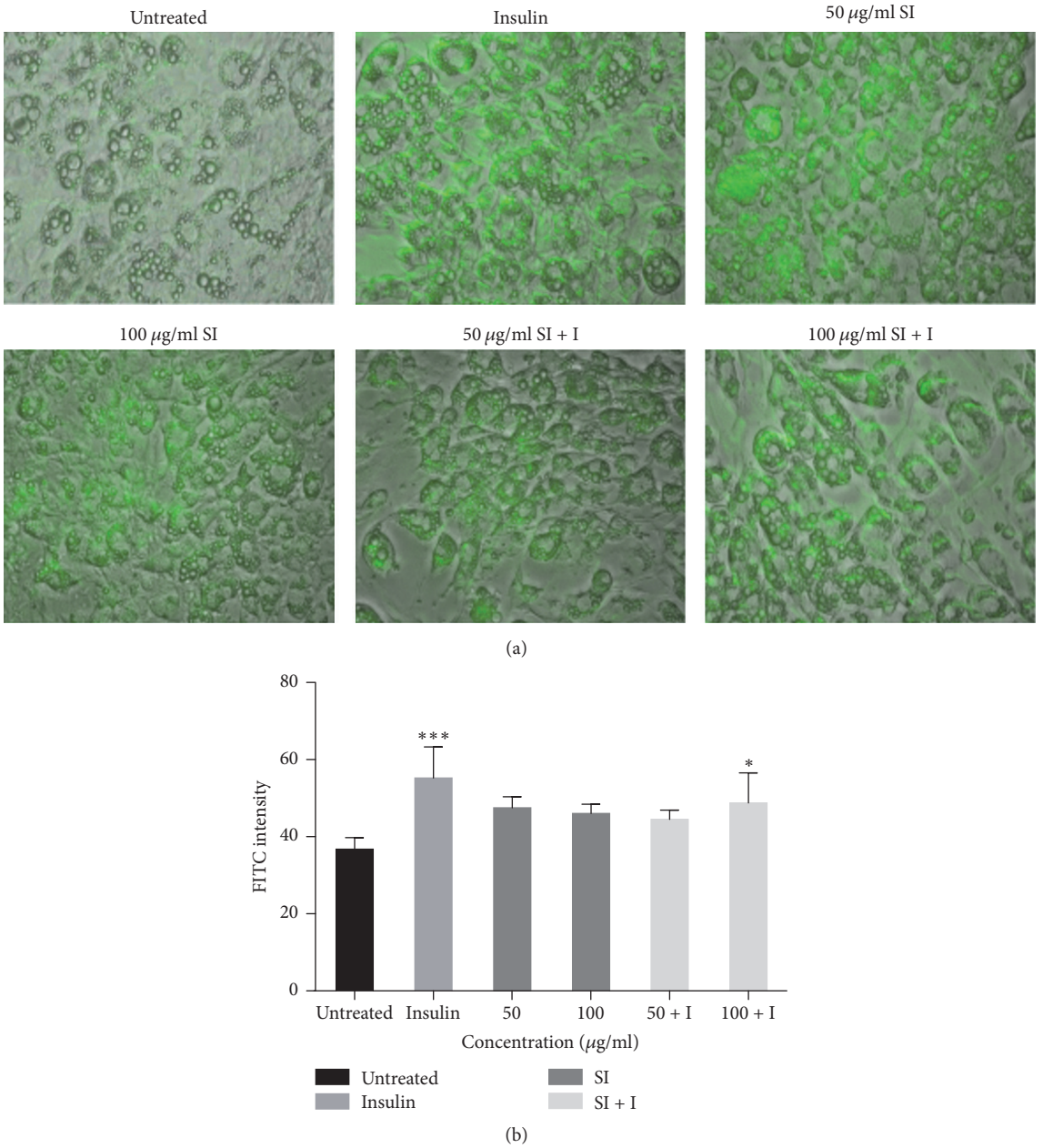

Figure 7: Effect of *S. italica* on translocation of GLUT4 to the plasma membrane of differentiated 3T3-L1 adipocytes. The cells were treated with 50 μg/ml and 100 μg/ml of the plant extract in the presence or absence of 1 μM insulin and viewed with fluorescence microscope (40x magnification) (a) and quantitative immunofluorescence was measured (b). Data represents the ± SEM of 3 independent replicate experiments, $^{***}p < 0.001$ and $^{*}p < 0.05$.

of the adipokines that produces insulin sensitising effect. Based on the current findings, it can be suggested that the pure compound(s) from this extract that elicit the desired functions that may not negatively affect the expression level of adiponectin could be isolated.

Glucose homeostasis is determined by glucose production and utilisation in insulin sensitive organs and tissues, including muscle, liver, and adipose tissue. Glucose uptake in adipose tissues plays a fundamental role in the body glucose control [14]. Decrease in intracellular pool of transporters results from insulin resistance in peripheral tissues at the molecular level which is connected with defects in the glucose transport system. As a result, fewer transporter molecules are available for translocation to the plasma membrane in response to insulin, thus affecting the process of glucose uptake and leading to insulin resistance [28]. Thus, substances that escalate the peripheral sensitivity to insulin are useful in the treatment of type II diabetes mellitus. A previous study from our laboratory (unpublished data) has shown that *S. italica* acetone leaf extract exhibits potential in inducing glucose uptake in C2C12 muscle cells. In the present study, the effect of the extract in stimulating glucose uptake in 3T3-L1

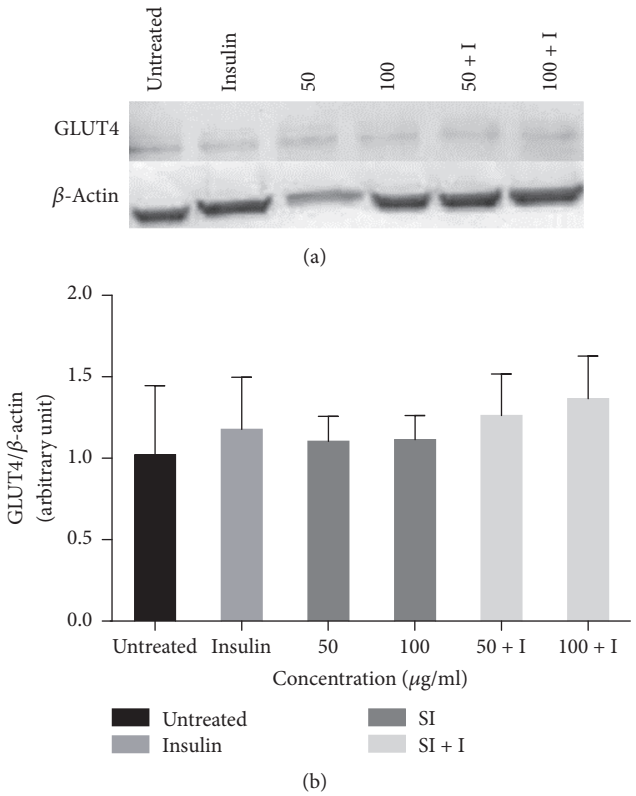

Figure 8: Western blot analysis of the effect of *S. italica* acetone leaf extract on the expression level of glucose transporter 4 (GLUT 4) in 3T3-L1 preadipocytes. Cells were treated with 50 μg/ml and 100 μg/ml of *S. italica* acetone leaf extract in the absence and presence of 1 μM insulin. Data represents the ± SEM of 3 independent replicate experiments.

and its possible mechanism of action were evaluated through the inhibition of PI3K.

The results showed a slight ability of the extract to induce glucose uptake in 3T3-L1 adipocytes, although the observed activity was not significant. A nonsignificant antagonistic effect was also observed when the effect of the extract was evaluated in combination with insulin, suggestive that the extract may contain compound(s) that interfere with insulin action in 3T3-L1 adipocytes. Previous findings in our laboratory showed that the extract exhibits high glucose uptake when in combination with insulin compared to insulin alone in C2C12 muscle cells, possibly due to the fact that different cell lines respond differently through different mechanisms (unpublished data). For decades, muscles have been considered to be the main site of insulin stimulated glucose uptake, with adipose tissue contributing relatively little to total body glucose disposal [29]. Reference [30] has reported that *berberine* stimulates glucose uptake in 3T3-L1 adipocytes and L6 myoblasts in an AMPK dependent manner. In this study the results showed that, during the inhibition of PI3K pathway, the glucose uptake decreased in all treatments, suggestive of its involvement in the extract-induced glucose uptake.

The translocation of GLUT4 occurs from intracellular storage sites to the plasma membrane in response to insulin. At the cell surface, GLUT4 facilitates the passive transport of glucose into muscle and adipose tissue [31]. Increased GLUT4 expression on the plasma membrane is important for the uptake of glucose into the adipose and muscle tissues and plays a key role in maintaining normal blood glucose level [32].

The current findings showed *S. italica* acetone leaf extract to have increased GLUT4 translocation, even though the increase was not as significant when compared to the positive control. Cotreatment with insulin showed a nonsignificant antagonistic effect, again suggesting the presence of substances within the extract that interfere with insulin activity. The AKT pathway has been reported to increase translocation of GLUT4 to the plasma membrane in muscle and adipose tissues [33]. In another study, [34] attributed resveratrol-mediated activation of AKT in their study to have played a vital role in GLUT4 translocation. Since resveratrol has been isolated from *S. italica*, the possibility of its involvement in facilitating glucose uptake in this study is paramount. Findings by [32] demonstrated that gallic acid induced GLUT4 translocation through the PI3K pathway in 3T3-L1 adipocytes. It is highly likely that *S. italica* might also be inducing GLUT4 translocation through a similar pathway, in this instance. This might be confirmed by the inhibitory effect of LY294-002 on *S. italica*-induced glucose uptake.

The expression of GLUT4 levels in treated cells was also assessed. GLUT4 is selectively expressed in insulin responsive tissues such as adipose and skeletal muscle cells [14]. According to [35], GLUT4 is not highly expressed in fibroblastic state. In this study 3T3-L1 preadipocytes were used to determine the effect of *S. italica* on GLUT4 expression. The results show that *S. italica* extract increased GLUT4 expression, as evidenced by the increase in GLUT4 protein band density following treatment with the extract (Figure 8(a)). Increase in GLUT4 expression might be due to the presence of flavonoids in the extract. Several studies have suggested the important role of flavonoids in enhancing the expression of GLUT4 [36]. The extract in combination with insulin resulted in higher GLUT4 expression. This shows a synergy between the extract and insulin in inducing GLUT4 expression levels.

In conclusion, the results suggest that *S. italica* stimulates glucose uptake through the PI3K-dependent pathway. The extract might play a role as a therapeutic agent for obesity through its ability to downregulate some of obesity-associated adipokines. Furthermore, the extract might have compounds that have antiglycation capabilities. However, further studies are necessary in order to understand which compound(s) is/are responsible for the regulation of obesity-associated adipokines. *In vivo* studies are worth undertaking in order to determine the effect of *S. italica* extract within the living system.

Conflicts of Interest

The authors declare that they have no conflicts of interest.

Acknowledgments

This work was made possible and was supported by grants from the South African Medical Research Council (through

funding received from the South African National Treasury) awarded to Leseilane Mampuru, National Research Foundation (NRF) (Thuthuka) awarded to Matlou P. Mokgotho, and the University of Limpopo, as well as Dr. C. Müller of the SAMRC.

References

[1] P. R. Njølstad, J. V. Sagen, L. Bjørkhaug et al., "Permanent Neonatal Diabetes Caused by Glucokinase Deficiency: Inborn Error of the Glucose-Insulin Signaling Pathway," *Diabetes*, vol. 52, no. 11, pp. 2854–2860, 2003.

[2] American Diabetes Association, "Diagnosis and classification of diabetes mellitus," *Diabetes Care*, vol. 36, supplement 1, pp. S67–S74, 2013.

[3] Z. Cheng, S. Guo, K. Copps et al., "Foxo1 integrates insulin signaling with mitochondrial function in the liver," *Nature Medicine*, vol. 15, no. 11, pp. 1307–1311, 2009.

[4] U. J. Jung and M. S. Choi, "Obesity and its metabolic complications: the role of adipokines and the relationship between obesity, inflammation, insulin resistance, dyslipidemia and nonalcoholic fatty liver disease," *International Journal of Molecular Sciences*, vol. 15, no. 4, pp. 6184–6223, 2014.

[5] J. M. Forbes and M. E. Cooper, "Mechanisms of diabetic complications," *Physiological Reviews*, vol. 93, no. 1, pp. 137–188, 2013.

[6] American Diabetes Association, "Diagnosis and classification of diabetes mellitus," *Diabetes Care*, vol. 27, supplement 1, pp. S5–S10, 2004.

[7] E. S. Ranaweera KKDS, "Antiglycation and Antioxidant Activities of a Ready to Serve Herbal Drink of Syzygium Cumini Bark Extract," *Medicinal & Aromatic Plants*, vol. 03, no. 01, 2014.

[8] D. C. Wijetunge, H. K. I. R, and H. K. I. Perera, "A novel in vitro method to identify protein glycation inhibitors," *Asia Journal of Medical Sciences*, vol. 5, no. 3, pp. 15–21, 2014.

[9] S. S. Gololo, N. S. Mapfumari, L. S. Sethoga, M. T. Olivier, L. J. Shai, and M. A. Mogale, "Identification of phytochemical constituents within the n-hexane leaf extract of Senna italica (Mill) using gas chromatography-mass spectrometry (GC-MS) analysis," *Journal of Pharmaceutical Sciences and Research*, vol. 8, no. 10, pp. 1141–1143, 2016.

[10] L. J. Shai, P. Masoko, M. P. Mokgotho et al., "Yeast alpha glucosidase inhibitory and antioxidant activities of six medicinal plants collected in Phalaborwa, South Africa," *South African Journal of Botany*, vol. 76, no. 3, pp. 465–470, 2010.

[11] N. Matsuura, T. Aradate, C. Sasaki et al., "Screening system for the Maillard reaction inhibitor from natural product extracts," *Journal of Health Science*, vol. 48, no. 6, pp. 520–526, 2002.

[12] T. Mosmann, "Rapid colorimetric assay for cellular growth and survival: application to proliferation and cytotoxicity assays," *Journal of Immunological Methods*, vol. 65, no. 1-2, pp. 55–63, 1983.

[13] S. E. Mazibuko, E. Joubert, R. Johnson, J. Louw, A. R. Opoku, and C. J. F. Muller, "Aspalathin improves glucose and lipid metabolism in 3T3-L1 adipocytes exposed to palmitate," *Molecular Nutrition & Food Research*, vol. 59, no. 11, pp. 2199–2208, 2015.

[14] Y. He, W. Li, Y. Li, S. Zhang, Y. Wang, and C. Sun, "Ursolic acid increases glucose uptake through the PI3K signaling pathway in adipocytes," *PLoS ONE*, vol. 9, no. 10, Article ID e110711, 2014.

[15] A. Noor, S. Gunasekaran, A. Soosai Manickam, and M. A. Vijayalakshmi, "Antidiabetic activity of Aloe vera and histology of organs in streptozotocin-induced diabetic rats," *Current Science*, vol. 94, no. 8, pp. 1070–1076, 2008.

[16] C. A. Luque and J. A. Rey, "Sibutramine: a serotonin-norepinephrine reuptake-inhibitor for the treatment of obesity," *Annals of Pharmacotherapy*, vol. 33, no. 9, pp. 968–978, 1999.

[17] N. Poulose, C. V. Prasad, P. N. Haridas, and G. Anilkumar, "Ellagic Acid Stimulates Glucose Transport in Adipocytes and Muscles through AMPK Mediated Pathway," *Journal of Diabetes & Metabolism*, vol. 02, no. 05, 2011.

[18] P. Anand, K. Y. Murali, V. Tandon, P. S. Murthy, and R. Chandra, "Insulinotropic effect of cinnamaldehyde on transcriptional regulation of pyruvate kinase, phosphoenolpyruvate carboxykinase, and GLUT4 translocation in experimental diabetic rats," *Chemico-Biological Interactions*, vol. 186, no. 1, pp. 72–81, 2010.

[19] A. Ghorbani, R. Moradi Marjaneh, Z. Rajaei, and M.-A. Hadjzadeh, "Effects of Securigera securidaca Extract on Lipolysis and Adipogenesis in Diabetic Rats," *Cholesterol*, vol. 2014, Article ID 582106, 2014.

[20] D. Arome and E. Chinedu, "The importance of toxicity testing," *Journal of Pharmaceutical and BioSciences*, pp. 146–148, 2013.

[21] S. Parasuraman, "Toxicological screening," *Journal of Pharmacology and Pharmacotherapeutics*, vol. 2, no. 2, pp. 74–79, 2011.

[22] A. Meeprom, W. Sompong, C. B. Chan, and S. Adisakwattana, "Isoferulic acid, a new anti-glycation agent, inhibits fructoseand glucose-mediated protein glycation in vitro," *Molecules*, vol. 18, no. 6, pp. 6439–6454, 2013.

[23] S. Adisakwattana, T. Thilavech, and C. Chusak, "*Mesona chinensis* Benth extract prevents AGE formation and protein oxidation against fructose-induced protein glycation in vitro," *BMC Complementary and Alternative Medicine*, vol. 14, no. 1, article 130, pp. 1–9, 2014.

[24] M. P. Mokgotho, S. S. Gololo, P. Masoko et al., "Isolation and chemical structural characterisation of a compound with antioxidant activity from the roots of senna italica," *Evidence-Based Complementary and Alternative Medicine*, vol. 2013, Article ID 519174, 2013.

[25] M. Khazaei, J. Karimi, N. Sheikh et al., "Effects of resveratrol on receptor for advanced glycation end products (RAGE) expression and oxidative stress in the liver of rats with type 2 diabetes," *Phytotherapy Research*, vol. 30, no. 1, pp. 66–71, 2016.

[26] A. Lasa, M. Schweiger, P. Kotzbeck et al., "Resveratrol regulates lipolysis via adipose triglyceride lipase," *The Journal of Nutritional Biochemistry*, vol. 23, no. 4, pp. 379–384, 2012.

[27] G. F. Wei and S. H. Dong, "Algebraic approach to energy spectra of the Scarf type and generalized Pöschl–Teller potentials," *Canadian Journal of Physics*, vol. 89, no. 12, pp. 1225–1231, 2011.

[28] S. A. Kalekar, R. P. Munshi, S. S. Bhalerao, and U. M. Thatte, "Insulin sensitizing effect of 3 Indian medicinal plants: An in vitro study," *Indian Journal of Pharmacology*, vol. 45, no. 1, pp. 30–33, 2013.

[29] B. B. Kahn and J. S. Flier, "Obesity and insulin resistance," *The Journal of Clinical Investigation*, vol. 106, no. 4, pp. 473–481, 2000.

[30] Y. S. Lee, W. S. Kim, K. H. Kim et al., "Berberine, a natural plant product, activates AMP-activated protein kinase with beneficial metabolic effects in diabetic and insulin-resistant states," *Diabetes*, vol. 55, no. 8, pp. 2256–2264, 2006.

[31] R. T. Watson and J. E. Pessin, "Bridging the GAP between insulin signaling and GLUT4 translocation," *Trends in Biochemical Sciences*, vol. 31, no. 4, pp. 215–222, 2006.

[32] C. N. Vishnu Prasad, T. Anjana, A. Banerji, and A. Gopalakrishnapillai, "Gallic acid induces GLUT4 translocation and glucose uptake activity in 3T3-L1 cells," *FEBS Letters*, vol. 584, no. 3, pp. 531–536, 2010.

[33] J. Gao, J. Li, Y. An et al., "Increasing effect of Tangzhiqing formula on IRS-1-dependent PI3K/AKT signaling in muscle," *BMC Complementary and Alternative Medicine*, vol. 14, article no. 198, 2014.

[34] S. V. Penumathsa, M. Thirunavukkarasu, L. Zhan et al., "Resveratrol enhances GLUT-4 translocation to the caveolar lipid raft fractions through AMPK/Akt/eNOS signalling pathway in diabetic myocardium," *Journal of Cellular and Molecular Medicine*, vol. 12, no. 6, pp. 2350–2361, 2008.

[35] H. Hauner, K. Röhrig, M. Spelleken, L. S. Liu, and J. Eckel, "Development of insulin-responsive glucose uptake and GLUT4 expression in differentiating human adipocyte precursor cells," *International Journal of Obesity*, vol. 22, no. 5, pp. 448–453, 1998.

[36] F. Hajiaghaalipour, M. Khalilpourfarshbafi, A. Arya, and A. Arya, "Modulation of glucose transporter protein by dietary flavonoids in type 2 diabetes mellitus," *International Journal of Biological Sciences*, vol. 11, no. 5, pp. 508–524, 2015.

Hindawi
Evidence-Based Complementary and Alternative Medicine
Volume 2017, Article ID 4393529, 8 pages
https://doi.org/10.1155/2017/4393529

Research Article

Wushenziye Formula Improves Skeletal Muscle Insulin Resistance in Type 2 Diabetes Mellitus via PTP1B-IRS1-Akt-GLUT4 Signaling Pathway

Chunyu Tian,[1,2] Hong Chang,[1,2] Xiaojin La,[1,2] and Ji-an Li[1,2]

[1]*North China University of Science and Technology, Tangshan 063210, China*
[2]*Pharmacology Analysis Key Laboratory for Prevention and Treatment of Diabetes of Traditional Chinese Medicine in Hebei Province, Tangshan 063210, China*

Correspondence should be addressed to Chunyu Tian; tcy4479@sina.com

Received 8 September 2017; Revised 25 November 2017; Accepted 4 December 2017; Published 31 December 2017

Academic Editor: Akhilesh K. Tamrakar

Background. Wushenziye formula (WSZYF) is an effective traditional Chinese medicine in the treatment of type 2 diabetes mellitus (T2DM). *Aim.* This study aimed to identify the effects and underlying mechanisms of WSZYF on improving skeletal muscle insulin resistance in T2DM. *Methods.* An animal model of T2DM was induced by Goto-Kakizaki diabetes prone rats fed with high fat and sugar for 4 weeks. Insulin resistance model was induced in skeletal muscle cell. *Results. In vivo*, WSZYF improved general conditions and decreased significantly fasting blood glucose, glycosylated serum protein, glycosylated hemoglobin, insulin concentration, and insulin resistance index of T2DM rats. *In vitro*, WSZYF enhanced glucose consumption in insulin resistance model of skeletal muscle cell. Furthermore, WSZYF affected the expressions of molecules in regulating T2DM, including increasing the expressions of p-IRS1, p-Akt, and GLUT4, reducing PTP1B expression. *Conclusion*. These findings displayed the potential of WSZYF as a new drug candidate in the treatment of T2DM and the antidiabetic mechanism of WSZYF is probably mediated through modulating the PTP1B-IRS1-Akt-GLUT4 signaling pathway.

1. Introduction

Diabetes mellitus characterized by deregulation of glucose and lipid metabolism seriously affects human health. It affected an estimated 366 million people in 2011 and the number is projected to be 600 million by the year 2035 [1]. Type 2 diabetes mellitus (T2DM), one of the most common types of diabetes with the characteristics of insensitivity to insulin, has attracted great attention [2]. Insulin resistance (IR), an impaired biological response to insulin, is the pathological basis of T2DM. It refers to the decreased sensitivity of tissues to insulin, resulting in the reduction in glucose uptake and utilization [3]. In the body, skeletal muscle is the main target organ that consumes glucose and completes approximately 80% of the postprandial glucose intake and consumption caused by insulin stimulation [4, 5]. However, under the condition of IR, insulin-stimulated glucose disposal in skeletal muscle is severely damaged and could not respond to insulin properly. This leads to a defect in the insulin signaling pathway in muscle and elevating blood glucose level, which is a key feature of IR in T2DM. Therefore, skeletal muscle was selected as a therapeutic target of WSZYF in the battle against T2DM.

The main proteins in the phosphatidylinositol 3-kinase (PI3K) signaling pathway, including PI3K, Akt, and glucose transporter type 4 (GLUT4), play important roles in insulin signaling transduction. The abnormality of this pathway is the major cause of T2DM [6]. The signaling cascade is triggered when insulin connects with the membrane receptor of target cells. Insulin receptor substrate-1 (IRS-1) phosphorylated by the activated insulin receptor leads to PI3K and Akt activation [7]. GLUT4, downstream of PI3K, is the pivotal protein in controlling glucose uptake and glycogen metabolism [8]. In T2DM, not only is the sensitivity of skeletal muscle to insulin abated, but also the expression of GLUT4 is decreased, which decreases the glucose uptake and utilization and raises blood glucose level [9, 10]. Moreover, the lack activity of IRS-1 leads to the reduced phosphorylation of PI3K and

thereby decreased GLUT4 expression in skeletal muscle cells, resulting in IR [11]. Thus, the modulation of IRS1-Akt-GLUT4 signaling pathway is quite associated with the treatment of IR.

Protein tyrosine phosphatase-1B (PTP1B), which leads to the dephosphorylation of insulin receptor, has the negative regulation in insulin signal transduction [12]. Studies [12–14] have demonstrated that inhibition of PTP1B could result in the phosphorylation of insulin receptor and insulin receptor substrates (IRS), thus improving insulin sensitivity and decreasing blood glucose level. Therefore, targeting on PTP1B may be a novel approach for the treatment of T2DM.

Traditional Chinese medicine has made significant contributions to the prevention and treatment of T2DM. WSZYF is an effective compound in the treatment of T2DM in clinic. It consists of four Chinese medicines, including Radix Polygoni Multiflori Preparata, Mori fructus, Mori folium, and Cassiae semen. It was testified that components in WSZYF, like resveratrol and 2-styrene glucoside [15, 16], had the effects on improving insulin sensitivity. The antidiabetic effect and underling mechanism of WSZYF have not been clearly explained. In this study, a T2DM rat model and an IR model of skeletal muscle cell were established to investigate whether WSZYF could improve glucose metabolism and IR or not and how to regulate PTP1B-IRS1-Akt-GLUT4 signaling pathway by WSZYF.

2. Materials and Methods

2.1. Materials. Insulin assay kit was obtained from Millipore (USA). Dulbecco's modified Eagle's medium (DMEM) and fetal bovine serum (FBS) were from Gibco (USA). Metformin was purchased from Squibb Pharmaceutical (Shanghai, China). Blood sugar meter and blood sugar test paper were purchased from Sannuo Biosensors (China). Assay kits of glycosylated serum protein and glycosylated hemoglobin were from Nanjing Jiancheng Bioengineering Institute (Nanjing, China). The primary antibodies against PTP1B, p-Akt (phospho S473), GLUT4, and GAPDH were from Bioworld Technology (USA) and antibody against p-IRS1 (phospho Y612) was from Abcam (USA). The secondary antibodies were purchased from Beyotime Biotechnology (China). The herbs in WSZYF were purchased from Tongrentang Pharmacy (Tangshan, China).

2.2. Animals and Experimental Design. All the procedures were conformed to the Guide for the Care and Use of Laboratory Animals published by the National Institutes of Health (NIH Publications number 85-23, revised 1996). Goto-Kakizaki (GK) rats weighing 200 to 300 g were purchased from Shanghai Slack Animal Center (certificate number SCXK (Shanghai) 2012-0002). Rats were raised in specific pathogen-free (SPF) room in North China University of Science and Technology. After one-week acclimation, rats were fed with high glucose and fat for 4 weeks to induce T2DM model. Rats with fasting blood glucose $\geqslant$ 11.1 mmol/L and blood glucose $\geqslant$ 16.7 mmol/L were randomly divided into five groups: model group (n = 6, oral administration of equivalent volume of normal saline), metformin group (n = 6, oral administration of metformin, 85 mg/kg/day), WSZYF low-dose group (WSZYF (L), n = 6, oral administration of WSZYF, 300 mg/kg/day), WSZYF medium-dose group (WSZYF (M), n = 6, oral administration of WSZYF, 600 mg/kg/day), and WSZYF high-dose group (WSZYF (H), n = 6, oral administration of WSZYF, 1200 mg/kg/day). The Wistar rats orally given equivalent volume of normal saline served as the control group. All the rats were raised for 8 weeks. At the end of the study, general conditions were measured and indexes related to blood glucose and insulin were tested. Muscle tissues were stored at −80°C for further analysis.

2.3. Body Weight, Food Intake, Water Intake, and Urine Output. The body weight, food intake, water intake, and urine output of the rats were monitored at the time points of 0, 1, 4, and 8 weeks and the data of 8 weeks were selected in this study. For urine output, rats were put into the metabolic cage after fasting for 12 hours. Urine in 24 hours was collected. During this time, they were only provided with food but no water.

2.4. Blood Chemistry Assay. After eight weeks, blood samples were collected for blood chemistry measurements. Fasting blood glucose was measured by using blood sugar meter and blood sugar test paper. Glycosylated hemoglobin, glycosylated serum protein, and insulin were detected by kits analysis according to manufacturer's instruction. Insulin resistance was assessed by a homeostasis model assessment of IR index as previously described [17].

2.5. Glucose Concentration in the Cell Supernatant Analysis. Primary cell culture of skeletal muscle was performed as previous study [18]. Muscle tissue was dissected from the soleus and cut into small pieces at the size of 0.1 cm^3 and washed 3 times with PBS and DMEM (mixed with 10% FBS and 2% penicillin/streptomycin). Then the small pieces of muscle tissue were seeded in culture flasks which were upside down in in a humidified incubator with 5% CO_2 at 37°C. After 2 hours, the culture flasks were right side up and 3–5 ml culture medium was added. The culture medium was renewed every three days, while cultures were monitored by daily observation under an inverted microscope (Olympus, Japan). Then the cells were purified by differential adherence and the second generation was used in the experiment. When the skeletal muscle cells reached 70% confluence, they were induced to differentiation by DMEM supplemented with 2% FBS, 100 U/ml penicillin, and 100 μg/ml streptomycin. The successful differentiation showed that most of the myocytes had differentiated into multinucleated myotubes and could be easily identified as muscle cells. Then cells were divided into several groups: control group, model group, WSZYF-L (25 μg/L) group, WSZYF-M (100 μg/L) group, and WSZYF-H (400 μg/L) group. In the model group, cells were washed three times with PBS and insulin (5×10^{-7} mol/L) with DMEM 200 μl was added for 12 hours. Then the supernatant was removed and DMEM was added for 24-hour incubation. Cells in the treatment groups were treated in a similar way, except that the culture media contained WSZYF in the later 24 hours. In the control group, fresh nutrient solution was changed at the time points of 12 and 24 hours.

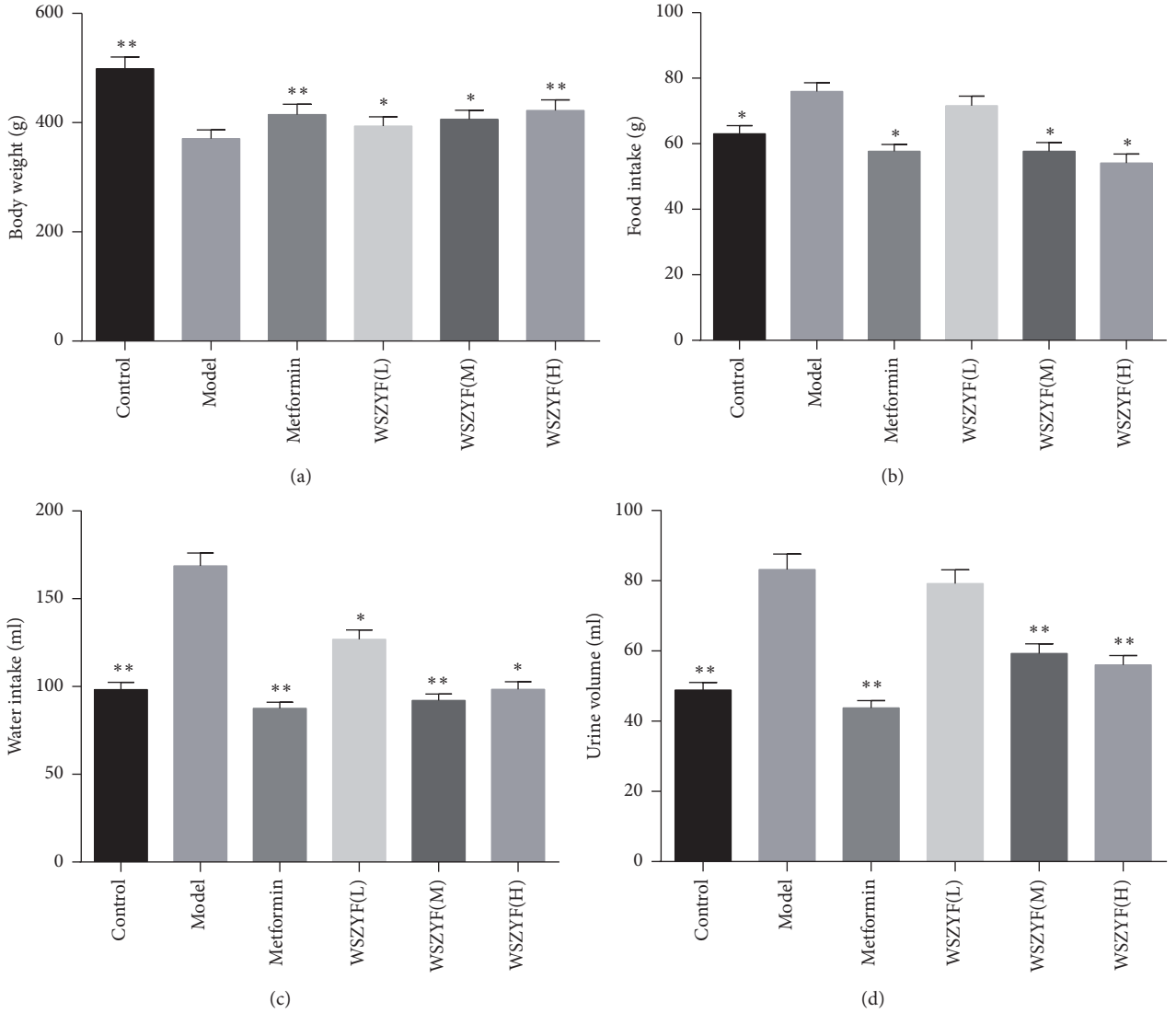

Figure 1: Effects of WSZYF on general conditions in T2DM rats. (a) Body weight, (b) food intake, (c) water intake, and (d) urine volume. $^{*}P < 0.05$, $^{**}P < 0.01$ compared with model group.

2.6. Western Blotting Analysis on Proteins Related to Regulating Insulin Resistance. Proteins related to regulating insulin resistance were detected by *in vivo* study. The collected muscle tissues (120 mg) were prepared with RIPA buffer (PPLYGEN, China) and proteins were extracted according to the manufacturer's instruction. Protein contents were measured with BCA protein assay kit (PPLYGEN, China). After addition of loading buffer boiled for 5 minutes, tissue samples were separated by 10% SDS-PAGE and transferred to NC membranes (Millipore, Germany). After being blocked with 5% nonfat dry milk for 2 hours, the membranes were incubated with different primary antibodies overnight at 4°C. After washing with TBST three times, the membranes were incubated with HRP-conjugated secondary antibodies for 1 hour at room temperature. Washed three times with TBST, the proteins were detected with an enhanced chemiluminescence agent (GE, USA) and quantified by densitometry using an image analyzer (Bio-Rad, USA). Mouse anti-GAPDH monoclonal antibody served as an internal control.

2.7. Statistical Analysis. Data were expressed as the mean ± standard deviation (SD). Statistical analysis was undertaken by one-way analysis of variance (ANOVA) and Dunnett's test. Differences between groups were considered as statistically significant when $P < 0.05$.

3. Results

3.1. Effects of WSZYF on General Conditions in T2DM Rats. Food and water intake and urine output in the model group were significantly higher and body weight was lower than that of control group. Treatments of WSZYF (M, H) and metformin increased body weight and decreased food and water intake and urine output compared with the model group. These results indicated that WSZYF could ameliorate the general conditions of T2DM rats. Low dose of WSZYF had no significance in food intake or urine volume (Figure 1).

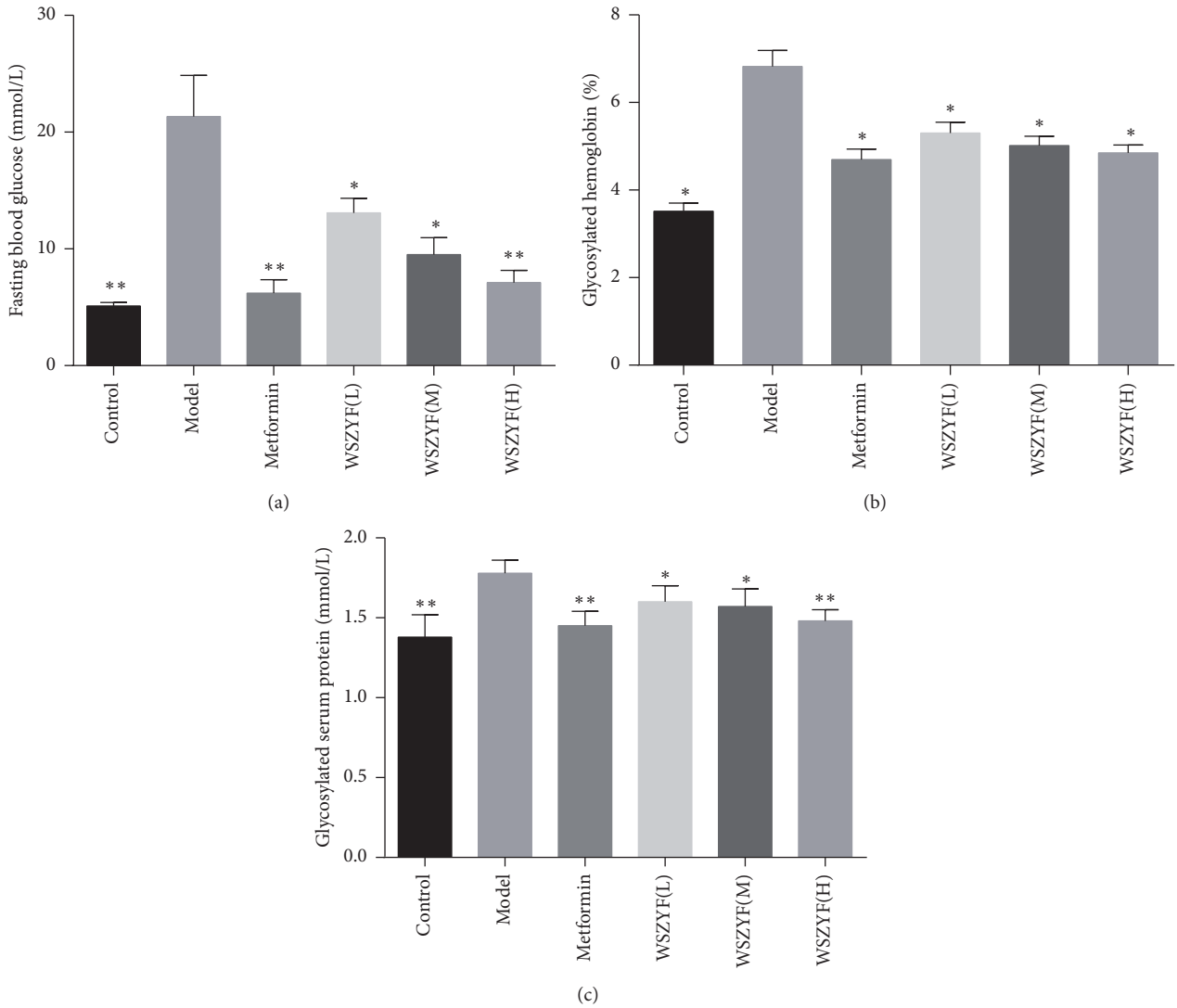

Figure 2: Effects of WSZYF on fasting blood glucose, glycosylated hemoglobin, and glycosylated serum protein. (a) Fasting blood glucose, (b) glycosylated hemoglobin, and (c) glycosylated serum protein. $^{*}P < 0.05$, $^{**}P < 0.01$ compared with model group.

3.2. Effects of WSZYF on Glucose Metabolism Disorders. As shown in Figure 2, fasting blood glucose, glycosylated hemoglobin, and glycosylated serum protein increased significantly in T2DM model group. These results suggested that glucose metabolism was disrupted. Treatments of WSZYF and metformin lowered all the three indexes mentioned above, indicating that they could restore glucose metabolism disorders.

3.3. Effects of WSZYF on Insulin Sensitivity. Insulin plays a critical role in the maintenance of blood glucose homeostasis. Further studies displayed the effects of WSZYF on insulin sensitivity. Insulin concentration and IR index increased in model group, which proved the IR occurrence. After treatments, these two indicators were decreased to be normal, demonstrating that WSZYF had the ability to enhance insulin sensitivity (Figure 3).

3.4. Effects of WSZYF on Glucose Consumption. In order to test the effect of WZSYF on glucose uptake, an IR model of skeletal muscle induced by insulin stimulation was established. In Figure 4, the glucose concentration in the cell supernatant of model group was higher than that of control group, indicating that glucose consumption was decreased in model group. Treatments of WZSYF decreased glucose concentration in the cell supernatant, which proved WSZYF could enhance glucose uptake of skeletal muscle cells.

3.5. Effects of WSZYF on Expressions of Insulin Signaling Transduction-Related Proteins. We further investigated the mechanism of WSZYF in the regulation of insulin signal transduction. As shown in Figure 5, the expressions of P-IRS1, P-Akt, and GLUT4 decreased, whereas PTP1B expression increased in model group compared with control group, indicating that insulin signal transduction was disrupted in

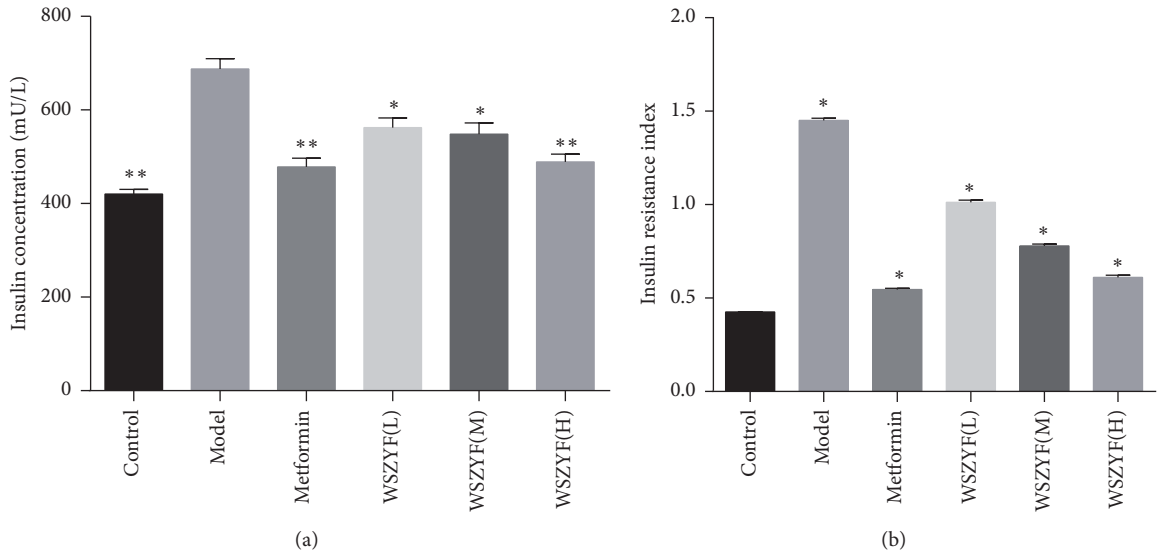

Figure 3: Effects of WSZYF on insulin and IR index. (a) Insulin concentration and (b) IR index. $^{*}P < 0.05$ and $^{**}P < 0.01$ compared with model group.

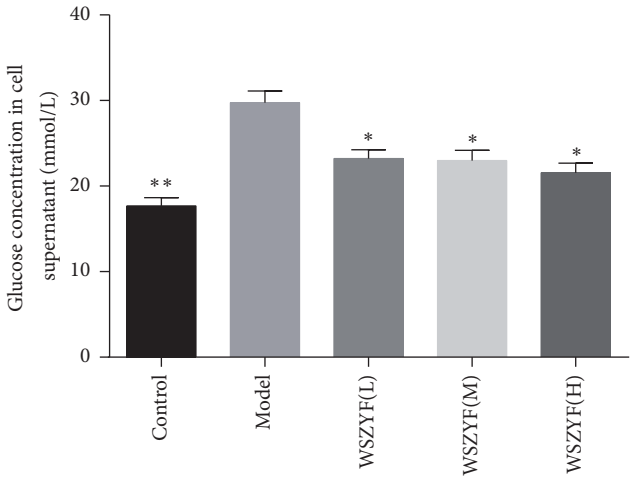

Figure 4: Effects of WSZYF on glucose consumption. $^{*}P < 0.05$ and $^{**}P < 0.01$ compared with model group.

T2DM rats. Expressions of these proteins were reverted to normal levels in treatment of WSZYF and metformin. The results showed that the antidiabetic effect of WSZYF may be mediated by modulating PTP1B-IRS1-Akt-GLUT4 anti-insulin resistant signaling pathway.

4. Discussion

Insulin resistance of skeletal muscle has been shown to play a vital role in the pathogenesis of T2DM. In this study, we demonstrated that WSZYF could exert antidiabetic effect by improving IR in skeletal muscle. Further *in vivo* study suggested that the anti-insulin resistant effect of WSZYF was potentially triggered by regulating PTP1B-IRS1-Akt-GLUT4 signaling pathway.

In T2DM patients, insulin sensitivity decreases in most organs and tissues, accompanied with symptoms like hyperglycemia, hyperlipidemia, hyperinsulinism, and so on [19]. GK rats, a model of T2DM prone rats, were characterized by hyperglycemia, hyperinsulinemia, and IR [20]. Due to these symptoms being similar to T2DM in human, GK rats are widely used in T2DM research. In this study, GK rats fed with high fat and glucose for 4 weeks exhibited a series of T2DM symptoms, including increases of food and water intake as well as urine volume but reduction of body weight. Compared with model group, WSZYF could alleviate the above-mentioned symptoms and better effect was obtained in a higher dose. Moreover, WSZYF also observably decreased fasting blood glucose, glycosylated serum protein, glycosylated hemoglobin, insulin, and IR index compared with those in model group. Meanwhile, *in vitro* results showed that WSZYF could also enhance glucose consumption in IR model of skeletal muscle cells. All of these suggested that WSZYF could regulate glucose metabolism disorders and improve IR in T2DM rats.

There are three signaling pathways mentioned in insulin signal transduction pathways including PI3K pathway, mitogen activated protein kinase pathway, and C-Cbl related protein pathway. Among them, PI3K signaling pathway is the classical one [21–24]. The normal transduction of PI3K signaling pathway is directly related to the normal metabolisms of glucose, fat, and protein. Meanwhile, any abnormalities of PI3K signaling pathway transduction may lead to IR [25]. In the normal process, IRS is phosphorylated when insulin combines with its receptor in the surface of skeletal muscle cell, followed by PI3K activation. The activated PI3K can catalyze phosphatidylinositol 4,5-bisphosphate (PIP2) to PIP3, which activates sequence downstream signaling factor Akt. Phosphorylated Akt translocates GLUT4 to the plasma membrane to uptake glucose into the muscle, which contributes to decreasing plasma glucose concentrations [26].

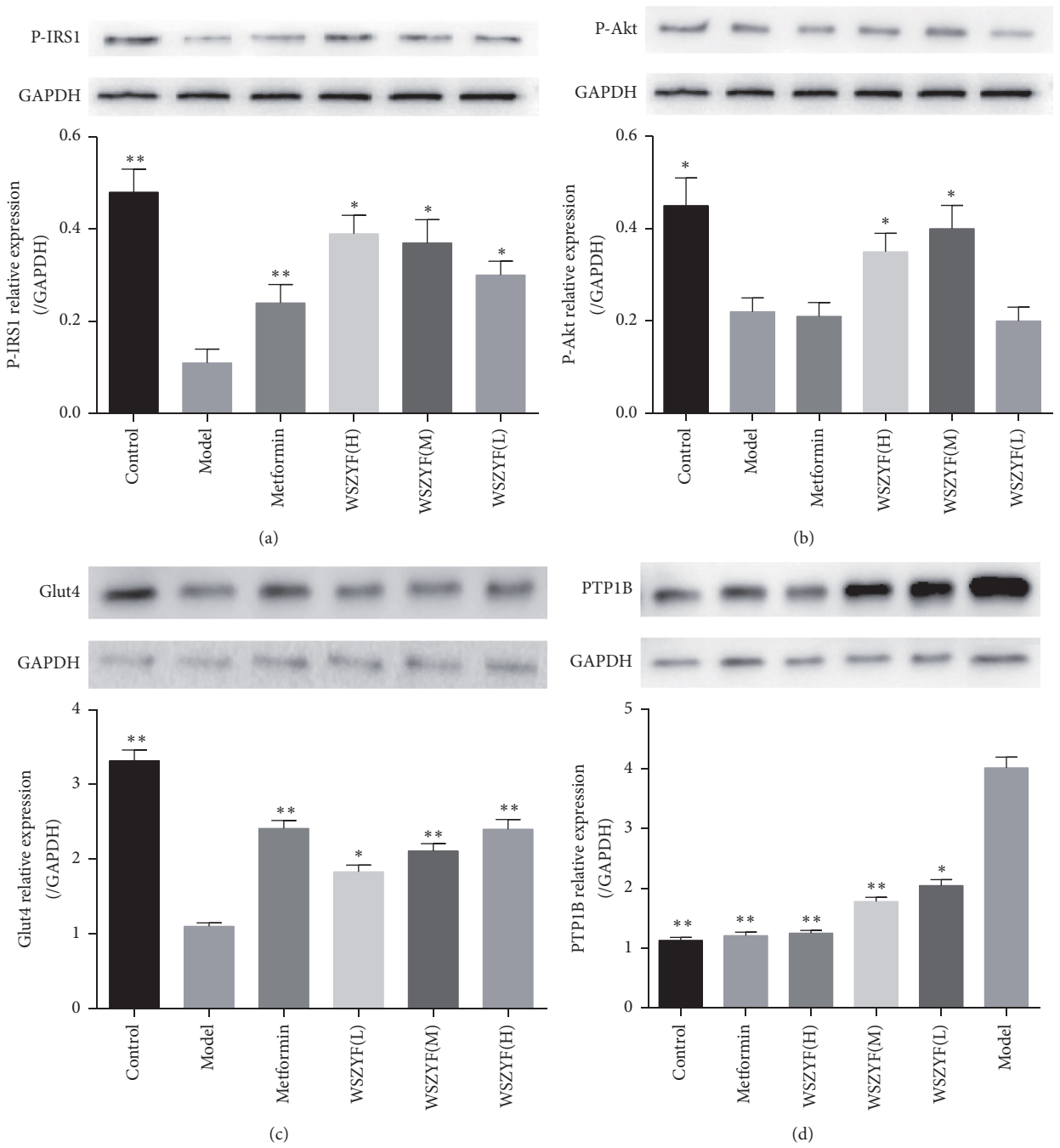

Figure 5: Effects of WSZYF on proteins related to insulin signal transduction. (a) P-IRS1 relative expression, (b) P-Akt relative expression, (c) GLUT4 relative expression, and (d) PTP1B relative expression. $^{*}P < 0.05$ and $^{**}P < 0.01$ compared with model group.

Therefore, IRS-PI3K/Akt-GLUT4 signaling pathway exerts vital regulative effect in insulin signaling transduction of skeletal muscle. Any disorder in this pathway can reduce the sensitivity of skeletal muscles to insulin, resulting in impaired glucose uptake, utilization, glucose tolerance, and elevated blood glucose level [27]. Compared with control group, the expressions of p-IRS1, p-Akt, and GLUT4 decreased significantly in model group, indicating that insulin signaling transduction of skeletal muscle was abnormal and IR occurred. With the treatment of WSZYF, expressions of the signal molecules mentioned above had been elevated, verifying that WSZYF improved IR via restoring insulin signaling transduction of skeletal muscle.

Protein tyrosine phosphatase-1B is an important target for T2DM treatment and has been proved to play a vital role in the negative regulation of insulin signaling transduction. It promotes the dephosphorylation of insulin receptor and IRS and downregulates insulin signaling transduction, ultimately

leading to IR [13]. The expression of PTP1B increased in model group, thus inhibiting IRS1-Akt-GLUT4 signaling pathway and resulting in IR. This was similar to other studies [12, 14]. WSZYF reduced PTP1B expression in a dose-dependent manner, followed by the restoration of IRS1-Akt-GLUT4 signaling pathway and mitigation of IR.

5. Conclusion

In summary, we investigated the antidiabetic effect of WSZYF in T2DM animal model and IR model of skeletal muscle in this study. The results demonstrated that WSZYF could regulate glucose mechanism and IR through modulating PTP1B-IRS1-Akt-GLUT4 signaling pathway. This study provides basis for further research on effective components in the treatment of T2DM.

Conflicts of Interest

The authors declare that they have no conflicts of interest regarding the publication of this manuscript.

Authors' Contributions

Chunyu Tian and Hong Chang contributed to the paper equally.

Acknowledgments

This paper was supported by the Natural Science Foundation of Hebei Province (H2015209025) and Scientific Research Program by Hebei Chinese Medicine Bureau (2016070).

References

[1] D. R. Whiting, L. Guariguata, C. Weil, and J. Shaw, "IDF Diabetes Atlas: global estimates of the prevalence of diabetes for 2011 and 2030," *Diabetes Research and Clinical Practice*, vol. 94, no. 3, pp. 311–321, 2011.

[2] P. Zimmet, K. G. M. M. Alberti, and J. Shaw, "Global and societal implications of the diabetes epidemic," *Nature*, vol. 414, no. 6865, pp. 782–787, 2001.

[3] American Diabetes Association, "Diagnosis and classification of diabetes mellitus," *Diabetes Care*, vol. 37, supplement 1, pp. S81–S90, 2014.

[4] B. He, M. Shi, and L. Zhang, "Beneficial effect of galanin on insulin sensitivity in muscle of type 2 diabetic rats," *Physiology & Behavior*, vol. 103, no. 3-4, pp. 284–289, 2011.

[5] J. D. Best, S. E. Kahn, M. Ader, R. M. Watanabe, T.-C. Ni, and R. N. Bergman, "Role of glucose effectiveness in the determination of glucose tolerance," *Diabetes Care*, vol. 19, no. 9, pp. 1018–1030, 1996.

[6] F. Kanai, K. Ito, M. Todaka et al., "Insulin-Stimulated GLUT4 Translocation Is Relevant to the Phosphorylation of IRS-1 and the Activity of PI3 Kinase," *Biochemical and Biophysical Research Communications*, vol. 195, no. 2, pp. 762–768, 1993.

[7] N. Yu, X. Fang, D. Zhao et al., "Anti-diabetic effects of Jiang Tang Xiao Ke granule via PI3K/Akt signalling pathway in type 2 diabetes KKAy mice," *PLoS ONE*, vol. 12, no. 1, Article ID e0168980, 2017.

[8] F. Favaretto, G. Milan, G. B. Collin et al., "GLUT4 defects in adipose tissue are early signs of metabolic alterations in alms1GT/GT, a mouse model for obesity and insulin resistance," *PLoS ONE*, vol. 9, no. 10, Article ID e109540, 2014.

[9] A. Zorzano, M. Palacín, and A. Gumà, "Mechanisms regulating GLUT4 glucose transporter expression and glucose transport in skeletal muscle," *Acta Physiologica Scandinavica*, vol. 183, no. 1, pp. 43–58, 2005.

[10] X. Yang, J. Yang, C. Xu et al., "Antidiabetic effects of flavonoids from Sophora flavescens EtOAc extract in type 2 diabetic KK-ay mice," *Journal of Ethnopharmacology*, vol. 171, pp. 161–170, 2015.

[11] L. Yang, Z. Wang, L. Jiang, W. Sun, Q. Fan, and T. Liu, "Total flavonoids extracted from oxytropis falcata bunge improve insulin resistance through regulation on the IKKbeta/NF-kappaB inflammatory pathway," *Evidence-Based Complementary and Alternative Medicine*, vol. 2017, Article ID 2405124, 6 pages, 2017.

[12] W. Ji, X. Chen, J. Lv et al., "Liraglutide exerts antidiabetic effect via PTP1B and PI3K/Akt2 signaling pathway in skeletal muscle of KKAy mice," *International Journal of Endocrinology*, vol. 2014, Article ID 312452, 9 pages, 2014.

[13] D. Patel, M. Jain, S. R. Shah et al., "Discovery of potent, selective and orally bioavailable triaryl-sulfonamide based PTP1B inhibitors," *Bioorganic & Medicinal Chemistry Letters*, vol. 22, no. 2, pp. 1111–1117, 2012.

[14] Q.-C. Liu, T.-T. Guo, L. Zhang et al., "Synthesis and biological evaluation of oleanolic acid derivatives as PTP1B inhibitors," *European Journal of Medicinal Chemistry*, vol. 63, pp. 511–522, 2013.

[15] T. Wang and Y. Fan, "Effect of tetrahydroxy stilbene glucoside from Polygoni Multiflori Radix for insulin resistance in skeletal muscle of type 2 diabetes rats," *China Medical Herald*, vol. 13, no. 12, pp. 25–28, 2016.

[16] C. Y. Yonamine, E. Pinheiro-Machado, M. L. Michalani et al., "Resveratrol improves glycemic control in type 2 diabetic obese mice by regulating glucose transporter expression in skeletal muscle and liver," *Molecules*, vol. 22, no. 7, p. 1180, 2017.

[17] F.-L. Hsu, C.-F. Huang, Y.-W. Chen et al., "Antidiabetic effects of pterosin A, a small-molecular-weight natural product, on diabetic mouse models," *Diabetes*, vol. 62, no. 2, pp. 628–638, 2013.

[18] X. M. Zhou, C. Y. Tian, X. J. La et al., "Effect of water extract of shizidaiping prescription on insulin resistance of skeletal muscle cells," *Natural Product Research and Development*, vol. 28, pp. 1139–1143, 2016.

[19] J. K. Prasain, N. Peng, R. Rajbhandari, and J. M. Wyss, "The Chinese Pueraria root extract (*Pueraria lobata*) ameliorates impaired glucose and lipid metabolism in obese mice," *Phytomedicine*, vol. 20, no. 1, pp. 17–23, 2012.

[20] K. Srinivasan and P. Ramarao, "Animal models in type 2 diabetes research: an overview," *Indian Journal of Medical Research*, vol. 125, no. 3, pp. 451–472, 2007.

[21] V. Saini, "Molecular mechanisms of insulin resistance in type 2 diabetes mellitus," *World Journal of Diabetes*, vol. 1, no. 3, pp. 68–75, 2010.

[22] K. Morino, K. F. Petersen, S. Dufour et al., "Reduced mitochondrial density and increased IRS-1 serine phosphorylation in muscle of insulin-resistant offspring of type 2 diabetic parents," *The Journal of Clinical Investigation*, vol. 115, no. 12, pp. 3587–3593, 2005.

[23] T. Shibata, A. Takaguri, K. Ichihara, and K. Satoh, "Inhibition of the TNF-α-induced serine phosphorylation of IRS-1 at 636/639

by AICAR," *Journal of Pharmacological Sciences*, vol. 122, no. 2, pp. 93–102, 2013.

[24] A. Koh, M. N. Lee, Y. R. Yang et al., "C1-Ten is a protein tyrosine phosphatase of insulin receptor substrate 1 (IRS-1), regulating IRS-1 stability and muscle atrophy," *Molecular and Cellular Biology*, vol. 33, no. 8, pp. 1608–1620, 2013.

[25] M. H. A. Bakar, K.-K. Cheng, M. R. Sarmidi, H. Yaakob, and H. Z. Huri, "Celastrol protects against antimycin A-induced insulin resistance in human skeletal muscle cells," *Molecules*, vol. 20, no. 5, pp. 8242–8269, 2015.

[26] N. Sharma, D. A. Sequea, C. M. Castorena, E. B. Arias, N. R. Qi, and G. D. Cartee, "Heterogeneous effects of calorie restriction on in vivo glucose uptake and insulin signaling of individual rat skeletal muscles," *PLoS ONE*, vol. 8, no. 6, Article ID e65118, 2013.

[27] Q. Liu, X. Li, C. Li, Y. Zheng, G. Peng, and D. J. McPhee, "1-deoxynojirimycin alleviates insulin resistance via activation of insulin signaling PI3K/AKT pathway in skeletal muscle of db/db mice," *Molecules*, vol. 20, no. 12, pp. 21700–21714, 2015.